Effect of HPGR on platinum bearing ores and the flotation response as compared to the conventional ball mill

Nomonde Solomon
BSc (Chem Eng), University of Cape Town

Thesis submitted in fulfillment of the requirements for the degree of
Master of Science in Engineering
MSc (Eng)
April 2010

UNIVERSITY OF CAPE TOWN
CENTRE FOR MINERALS RESEARCH

Declaration

I know the meaning of plagiarism and declare that all of the work in this document, save for that which is properly acknowledged, is my own

_____

Nomonde Solomon

Acknowledgments

I would like to offer sincere gratitude to my supervisors Dr Aubrey Mainza, Dr Megan Becker, Dr Jochen Petersen and Professor J P Franzidis for their guidance and assistance in this work. The management and staff in the in the CMR laboratory Jenny Wiese, Jason Waters, Mike Bekapi, Kenneth Maseko and Monde Bekapi are also acknowledged for their assistance. I would also like to thank Peter Harris for his assistance in the analysis of the flotation data and Dee Bradshaw for reading and commenting on parts of this thesis.

Sincere acknowledgements go to Polysius for allowing us to use their machine, Mintek for allowing us to perform the tests on their site and Victor Ross and Allen Hemphill at Lonmin for providing the ore and assisting with the logistics involved. This project could not have been made possible without the contribution from these companies and these people.

This thesis is dedicated to my family who has been a great source of strength and motivation during this work. Special thanks go to my sister Nandipha who put me through university and to my aunt Beryl for always having faith in my abilities. Words cannot describe how grateful I am for your support. I would not be where I am today without you. To my best friends Ntokozo, Lungiswa and Danna, thank you for making this journey a lot more insightful and enjoyable.

Executive Summary

This thesis focuses on the application of the high pressure grinding rolls (HPGR) on platinum bearing ores Merensky, UG2 and Platreef. These are very fine grained ores and due to the complexity of the ore bodies, platinum operations are looking to apply alternative comminution devices that can liberate the PGMs at a coarser grind, at reduced energy consumption and increased throughput. Conventional tumbling mills such as the ball mill that are typically applied on these ore types are highly energy intensive with a small percentage of the input energy being used for actual breakage. Rapidly increasing energy costs have contributed to the rising interest of the HPGR in the platinum industry particularly in plants processing UG2 and Platreef ores. Therefore, this thesis seeks to determine if the HPGR can be used as an alternative to the ball mill. Key aspects of interest are throughput, energy efficiency, PGE grade and recovery and PGM liberation.

Comminution and flotation tests were performed on the three platinum bearing ores obtained from the Bushveld Complex. The comminution tests involved the application of a small scale HPGR at different operational parameters. From these tests, it has been determined if the HPGR can produce a fineness of grind suitable for flotation tests. Comparative pilot scale ball mill tests were performed on all three ore types. Batch flotation tests were then performed on selected HPGR samples to determine the effects on PGM recovery. In order to determine the benefits of the HPGR in terms of energy consumption, throughput and PGM recovery, ball mill tests were also performed as a comparison.

Based on the sizing analyses, it was found that a circuit with a series of HPGRs could be applied as an alternative to the ball mills particularly in the primary comminution stage. Grinds of up to 41.5%, 47.6% and 36.9% passing 75μm were obtained after five passes for Merensky, UG2 and Platreef, respectively. This is within the range of grinds applied in the primary comminution circuits in platinum processing plants. Depending on the grind required, the HPGR parameters can be adjusted to ensure that more energy efficient conditions are applied.

The relationship between the reduction ratio and the specific energy consumed was used to determine the variables where more energy efficient application of the HPGR could be obtained for each ore type. Differences in reduction ratio – specific energy relationship were obtained for different ore types. Linear relationships were obtained for Merensky at varying pressures while UG2 and Platreef exhibited non-linear relationships. It was found that although Platreef consumed more energy compared to Merensky and UG2, it was more energy efficient to apply the HPGR due to the increasing slopes of the curves generated.

While the reduction ratio-specific energy relationship is essential for determining the most energy efficient operational conditions of the HPGR for each ore type, it does not take into account the saturation points. Therefore reference to the grinds and specific energy relationships is required to determine possible HPGR operational variables for each ore type.

Comparisons of the PGE grade and recoveries obtained with the HPGR were made to those from the ball mill tests. Although material comminuted with the HPGR was able to float, the PGE grade and recoveries were less than those obtained with the ball mill. Grinds obtained with the ball mill show that the lower coarse content in the 125µm - 1000µm size range for Merensky and UG2. Platreef on the other hand showed coarser grinds obtained with the ball mill compared to the HPGR.

Table of Contents

List of figures

List of tables

Abbreviations and Nomenclature

ρ	material specific gravity (t/m^3)
AG/SAG	Autogenous/Semi-autogenous
ANOVA	Analysis of variance
BMS	base metal sulphides
BSE	back scattered electrons
BWI	Bond work index (kWh/t)
CSIRO	Commonwealth Scientific and Industrial Research Organisation
D	diameter of HPGR rolls (m)
E_{sp}	specific energy (kWh/t)
EDS	energy dispersive spectrometer
F	grinding force (N)
F_{sp}	specific grinding force (N/mm^2)
F_{50}	feed median size (μm)
HPGR	High Pressure Grinding Rolls
JKMRC	Julius Kuttschnitt Mineral Research Centre
L	width of the HPGR rolls (m)
MLA	Mineral Liberation Analyser
PGE	Platinum Groups Elements
PGM	Platinum Group Minerals
P_{50}	Product median size (μm)
QEMSCAN	Quantitative Evaluation of Minerals using Scanning Electron Microscopy

UG2	Upper Group 2
u	Rolls speed (m/s)
Working gap, x_g	The maximum gap measured between the rolls of the HPGR during operation (m)
Zero gap	The initial gap between the rolls of the HPGR

Chapter 1

1 Introduction

1.1 Background

The Bushveld Complex of South Africa contains approximately 80% of the world's reserves of platinum group minerals (Liddell *et al*, 1986). The Complex consists of three major reefs: the Merensky reef, the Upper Group 2 (UG2) reef and Platreef. Due to the differences in mineralogical characteristics, these ore types exhibit different behaviour during processing for the extraction of the valuable minerals. Figure 1-1 shows the three main stages in mineral processing that the ore from the mine goes through for the extraction of these valuable minerals. The valuable minerals are first liberated from the unwanted gangue minerals and are then separated through flotation into concentrate and tails. The concentrate goes for further hydrometallurgical and refining processing while the tails are disposed of.

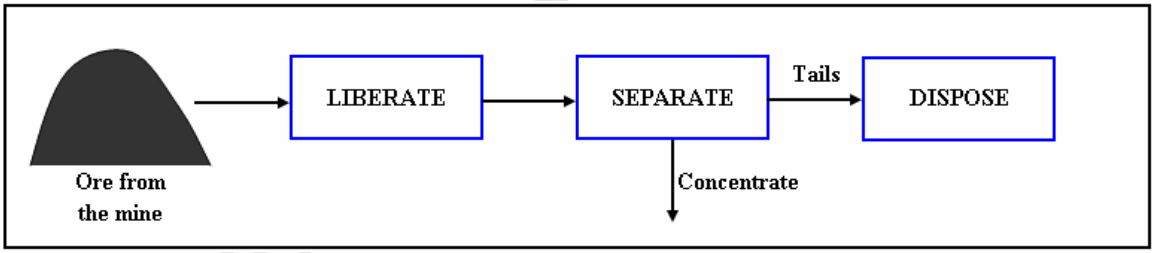

Figure 1-1: Sub-processes involved in mineral processing (Cramer, 2001)

In the liberation stage, comminution is the process of size reduction by which the valuable minerals are exposed and prepared for separation from the unwanted gangue minerals. Ideally, the ore goes through several stages of comminution in order to reach a particle size distribution where optimum liberation of the valuable minerals has occurred. The comminution circuit on a mineral processing plant can be sub-divided into two stages known as crushing and grinding. The grinding circuit is the final stage in the comminution circuit and is the most energy intensive. Approximately 70% of all the energy consumed in a mineral processing circuit is utilised in comminution (Fuerstenau

et al, 1999). The amount of energy utilised in comminution circuits is dependent on several variables which include the ore characteristics, the comminution devices applied and the circuit configuration (Wen *et al*, 1998). The comminution stage is also the throughput limiting stage in mineral processing circuits. Therefore, the optimisation of this stage in terms of energy efficiency and throughput will improve the overall mineral processing circuit.

Characteristics of the ore such as hardness and mineral compositions are key variables in the determination of comminution energy consumption and plant throughput. According to the comminution characterisation indices, the three ore types Merensky, UG2 and Platreef are considered to be very hard ores and they vary in hardness depending on the location in the reef (Cramer, 2001; Mainza and Powell, 2006). Therefore, in order to achieve optimum mineral liberation of these ore types, a considerable amount of energy is utilised by conventional tumbling mills such as the autogenous, semi-autogenous (AG/SAG) and ball mills. These mills are highly energy inefficient, and may be up to 1-10% energy efficient (Fuerstenau and Abouzeid, 2002). A significant amount of energy is lost in overcoming friction and wear of media and mill liners. Furthermore, the uncertainty of a particle experiencing an impact force from the grinding media contributes to the high energy inefficiencies (Fuerstenau and Kapur, 1995).

Due to the processing of more complex ore types with very fine grained textures, some operations including the platinum industry need to grind the material ultrafine (<10μm) in order to sufficiently liberate the valuable minerals (Cole and Ferron, 2002). As a result, some operations have opted to add fine grinding technology such as the IsaMill to the comminution circuits to achieve optimum mineral liberation of these ore types. However, the production of more fines has resulted in metallurgical problems experienced in downstream separation processes such as flotation (Clarke and Wills, 1989). Losses in valuable mineral recovery have been experienced in some operations due to the production of ultra fine particles. Furthermore, the production of ultra fine particles has resulted in more energy consumption and lower throughput due to the limited capacity of ultrafine grinding comminution devices.

Potential methods of enhancing mineral liberation which focus on optimizing mineral liberation at a coarser grind have been discussed by Wills (1988). These methods include the application of alternative comminution methods using compression rather than impact breakage such as the high pressure grinding rolls (HPGR) as a pre-treatment method for conventional comminution devices. The HPGR has been applied in various comminution circuits in the copper, nickel, gold, iron and platinum industries. Benefits of the application of the HPGR in these industries that have been reported in several publications include improved energy efficiency (10 – 30%), enhanced mineral liberation, increased throughput in existing comminution circuits including those processing hard ore types and lower operational costs (Humphries, 2006; Patzelt *et al*, 1995; Aydogan *et al*, 2006; Siedel *at al*, 2006; Brachthäuser and Kellerwessel, 1988)

The micro-fissures and cleavages reportedly induced by the HPGR in particles from selected ore types have resulted in reduced energy consumption in downstream grinding processes and increased mineral recovery particularly in leaching processes (Dunne *et al*, 1996; Tavares, 2005). Several possible applications of the HPGR in comminution circuits include the following (Brachthauser and Kellerwessel, 1988):

- one step comminution in the fine crushing to coarse grinding size range
- pre-treatment of the feed of a conventional tumbling mill in open or closed circuit
- production of the final product in closed circuit

The above applications have been applied extensively in various comminution circuits with each showing improvements in energy efficiency of 10 – 30% (Parker *et al*, 2001; Shi *et al*, 2006; Aydoğan *et al*, 2006).

Rapidly increasing energy costs have contributed to the rising interest of the HPGR in the platinum industry particularly in plants processing UG2 and Platreef ores. The goal is to improve plant capacity in Platreef plants and increase recovery in UG2 plants. Therefore, the opportunity for improvement of existing platinum plants using HPGR technology is expected to play a significant role in future platinum processing (Rule *et al*, 2008). For this reason, this project is focused on determining the effect of the application of the HPGR on the three platinum bearing ores under consideration, Merensky, UG2 and

Platreef. Aspects of interest to this study include throughput, energy efficiency, mineral liberation and flotation recovery of the platinum group minerals in these ore types. The following sub-section gives some motivations for this project.

1.2 Motivation

There are several operational and design variables of the HPGR that have significant effects on energy consumption and the degree of mineral liberation. Various studies have been performed on different ore types to determine the effects on these variables and to establish the optimum operating conditions (Lim *et al*, 1996; 1997). The results obtained from these studies indicate that ore type has an influence on the outcome in terms of energy consumption and the extent of size reduction. Very few studies of this nature have been performed on platinum bearing ores and the findings from these have not been published. Most studies on the HPGR have investigated its application as a pre-grinding stage where the product is fed to a ball mill (Patzelt *et al*, 1995; Wightman *et al*, 2008; Dunne *et al*, 1996). However, there have been no studies published that focus on determining if the product from the HPGR could be sufficiently liberated for the primary flotation circuit without any subsequent grinding requirements.

In a study performed by Daniels (2007) on the platinum bearing ore, UG2, it was shown that the HPGR does show some signs of preferential mineral liberation for minerals that are typically associated with the PGMs. This however, did not translate to the preferential liberation of the PGMs. It was therefore concluded that more work need to be performed to determine if preferential liberation could be achieved on the PGMs with the application of the HPGR. Wightman *et al* (2008) on the other hand, found that despite the comminution device applied on copper and a silver/lead/zinc ores, there were no variations in the deportment of liberated valuable minerals in different size classes.

Dunne *et al* (1996) performed a series of tests to determine the effects of the HPGR on downstream recovery processes such as leaching, flotation and gravity settling for gold ores. Although no benefits were observed in the flotation and gravity settling processes,

significant improvements in gold recovery were observed with the leaching process. This showed the benefits of the HPGR in terms of downstream recoveries, particularly for leaching processes, but does not necessarily show the efficiency of the comminution devices in terms of mineral liberation.

The above mentioned studies are more fully discussed further in the literature review. However, none of these studies has shown the links between energy efficiency, mineral liberation and the effect on downstream processes such as flotation and leaching for a particular ore type. Therefore, the following key questions convey the motivations of this study:

1. Is it possible to apply the HPGR as an alternative to the highly energy inefficient ball mill in a grinding circuit processing platinum bearing ores?
2. How does the application of the HPGR affect downstream PGM recovery?
3. How does the HPGR affect the energy efficiency and size reduction of each ore type?

1.3 Hypotheses

Based on the background and the motivation presented in the previous section, the following are the hypotheses of this work:

1. The operational variables where the HPGR can comminute the ore with minimal energy requirements vary for different ore types because material with dissimilar mineralogical compositions will respond differently to the applied force.
2. The HPGR can be used to prepare the ore for flotation without any subsequent grinding at reduced specific energy input. This is due to the different breakage mechanism applied by the HPGR can potentially liberate valuable minerals at a coarser grind.

1.4 Objectives

The main objectives of this study are to perform experiments to determine if:

1. To determine the most energy efficient HPGR variables that can be applied on platinum bearing ores.
2. To compare PGE recoveries from product generated with the use of the HPGR to that obtained from the ball mill.
3. To compare liberation profiles of the product generated from the HPGR to that obtained from the ball mill.
4. To determine the benefits of the application of the HPGR as a pre-grinding stage to a pilot scale ball mill in terms of throughput and energy consumption.

1.5 Methodology of solution

A small scale HPGR with roll dimensions 250mm diameter and 100mm length was used to address the main objectives of this project. Various tests were performed at different operational variable of the HPGR on the three ore types Merensky, UG2 and Platreef. The following variables were considered in the test work:

- Pressure (bar)
- Zero gap – the initial gap between the rolls
- Ore type
- Feed top size

Tests involving several passes through the HPGR were performed to determine the limit to which the HPGR could comminute each ore type. From this, it could be determined if sufficiently liberated ore could be obtained with the application of the HPGR alone. The cumulative energy expended after various passes could be determined for each ore type.

Operations processing platinum bearing ores typically apply flotation as the method of separation and concentration. Therefore, batch flotation tests were performed on selected HPGR products. The samples that had a fineness of grind that was similar to that applied in typical primary flotation circuit processing platinum bearing ores. The effect of the HPGR on grade and recovery of PGMs could thus be determined from the flotation tests.

In order to substantiate the benefits of applying the HPGR relative to ball mills, a comparison of the two comminution devices was performed. A pilot scale ball mill with dimensions 0.9m diameter and 1.5m length was utilised. Two types of tests were performed with the ball mill:

1. Ball mill tests where 6mm feed top size of each ore type was ground
2. Hybrid tests were 6mm feed top size of each ore type was crushed with the HPGR and subsequently ground in the ball mill.

These tests served to highlight the difference between the two comminution devices by performing a comparison of the measured outputs: specific energy consumption, mineral liberation, flotation recovery and throughput.

The Quantitative Evaluation of Minerals using Scanning Electron Microscopy (QEMSCAN) was used to perform a bulk mineralogical analysis to characterise each of the three platinum ores investigated in this study. The Mineral Liberation Analyser (MLA) was used to characterise the PGMs and to generate liberation profiles of some of the products obtained from the HPGR and the ball mill.

Figure 1-2 gives an overview of how the different mineral processing aspects interlink and the areas of contribution from this study. This study is concerned with the first two stages of mineral processing shown as Liberate and Separate in Figure 1-2. The effect of HPGR on the Disposal of the unwanted gangue minerals is beyond the scope of this work.

1.6 Thesis lay out

Chapter 1 discusses the background, motivation, hypothesis, objectives and scope of this thesis. Chapter 2 contains relevant literature that considers the HPGR applications in different comminution circuit configurations and the benefits of these applications. A review of the PGM ores and how these ore types may benefit from this work has also been given. A review of the techniques relevant to this study has also been performed in this chapter.

Chapter 3 provides a detailed description of the experimental set up that was applied in order to accomplish the objectives of the thesis. Descriptions of each of the experiments performed using the HPGR, ball mill and in flotation are given.

Chapter 4 gives the results obtained from the HPGR and ball mill experimental work. The aim of this chapter is to give a comprehensive account of the effects of the different HPGR variables on throughput, size reduction and specific energy of the three ore types under consideration. On this basis, comparisons between the HPGR and the ball mill have been made. Chapter 5 gives the results from the flotation tests and the QEMSCAN and MLA analyses.

Chapter 6 is a discussion of the results presented in Chapters 4 and 5 and mainly focuses on the interpretation of the data presented and how they compared to published work. Conclusions and recommendations based on the outcomes of this study are discussed in Chapter 7.

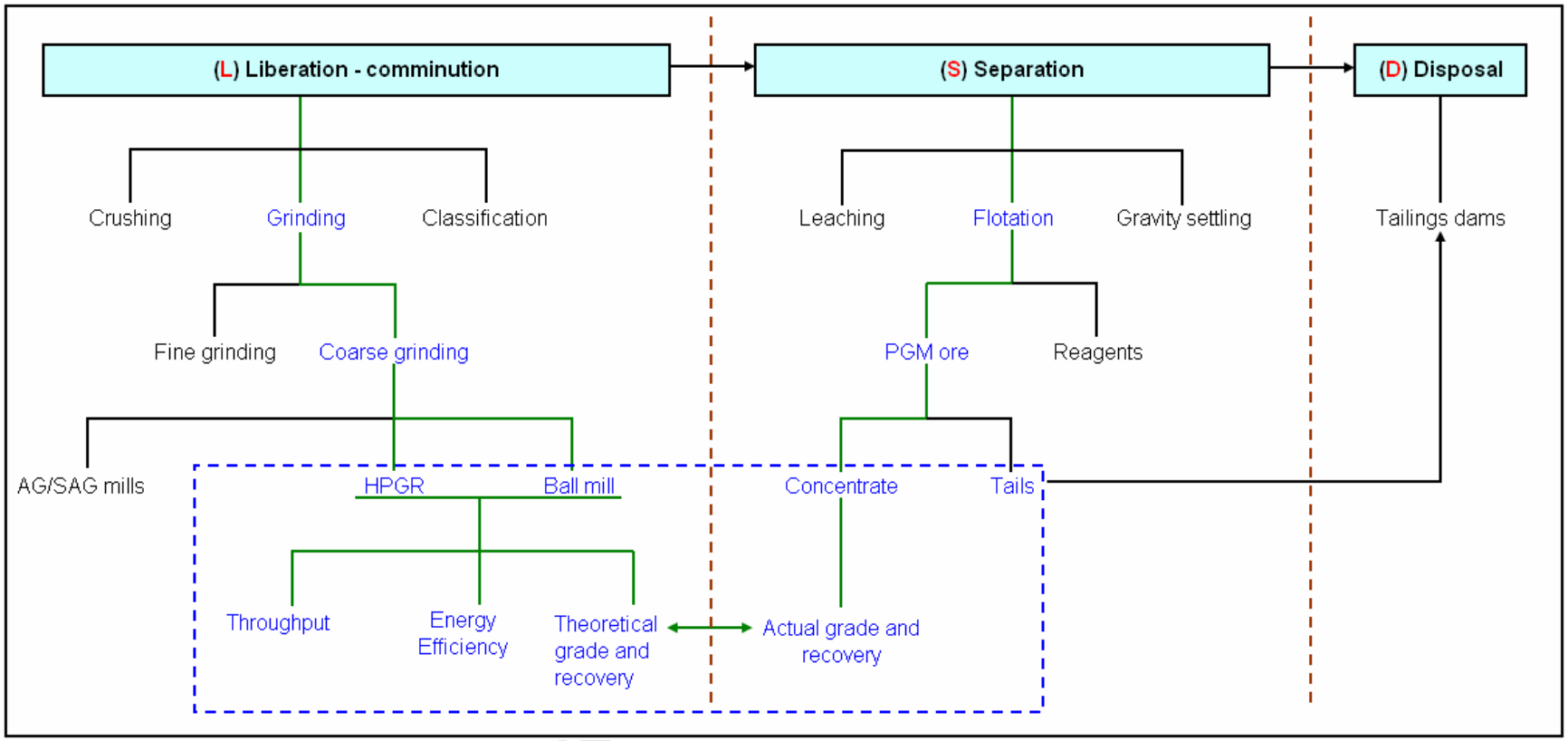

Figure 1-2: Project overview and scope

Chapter 2

2 Literature Review

Overview: This chapter is a review the literature that is relevant to this study. The focus is mainly on studies that have been performed with the application of the HPGR on various comminution circuit configurations. Methodologies and techniques applied that are applicable to this thesis have also been reviewed.

2.1 Platinum bearing ores from the Bushveld Complex

The Bushveld Complex of South Africa is the largest layered intrusion in the world which consists of the major known deposits of chrome, vanadium and platinum group minerals (PGM) (Clarke *et al*, 2008). The major reefs, Merensky, UG2 and Platreef which account for up to 80% of the world's reserves are exploited mainly for the base metal sulphides (BMS) and platinum group minerals (PGM) (Liddell *et al*, 1986).

2.1.1 Mineralization in Merensky, UG2 and Platreef

The total platinum group element (PGE) abundance of these reefs ranges between 4 and 8g/t and is sometimes lower (1 – 3g/t) with grain sizes ranging from less than 10μm up to 350μm (Lee, 2000; Cabri, 2004). The Merensky reef is the most abundant in PGM content followed by UG2 and then Platreef (Lee, 1996). The PGMs are typically associated with the base metal sulphides. However in the UG2 reef, the PGMs can vary from being predominantly associated with the BMS to being predominantly associated with the gangue minerals depending on the location of the reef (Penberthy *et al*, 2000).

The major BMS present in the three reefs include chalcopyrite ($CuFeS_2$), pyrrhotite ($Fe_{1-x}S$), pentlandite ($(Fe,Ni)_9S_8$) and pyrite (FeS_2). These BMS are present in varying amounts at different locations in each of the three reefs. The Merensky reef which is the most abundant in total BMS content consists of approximately 1% while UG2 has <0.1% (Lee, 1996). Platreef on the other hand has BMS mineralization and PGM concentrations

that were found to be irregular both in value as well as in distribution (Lee, 2000; Holwell *et al*, 2006).

The three reefs have similarities in the type of major gangue minerals present but with differences in abundance and association. The Merensky reef predominantly consists of the silicate, orthopyroxene (70 – 90%) and up to 30% of plagioclase. The UG2 reef predominantly consists of chromite (60 – 90%) and between 5 – 25% orthopyroxene and 1 – 10% plagioclase (Lee, 1996). Platreef on the other hand consists of a complex assemblage of pyroxenites, serpentinites and calc-silicates (Lee, 2000).

The reefs contain economic amounts of the PGM but they differ in mineralogical characteristics. This has an effect on the method and operational variables of the concentration process applied. Therefore, knowledge of the mineralogy of these ore types can be used for the optimisation of the beneficiation of PGMs. Information such as the grain sizes, mineral proportions and associations are needed to ensure that maximum recovery of the PGMs can be achieved (Schapiro, 1981; Henely, 1983).

2.1.2 Beneficiation of platinum group minerals

The same basic process is applied in the beneficiation of the PGMs and BMS from the three ore types. Cramer (2001) showed the typical stages involved in the beneficiation of the platinum bearing ores in Figure 2-1. Some operations apply the MF2 process which consists of primary and secondary stages of comminution each followed by flotation to ensure optimum recovery of the valuable minerals. Due to the differences in mineralogical content, variations in the operational conditions of the process equipment have been implemented to ensure maximum recovery for each ore type. However, a common thread in the processing of these ores is that the greatest losses in PGMs recovery occur due to inefficiencies in the first stage of the beneficiation process. PGMs recoveries of 80 – >90% are typically obtained in the concentration stage while the smelting and refining stages yield recoveries of 95 – 99% (Merkle and McKenzie, 2002).

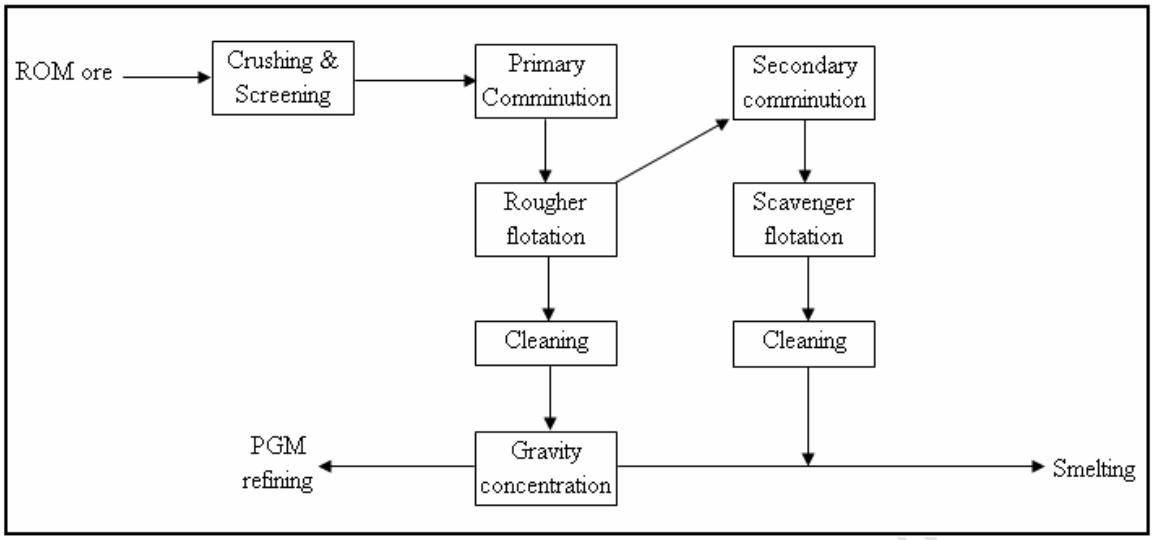

Figure 2-1: A typical concentrator flow sheet used in platinum operations (Cramer, 2001)

The platinum bearing ores have different competencies in terms of the comminution characterisation indices shown in Table 2-1 (Mainza and Powell, 2006). The average bond work indices (BWI) and breakage parameters (AxB) obtained from the Julius Kruttschnitt (JK) drop weight test for Merensky, UG2 and Platreef are given in Table 2-1. At closing screens 300µm and 75µm, UG2 has a lower BWI compared to Merensky and Platreef ore. The higher breakage parameters from the JK drop weight tests indicate that UG2 is the softest of the three ore types (Mainza and Powell, 2006).

The amount of energy consumed in the comminution stage is dependent on the hardness of the ore, the circuit configuration and the fineness of grind required to achieve the desired size distribution where optimum mineral liberation is obtained (Napier-Munn *et al*, 2006). Due to the very fine grained nature of the PGMs, typically large size reductions are required for the platinum bearing ores. This gives rise to higher chances of over-grinding the ore which would result in unnecessary use of energy and poor recoveries of the PGMs in flotation circuits. As a result, some operations have had to ensure a balance between adequate liberation without the generation of excessive fines (Merkle and McKenzie, 2002).

Table 2-1: Comminution characterisation indices of Merensky, UG2 and Platreef ore (Mainza and Powell, 2006)

Ore type	BWI at 300µm (kWh/t)	BWI at 75µm (kWh/t)	AxB	Ta
Merensky Reef	21	25	77	0.63
UG2 Reef	18	21	151	1.25
Platreef	18 – 25	23 – 27	30 – 40	0.11 – 0.21

In the comminution stage, conventional tumbling mills such as the autogenous, semi-autogenous (AG/SAG) and ball mills are applied. In the primary comminution stage, the ore is ground to approximately 30% passing 75µm for the rougher flotation circuit (Cramer, 2001). In the secondary comminution stage, grinds of approximately 60% passing 74µm are achieved for Merensky and UG2 ore (Cramer, 2001). However, many operations prefer 40 – 50% passing 75µm in the primary and close to 80% passing 75µm in the secondary/tertiary grinding stages due to the processing of more fine grained ore types. For Platreef ore, final grinds of approximately 75% passing 75µm are required to adequately liberate the valuable minerals (Cramer, 2001).

It is well known that the conventional comminution process is highly energy inefficient and accounts for up to 70% of the total energy required in the beneficiation process (Fuerstenau *et al*, 1999; Tromans, 2008). This is mainly due to the application of tumbling mills such as the AG/SAG and ball mills in which most of the energy is expended in moving the bulk charge around. Up to 1 – 10% of the total energy utilised by the ball mill is used for actual breakage of ore being milled (Fuerstenau *et al*, 2002). While these mills have been said to be robust and effective for the past few decades, they are highly energy inefficient (Fuerstenau and Kapur, 1995).

Recovery by flotation is performed on the comminution product to separate the liberated valuable minerals from the unwanted gangue minerals. The nature of the grind in terms of liberation and fineness has enormous effects on the PGM grade and recoveries obtained in the flotation stage (Wills, 2005). PGM flotation circuits have often suffered

from poor recoveries due to over-grinding in the comminution stage. Recovery of gangue minerals by entrainment as a result of the very fine particles has resulted in lower concentrate grades (Wills, 2005). Depressants are normally added to the system to reduce the recovery of these unwanted gangue minerals. However, complete depression of the gangue minerals could result in the loss of BMS and PGE as a result of the suppression of partially liberated PGMs and liberated grains coated with talc slimes (Merkle and McKenzie, 2002).

The comminution and flotation stages are where the losses in energy efficiency and recovery are highest during the beneficiation of PGM. In a climate where energy costs are rapidly increasing and metal prices are low, operations including the platinum industry are investigating the possibility of applying more energy efficient methods of comminution that can lead to improved mineral liberation at a coarser grind. The platinum operations are also looking to improve capacity, recovery and reduce operating costs in the beneficiation stage (Rule *et al*, 2008). One such way is through the application of alternative comminution devices such as the high pressure grinding rolls (HPGR) which was developed by Schönert in the 1970s (Lim *et al*, 1997). Various studies performed on different ore types have shown that the HPGR has the potential to achieve the previously mentioned desired outcomes (Dunne *et al*, 1996; Daniels, 2007; Fuerstenau and Kapper, 1995; Apling and Bwalya, 1997; Patzel *et al*, 1995). The following section therefore, looks at some of the applications of the HPGR in existing circuits and the benefits that have resulted.

2.2 The High Pressure Grinding Rolls (HPGR)

The (HPGR) was developed by Schönert in the late 1970s and was first applied in the cement industry in the 1980s. Its application in the mineral processing industry lagged due to the processing of more abrasive material which resulted in the extremely high wear rates of the rolls, making it a costly process (Lim *et al*, 1997). The manufacturers KHD and Krupp Polysius have since developed different types of roll surfaces to suit

these abrasive ores. Figure 2-2 shows examples of the roll surfaces of the HPGR. The wear rate is reduced due to the lower slip and extrusion effects on the roll surface compared to the previously used smooth rolls (Daniel and Morrell, 2004; Lim and Weller, 1998). The improvements in the roll design and materials of construction have lead to favourable increases in HPGR installations in the minerals industry (Daniel and Morrell, 2004). Of these, two significant installations have been pioneered in platinum comminution circuits (Rule *et al*, 2008).

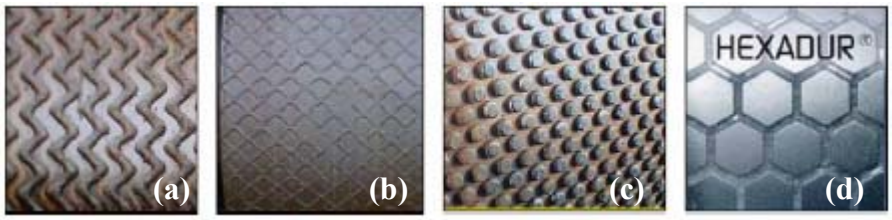

Figure 2-2: Roll surface patterns: welded (a), chevron (b), studded (c) and hexadur (d) (Daniel and Morrell, 2004)

The HPGR consists of two counter rotating rolls; one is fixed while the other known as the floating roll is movable as illustrated in Figure 2-3 (Napier-Munn *et al*, 1996). The floating roll is connected to a hydro-pneumatic spring system which applies a force on the roll which in turn applies a force on the ore being ground. The feed is choke-fed into the HPGR through a hopper situated above the rolls. The feeding mechanism and the rotating rolls allow for continuous rather than batch processing of the ore. The ore being crushed experiences a compression force as it passes between the two rolls. As a result, the compressed bed experiences high inter-particle stress which in turn causes breakage along zones of structural weakness (Ntsele and Sauermann, 2007). The force applied on the movable roll and the gap between the rolls can be manipulated in order to optimise the operating conditions.

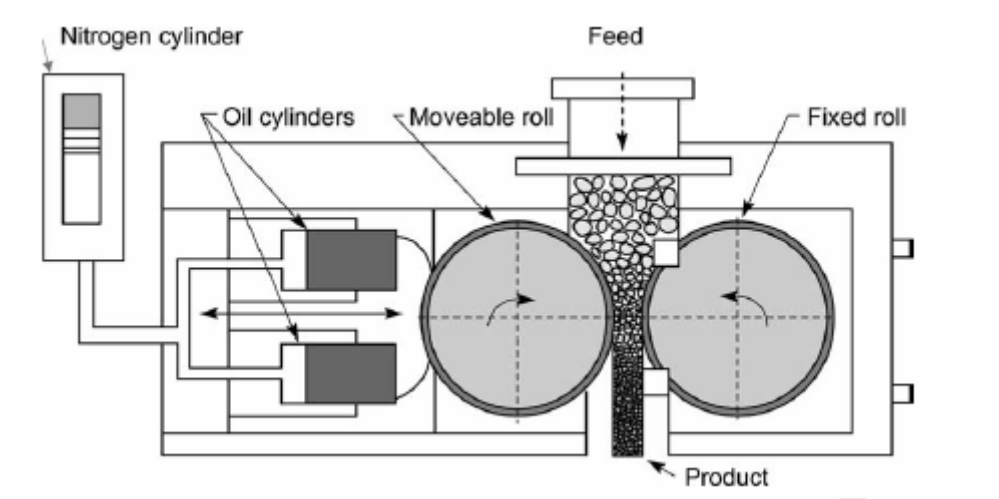

Figure 2-3: Schematic diagram of the HPGR (Napier-Munn *et al*, 1996)

Lim and Weller (1998) described three zones that exist between the rolls of the HPGR as ore is being crushed (Figure 2-4). The first zone known as the acceleration zone is where the ore is pulled downwards due to gravity. Particles larger than the gap between the rolls are nipped in this zone at a nip angle α_c and are pre-broken before entering the second zone known as the compression zone. The beginning of the compression zone is denoted by x_c where particles are nipped and broken by high compressive forces. The compression force reaches its maximum at an angle α_{max} located slightly above the axis of the rolls. The compression force is quickly reduced to zero in the third zone known as the relaxation zone. This is where the flakes formed in the compression zone expand due to the release of pressure. Extrusion effects occur in the relaxation zone where the volumetric expansion causes the flake to travel faster than the rolls speed. The extrusion of hard minerals such as quartz may cause the packed bed to abrade the rolls surface. Figure 2-5 shows how the pressure varies at the different zones between the rolls (Lim and Weller, 1998).

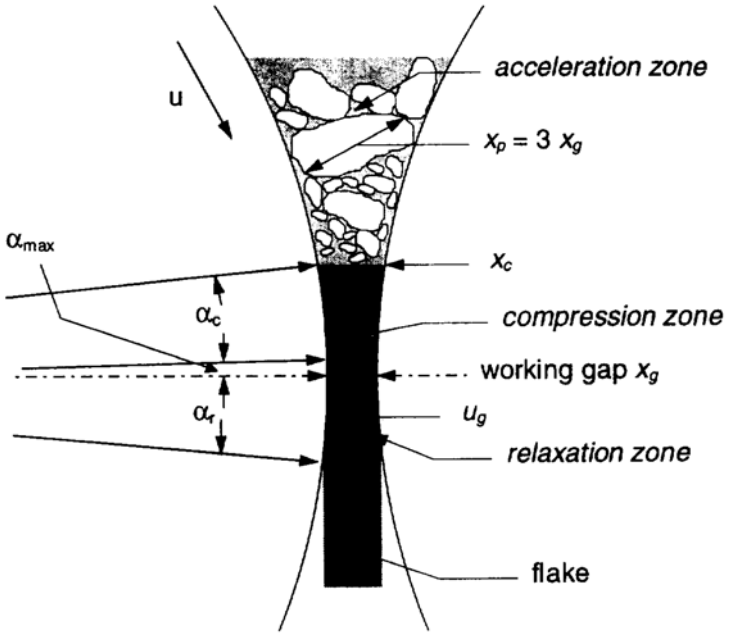

Figure 2-4: A schematic diagram of the three zones between the HPGR rolls (Lim and Weller, 1998)

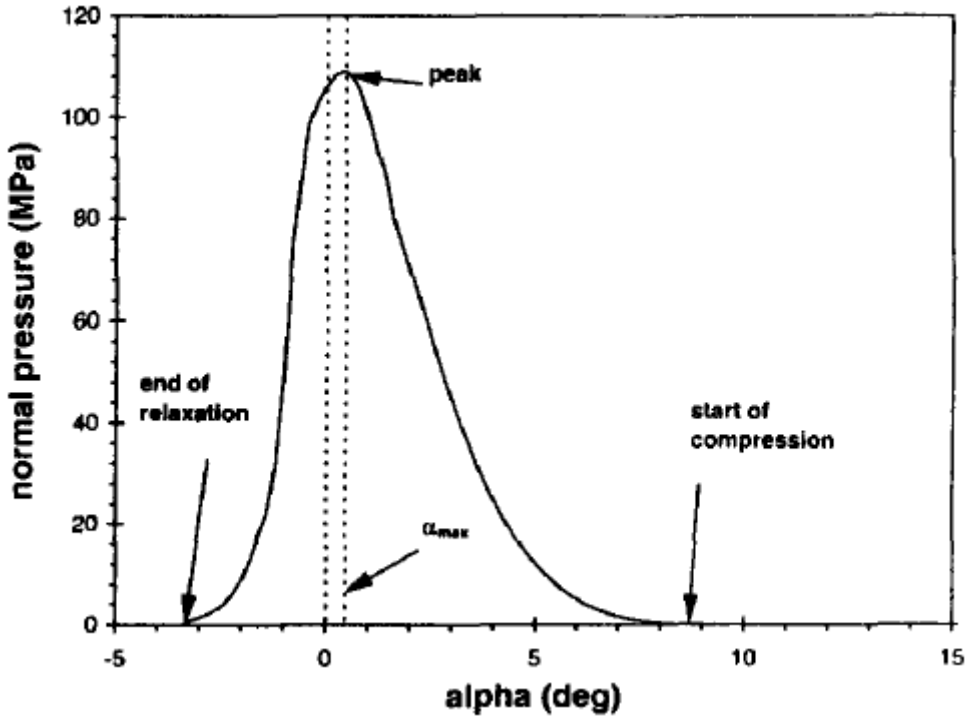

Figure 2-5: Variations in pressure at the different zones between the rolls of the HPGR (Lim and Weller, 1998)

Other zones between the HPGR rolls described by Van der Meer and Gruendken (2009) are known as the edge and centre zones (Figure 2-6). The HPGR product consists of 80 – 90% centre material from the zone of highest pressure between the rolls. The edge zone consists of product from the low pressure zones along the rolls as shown in Figure 2-6. The edge product is coarser and is closer to the feed size distribution. In some operations, a splitter is installed to separate the edge from the centre zone product. The centre material is taken as the final product while the edge zone is recycled for further breakage. A portion of the centre zone product is sometimes recycled to assist in the generation of more fines (Van der Meer and Gruendken, 2009).

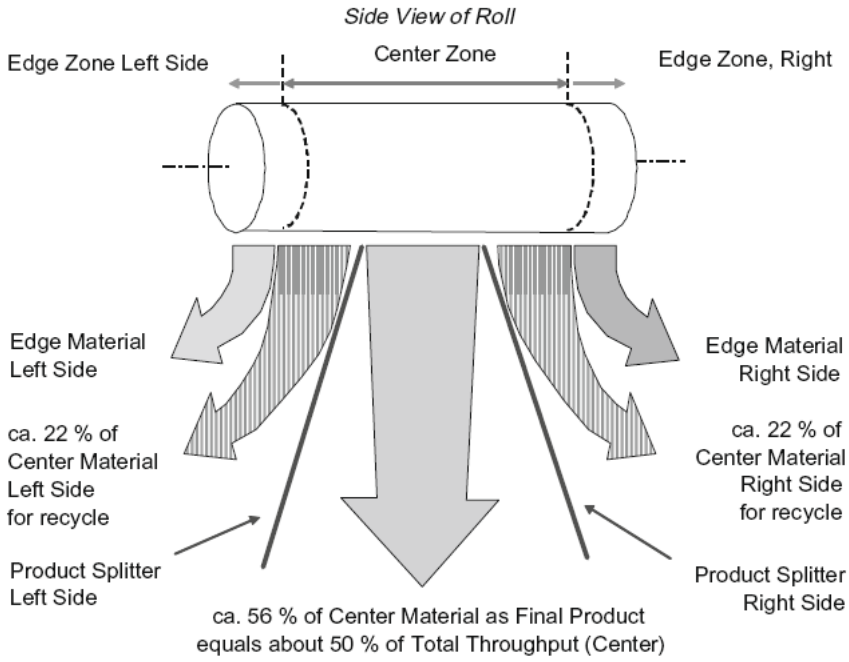

Figure 2-6: Edge and center zones of the HPGR (Van der Meer and Gruendken, 2009)

The flakes formed in the compression zone have a density in the range 70 – 85% by volume (Klymowsky *et al*, 2002). The size and stability of these flakes is dependent on the operational variables of the HPGR and the ore characteristics. Therefore, depending on the hardness of the flakes, a de-agglomeration stage is sometimes required in comminution circuits to break the flakes that have been formed before going on to subsequent processing stages (Aydoğan *et al*, 2006).

Part of the attraction of the HPGR to the minerals industry was due to the potential to preferentially liberate valuable minerals. Several studies have shown some improvements in mineral liberation with the application of the HPGR compared to other comminution devices such as the rod/ball mills. These studies have been performed on ore such as the diamond, coppers and cement (Celik and Oner, 2006; Tavares, 2005; Ntsele and Sauermann, 2007). Other studies on the other hand, have found this to be untrue particularly at the finer size fractions below 150μm (Shi *et al*, 2006; Daniel, 2007). For studies that have shown improvements in mineral liberation, this has been attributed to the different breakage mechanism applied by the HPGR compared to other comminution devices. The following section describes the different breakage mechanisms that exist and how those applied by the HPGR differ from those applied by conventional comminution devices.

2.2.1 Breakage mechanisms of the HPGR

The breakage mechanisms that can be achieved by applying different comminution devices include single particle, particle bed compression and random impact breakage as shown in Figure 2-7 which was adapted from Patzelt *et al* (1997). In single particle breakage, a particle experiences a force from the comminution device. When the force experienced exceeds the strength of the particle, fracturing occurs at the points of contact between the particle and the comminution device as explained and shown by Viljoen *et al* (2001) in Figure 2-8. The fractures propagate roughly along the line joining the points of contact between the particle and the device. Further application of the force causes more breakage known as secondary breakage, which results in the formation of coarse and fine particles (Figure 2-8). Comminution devices such as the roll crusher apply this breakage mechanism.

A similar breakage mechanism is obtained with random impact breakage however, the force applied is greater and hence more fines are produced. Tumbling mills such as the ball, rod and AG/SAG mills apply this kind of breakage. Particles experience impact from the grinding media and the mill shell.

In particle bed compression, a particle experiences the initial breakage similar to that of the single particle breakage case. However as the force applied is increased, the product from the fractured particle is shielded by surrounding particles and the voids between the particles, preventing further breakage. If the force is further applied and the bed has been compressed to an extent where the voids between the particles have been filled, the product formed from the initial fracture experiences secondary breakage shown in Figure 2-9 (Viljoen *et al*, 2001). The HPGR applies this type of breakage mechanism.

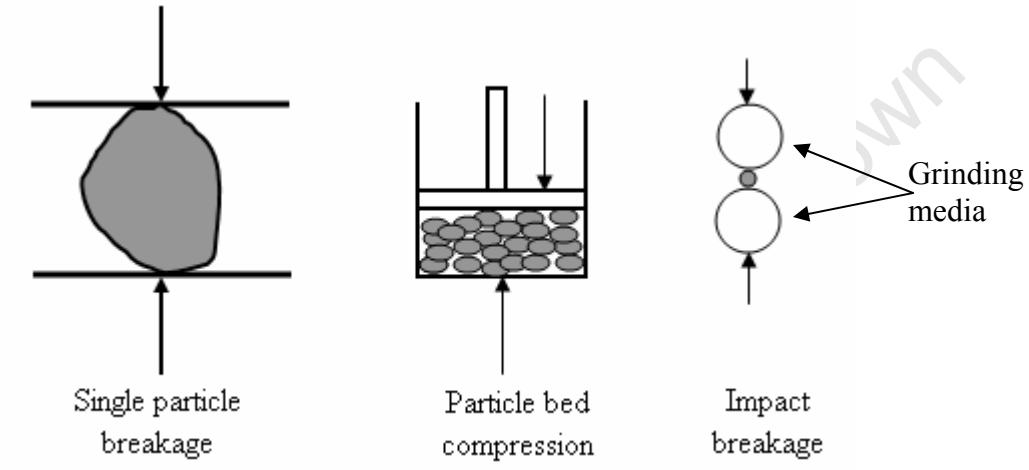

Figure 2-7: Breakage mechanisms applied in comminution (Patzelt *et al*, 1997)

Viljoen *et al* (2001) suggest that conditions that would minimise over-grinding due to secondary fracture include:

- the use of particles to shield primary breakage fragments
- the limitation of the applied force such that secondary fracture is prevented
- maximising the porosity of the bed

The application of the HPGR could potentially result in the fulfilment of the above characteristics due to the type of breakage mechanism it applies. However this is dependent on variables such as the HPGR settings and the ore characteristics which are discussed in section 2.2.3.

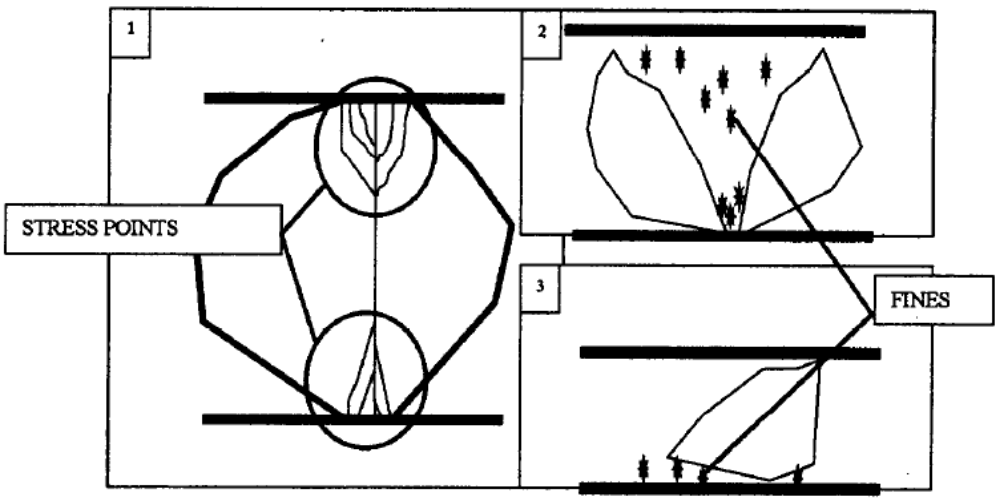

Figure 2-8: Effects of single particle breakage (Viljoen *et al*, 2001)

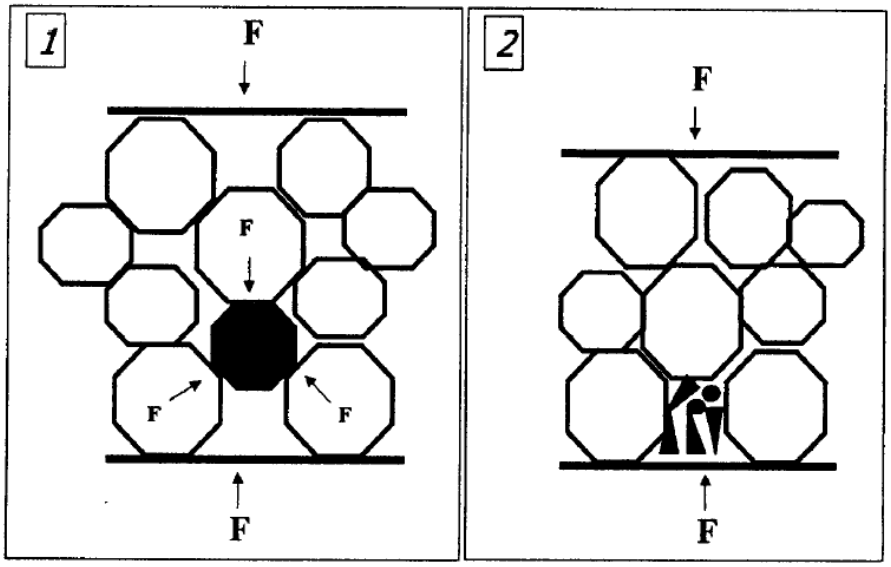

Figure 2-9: Effect of particle bed compression (Viljoen *et al*, 2001)

During compression with the HPGR, micro-cracks are formed on the particles in the particle bed. The particles fracture along zones of structural weakness causing different types of breakage and these are shown in Figure 2-10, an adaptation of the image by Daniels (2007). Inter-granular, trans-granular, and preferential mineral breakages are some of the types of breakages that occur in HPGR applications. In trans-granular breakage, the cracks propagate across different phases of minerals, resulting in breakage

across grain boundaries as shown in Figure 2-10. In inter-granular breakage, the cracks propagate within a particular mineral causing structural weakening of the mineral. In preferential mineral breakage, breakage occurs along grain boundaries, resulting in the separation of different mineral phases. It is due to the latter type of breakage that it is believed that the HPGR has the potential to improve mineral liberation.

In terms of energy efficiency, single particle breakage is the most energy efficient due to the direct energy transfer from the breakage device to the particle (Fuerstenau and Kapur, 1995). Random impact breakage is the most energy inefficient of the three due to the uncertainty of a particle experiencing an impact force from the grinding media (Fuerstenau and Kapur, 1995). In particle bed compression, not all the particles experience direct energy transfer from the device. Energy is transferred only to the particles that are in direct contact with the device which then transfer energy to the other particles in the bed.

Figure 2-11 shows the difference between particles obtained from the HPGR and a conventional crusher (Klymowsky *et al*, 2002). The particle obtained from the HPGR looks more fragile compared to that obtained from the conventional crusher. The weakening of the ore body due to compression breakage results in reduced energy requirements for subsequent grinding (Tavares, 2005). Therefore due to the breakage mechanism applied by the HPGR, benefits such as reduced energy consumption in subsequent grinding processes can be experienced. However this is dependent on the circuit configurations and the ore type. The following section discusses the various circuit configurations in which the HPGR is applied in industry and the benefits that have been realised.

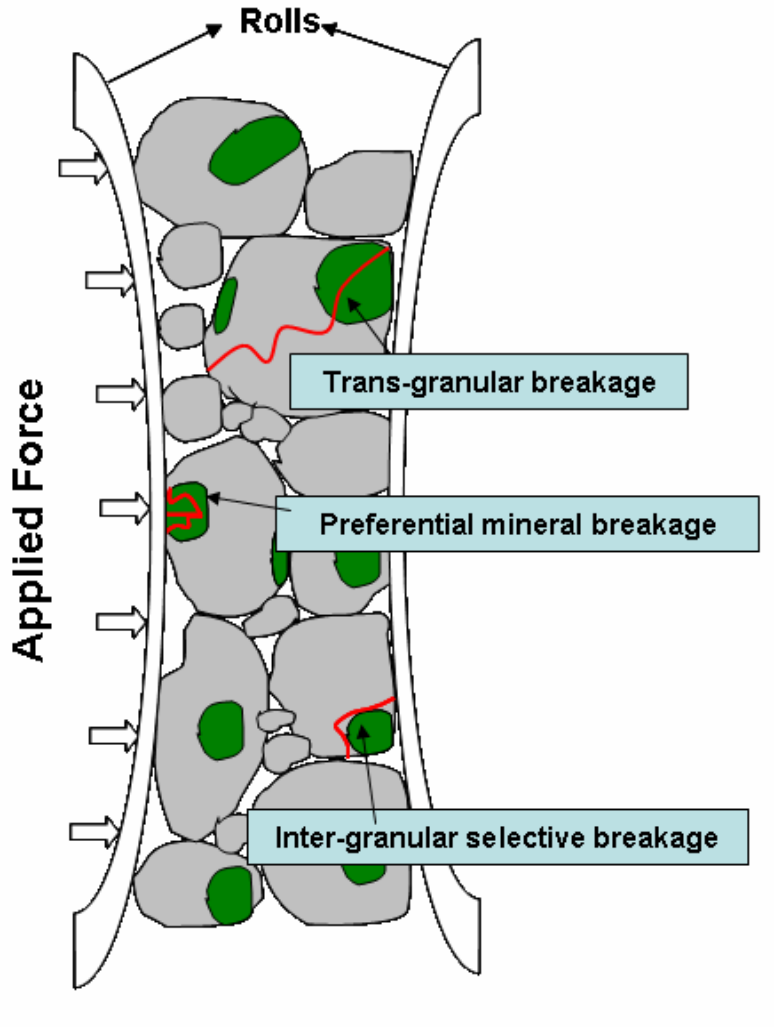

Figure 2-10: Cracks formed due to compression breakage applied by the HPGR (Daniels, 2007)

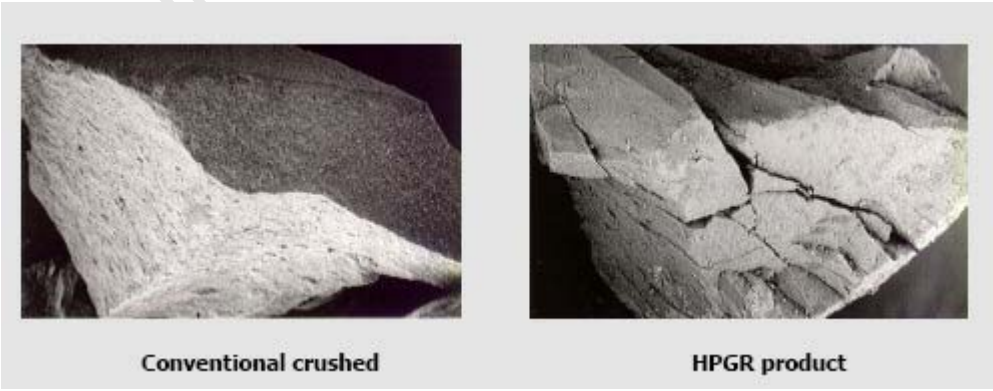

Figure 2-11: Micro-cracks formed from the application of the HPGR compared to the application of the conventional crusher (Klymowsky *et al*, 2002)

2.2.2 Application of HPGR in various circuit configurations

As part of the objectives of this work, the determination of the benefits of the application of the HPGR in existing platinum processing circuits is essential. As previously mentioned one of the main aims of platinum processing plants is to improve throughput and reduce energy consumption (Rule *et al*, 2008). Therefore, this section reviews some of the HPGR circuit configurations that have been applied and their advantages and disadvantages.

HPGR configurations

Patzelt *et al* (1995) discussed the use of the HPGR in different comminution circuit configurations for a gold leaching plant. Figure 2-12 shows the three categories of the HPGR applications that were discussed. The one pass grind application exposes the ore to a single pressure and is suitable for pre-grinding the ore with the use of the HPGR to increase the capacity of a plant Figure 2-12(a). Other benefits include minimized power consumption and improved recovery.

For the multiple pass grinding application (Figure 2-12(b)), the ore is exposed to more grinding energy where some of the product from the previous pass is recycled to the HPGR. The fines from the recycled feed are meant to promote the generation of more fines. However, there have been contradictions as to weather the presence of fines in the feed is beneficial in HPGR applications. Viljoen *et al* (2001) recommend that the fines be removed as they are formed so as to avoid over-grinding the material. Aydoğan *et al* (2006) on the other hand found that the recycled feed assisted in the generation of more fines which was desirable for cement applications. Therefore, how the HPGR is applied in any comminution circuit is dependent on the desired outcomes of the mineral processing plant.

The multiple pass grinding with screening application (Figure 2-12(c)) is applied in circuits where the downstream process requires a maximum particle size. Several comminution circuits such as the Phoenix and Boddington projects apply the HPGR in

this configuration (Siedel, *et al*, 2006). The results obtained from these projects are discussed later in this section.

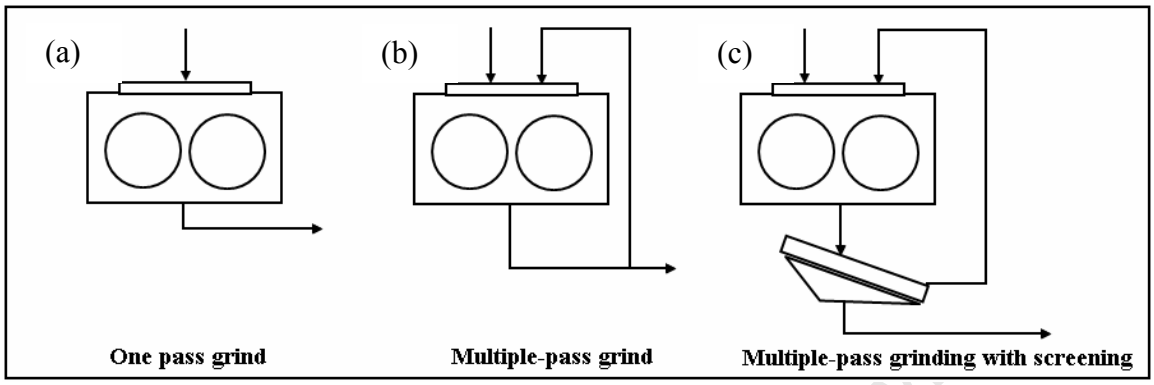

Figure 2-12: HPGR applications in comminution circuits (Patzelt *et al*, 1995)

Patzelt *et al* (1995) found that the benefits that come with the application of the HPGR are ore specific. The one pass and the multiple pass grinding were suitable for more brittle ores, while ore types with excessive slimes required wet screening. Other circuit configurations have been applied on different ore types such as diamond, iron, copper and platinum ores. These can be considered to be a variation of the three main applications that have been discussed so far. Morley (2006) discusses the different flowsheets for HPGR applications.

HPGR circuit configuration aims

Morley (2006) categorises the different HPGR circuit configurations according to the desired outcome of a particular plant. Four main outcomes which include:

- energy efficiency,
- debottlenecking,
- metallurgical performance and
- differential comminution

The different variations of the circuit configurations described by Morley (2006) for energy efficiency improvements can generally be described as multiple pass grinding

with screening shown in Figure 2-12. The shortcomings that are associated with this application include accelerated wear rates of the roll surface due to the processing of truncated feed particularly with respect to more abrasive ores. However, this could be accommodated through the recycling of the fines produced. Dust is also a major challenge with this application as dry grinding is typically applied with the HPGR. The addition of wet screening was introduced to the HPGR product to alleviate this problem.

The main aim for debottlenecking is to improve the overall throughput of a comminution circuit. To achieve this outcome, the HPGR is typically applied in the one pass grind application (Morley, 2006). Bottlenecking is characteristically a problem in circuits that apply the AG/SAG mills due to a build up of a critical size in the mill (Patzelt *et al*, 2001). The addition of the HPGR to AG/SAG circuits showed improvements such as increased throughput and reduced power consumption in plants processing iron ores. However, a consequence of the addition of the HPGR was the requirement for more equipment which made the process more complicated with higher capital costs (Patzelt *et al*, 2001; Siedel *et al*, 2006). As such, the elimination of the AG/SAG mill by replacing it with the HPGR was considered. Higher fines content, increased grinding capacity in ball mills and a reduction of the work index of the ore are some of the benefits that have been realised with this circuit configuration. It was these benefits that were realised in a Chilean iron ore mine that resulted in the renewed interest of the HPGR in gold and copper processing plants (Patzelt *et al*, 2001).

The third outcome for HPGR application discussed by Morley (2006) is enhanced metallurgical performance. For this application, edge recycle is preferred to screening as it is less complex and less costly. During HPGR operation, the particle bed experiences a higher force in the middle of the rolls. As a result, the middle product is finer than the edge product. The edge product is thus recycled to ensure enhanced breakage is achieved. Very few studies have been found that apply this HPGR configuration in existing comminution circuits. However, benefits such as better leach rates and recoveries are expected with this configuration (Morley, 2006).

The fourth outcome for HPGR application is for differential comminution in which the breakage mechanism is of particular interest for processing. Preferential liberation of targeted minerals is more efficient with the HPGR than with conventional comminution devices such as the ball mill. Benefits of the HPGR in this regard have been observed for ore types such as diamond and gold ore containing nuggets. This preserves the particle shape of the targeted mineral particularly in diamond processing (Morely, 2006; Ntsele and Sauermann, 2007).

The aim of each of the circuit configurations discussed above is mainly to improve energy consumption, increase throughput, improve effects on downstream processes such as leaching and improve mineral liberation, respectively. Although a plant may be looking to achieve a certain objective, there is some overlap that occurs in the outcomes that are achieved. However, both authors Patzelt (1995) and Morley (2006) have similar comminution configurations that can be described under the same headings: one-pass grind, multiple-pass grind and multiple-pass grind with screening. The following section gives a description of where some of the circuit configurations discussed above have been applied and the outcomes.

HPGR circuit configuration applications

In a study performed by Aydoğan *et al* (2006), several cement grinding circuit configurations applying the HPGR were tested to determine the effects on size distribution, size reduction and specific energy consumption. Table 2-2 shows the circuit configurations for the different case studies performed. Tests were performed with the HPGR in open and in closed circuits with some case studies consisting of a recycle stream. Hybrid grinding tests were performed where the HPGR was applied on a cement sample prior to ball milling.

Table 2-2: Case studies analysed at different HPGR circuit configurations for cement (Aydoğan *et al*, 2006)

Case	Configuration
Case study 1	Open circuit HPGR – closed circuit ball milling
Case study 2	Open circuit HPGR with partial recycling – closed circuit ball milling
Case study 3	Hybrid grinding
Case study 4	Closed circuit HPGR – closed circuit ball mill grinding
Case study 5	Semi-finish grinding

The findings from this study indicate that the circuit configuration has an impact on the specific energy consumed by the HPGR. Therefore the differences in circuit configurations such as open or closed circuit, circulation load ratio and feed size distributions can affect the specific energy consumed by the HPGR. Aydoğan *et al* (2006) found that as the amount of work put in by the HPGR increased, the overall specific energy of the comminution circuit decreased. For closed circuit applications of the HPGR, significantly higher reduction ratios (F_{80}/P_{80}) were obtained compared to the open circuit cases. The open circuit applications (case studies 1 and 2) had reduction ratios of 4.4 and 3.5 respectively while the closed circuit applications (case studies 4 and 5) had reduction ratios of 308.2 and 242.5 respectively.

The general findings from the study performed by Aydoğan *et al* (2006) were:

- improved capacity particularly for open circuit hybrid configurations
- substantial energy savings for closed circuit HPGR configurations
- the addition of the HPGR to existing cement plants would significantly change the feed size of the ball mill circuit which would require optimisation of the ball mill circuit to ensure full advantage of the HPGR addition is realised.

Norgate and Weller (1994) investigated the effects of converting from single-stage to a multi-stage HPGR circuit configuration on zinc and gold ores. One-pass tests with screening were performed with the HPGR as a pre-grinding stage to a ball mill in open and in closed circuit. Table 2-3 shows some of the results that were obtained in this study.

Table 2-3: Summary of specific energies consumed for open and closed HPGR application at different specific forces (Norgate and Weller, 1994)

	Open circuit		Closed circuit	
Specific grinding force (Nmm^2)	2.76	10.10	2.76	10.10
P_{80} (μm)	75	75	75	75
HPGR (kWh/t)	2.4	9.6	2.4	9.6
Ball Mill (kWh/t)	16.9	12.7	15.6	12.2
Overall specific energy	**19.3**	**22.3**	**18.6**	**21.8**

No significant difference in overall specific energy consumption was obtained when comparing the open circuit to the closed circuit configuration. However, a 15% and 21% increase in overall specific energy was observed when changing from low ($2.76N/mm^2$) to high ($10.1N/mm^2$) specific force for the open and closed circuit configurations, respectively. These results are contradictory to the results obtained by Aydoğan *et al* (2006) who found that substantial savings were obtained for the closed circuit application compared to the open circuit application. This could be as a result of the differences in material characteristics being tested. Djordjevic and Morrison (2006) suggest that the experience gained from the cement industry in terms of HPGR applications is not considered likely to be representative of the behaviour of hard ores such as those processed in the minerals industry.

Siedel *et al* (2006) performed comparative studies between the SAG and ball mill circuit known as SABC and a crusher/HPGR/ball mill circuit on two low grade gold/copper processing plants known as the Phoenix and Boddington projects. For both projects, the HPGR was applied in the multiple pass with screening method. However, the Boddington project included wet screening of the HPGR product. In terms of power requirements, the crush/HPGR/ball mill circuit of the Phoenix project was 15% less than that of the corresponding SABC circuit. However, the overall power requirements for the HPGR circuit was an insignificant 2% less than the SABC circuit. Higher capital costs (35%) were experienced with the HPGR circuits due to more equipment requirements. The operating costs on the other hand were 5% less for the HPGR circuit. However this was

not enough to offset the capital costs. Therefore, for the Phoenix project, the SABC was chosen over the HPGR circuit. For the Boddington project on the other hand, the HPGR circuit was chosen because the capital costs were only 7% higher and the operating costs were 12% lower than those obtained with the SABC circuit. However, some operations may consider the differences in capital and operating costs between the HPGR and SABC circuits to be insignificant due to plant instability as a result of throughput variations. Table 2-4 is a summary of the project outcomes.

Oestreichner and Spollen (2006) performed a similar feasibility analysis for the Los Bronces expansion on different quartz containing ores with varying hardness. It was also found that while the capital costs associated with the HPGR circuit were 17% higher than the SABC circuit, the operating costs were 20% lower. However, further feasibility studies were still in progress for this project.

Table 2-4: Summary of results showing the effect of the application of the HPGR circuit compared to the SABC in the Phoenix and Boddington projects (Siedel *et al*, 2006)

Quantity	Phoenix project	Boddington project
Design power	15% less	14% less
Overall power	2% less	5% less
Capital costs	35% more	7% more
Operation costs	5% less	12% less
Circuit chosen	SABC	HPGR

Rule *et al* (2008) discussed the benefits of the installation of a full scale HPGR (950mm diameter x 650mm width) at the Northam Platinum UG2 plant. Some of the desired objectives from this installation were improved throughput, reduced operation costs, reduced energy consumption, increased PGM recovery and reduced chrome content in the concentrate. The circuit configurations tested were rod mill, HPGR/rod mill and HPGR/ball mill. The desired outcomes were realised and are summarised in Table 2-5 for the comparison between the HPGR/rod and HPGR ball mill configurations. Although the

results obtained were preliminary, the throughput obtained surpassed design capacity and a 20 – 30% decrease in specific energy was achieved. For a Platreef processing plant (Mogalakwena North) also discussed by Rule *et al* (2008) it was found that there was an increase in primary flotation recovery from 77.8% to 81.6% when the HPGR/rod and HPGR ball mill circuits were compared. The HPGR was applied in the one pass configuration at the Northam UG2 plant while at Mogalekwena North the HPGR was applied in the multiple pass with screening configuration.

Table 2-5: Initial results obtained from the comparison of the HPGR/rod and the HPGR/ball mill circuits at the Northam UG2 plant (Rule *et al*, 2008)

Quantity	Initial result
Throughput	Increased to 160tph, beyond design capacity (150tph)
Total energy consumption	20 – 30% lower
Grind	42% passing 75µm (increased from 22% passing 75µm)
PGM recovery	84% (4% increase)
Chrome content	Lower (1.9%) chrome content in final flotation concentrate

This section pointed out the different HPGR circuit applications and configurations. The effects of the different comminution circuit configurations on throughput, specific energy consumption, size distributions and reduction ratios were shown. However, a key variable that has not been discussed is the effects on mineral liberation. Reported improvements in recovery such as that by Rule *et al* (2008) is not evidence that preferential mineral liberation has occurred. Factors such as the generation of a finer grind have an effect on the liberation properties of any material. Therefore, part of the objective of this study is to determine if preferential PGM liberation can be obtained with the application of the HPGR. The effect of the HPGR on mineral liberation in previous studies is discussed in section 2.2.6.

In addition to circuit configuration during performance optimisation of plants applying the HPGR, changing the variables of the HPGR play a significant roll. The following

section gives an overview of the different HPGR variables and how they affect energy efficiency, throughput and size reduction.

2.2.3 HPGR variables

The following HPGR variables have effects on throughput, specific energy, size reduction and mineral liberation.

- Pressure (bar)
- Zero gap (mm)
- Rolls speed (m/s)
- Rolls surface pattern – shown in Figure 2-2
- Feed characteristics

While literature has shown that the rolls speed and the rolls surface pattern have significant effects of throughput and the size reduction achieved are not part of this study. Therefore this section only discusses the variables that are relevant to this study.

Pressure (bar)

According to Klymowsky *et al* (2002), the grinding pressure controls the product fineness and can be quantified by various parameters one of which is the specific grinding force. The specific grinding force, F_{sp} (equation 1) can be used for establishing correlations between grinding pressure, the particle bed and the achievable product fineness. It is also used for comparing the grinding force between HPGR of different sizes. The grinding force, F is in turn related to the grinding pressure and the cross-sectional area of the piston in the hydraulic system (equation 2). In this work, the roll dimensions were kept constant therefore the pressure will be used and not the specific force as is typically done in most studies. The pressure effects are discussed in section 2.2.4.

$$F_{sp} = \frac{F}{1000 * L * D} \quad (1)$$

$$F = P * \pi * d^2 \quad (2)$$

Where P = grinding pressure (bar)

d = diameter of hydraulic spring system (dm)

F_{sp} = specific grinding force (N/mm^2)

F = grinding force (kN)

L = roll width (m)

D = roll diameter (m)

Zero gap

The zero gap is the distance between the rolls of the HPGR that is set prior to operation. There have been very few published studies that have investigated the effect of the zero gap in HPGR applications. The gap setting could play a roll in throughput, specific energy consumption and size distribution. Therefore, this HPGR variable has been considered in the investigation of the effects on platinum bearing ores in this work.

Feed characteristics

The feed characteristics play a major roll in the outcome of any comminution circuit (Hosten and Cimilli, 2009; Kylymowsky *et al*, 2002). Feed characteristics such as top size, size distribution, hardness and mineralogical characteristics have been considered in this study. The effects of the feed characteristics have been discussed in section 2.2.7.

2.2.4 Pressure effects

In this section, the effects of pressure on throughput, size distribution, specific energy, size reduction and mineral liberation presented in literature have been discussed.

Throughput

Several studies have been performed that determine the effect of the HPGR variables on throughput (Lim *et al*, 1997; Lim and Weller, 1998; Lubjuhn and Schönert, 1993). While the rolls speed and surface pattern are not of interest in this study, they are the most influential variables on HPGR throughput. Lubjuhn and Schönert (1993) and Klymowsky *et al* (2002) have shown that the pressure or the specific force have a limited effect on throughput for various ore types such as quartz, limestone, iron, gold and kimberlite. Slight decreases in throughput with increasing pressure were observed. This is consistent with results obtained by other authors such as Lim *et al* (1997), Austin *et al* (1993), Schönert (1988), Brachthäuser and Kellerwessel (1988). However, it was found that if the feed to the HPGR is moist and has high fines content, then the decrease in throughput with increasing pressure was greater (Klymowsky *et al*, 2002).

The working gap is the distance between the rolls during HPGR operation. As the pressure increases, the working gap between the rolls decreases. As a result, the bulk density of the material passing through the gap increases. This implies that the separation of the rolls at the critical angle (α_c) is less so the material is pulled in between the rolls at a slower rate (Austin *et al*, 1993). Therefore, if all other variables are kept constant, the variation of the gap between the rolls during operation can be assumed to have a direct effect on the throughput. This can be confirmed by equation 3 which relates the throughput to HPGR variables rolls speed (u), diameter (L) and length (D). If the variables u, L, and D are kept constant, the changes in throughput can be attributed to changes in the material specific gravity multiplied by a dimensionless factor m known as the specific throughput. The specific throughput is used when comparison between HPGRs of different scales or are being made (Lim and Weller, 1998). In this thesis, the scale and rolls speed will be kept constant so the specific throughput will not be used.

$$m = \frac{M}{\rho u L D} \tag{3}$$

Where m = specific throughput (dimensionless)

M = throughput (t/h)

ρ = material specific gravity (t/m^3)

u = rolls speed (m/s)

L = width of the rolls (m)

D = diameter of the rolls (m)

Lim and Weller (1998) used the specific throughput to compare the effects of HPGR scale at different operating conditions, ore types and feed size. The results showed that the studded rolls always had higher specific throughputs regardless of the ore type. An increase in specific throughput of approximately 11% was observed at a low specific grinding force of $1.6N/mm^2$ and at constant rolls speed of 0.38m/s for the smooth rolls. However, the effects of feed top size showed decreasing throughput as the specific grinding force increased at a rolls speed of 0.38m/s for smooth rolls.

Product Size distributions

Shi *et al* (2006) showed the difference in size distribution between product obtained from an HPGR and from a roll crusher (Figure 2-13). It can be seen that broader size distributions with higher fines content was produced from the HPGR compared to the roll crusher. This is proposed to be due to the difference in breakage mechanisms applied by the two devices (Klymowsky *et al*, 2002; Palm *et al*, 2009). The HPGR applies inter particles breakage while the roll crusher applies single particle breakage. The differences in design and feeding mechanism of the HPGR that allow for the dynamic roll are the main causes of the differences in breakage mechanisms. The roll crusher has a pre-set, fixed working gap where particles that are finer than the working gap can go through unbroken. The HPGR on the other hand is choke-fed and the working gap changes during operation. Therefore, particles that are finer than the gap between the rolls also experience compression forces and can be reduced further.

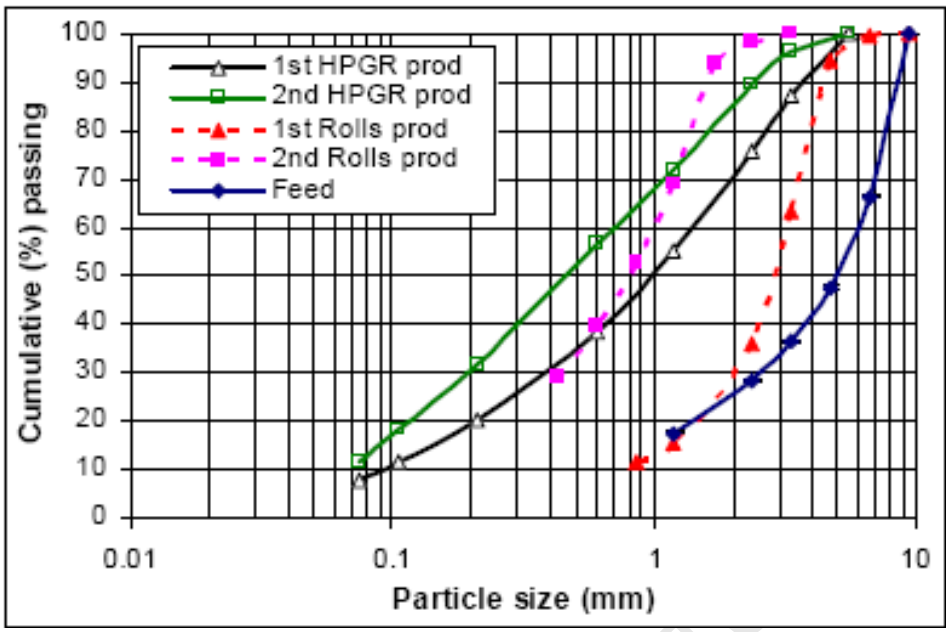

Figure 2-13: Comparison of size distributions of HPGR products with conventional crusher product (Shi *et al*, 2006)

Pressure plays a significant roll in the product size distribution obtained in HPGR applications. Lim *et al* (1997) found that while the shape of the product size distribution did not change with an increase in the specific force applied, the product became finer. Similar results were obtained by Schönert (1988) for quartz. Klymowsky *et al* (2002) found that continued increase in the specific force resulted in increasing fineness of the product until a point was reached where no further reduction of the ore can be achieved. This effect was observed on ores such as phosphate, copper and kimberlite. The point where no further reduction could be obtained regardless of the specific force applied is known as the saturation point. This point coincides with the maximum specific energy that can be applied on a particular ore type after which it becomes energy inefficient to apply the HPGR (Klymowsky *et al*, 2002).

Specific Energy (kWh/t)

The specific energy consumed for any ore type is related to the applied specific grinding force. Linear relationships between the specific energy and the specific force were obtained for iron, gold and kimberlite ores for a specific force range of 1 – 7N/mm^2

(Klymowsky, 2002). Similar results were obtained by Norgate and Weller (1994) for gold and zinc ores for specific forces in the range 2 – 12N/mm^2. However, non linear relationships were observed by Lim *et al* 1997 and Schönert (1988) for gold and quartz, respectively. These relationships have become non-linear due to the requirement of the specific energy to reduce to zero at zero specific force Schönert (1988).

Fuerstenau *et al* (1991) developed a relationship (equation 3) for the HPGR which relates the size reduction ratio (F_{50}/P_{50}) to the specific energy consumption. The reduction ratio is based on the product (P_{50}) and feed median sizes (F_{50}). It was found that for the specific ore types that were tested, a linear relationship between the reduction ratio and the specific energy consumed was obtained. However, this was tested over a short range of specific energies (1 – 4N/mm^2). Further testing of this equation on different ore types by Norgate and Weller (1994) for a wider range of specific energies showed that a more suitable fit was the power law represented by equation 4. Constants k and b are ore dependent, however there have been no tests that quantify these constants as has been done for the constants in the Bond equation for different ore types.

$$\frac{F_{50}}{P_{50}} = kE + c \tag{4}$$

$$\frac{F_{50}}{P_{50}} = kE^b + c \tag{5}$$

where F_{50} is 50% cumulative passing size of feed

P_{50} is 50% cumulative passing size of product

E is the specific grinding energy (kWh/t)

c is a constant that is theoretically equal to unity

k and b are ore dependent constants

Application of equation 4 shows increasing specific energy consumed with increasing reduction ratio. Lim *et al* (1996) applied equation 4 on different ore types for different rolls speeds. The results suggest that it was more energy efficient to operate the HPGR at

lower specific grinding energies because the reduction ratio increased linearly at lower specific energies. Further increases in specific energies resulted in a non-linear relationship with decreasing slopes. Apling and Bwalya (1997) also suggest that it is preferable to operate the HPGR at lower intensities because inter-granular breakage is more likely to occur whereas at higher intensities, more random breakage occurs.

Norgate and Weller (1994) found that larger reduction ratios could be obtained if the HPGR were applied as a multi-stage operation at low specific energies as opposed to a single stage operation at higher specific forces. A gold ore was exposed to four passes in the HPGR at a specific force of 3N/mm^2. The results obtained from these tests were compared to single pass tests of the same ore type at varying specific forces up to 12N/mm^2. Figure 2-14 shows the results that were obtained. Although the linear model applied did not fit well to the multi-pass data, it is apparent that greater reduction ratios can be obtained with the application of the HPGR as a multi-stage operation.

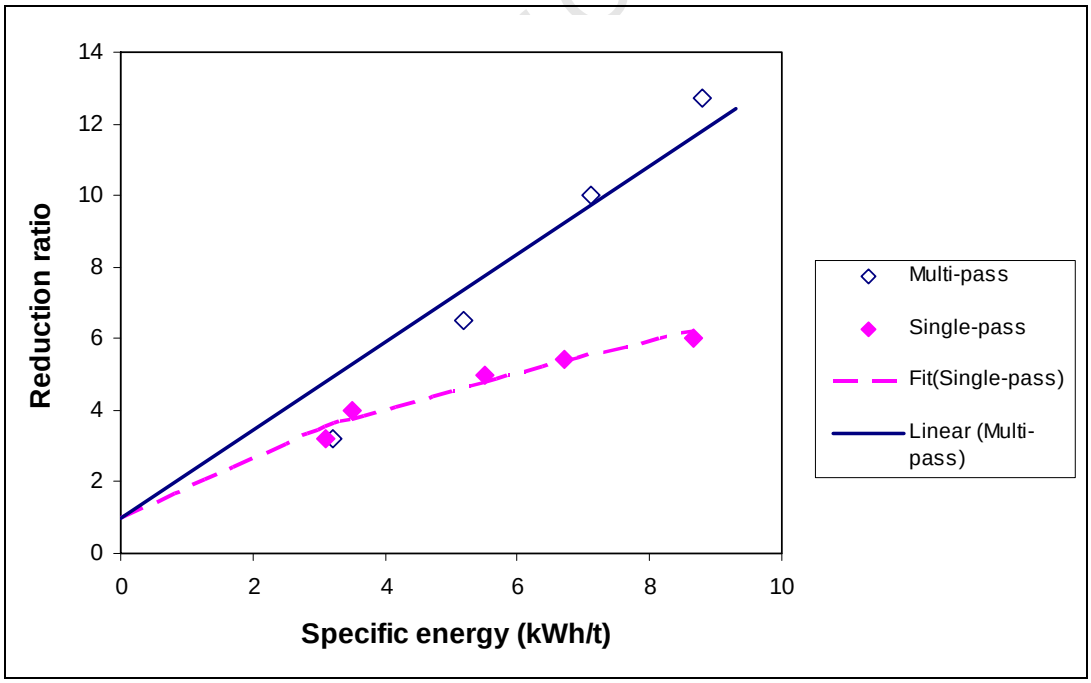

Figure 2-14: Specific energy-reduction ratio relationship for multi-pass and single-pass HPGR applications on a gold ore (Norgate and Weller, 1994)

Further tests performed by Norgate and Weller (1994) to determine the energy consumption of the ball mill when multi-stage and single stage products were ground. The results obtained are presented in Table 2-6 for a gold ore. It was found that multistage operation of the HPGR at low specific grinding forces did not change the overall specific energy of the circuit when compared to a single stage application at higher specific force (7.7N/mm^2).

Table 2-6: Energy consumed by ball mill when multi-stage and single stage product was ground (Norgate and Weller, 1994)

		Multi-stage	Single-stage
High pressure grinding rolls			
Specific grinding force	(N/mm^2)	3.0	7.7
P_{80} rolls product (um)	(μm)	3980	3980
Specific energy - rolls 1	(kWh/t)	2.5	5.6
- rolls 2	(kWh/t)	1.7	
- total	(kWh/t)	4.2	
Ball Mill			
Bond Work Index	(kWh/t)	18.7	17.3
F_{80} ball mill circuit feed	(μm)	3980	3980
P_{80} ball mill circuit product	(μm)	75	75
Specific energy	(kWh/t)	18.6	17.2
Overall specific energy	**(kWh/t)**	**22.8**	**22.8**

2.2.5 Effect of HPGR on downstream processes

One of the main attractions of the HPGR to the mineral processing industry is that it reportedly preferentially liberates minerals at a coarser grind through breakage along grain boundaries and zones of structural weakness. It has been suggested that if the same ore is subjected to different comminution devices such that the resultant particle size distributions are similar yet subsequent downstream treatment shows substantial

differences, then there is reason to believe that preferential mineral liberation has occurred (Celik and Oner, 2006).

Dunne *et al* (1996) compared the effect of HPGR and ball mill on downstream processes such as flotation, cyanide leaching and gravity separation on a zinc and gold ore. It was found that leaching tests had the most significant difference between recoveries of the valuable minerals. Higher recoveries were obtained in the leaching tests with the HPGR compared to the ball mill. A larger difference in recovery of 20% between the comminution devices was observed at the coarser size fractions (4000μm) than at the finer size fractions (425μm and 325μm) where the difference was 9%. Therefore based on these results, for leaching purposes, it is preferable to generate coarser grinds with the HPGR to obtain better recoveries. Better propagation of micro-cracks occurs at the coarser grinds thus making it easier for leaching reagents to access the valuable minerals (Dunne *et al*, 1996). For flotation and gravity separation on the other hand, no significant differences in recovery were observed. Effective recovery of valuable minerals by flotation and gravity settling techniques are highly dependent on the degree of mineral liberation. Therefore, based on the flotation and gravity separation results, no evidence of preferential liberation could be observed.

Esna-Ashari *et al* (1988) found that better leaching was obtained for compressive breakage compared to conventional grinding of a South African gold ore. More than 95% recovery was obtained for size fractions less than 1mm with compression breakage. In conventional grinding, 95% recoveries could only be obtained for size fractions less than 0.2mm. This observation confirms that better recoveries can be obtained at coarser grinds with the application of the HPGR for leaching processes.

Although the tests discussed above show the effects of the HPGR in terms of downstream recoveries, they do not show the degree of liberation attained as a result of the application of the HPGR. This author is of the opinion that analysing the liberation characteristics from the different comminution devices would assist in explaining some findings from

the work performed by Dunne *et al* (1996) and Shi *et al* (2006). The following section discusses studies that investigated the effect of HPGR on mineral liberation.

2.2.6 Effect of HPGR on mineral liberation

Daniel (2007) applied mineralogical techniques to measure the liberation of minerals from different comminution devices. Theoretical grade-recovery curves of the minerals of interest were generated as a method of analysis. The results obtained showed that the HPGR effects are ore dependent. While the bauxite and lead/zinc ores examined did not exhibit differences in mineral liberation, the PGM ore investigated showed differences in mineral liberation particularly for the coarse chromite minerals. This however does not translate to the liberation of PGM. As such, Daniel (2007) concluded that this is an area that needs to be studied further.

Wightman *et al* (2008) also performed a study to compare the degree of mineral liberation obtained from various modes of breakage such as the rod mill, hammer mill, stirred mill and the piston and die. The MLA was used to measure the degree of mineral liberation obtained. It was found that despite the comminution devices applied, there were no deviations in the deportment of the liberated particles towards each size fraction particularly at the finer size fractions for the valuable minerals. However for the gangue material such as the silicates, there were no deviations for all size fractions. Hosten and Ozbay (1998) on the other hand found that better degrees of liberation were obtained with the HPGR compared to the rod mill at different size fractions. The contradiction of the results obtained from Wightman et al (2008) and Hosten and Ozbay could be due to differences in ore type.

The method of determining the preferential mineral liberation applied by Daniels (2007) and Wightman *et al* (2008) showed the potential of the separation process through the generation of the theoretical grade-recovery curve. This also showed that the efficiency of the comminution device in terms of mineral liberation could be determined. Therefore,

the operational conditions of the comminution device can be optimized and those that show improved mineral liberation can be determined.

2.2.7 Effect of feed characteristics

While the previous sections have shown that the HPGR variables affect the results obtained, it should also be noted that the characteristics of the feed have significant effects on the product obtained. Feed characteristics such as size distributions and mineralogical characteristics of the feed have effects on the throughput, specific energy, product size distributions, reduction ratios and mineral liberation.

Klymowsky *et al* (2002) performed a comparison of the effect of two full feed size distributions (0 – 18mm and 0 – 40mm) to a truncated feed (6 – 40mm). It was found that the truncated feed produced the coarsest product. This suggests that the presence of fines in the feed assisted in the generation of finer product.

Hosten and Cimilli (2009) showed the effects of the feed size distribution on confined-bed comminution of quartz and calcite in a piston-die press. The breakage mode applied with the piston-die press system was applied by Hosten and Cimilli (2009) as a convenient tool for the study and analysis of various size reduction aspects of the HPGR. For all the tests performed by Hosten and Cimilli (2009), a constant feed top size of 3.35mm was used with variations in fines content for both quartz and calcite. It was found that feeds with narrower size distributions generated finer product. This contradicts the findings obtained by Klymowsky *et al* (2002) who found that broader size distribution generated finer product.

The contradiction between the results obtained by Hosten and Cimilli (2009) and Klymowsky *et al* (2002) could be due to the differences in the devices used. The piston-die press system used by Hosten and Cimilli (2009) is not a true representation of the compression zone in the HPGR. Several zones exist between the rolls of the HPGR in which different pressures are experienced as discussed in section 2.2. Edge effects are a

major characteristic of the compression zone of the HPGR. However, a good representation of the effects of the feed size distribution on variables such as product size distributions, specific energy and the breakage kinetics was shown by Hosten and Cimilli (2009).

Hosten and Cimilli (2009) showed that the limit of size reduction achieved is not only dependent on the feed size distribution but is also dependent on the ore type. Calcite, which is softer than quartz, had finer size distributions compared to quartz at the different feed size distributions tested. Similarly, it could be determined from the data produced by Lim *et al* (1996) that the ore type had an effect on the fineness of grind produced.

In the study performed by Lim *et al* (1996) the focus was on the effect of rolls speed and rolls surface pattern on HPGR performance for different ore types. The authors do not mention this in their article but some of the graphs appear to indicate that the specific throughput varies significantly with the ore type. Approximately 27% higher throughput was obtained with a diamond ore compared to a gold ore tested under similar HPGR conditions. This is postulated to be due to the differences in mineralogical characteristics of the ore types.

This section gave an overview of the various studies that have been performed with the application of the HPGR. The effects of the different HPGR variables on throughput, energy efficiency, downstream processes and mineral liberation were discussed. Of importance to this work, is the determination of the effect of HPGR on PGM flotation recovery and liberation. Therefore, the following sections describe the techniques applied in flotation and process mineralogy that are required this work.

2.3 Flotation

As previously mentioned, flotation is the separation process applied in the beneficiation of the liberated valuable minerals from the ore. The comminuted ore goes through several stages of flotation to ensure optimum recovery of the valuable minerals (Cramer, 2001; Merkle and McKenzie, 2002). In this work, the effect of HPGR on flotation recovery of PGMs has been investigated. Therefore, the following section discusses the principles of flotation and the factors that affect mineral recovery.

2.3.1 Principles of flotation

The flotation process uses the differences in the physico-chemical surface properties to separate the valuable minerals from the unwanted gangue minerals (Wills and Napier-Munn, 2005). Figure 2-15 is a schematic of the processes involved in flotation. Reagents are added to the pulp to render the valuable minerals hydrophobic and the unwanted gangue minerals hydrophilic. Reagents such as collectors, frothers, activators and depressants are used in flotation cells in order to enhance these differences on the mineral surfaces. The collectors promote the hydrophobicity of the valuable mineral while the activators increase the effectiveness of the collectors. The frother stabilises the water-air interface allowing for collection of the valuable mineral as concentrate and the depressants reduce the recovery of the unwanted gangue minerals (Wills and Napier-Munn, 2005).

This process usually takes place in an agitated cell with air being fed from the bottom of the cell. During flotation, minerals are recovered by three main sub-processes which include true flotation, entrainment and entrapment (Wills and Napier-Munn, 2005). True flotation occurs when the valuable minerals attach onto the bubbles and are transported through the pulp phase into the froth phase where they are removed as concentrate. Recovery by entrainment occurs when the suspended minerals are recovered with water which passes through with the froth. This is a non-selective process and is the main cause of the recovery of fine liberated unwanted gangue minerals (Wills and Napier-Munn,

2005). Entrapment occurs when a mineral is physically trapped by a particle attached to a bubble.

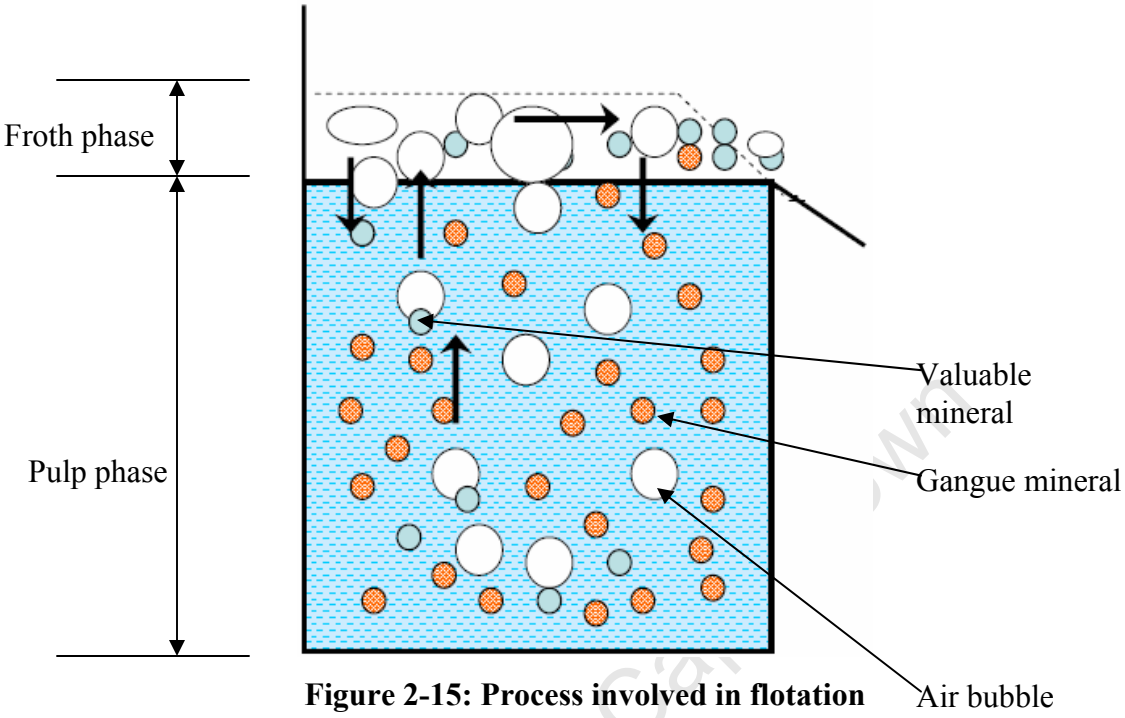

Figure 2-15: Process involved in flotation

Three main components such as the reagents used, the equipment applied and the operational parameters affect the outcome of flotation (Klimpel, 1984). Equipment components such as the cell design, agitation and air flow affect the flotation process. While the reagent and the equipment components strongly affect the optimum operation of a flotation plant, they are not the focus of this thesis. Operational parameters that affect the flotation outcome include the feed rate, mineralogy, particle size, pulp density, temperature and circuit design (Klimpel, 1984). For the purposes of this study, only the mineralogy and the particles size have been discussed in the following sections.

2.3.2 Effect of mineralogy

The mineralogy of the ore determines the grind required to adequately liberate the valuables mineral in the comminution process. While the three ore types of interest in this study are all PGM ores, the differences in mineralogy determine the necessary flotation conditions for each ore type.

2.3.3 Effect of particle size

The particle size plays a critical roll in the probability of a particle colliding with a bubble and remaining attached in the pulp phase. Fine particles have slow recovery rates due to decreased particle-bubble collisions and are more likely to be recovered by entrainment which has negative effects on the concentrate grade. The particle-bubble aggregate with coarse particles is less buoyant relative to the pulp and is more likely to detach in turbulent zones (Feng and Aldrich, 1999). Therefore, to determine the optimum particle size for the flotation process the mineral size and the fineness of grind must be considered (Wills and Napier-Munn, 2005).

Grano (2009) found that the grinding environment had an influence on the recovery of the fine (<10µm) valuable minerals in a copper ore. Full autogenous grinding resulted in better recoveries of the finer minerals compared to the conventional ball mill for the same grind (d_{80} = 130µm). Grano (2009) also reported that differences in grinding media showed differences in chalcopyrite and pyrite recoveries obtained. Better chalcopyrite grades and recoveries were obtained with ceramic balls as opposed to mild steel balls. This was postulated to be due to the differences in breakage rates applied by the different grinding media which resulted in differences in the size distribution of the chalcopyrite in the feed. Similarly, in HPGR and conventional ball mill studies, the differences in breakage rates and hence size distributions of the valuable minerals could explain differences observed for feeds with similar grinds.

Dunne *et al* (1996) found insignificant differences in flotation recovery of gold and zinc ore when comparing the HPGR to conventional devices with similar grinds. Shi *et al* (2006) performed tests to determine the effects of HPGR, applied as a pre-grinding stage on flotation recovery by comparing it to a conventional crushing device. The results in Figure 2-16 presented are of the sulphur recoveries from a PGM ore. It was found that the HPGR treated ore had slightly better flotation responses at coarser grinds of 70% passing 150µm and 106µm while at a finer grind of 70% passing 75µm, the conventional crusher had significantly higher recoveries. The recoveries however were much at the coarser sizes (150µm and 106µm) compared to the finer size (75µm).

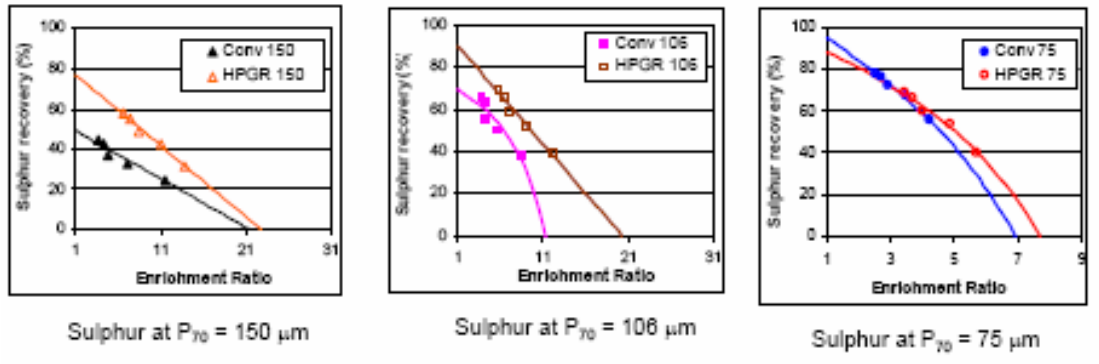

Figure 2-16: Effect of HPGR on flotation recovery of nickel (Shi *et al*, 2006)

2.4 Process Mineralogy

Process mineralogy is the application of mineralogical techniques to characterise an ore body so as to determine necessary metallurgical processing routes for optimum beneficiation of valuable minerals. Petruk (2000) defines process mineralogy as "the application of mineralogical information to understanding and solving problems encountered during the processing of ores, concentrates, smelter products and related materials". The mineralogy of the ore body provides the metallurgist with valuable information for the development and optimisation of metallurgical flow sheets (Henley, 1983).

Henley (1983) gives a detailed description of the application of process mineralogy in the development of mineral processing plants (Figure 2-17). The description begins from the exploration of an ore body to the start up of the plant, showing the importance of process mineralogy at each stage. Henley (1983) points out that even during the running of the plant, frequent testing of the ore body is essential to determine any metallurgical changes that may be necessary. Some industrial plants that are already in existence apply process mineralogy so as to determine any metallurgical changes in the ore and therefore can change the process accordingly.

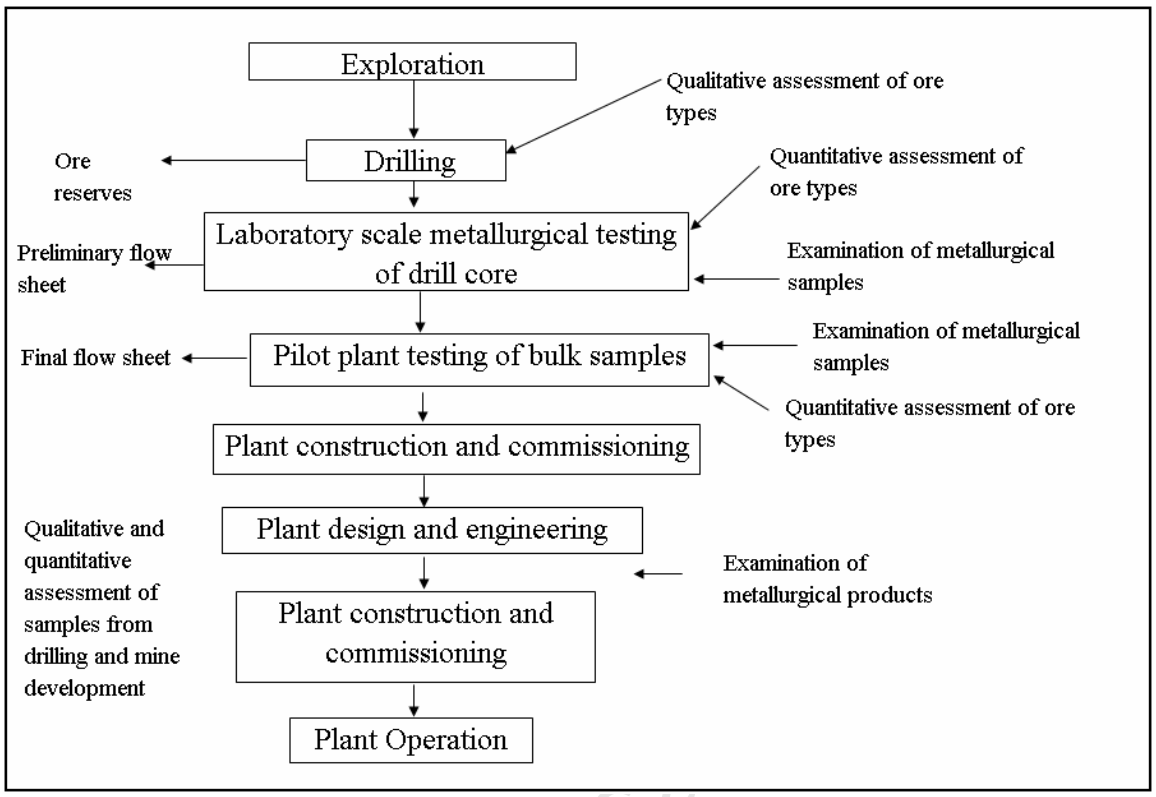

Figure 2-17: Linking process mineralogy to metallurgy (Henley, 1983)

Process mineralogy has been applied successfully in the characterisation of ores such as gold ores (Goodall *et al*, 2005), platinum ores (Xiao and Laplante, 2004), and coal and ash (Van Alphen, 2006). In cases such as platinum operations, the development of some flow sheets for the processing of these ores was determined through process mineralogy (Humphries *et al*, 2006). Cabri *et al* (2005) used the newly developed and patented technology of hydro-separation to study two samples from the Skaergaard intrusion in Greenland to determine the nature of precious metal minerals and to provide guidance for mineral processing. They found that the mineralogical data obtained proved useful to the metallurgical test work on the bulk samples.

2.4.1 Characterisation of ore bodies

Characteristics of an ore body such as mineral identities, grain size, mineral associations, degree of liberation and the distribution of the minerals present are determined. The identification of all minerals and their proportions in an ore body is essential for the

prediction of their response to various treatment processes. This information coupled with the distribution and compositions of the identified minerals will help identify trace elements that may affect the process and the purity of the refined metal. Knowledge of the grain size of the valuable minerals present will give an indication of the size to which the ore must be ground in order to achieve optimum degrees of liberation (Schapiro, 1981). This reduces chances of over grinding which can lead to loss of recovery in separation process such as flotation (Viljoen *et al*, 2001).

The grind is analysed for mineral liberation with the use of image analysis with the application of mineralogical techniques (Petruk, 2000). The association of the minerals gives an indication of where the valuable mineral is located with respect to other minerals present. If it is located at the grain fractures, liberation will be easier, whereas if the grains are locked or inter-grown then liberation becomes difficult (Lee, 2000).

In the past, constituents in the ore were determined by considering the ore grade, extent of reserves, transportation services and political structure. This was based on the assumption that conventional separation technology could be used (Schapiro, 1981). However, in an era where reserves are depleting with an ever increasing demand, operations are resorting to processing more complex deposits (Xiao and Laplante, 2004). Therefore, additional information such as, structural and textural nature of the valuable minerals in the ore body are desired. The mineralogical industry has been active in the development of technology that can routinely supply this type of information.

2.4.2 Techniques applied in process mineralogy

In the past, the characterisation of ore types such as platinum bearing ores has been difficult due to the fine grained nature of the minerals present in these ore types. Techniques such as optical microscopy and x-ray diffraction (XRD) were applied to characterise the ore. Obtaining liberation information through optical microscopy can lead to significant misinterpretation of the data due to a lack of human eye precision and difficulty in obtaining statistical data (Fonseca and Sá, 2005).

The development of the automated mineralogy techniques such as the Quantitative Evaluation of Minerals with Scanning Electron Microscopy (QEMSCAN) and the Mineral Liberation Analyser (MLA) has made it easier to characterize complex ore types. QEMSCAN was developed by the Commonwealth Scientific and Industrial Research Organization (CSIRO) in Australia while the MLA was developed by the Julius Kruttschnitt Mineral Research Centre (JKMRC) also in Australia. Both techniques work by gathering back scattered electron (BSE) images in the initial spatial survey. MLA combines the BSE and the energy dispersive spectrometer (EDS) information to characterize minerals while QEMSCAN uses the EDS detectors to collect elemental X-ray information to differentiate the minerals (Lastra, 2007).

Both techniques are used for ore characterisation, liberation analysis, process optimisation, process modeling and plant problem solving (Xiao and Laplante, 2004). A quantitative distribution of minerals in plant and test products can be obtained. These are highly automated instruments which ensure reliable results. The data obtained can be represented in tabular form, giving a size-by-size and mineral-by-mineral breakdown as well as a pictorial representation in which an outline of each particle and phase is given. This allows for a full assessment of the ore body which could improve plant recovery and maintain the quality of the product. Accurate identification of minerals can be obtained for particles in the size range 2-600μm (Xiao and Laplante, 2004).

2.4.3 Mineral liberation measurement with QEMSCAN and MLA

Two methods of determining the degree of liberation can be applied with the use of the automated mineralogical techniques and these are (Lastra, 2002):

- Comparing the cross-sectional area of the valuable mineral in a particle to that of the whole particle.
- Comparing the perimeter/exposed section of the valuable mineral to the perimeter of the whole particle.

Fonseca and Sà (2005) showed that there is a small difference in the degree of liberation obtained by considering the cross-sectional areas and the perimeter/exposed section of the minerals. However Lastra (2002) inferred that obtaining the liberation with the use of perimeters may be preferably applied for materials containing minerals with non-complex textures such as particle (a) shown in Figure 2-18.

(a) (b) (c)

Figure 2-18: Particles showing varying degrees of complexity in texture

Determining the liberation of binary particles such as (a) in Figure 2-18 using perimeters can be done easily. However for binary particles where the valuable mineral is located at the edge of a gangue particle with a small section of the gangue particle exposed such as (b), the measurement of liberation using perimeters would result in highly inaccurate data. For particles with more complex textures such as (c) it would be difficult due to the complexity of the texture of the particle. Therefore in the case of particles (b) and (c) it would be preferable to use cross-sectional areas to determine liberation.

Difficulties are sometimes experienced in estimating the mineral liberation and the grain size of a sample with the use of automated mineralogy known as stereology. A composite grain may appear liberated when sectioned and the image of particles may appear less than or equal to the actual size of the grain (Gay and Morrison, 2005; Sutherland, 2006). Several techniques can be applied for stereological corrections for liberation measurements using cross-sectional areas (Lastra, 2002). Therefore, comparison of liberation data obtained by the application of other mineralogical techniques or performing chemical assays should be performed to ensure reliable data.

2.5 Summary of Literature Review

The studies performed with the application of the HPGR that have been discussed concentrated mainly on its application as a pre-grinding stage in conventional comminution circuits. The main points that have been brought up are that the application of the HPGR results on the generation of propagating micro-cracks which potentially result in preferential mineral liberation. These micro-cracks make it easier for separation processes such as leaching at coarser grinds as discussed by Dunne *et al* (1996) and Esna-Ashari and Kellerwessel (1988). Most of these studies also report that the application of the HPGR in comminution circuits has resulted in energy savings ranging between 20-50%. However, studies that determine if the HPGR can be applied as an alternative to the ball mill have not been found.

The energy efficiency of a comminution circuit is dependent on how the HPGR has been incorporated in the comminution circuit. Therefore comprehensive tests of the HPGR in its application in existing comminution circuits must be performed in order to determine the most energy efficient method. This also entails the application of mineralogical techniques that could assist in the characterisation of the ore in terms of mineral liberation. This would give a robust analysis of the performance of comminution circuits as well as predict the performance of downstream processes such as flotation and leaching.

Very little evidence of preferential mineral liberation occurring as a result of the application of the HPGR has been published. In the studies by Wightman *et al* (2008) and Daniels (2007) it was found that little evidence of preferential mineral liberation was observed for different comminution devices, particularly at finer size fractions. Therefore in an effort to achieve the objectives set out in this work, the following chapter gives a detailed outline of the experimental procedure performed.

Chapter 3

3 EXPERIMENTAL PROCEDURE

Overview: This chapter describes the experimental work that was performed in order to test the hypotheses and answer the key questions outlined in chapters 1.

Comminution and flotation tests were performed on three platinum bearing ores Merensky, UG2 and Platreef obtained from the Bushveld Complex. The comminution tests involved the application of a small scale HPGR at different operational parameters. From these tests, it has been determined if the HPGR can produce a fineness of grind suitable for flotation tests. Comparative pilot scale ball mill tests were performed for all three ore types. Batch flotation tests were then performed on selected HPGR samples to determine the effects on PGM recovery. In order to determine the benefits of the HPGR in terms of energy consumption, throughput and PGM recovery, ball mill tests were also performed as a comparison.

3.1 Ore preparation

Bulk samples of run of mine Platreef ore obtained from the Northern limb and Merensky and UG2 obtained from the western limb of the Bushveld complex was used in this work. The bulk samples were transported to MINTEK for ore preparation and HPGR experimental test work. Preparation of this ore included crushing the ore down to the required top sizes for the HPGR and ball mill pilot plant tests. Approximately 15 tonnes of each ore type was available for the test work.

The top size used for the HPGR and the ball mill tests were 12mm and 6mm. The same preparation procedure was used for all three ore types. Each 15 tonne bulk sample was crushed to 100% passing 12mm. Following which, the bulk samples were then blended and split into approximately 500kg bulk samples. Half the bulk samples, that is, 7.5

tonnes of each ore type was then further crushed to 100% passing 6mm. The crushed 7.5 tonne bulk samples were then blended and split into 500kg samples.

Figure 3-1 shows photographs of the crushed material for the three ore types. It was observed that the fines content varied depending on the ore type. Table 3-1 shows the differences in Bond Work Indices and the breakage characteristics of the three ore types tested in this work which were discussed in section 2.1 on page 12 (Mainza and Powell, 2006). Therefore, differences in behavior in terms of energy consumption and size reduction are expected.

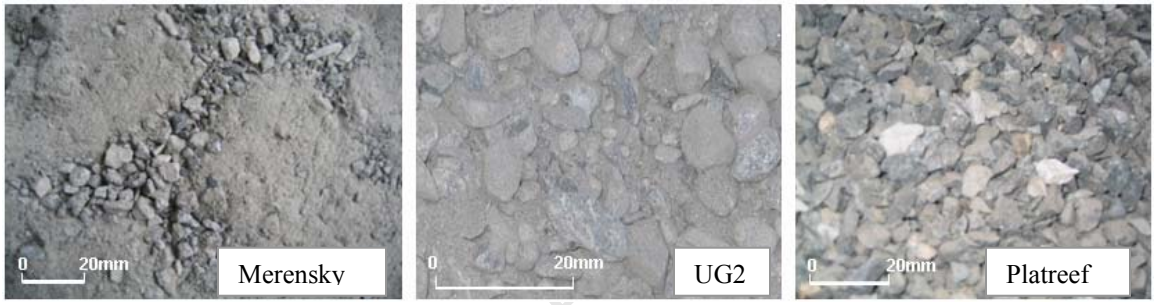

Figure 3-1: Photos of the three platinum bearing ores tested showing differences in coarse content which is an indication of the relative hardness of three ore types

Table 3-1: Comminution characterisation indices of Merensky, UG2 and Platreef ore (Mainza and Powell, 2006)

Ore type	BWI at 300µm (kWh/t)	BWI at 75µm (kWh/t)	AxB	Ta
Merensky Reef	21	25	77	0.63
UG2 Reef	18	21	151	1.25
Platreef	18 – 25	23 – 27	30 – 40	0.11 – 0.21

3.2 Representative sampling

Belt cuts of the feed were collected from each 500kg sample for each ore type and for each feed top size. Size distributions of each feed sub sample were obtained and

compared. The feed size distribution results appear to be representative with slight deviations from the observed as illustrated in Figure 3-2. These deviations could be due to the sampling technique applied where cuts were taken at different points on the belt with only a portion of the feed on the belt just before the test.

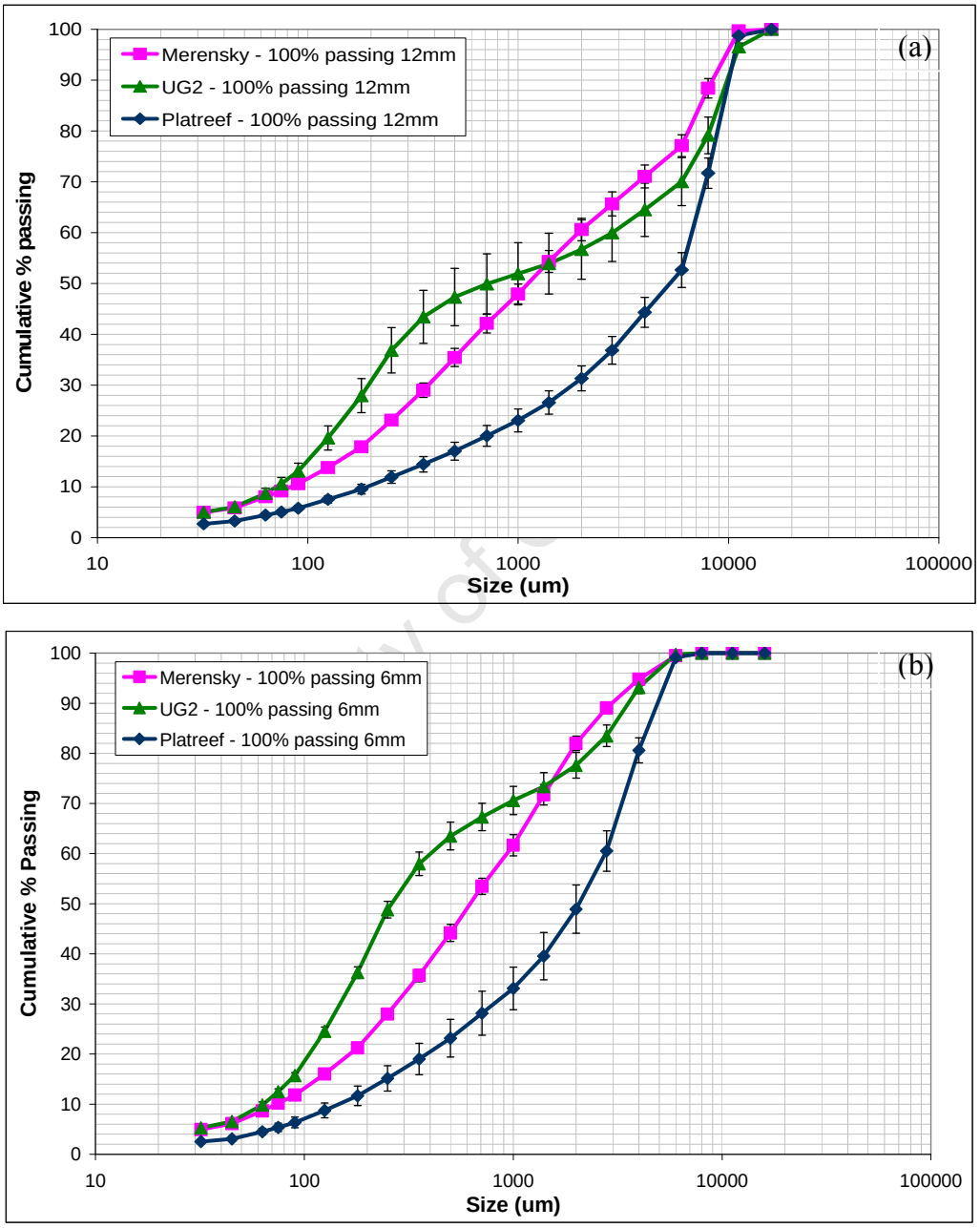

Figure 3-2: Graph showing feed size distributions of the three ore types at feed top sizes 12mm (a) and 6mm (b)

3.3 Comminution tests

Figure 3-3 shows the three comminution circuit configurations that were investigated in this study. The first set of tests was performed by passing each of the three ore types under consideration multiple times through the HPGR at different variables. The second set of tests was performed using a pilot scale ball mill. Comparisons between the two sets of experiments in terms of flotation recovery and mineral liberation were performed. The third set of tests was hybrid tests performed by pre-grinding the ore with the HPGR before ball mill. The hybrid tests were performed mainly to determine the effects of HPGR on ball mill throughput and specific energy consumption.

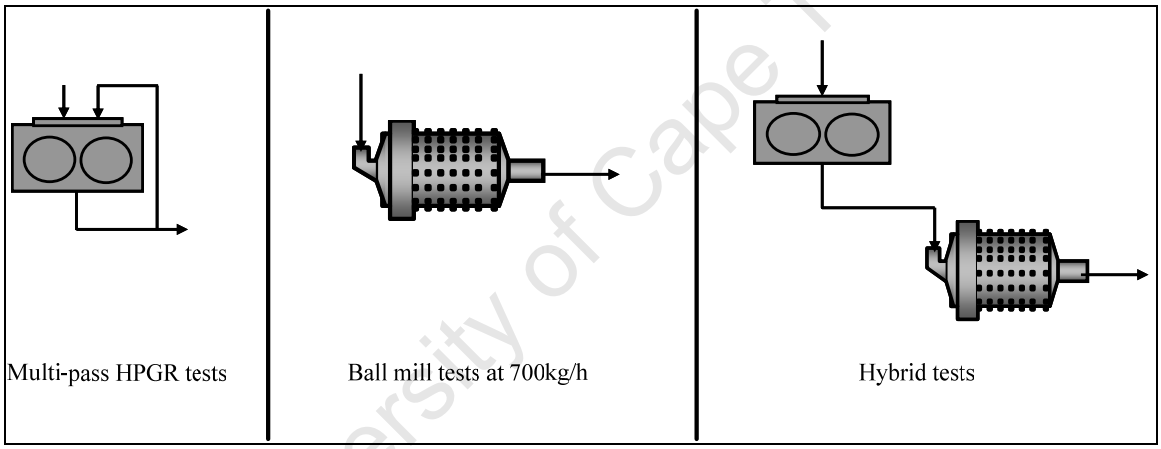

Figure 3-3: Comminution circuits investigated

In the first set of experiments, the ore was passed through the HPGR multiple times in order to ensure that a fineness of grind suitable for flotation was obtained for some of the tests. Based on the grind achieved, selected samples from these tests were floated to determine PGE recoveries. The PGE recoveries from the first set were compared to those from the second set of tests. Liberation profiles from both tests were obtained to assist in the explanation of the PGE recovery results obtained. In the hybrid tests, the product obtained from a single pass through the HPGR was fed to the ball mill.

3.3.1 High Pressure Grinding Rolls (HPGR) tests

As discussed in section 2.2, the various design and operational variables of the HPGR have effects on energy consumption, size reduction, throughput, mineral liberation and downstream recovery. Most importantly, for an HPGR without a variable speed drive like the unit used in this study, the essential variables are the specific grinding force and the zero gap. Therefore, these variables have been investigated in this study.

HPGR procedure

Tests were performed on a 250mm diameter by 100mm wide HPGR unit manufactured by Krupp Polysius shown in Figure 3-4. The front view shown in Figure 3-4(a) shows the fixed and movable rolls and Figure 3-4(b) is the side view showing the hopper through which the feed was introduced and the pressure system. Although this device has a maximum operating pressure of 200bar, in this study the pressure was varied between 60bar to 150bar. Figure 3-4(c) is the view from the top inside the feed hopper showing the studded rolls and the gap between the rolls through which the ore passed. The design and fitting of the hopper ensured that no gaps were left on either side of the rolls. This was done to avoid spillage of the feed on either side of the rolls. To ensure the hopper did not overflow during operation, a level controller was used as shown in Figure 3-4(d). The device was fitted with a digital energy meter (Figure 3-4(e)) for the direct measurement of the net comminution energy.

Figure 3-5 shows the flow chart that was used in this study for the HPGR experimental work. The ore was placed in the feed hopper before the beginning of the procedure. From the feed hopper, the ore was transferred to the HPGR by conveyor belt. At pre-set conditions of the HPGR, the ore was ground and collected on the product conveyor belt and transferred to the product hopper. Sampling was performed below the product hopper for the duration of each run and collected in two 20L buckets. At the end of the run when sample was collected and set aside, the remaining product was sent back to the feed hopper for further grinding. This flow sheet was used for the three ore types tested at different operational variables of the HPGR.

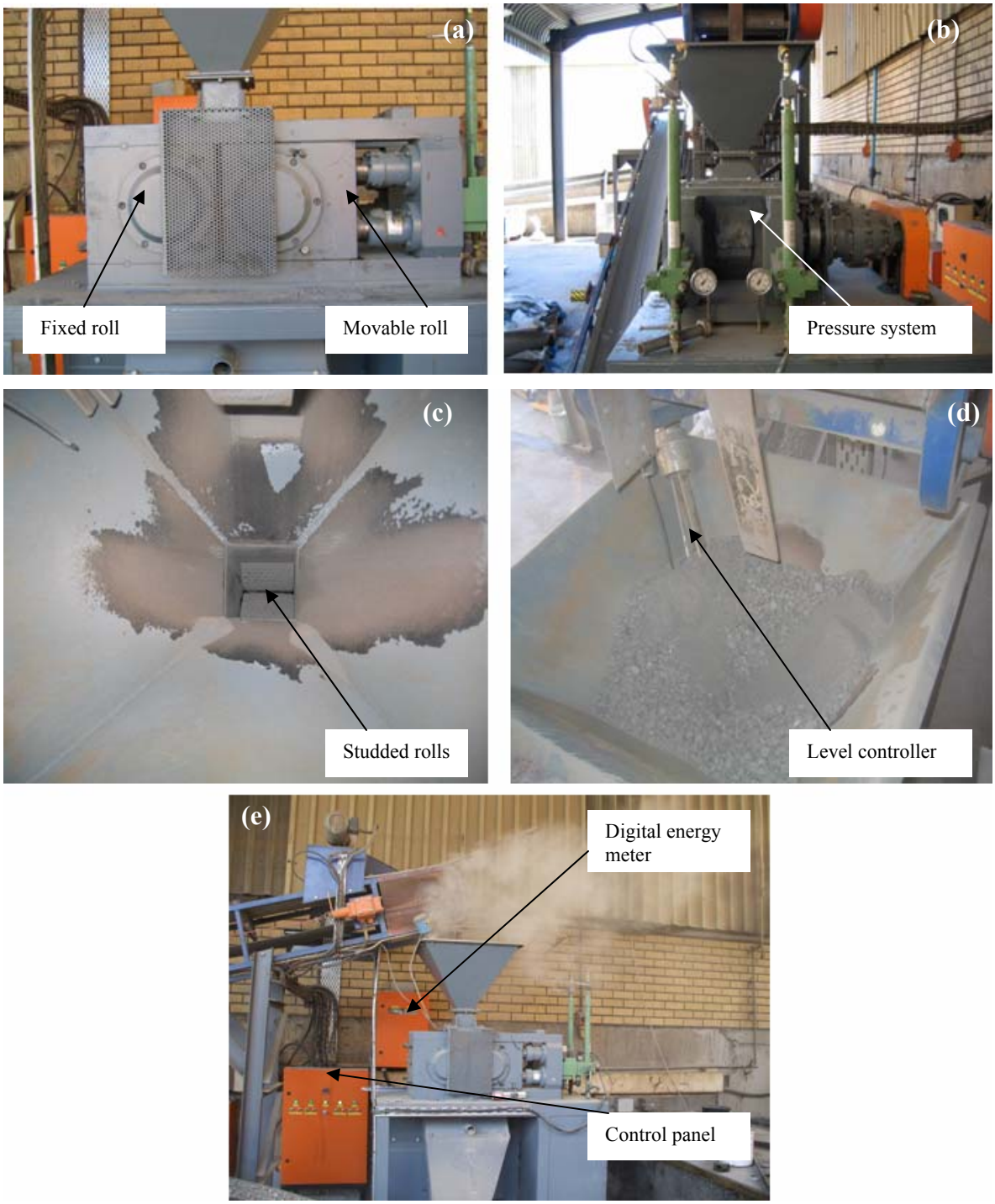

Figure 3-4: The laboratory scale HPGR utilised in this test work with a digital energy meter and level control in the feed hopper

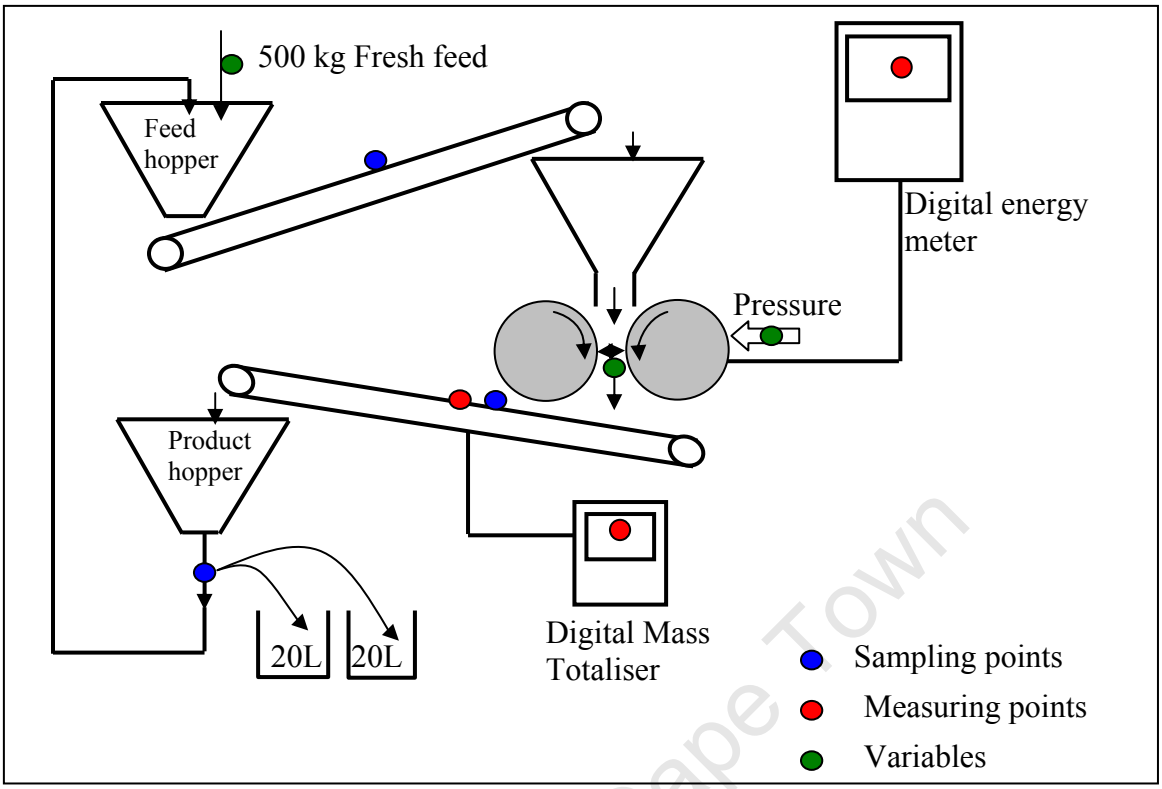

Figure 3-5: Flow chart of the HPGR system showing sampling points, measuring points and the input variables

The power source was isolated and the whole current circuit equipment locked out. The first step was to ensure that the machine was clean and no residuals from the previous test were in the hopper or between the two rolls. The second step was to grease the unit by way of a grease pump, making sure that all the bolts through which greasing was done had been attended to. The main power supply to the whole unit was then switched on and the process of setting the pressure started. The oil pump used for setting the hydraulic pressure was filled with oil with the use of a funnel and the Nitrogen cylinder had gas already.

The pneumatic pressure was set first by opening the valve on the Nitrogen cylinder to allow gas to flow to the Nitrogen accumulators. The hydraulic pressure was then set using an oil pump and the value was set in such a way that the ratio of hydraulic pressure to pneumatic pressure was always 3:2 The zero or initial gap between the rolls was then set. For the purposes of this work, the three zero gaps used were: 1.5mm, 3mm and

4.5mm. Once the pressure was set, the high pressure grinding roll was started up and the no load power was recorded. Four pressures were tested: 60 bar, 90bar, 120bar and 150bar.

Once the variables were set, approximately 500kg feed was choke-fed to the HPGR through the hopper. The sampling procedure was started approximately 20 seconds after the beginning of each run and stopped approximately 20 seconds before the end of the run. Samples were collected at intervals for the duration of the sampling period. The duration of the intervals during sampling depended on the throughput of each test.

Samples were cut using a tray that was wide enough to cover the entire width of the product hopper outlet. The large width was required to ensure that no material spilled from the cutter during sampling. For each pass the samples cut at various intervals were collected in two 20L buckets and then transferred into labeled plastic bags after each test. For each test a sample between 60 and 80kg was collected for further investigation. The remaining sample was then sent back to the HPGR for the subsequent pass and the sampling process repeated to obtain pass 2 products. This procedure was repeated for approximately three further passes for each 500kg batch of sample.

Power was monitored during the process by recording the power reading before and after each test in order to determine the power consumed during each test. The total time the material passed through the rolls was measured by observing the power meter and starting up the stop watch immediately when there was an indication of load between the rolls. The stop watch was stopped immediately after the decrease to no load power was observed. Table 3-2 is a matrix of the tests performed for the three ore types at varying pressure, zero gaps and feed topsizes.

All samples generated during the HPGR test work were bagged and stored for the sample preparation procedure described in section 3.4.

Table 3-2: Tests performed with the HPGR on each of the three ore types

Ore Type	Pressure (bar)	Feed topsize (mm)	Zero gap (mm)		
			1.5	3	4.5
Merensky	60	6	√	√	-
		12	√	√	-
	90	6	√	√	-
		12	√	√	-
	120	6	√	-	-
		12	√	-	-
	150	6	√	√	-
		12	√	√	-
UG2	60	6	√	√	-
		12	√	√	√
	90	6	√	√	-
		12	√	√	√
	120	6	√	-	-
		12	√	-	√
	150	6	√	√	-
		12	√	√	√
Platreef	60	6	√	√	-
		12	√	√	-
	90	6	√	√	-
		12	√	√	-
	120	6	-	-	-
		12	-	-	-
	150	6	√	√	-
		12	√	√	√

Repeatability analysis

Selected tests from the HPGR experiments were performed in duplicate for a repeatability analysis. Due to the large number of tests performed, only selected tests were repeated and it has been assumed that the results could be carried on to the other tests. The following table shows the tests that were repeated for each ore type. The results of the repeatability analysis have been presented in section 4.1.

Table 3-3: Table showing the tests in which repeat analyses were performed

Ore Type	Pressure (bar)	Feed topsize (mm)	Zero gap (mm)		
			1.5	3	4.5
Merensky	60	6	-	-	-
		12	-	-	-
	90	6	-	-	-
		12	-	-	-
	120	6	-	-	-
		12	-	-	-
	150	6	-	-	-
		12	-	-	-
UG2	60	6	-	-	-
		12	-	√	-
	90	6	-	-	-
		12	-	-	-
	120	6	-	-	-
		12	-	-	-
	150	6	√	-	-
		12	√	-	-
Platreef	60	6	-	-	-
		12	-	-	-
	90	6	-	-	-
		12	-	-	-
	120	6	-	-	-
		12	-	-	-
	150	6	-	-	-
		12	√	-	-

Measurements taken

Table 3-4 is a summary of the measured and calculated inputs and outputs for each test (Daniel, 2007). The flake thickness was measured in order to infer the working gap which is the gap between the rolls when the rolls are furthest apart during operation. However, this is not an accurate measurement of the working gap because the flakes tend to expand after passing through the compression zone between the rolls as discussed in section 2.2. In this work, a minimum of ten flakes were taken off the product conveyor belt to measure the thickness with the use of vernier calipers. The thicknesses of the flakes presented in section 4.1 are the average thicknesses of the flakes measured for each

test performed with the HPGR. The results obtained from the HPGR tests are presented in chapter 4.

Table 3-4: List of input, measured and calculated experimental data

Data category	Experimental measurements
Measured input	Pressure (P) Roll width (L) Roll diameter (D) Roll speed (u) Feed size distribution
Measured output	Energy (kWh) Test duration (t) Flake thickness (x_{fg}) Sample mass (m) No load power ($P_{no\text{-}load}$)
Calculated output	Specific energy (kWh/t) Throughput (Q_m) Specific force (F_{sp}) Product size distribution

Table 3-5 shows some of the equations that were applied for the estimation of the calculated outputs mentioned in Table 3-4.

Table 3-5: Equations used for the calculated out put

Quantity	Equation
Measured throughput (Q_m)	$Q_m(t/h) = 3.6 * \frac{m}{t}$
Specific force (F_{sp})	$F_{sp}(N/mm^2) = F_{gf} * D * L * 1000$
Specific energy (E_{sc})	$E_{sc}(kWh/t) = \frac{P_{gross} - P_{noload}}{Q_m}$

Where m is the mass of the sample (kg)

t is the duration of the test (s)

F_{gf} is the grinding force applied (kN)

D in the diameter of the roll (mm)

L is the width of the rolls (mm)

P_{gross} is the calculated gross power (kW)

$P_{no\ load}$ is the no load power (kW)

3.3.2 Ball Mill procedure

A pilot scale ball mill with an internal diameter of 0.93m and 1.5m length was utilised at Lonmin Karee Pilot Plant. The pilot scale ball mill tests were performed to generate samples that could be compared to the HPGR samples in terms of flotation recovery and mineral liberation. For each ore type, two types of tests were performed. A conventional open circuit ball mill test and a hybrid test involving the application of the HPGR at the first pass and the product fed to the ball mill. Both tests were performed on a feed top size of 6mm.

The set up illustrated in Figure 3-6 consisted of a pilot scale ball mill, a feed hopper, a belt feeder with a variable feed drive, a production screen and a screen undersize sump. The ball mill was equipped with a variable speed drive which made it possible to operate at any desired speed. In this test work, a speed drive corresponding to a frequency of 40Hz which is equivalent to 50% of the critical speed was used. The maximum speed the mill motor could reach was 65% of the critical speed. However to avoid using the motor at full capacity, the mill was operated at 50% capacity (Mainza and Powell, 2006). A ball charge with a seasoned ball size distribution was used as grinding media. The mill was fitted with a discharge grate with 10mm diameter holes at an open area of 20%.

(a)

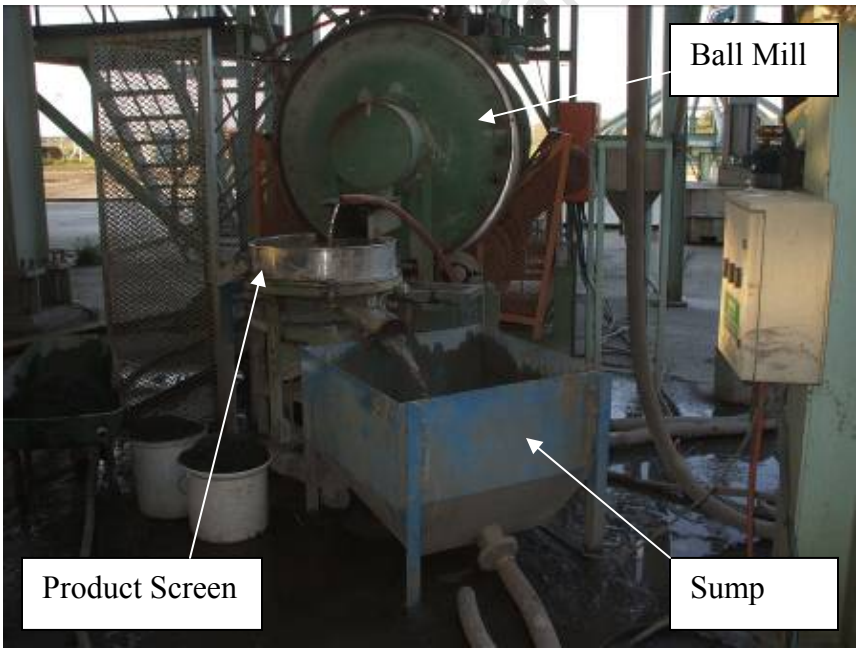

(b)

Figure 3-6: Pilot scale ball mill set up

Figure 3-7 shows the flow sheet that was used in this study for the ball mill tests. The ore was loaded into the feed hopper and was transferred into the ball mill inlet through the conveyor belt. At the ball mill inlet, water was added at an adjusted feed rate to ensure that the correct solids percent was obtained inside the mill. Slurry was discharged from the mill into the product screen where more water was added at an adjusted flowrate to ensure that the desired screen undersize solids concentration was obtained. The screen undersize was fed into a sump which operated as a feed to a Flotation Characterisation Test Rig (FCTR).

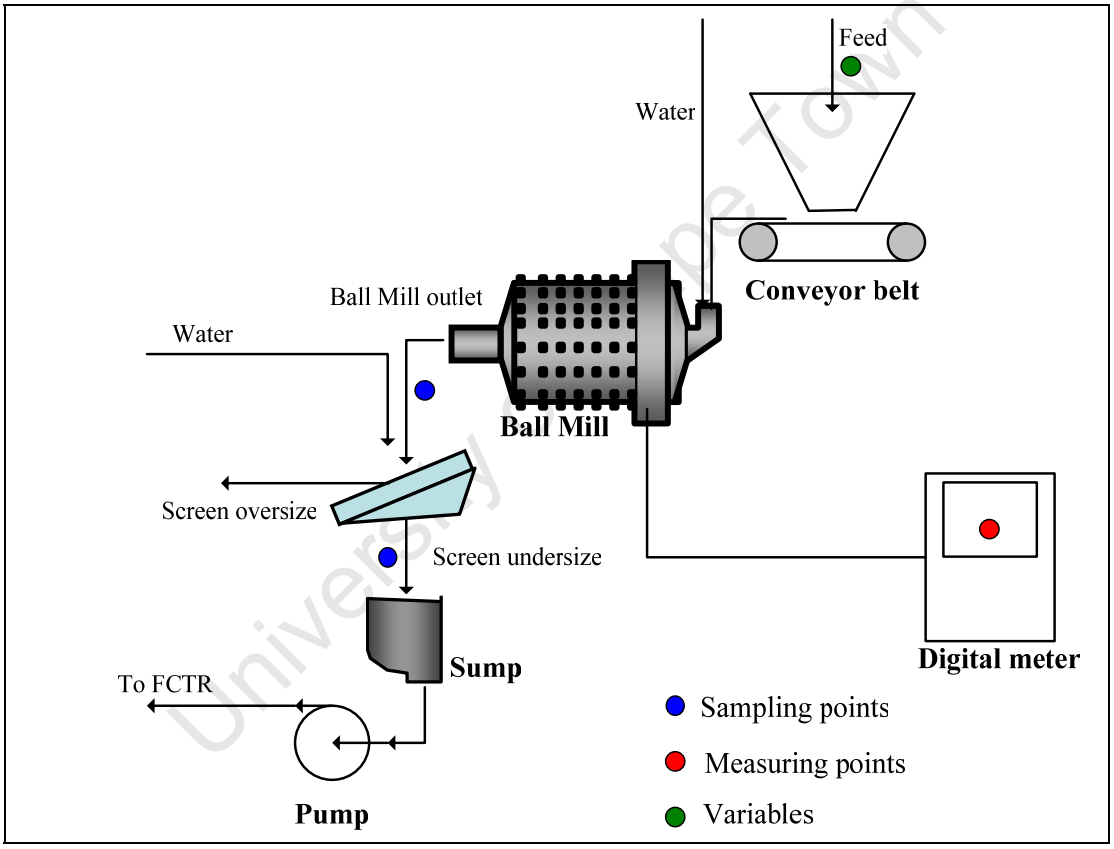

Figure 3-7: Flow sheet showing the sampling points, measuring points and variable of the ball mill tests

Mill operation

Previous tests performed by Powell and Mainza (2006) showed that the optimum throughput for this particular pilot scale ball mill set up was approximately 700kg/h. For the ball mill tests in this work the same throughput was used at a solids concentration in the range 75 – 80wt%. This is the optimum solids concentration range for any ball mill application. The water at the ball mill inlet was adjusted so that the desired solids concentration was applied. The following equation (6) was used to calculate the desired water flowrate at the mill inlet:

$$Water\,inlet(cm^3/s) = \frac{Throughput(kg/h)}{\%solids} * \frac{(100 - \%solids)}{3.6} \quad (6)$$

The throughput and the % solids applied in equation 6 were of the desired variables of 700kg/h and 78wt% respectively for all the ball mill tests performed in this work. The water flowrate was set with the use of a 2000cm^3 measuring cylinder and a stopwatch. The same procedure was used to set the flowrate of the water added to the product screen at the mill discharge. The flowrate was adjusted so that the screen undersize had a solids concentration of approximately 35wt% for the batch flotation tests to be performed. To obtain the flowrate of the water at the mill discharge, the following equation was applied:

$$Water\ flowrate(cm^3/s) = \frac{Throughput(kg/h)}{\%solids} * \frac{(100 - \%solilds)}{3.6} - water\,inlet(cm^3/s) \quad (7)$$

The % solids used in equation 7 is of the desired solids concentration of 35wt% at the mill discharge.

Test preparation

Once the variables had been set, approximately 15minutes was allowed for the system to reach steady state. For the first set of ball mill tests samples were the collected. As previously mentioned, the first set of ball mill tests involved grinding ore with a 6mm feed top size. For the second set of tests where the ore was pre-treated with the HPGR, the throughput was gradually increased from 700kg/h to approximately 900kg/h. This

was determined by measuring the percentage passing 75µm at each feed rate increment until the desired grind was reached. This procedure is described in the following section. Samples were collected at the initial throughput of 700kg/h and at the highest throughput reached.

Determining the percentage passing 75µm

To determine the percentage passing 75µm, a sample of the screen undersize was collected with the use of a sampling container. The sample was then carefully transferred into a 500ml beaker, ensuring that the entire sample went into the beaker. The beaker was then filled to the 500ml mark with water. The beaker, filled with the sample was then weighed. The sample was then wet screened on a 75µm screen and only the screen oversize was kept. Once the sample was thoroughly screened, the +75µm sample was transferred back to the 500ml beaker. Water was used to once again fill the beaker up to the 500ml mark. The new mass of the beaker was then obtained. Using these masses and equation 8, the percent passing 75µm was determined. This procedure was repeated at different throughputs.

$$\%passing75\mu m = \frac{SampleMass - +75\mu mMass}{SampleMass} * 100 \quad (8)$$

Table 3-6 is a summary of the tests performed with the pilot ball mill. The first tests were applied on the three ore types under consideration in this work at a throughput of approximately 700kg/h with a feed top size of 6mm. For the hybrid tests, the ore was pre-treated with the HPGR at a pressure of 60bar, a feed top size of 6mm and a zero gap of 3mm before being ground with the ball mill. For these tests, the low (~700kg/h) and high (~900kg/h) throughput results were recorded.

Table 3-6: Ball mill tests performed on all three ore types

Test	Ore type	Pressure (bar)	Feed top size (mm)	Zero gap (mm)	Throughput	
					~700kg/h	~900kg/h
Ball Mill	Merensky	-	6	-	√	-
	UG2	-	6	-	√	-
	Platreef	-	6	-	√	-
HPGR - Ball mill	Merensky	60	6	3	√	√
	UG2	60	6	3	√	√
	Platreef	60	6	3	√	√

Sampling procedure

Before sample began, throughput, the solids concentration of the mill discharge and the screen undersize were measured to ensure that they were in the desired ranges. The samples that were collected from the ball mill tests were for sizing, flotation and mineralogical analyses. For the sizing analysis, the samples were collected at the mill discharge above the product screen shown in Figure 3-7. Two 5L buckets were lined up next to the mill discharge for the sizing samples. A sample cutter that was wide enough to cover the width of the mill discharge was used. In 10s intervals, samples were cut for 5 seconds and alternately poured into the two buckets for an approximate period of 15minutes. The buckets were then weighed and set aside.

For the flotation and mineralogical sample, six 5L buckets were lined up next to the screen undersize where the samples were collected. Four of the buckets were for the flotation and two were for the mineralogy samples. A mark was placed at the 3L mark in each of these buckets. This was to ensure that enough samples were collected for the batch flotation tests. The same cutting procedure described above was used, ensuring that cutting was done until all six buckets were filled up to the 3L mark. The buckets were each weighed and set aside.

The sample preparation procedure described in section 3.4 was performed on the ball mill samples and the flotation procedure described in section 3.6 was used on the flotation

samples. The following is a summary of the measured variables and the equations applied to calculate the power draw and the specific energy.

Measurements taken

Table 3-7 shows that measurement and the respective quantities taken during the ball mill experimental work for the three ore types Merensky, UG2 and Platreef. The voltage and the current readings were used to calculate the specific energy consumed.

Table 3-7: Summary of test conditions measured during ball mill test work

System	Ore type	Throughput (kg/h)	Mill outlet % solids	Screen undersize %solids	Voltage (V)	Current (Amps)
Ball Mill	Merensky	720	75.6	32.0	424	11.2
	UG2	709	78.9	34.0	429	11.7
	Platreef	695	77.9	33.5	429	11.9
HPGR - Ball Mill	Merensky	743	77.8	33.2	424	11.2
	UG2	712	77.4	33.8	428	11.9
	Platreef	710	65.9	32.1	429	11.7
	Merensky	936	77.7	37.0	424	11.2
	UG2	932	77.3	34.1	428	11.9
	Platreef	943	68.5	33.1	429	11.7

Table 3-8 shows the equations that were applied for the calculation of the power draw and the specific energy.

Table 3-8: Equations applied for the ball mill data collected

Quantity	Equation
Power draw (kW)	$Power\ draw(kW) = \frac{\sqrt{3} * I * V * P_{factor}}{1000}$
Specific Energy, E_{sp} (kWh/t)	$E_{sp}(kWh/t) = \frac{Power\ draw(kW)}{Throughput(t/h)}$

Where I is the current (Amps)

V is the voltage

P_{factor} is the power factor, 0.75 was applied in this test work

3.4 Sample preparation

This section discusses the preparation of the HPGR and the ball mill samples for further analyses. The further analyses include particles size distributions, flotation tests and mineralogy analysis. A rotary splitter was used to split the samples obtained from the HPGR tests so as to obtain representative samples for the subsequent analyses.

3.4.1 HPGR product sample preparation

Figure 3-8 shows the flakes that were formed during the HPGR tests for Merensky (a), UG2 (b) and Platreef (c). The flakes formed varied in thickness and competence depending on the ore type and the settings of the HPGR applied. The first step was to de-agglomerate the flakes formed to ensure that representative sampling was performed during the splitting.

Figure 3-8: Flakes formed during the HPGR tests for all three ore types, Merensky (a), UG2 (b) and Platreef (c)

A 4.5mm screen shown in Figure 3-9(a) was used to manually de-agglomerate the flakes in the HPGR product without changing the particle sizes and the geometrical shape of the particles. Once the flakes in each sample were broken, the samples were weighed. The rotary splitter shown in Figure 3-9 which had a 100kg capacity was used to split the samples. Figure 3-10 shows the splitting procedure that was applied for the HPGR product. Samples for sizing analysis, flotation tests and mineralogical analysis were obtained. After splitting, each of the sub-samples were bagged and labeled in preparation for further processing. The sample labeled 45-60kg shown in Figure 3-10 was not used for the purposes of this study. Table 3-9 is a break down of the approximate mass of each

sample set aside for subsequent tests. The sizing and flotation procedures are described in section 3.5 and 3.6 respectively.

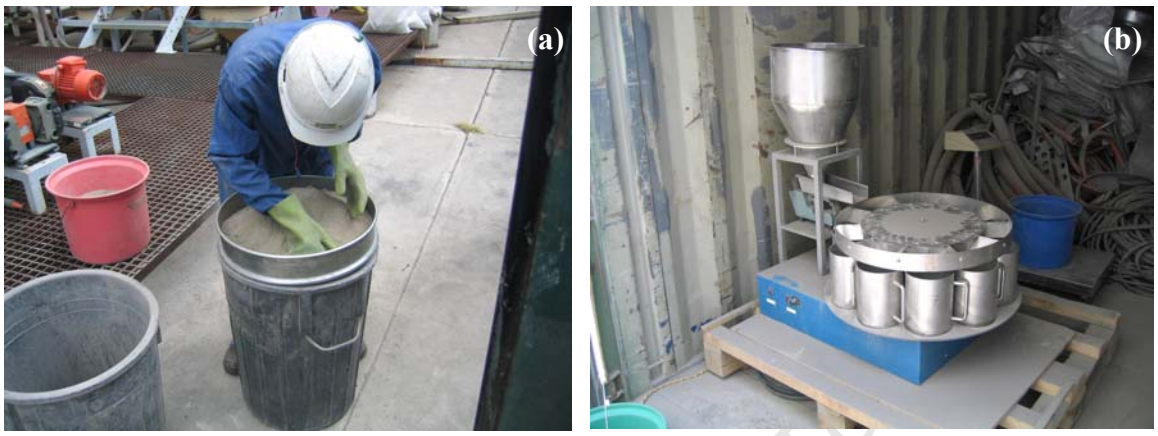

Figure 3-9: (a) Breaking up of any flakes present in the sample with the use of a 4.5mm screen, (b) Splitter used for dividing HPGR product into various sub samples

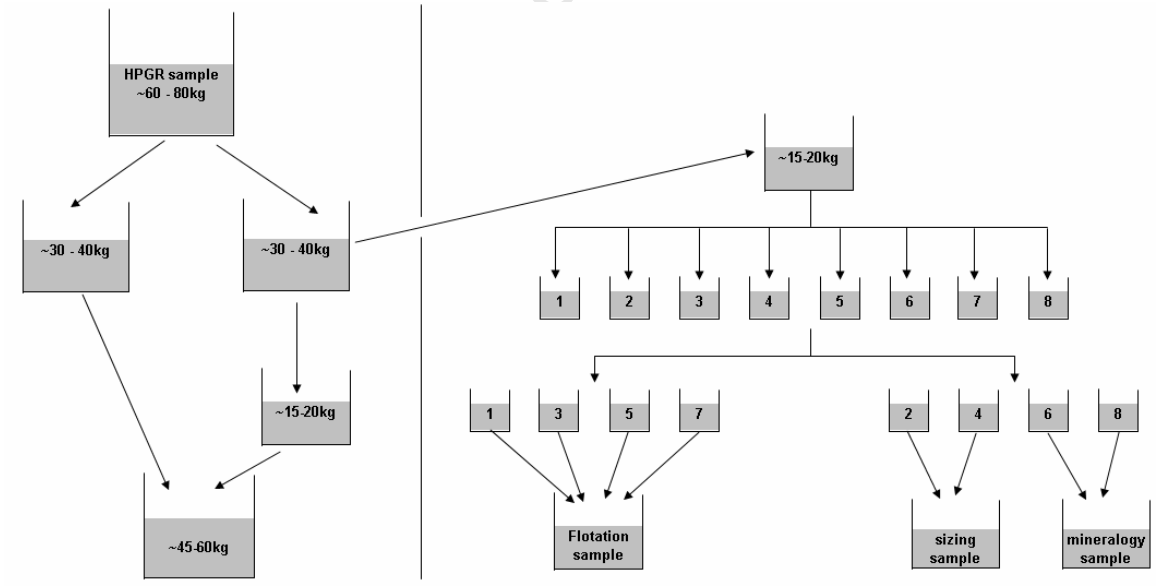

Figure 3-10: Schematic of splitting procedure to obtain sub-samples for further analyses

Table 3-9: Break down of the approximate amount of sample for each test

Test	Approximate mass (kg)
Particle size distribution	2
Flotation	8
Mineralogy	4

3.4.2 Ball mill product sample preparation

The samples that were collected for the flotation tests from the ball mill experiments were immediately transferred into a 3L Leeds batch flotation cell. Hot floats were then performed on the samples using the flotation procedure outlined in section 3.6.

The samples collected from the ball mill experiments for sizing and mineralogical analyses were weighed, filtered and placed in the oven to dry at a temperature of 80ºC. Once dried and cooled, the samples were weighed again. The solids percent was then calculated using the wet and dry masses with the application of equation 9. After weighing, the dry samples were bagged, labeled and stored for the sizing and mineralogical analyses.

$$\%solids = \frac{DryMass(g)}{WetMass(g)} * 100 \quad (9)$$

3.5 Size distribution analysis

To obtain particle size information, the samples for sizing from the HPGR and ball mill tests were screened according to the procedures outlined in this section. Wet screening was applied for finer sizes and dry screening for coarser sizes. Table 3-10 shows the size fractions where the wet and dry screening procedures were applied.

Table 3-10: Size fractions applied in the dry and wet screening processes

Dry screening		Wet screening
+11.2mm	+1000µm	+63µm
-11.2mm+8mm	-1000µm+710µm	-63µm+45µm
-8mm+5.6mm	-710µm+500µm	-45µm+32µm
-5.6mm+4mm	-500µm+355µm	-32µm
-4mm+2.8mm	-355µm+250µm	
-2.8mm+2mm	-250µm+180µm	
-2mm+1.4mm	-180µm+125µm	
-1.4mm+1mm	-125µm+90µm	
-1mm	-90µm+75µm	
	-75µm	

Dry screening of the +1mm sub-samples

The sizing samples from the HPGR and the ball mill test work were each weighed before being dry screened on a 1mm sieve. The +1mm and the -1mm samples were each weighed. Dry sieving was used for the +1mm samples. Each fraction was weighed and the sum of the mass of the fractions was obtained and compared to the initial mass of the +1mm sample to ensure the integrity of the sampling procedure.

The +1mm sub-sample was then dry screen using the screens in a root 2 series from +11.2mm to sub 1mm shown in Table 3-10. Each size fraction was weighed and the sum of the fraction was compared to the initial mass of the +1mm sub-sample to check that the procedure was performed satisfactorily.

Wet screening

The weighed -1mm sub samples were split with the use of a rotary splitter in order to obtain 300g samples. A and B samples of the -1mm sub samples were obtained in case a problem occurred with the A samples. The ~300g sample was weighed and wet screened using a single wet screening procedure. The samples were screened on three screens: 32µm, 45µm and 63µm.

The 32µm screen was firmly clamped to the vibratory sieve shaker. The sample was first mixed with water to form slurry before being poured onto the screen. The shaker was

turned on and water was introduced on the screen continuously throughout the procedure. The screen undersize was collected underneath the screen in a clean bucket. This procedure was continued until only clear water was discharged in the screen undersize. The bucket containing the sub 32µm sample was then set aside and replaced with another clean bucket. The 32µm screen was replaced with the 63µm screen and firmly clamped on the shaker.

The +32µm sample was then carefully transferred from the 32µm screen onto the 63µm screen. Wet screening was performed until only clear water was discharged in the screen undersize. The +63µm sub-sample was then carefully transferred into a drying pan. The bucket containing the sub 63µm sub-sample was replaced with a clean bucket and the 45µm screen was clamped on the vibratory shaker. The sub 63µm sample was then poured onto the 45µm screen to resume screening, ensuring that the entire sample was transferred.

Once the procedure was complete, the +45µm was transferred onto a drying pan while the bucket containing the sub 45µm sample was replaced with another clean bucket. The 32µm screen was once again clamped onto the shaker and the sub 45µm sample poured onto it for further screening. The +32µm sub-sample obtained was transferred into a drying pan while the remaining sub 32µm in the bucket was combined with the first -32µm sample generated at the beginning of the screening process. The sub 32µm sub sample was then filtered in a pressure filter on pre-weighed filter paper and was the placed in a drying pan.

The sub samples generated in the screening process were oven dried at approximately 80ºC. Once dried and cooled, each of the size fractions was weighed. The +63µm samples were then dry screened on a stack of sieves in a root 2 series from +1mm to -75µm. The masses of the size fractions were summed and compared to the initial mass.

The results from the HPGR, ball mill and sizing analysis are presented in chapter 4 and discussed in Chapter 6. The following section describes the flotation procedure.

3.6 Flotation tests

Flotation tests were performed on selected samples obtained from the HPGR and the ball mill tests. Table 3-11 shows the HPGR tests that were chosen for flotation tests. The samples were chosen based on the percent passing 75µm obtained using the sizing analysis data. The samples from the HPGR and ball mill tests where the grind was similar or close to the primary grind in platinum processes were selected for flotation tests. It will be shown in chapter 4 that the required grind was obtained after four passes with the application of the HPGR at pressure of 150bar. Comparisons in terms of PGE recovery obtained from the two devices were performed using grade-recovery curves.

Table 3-11: HPGR tests selected for flotation tests

Ore Type	Pressure (bar)	Feed topsize (mm)	Zero gap (mm)		
			1.5	3	4.5
Merensky	60	6	-	-	-
		12	-	-	-
	90	6	-	-	-
		12	-	-	-
	120	6	-	-	-
		12	-	-	-
	150	6	√	-	-
		12	√	√	-
UG2	60	6	-	-	-
		12	-	-	-
	90	6	-	-	-
		12	-	-	-
	120	6	-	-	-
		12	-	-	-
	150	6	√	-	-
		12	√	√	-
Platreef	60	6	-	-	-
		12	-	-	-
	90	6	-	-	-
		12	-	-	-
	120	6	-	-	-
		12	-	-	-
	150	6	√	-	-
		12	√	√	-

3.6.1 Batch flotation cell

A 3L Leeds Batch Flotation cell was used for all the flotation tests performed in this study. The cell which is shown in Figure 3-11 is fitted with an impeller which was operated at a speed of 1200rpm. The speed of the impeller was maintained manually throughout the duration of each test. An air flow rate of 7L/min was continuously supplied to the cell for the duration of each test.

Figure 3-11: ***Leeds batch flotation cell***

3.6.2 Flotation sample preparation

For each flotation test, a sample of approximately 1kg was required so as to ensure that the solids percent was 33 – 35wt%. In preparation for the tests, the flotation sub samples from the HPGR product were first weighed and then screened on a 1mm screen to remove coarse particles. The -1mm sub samples were weighed and rotary split into 1kg samples in preparation for the flotation tests which were performed according to the procedure described in the following section.

3.6.3 Flotation procedure

The 1kg dry samples from the HPGR were placed in a bucket and mixed with approximately 500ml of synthetic plant water to make slurry. The slurry was then transferred to the flotation cell and the impeller was immediately switched on to ensure homogeneity of the mixture. More synthetic plant water was then added to the cell up to the 3L mark so that the solids concentration was in the region 33 – 35wt%. A mixing time of approximately two minutes was allowed to ensure a homogenous mixture. Once the pulp was well mixed, a feed sample was collected with the use of a 50ml syringe. The reagents were prepared according to the following procedure.

Reagent preparation

Table 3-12 shows the reagents, dosages and conditioning times that were used in this testwork. The type of reagents and the dosages that were applied for each ore type in this testwork were recommended by Lonmin Platinum. A 1% solution of each reagent was prepared in 100ml volumetric flasks and well mixed until all the reagent had dissolved. For the depressants approximately one hour of mixing with the use of a magnetic stirrer was required before the beginning of the tests. Once dissolved, the required amounts of reagent for each test was measured into syringes and lined up next to the flotation cell. Equation 10 was used to determine the volume of each reagent required for the tests.

$$V_{reagent}(cm^3) = \frac{Dosage(g/t) * m(g)}{x(g/cm^3) * 10^6} \quad (10)$$

Where $V_{reagent}$ is the volume of the reagent solution required

m is the mass of the sample being floated

x is the fraction of the reagent in solution

For the purposes of this work, the density of the reagent solution used was $0.01 g/cm^3$ for a 1% solution. Once the reagents were ready, the procedure was started as outlined in the following section.

Table 3-12: Reagents and dosages used in flotation tests

Reagents	Condition time (min)	Merensky		UG2		Platreef	
		Type	Dosage (g/t)	Type	Dosage (g/t)	Type	Dosage (g/t)
Activator	5	$CuSO_4$	55	CuSO4	170	CuSO4	none
Collector	2	SNPX	200	SNPX	155	SIBX	250
Depressant	2	Dep 267	220	KU11	80	KU11	200
Frother	1	DOW200	40	DOW200	40	DOW200	40

Test preparation

Before the beginning of the procedure, it was ensured that there were four clean, weighed pans stacked on top of each other on the pan holder below the lip of the flotation cell. These were used for collecting concentrate samples during the procedure.

Four water bottles were numbered, filled with water, weighed and used for cleaning the scraper and lip of the flotation cell during the sampling procedure. This was to prevent any concentrate from going back into the cell.

The activator was added with a syringe to the homogenous pulp mixture in the cell. Simultaneously, a stop watch was started. The activator was allowed to condition for five minutes. Conditioning allows the reagents to absorb onto the mineral surfaces. Next, the collected was added and conditioned for two minutes followed by the depressant and the frother which conditioned for two and one minute, respectively.

Once the reagents had been conditioned, the air supply was immediately switched on, ensuring that the flowrate was steady at 7L/min. The impeller speed was checked and adjusted accordingly to ensure that the speed was maintained at 1200rpm. The level of the pulp in the cell was also checked and maintained with the use of plant water for the duration of the test.

Sampling procedure

Fifteen seconds after the air supply was turned on, froth was scraped off the top of the cell into the top pan, ensuring that the entire top of the froth was scraped off from the back of the cell to the lip of the cell. The scraping procedure was performed every 15 seconds for two minutes. After each scrape a water bottle was used to clean the scraper and the lip of the flotation cell, allowing the cleaning water to spill into the pan. Immediately after two minutes, the top pan containing the first concentrated was removed and scraping continued into the second pan. The first water bottle was set aside and replaced with the second bottle. The same scraping procedure was used for the collection of the second, third and fourth concentrates for four, six and eight minutes, respectively. The water bottles were changed every time a pan containing concentrated was removed. Once all four concentrates were collected two 50ml syringes of tails samples were collected.

Once the sampling procedure was complete, the flotation cell was emptied into a bucket and cleaned in preparation for the following flotation test. The remaining pulp was pressure filtered on weighed filter paper and then placed in the oven to dry.

The pans containing the concentrates and the four water bottles were weighed. The concentrates, feed and tails samples were the filtered using a vacuum filter on weighed filter paper. The filter papers containing the samples were folded and placed in a drying pan oven dried at a temperature of 80ºC. Once dried and cooled, the samples were weighed.

All the data collected during the flotation procedure was used for the calculation of the mass-water recoveries. These results have been presented in section 5.1.The flotation tests were performed in quadruplicate to check for repeatability and to ensure that enough sample was generated for PGE assays. The sample preparation of the PGE assay analysis is outlined in the following section.

3.6.4 Sample preparation of flotation samples for PGE assays

Table 3-13 shows the procedure that was used to combine the flotation samples in preparation for the PGE assay analysis. A and B samples were generated so as to asses repeatability. Concentrates C1 and C2 from floats 1 and 2 were combined and well mixed to form C1a while C3 and C4 formed C2a. Feeds F1 and F2 were combined to form Fa while T1 and T2 from both floats formed Ta. The same procedure was applied on floats 3 and 4 to form the B samples. Table 3-14 is a summary of the samples that were sent for PGE assays for each flotation test performed from the HPGR and ball mill tests. The results from the PGE assays are presented in Chapter 5.

Table 3-13: Tabulation procedure used to combine samples from flotation tests

	A Samples		B Samples	
Sample name	**Float 1**	**Float 2**	**Float 3**	**Float 4**
Feed	F1	F2	F3	F4
Concentrate 1	C1	C1	C1	C1
Concentrate 2	C2	C2	C2	C2
Concentrate 3	C3	C3	C3	C3
Concentrate 4	C4	C4	C4	C4
Tail 1	T1	T1	T1	T1
Tail 2	T2	T2	T2	T2

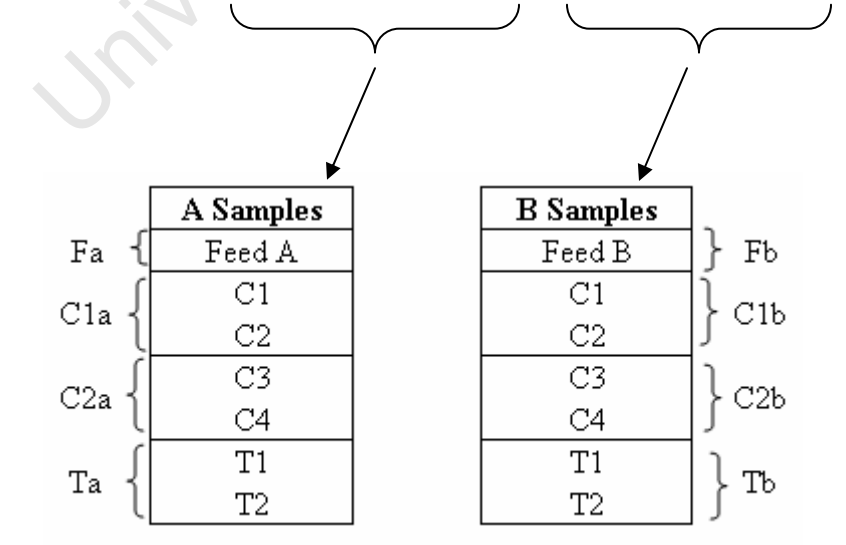

Table 3-14: Summary of the samples sent for PGE assaying

	A Samples	B Samples
Feed	Fa	Fb
Concentrate 1	C1a	C1b
Concentrate 2	C2a	C2b
Tails	Ta	Tb

3.7 Mineralogical Analyses

The mineralogical analyses were performed to characterise the PGMs and obtain liberation profiles of the HPGR and ball mill samples selected for flotation tests. The samples were selected according to the grind required for a primary flotation circuit on PGM processing plants. Therefore, sub samples of the flotation feed shown in Table 3-11 were also taken for mineralogical analysis. MLA was used for the characterisation of the PGMs. QEMSCAN was used to obtain a bulk mineralogical analysis of the three ore types. Sample preparation for the QEMSCAN and MLA analyses is described in the following sub-section.

3.7.1 QEMSCAN Analysis

For the QEMSCAN samples, 200g of each was ore type was wet screened using the procedure described in section 3.5 into size fractions -180+106µm, -106+53µm, -53+20µm and -20µm. The QEMSCAN tests were performed at Mintek where sized samples were required for the analysis. The mineralogical analysis data have been presented in Chapter 5 and discussed in Chapter 6.

Figure 3-12 shows the QEMSCAN that was used in this study at Mintek. Mounts of the samples were placed in the samples chamber for analysis. Bulk mineralogy data of each of the three ore types was obtained from these tests.

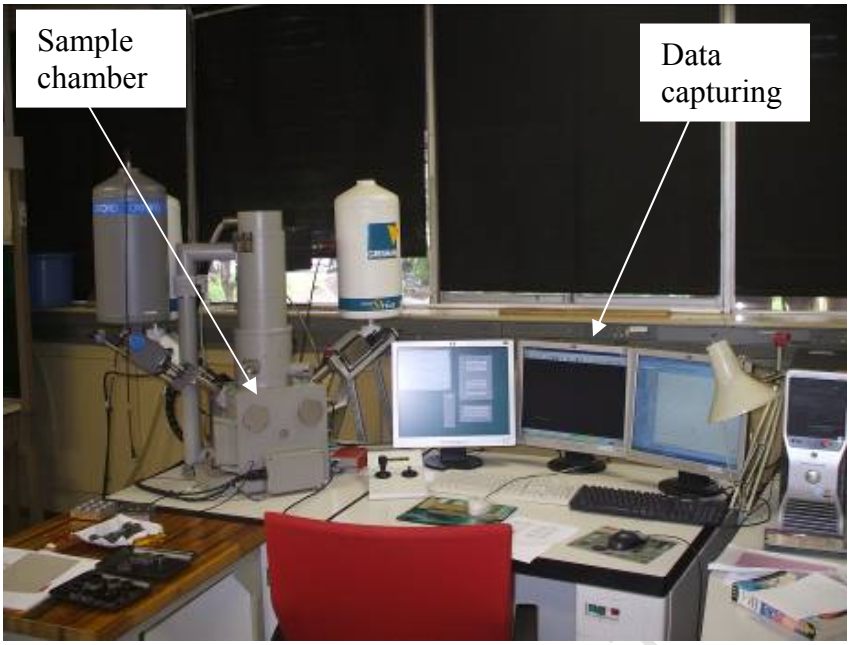

Figure 3-12: ***QEMSCAN used for obtaining a modal analysis of selected samples***

Analysis method

Two methods can be applied in the analysis of the samples: Particle Mineral Analysis (PMA) and Bulk Mineral Analysis (BMA). Based on these methods, a modal analysis of the QEMSCAN data can be obtained. The PMA gives a particle by particle analysis, producing false colour images of the particles. This method is suitable for a visual analysis of liberation and the determination of mineral associations. The second method, BMA produces images such as that illustrated in Figure 3-13. A line by line analysis of each mount was performed with a set spacing between the lines. The line spacing is set such that each line goes through each particle once in the x-direction. In this work, the BMA method was applied.

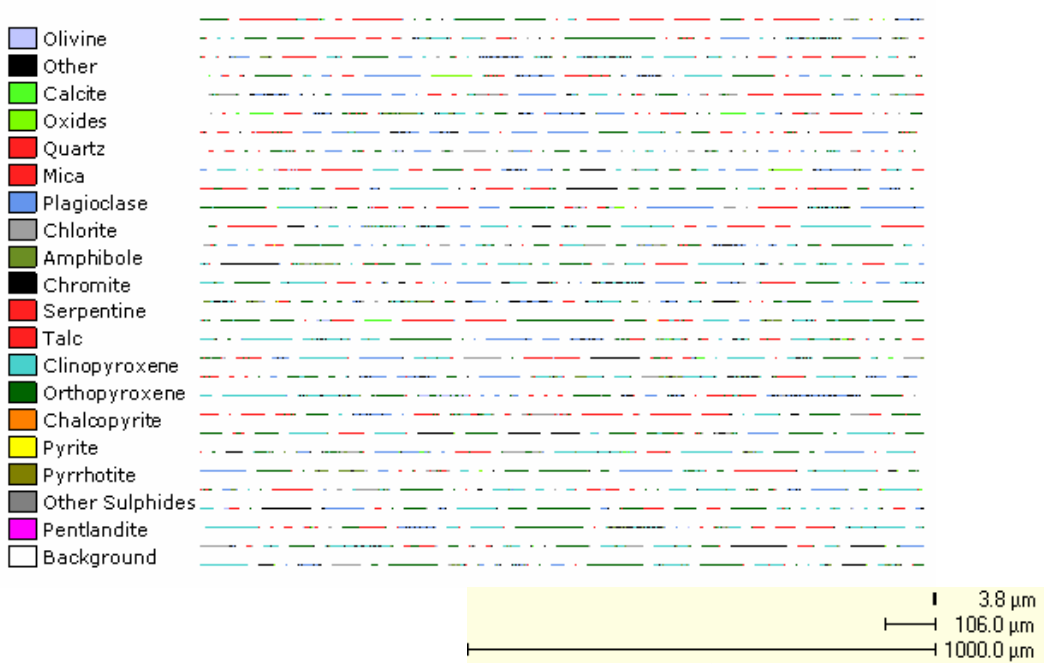

Figure 3-13: Bulk Mineral Analysis obtained from QEMSCAN with each colour representing a mineral

Data validation

The QEMSCAN data was validated by plotting the QEMSCAN assays against chemical assays. Satisfactory correlations between the QEMSCAN assays and the chemical assays are obtained for the major elements all three ore types as illustrated in Figure 3-14. This is shown by most of the points which lie on the line with a gradient of one. Departures from the line were observed particularly for calcium. This means that there was either an overestimation of the calcium content with the chemical assays or an underestimation with QEMSCAN.

3.7.2 MLA analysis

Approximately 4kg of the samples collected for mineralogical analysis as shown in Table 3-9. The samples were screened on a 1mm sieve to remove the +1mm particles. The -1mm sub samples were then rotary split into approximately 200g samples. A total of 12 samples collected at the different HPGR and ball mill tests discussed above were sent for to ALS Mineralogy in Australia for MLA analysis. The results generated from the QEMSCAN and MLA analyses are presented in Chapter 5.

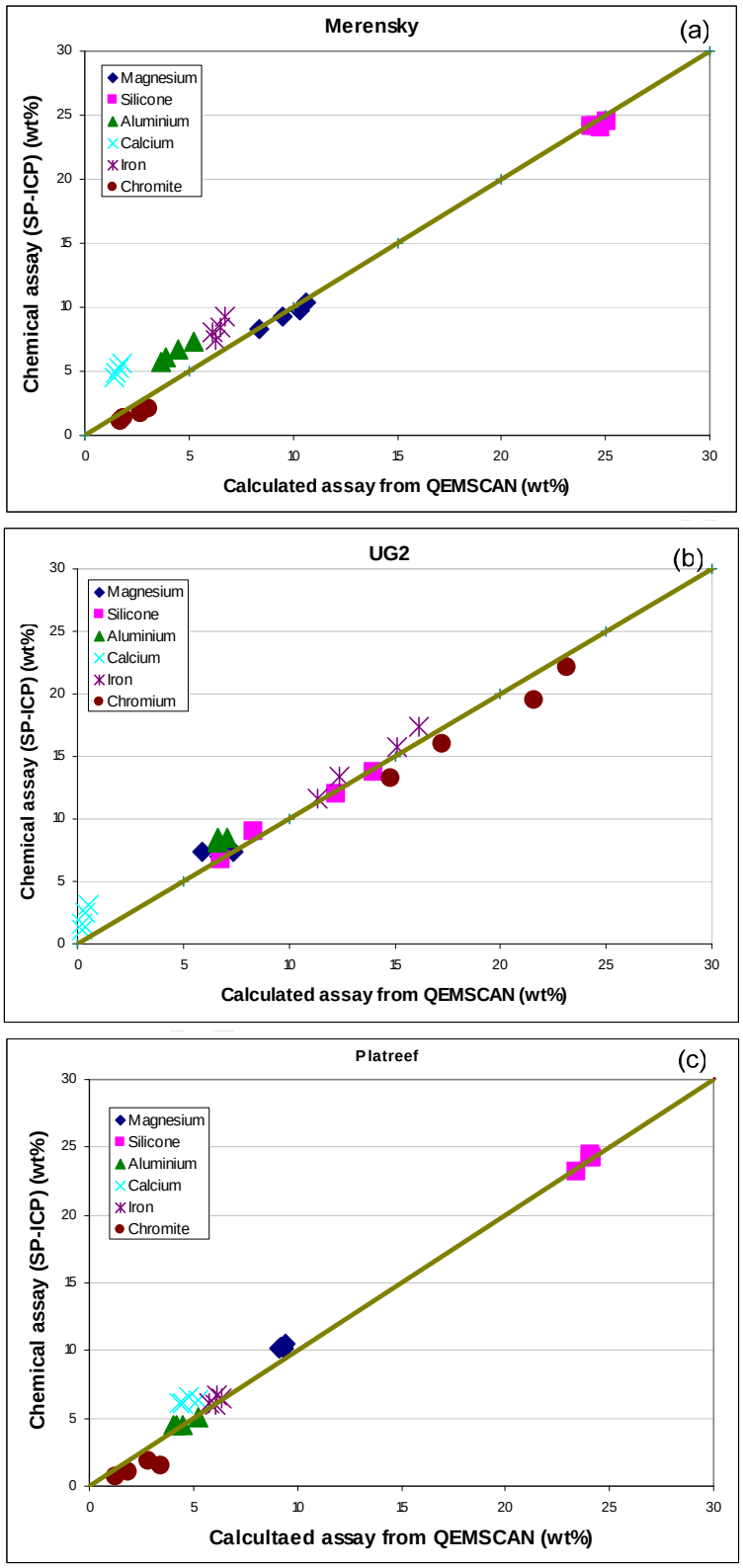

Figure 3-14: Data validation of QEMSCAN assays with chemical assays for (a) Merensky, (b) UG2 and (c) Platreef

Chapter 4

4 Effect of HPGR and Ball mill on platinum ores

Overview: This chapter presents the results obtained from the tests performed with the HPGR at different variables. The influence of HPGR variables on throughput, specific energy consumption and product size distributions for Merensky, UG2 and Platreef ores are presented. Ball mill test results have also been presented in this chapter focusing on throughput, product size distribution and specific energy consumption.

4.1 Effect of various operational and design features of HPGR

The results presented in this section show the effects of the two operating variables pressure and zero gap on specific energy consumption, throughput, size distributions, the reduction ratio (F_{50}/P_{50}) and the number of passes. The specific energy (kWh/t) was calculated in order to determine the amount of energy imparted by the comminution device on to the ore without the no-load power. This quantity was considered because it has been traditionally applied in literature as a basis to compare the energy consumption of different comminution devices. The relationship between the specific energy and the reduction ratio has been analysed to determine the efficiency of the HPGR at different variables for each ore type.

4.1.1 Repeatability analysis

Reproducibility tests were performed on selected HPGR tests as discussed in section 3.3.1 and the results can be obtained in Appendix A which gives the HPGR raw data. Table 4-1 shows the results obtained from the reproducibility analysis. Analysis of variance (ANOVA) was used to determine any differences between repeat tests. The results obtained show that confidence intervals less than 95% were obtained for the repeat tests performed. This indicates that there is no significant difference between the repeat tests performed suggesting that the HPGR tests were reproducible.

Table 4-1: Results obtained from the reproducibility analysis

Sample repeated	Confidence intervals (%)		
	Throughput	Specific energy	Power draw
	Merensky		
60bar, 6mm feed, 3mm zero gap	82.3	69.0	79.3
150bar, 12mm feed, 3mm zero gap	29.5	87.4	89.9
	UG2		
150bar, 12mm feed, 1.5mm zero gap	28.9	4.5	6.4
150bar, 6mm feed, 1.5mm zero gap	43.5	35.1	8.7
60bar, 12mm feed, 3mm zero gap	81.9	89.9	61.1
	Platreef		
150bar, 12mm feed, 1.5mm zero gap	6.9	15.2	8.1
60bar, 6mm feed, 3mm zero gap	89.6	89.9	17.0

4.1.2 Effects on throughput

Pressure effects

Figure 4-1 shows the relationship between the number of passes and throughput of the HPGR at various pressures (60 – 150bar) for Merensky (a), UG2 (b) and Platreef (c). The results shown were generated at the 1.5mm zero gap and 12mm feed top size. Merensky ore shows a general decrease in throughput as the number of passes increased at each pressure. Slight increases in throughput were observed after the third pass at pressures of 60bar, 120bar and 150bar. However, further decreases in throughput were observed at the fifth pass at the 90bar and 150bar pressures. In terms of pressure effects, while there was no significant difference in throughput between 90bar and 120bar, the general trend shows that there was a decrease in throughput as the pressure increased. However, pressure did not seem to affect throughput at the first pass at pressures 90bar, 120bar and 150bar, it was only from the second pass that the differences in throughput were observed.

UG2 ore (Figure 4-1 (b)) shows slight decreases in throughput as the number of passes increased. For pressures 90bar, 120bar and 150bar, there was no significant difference in pressure. At 60bar slightly higher throughputs were observed after the second pass.

Platreef ore (Figure 4-1(c)) showed similar throughputs between the first and second passes, suggesting that the coarse content at the second passes was still high. A steady decrease in throughput was observed between the second and fourth passes before leveling off between pass 4 and 5.

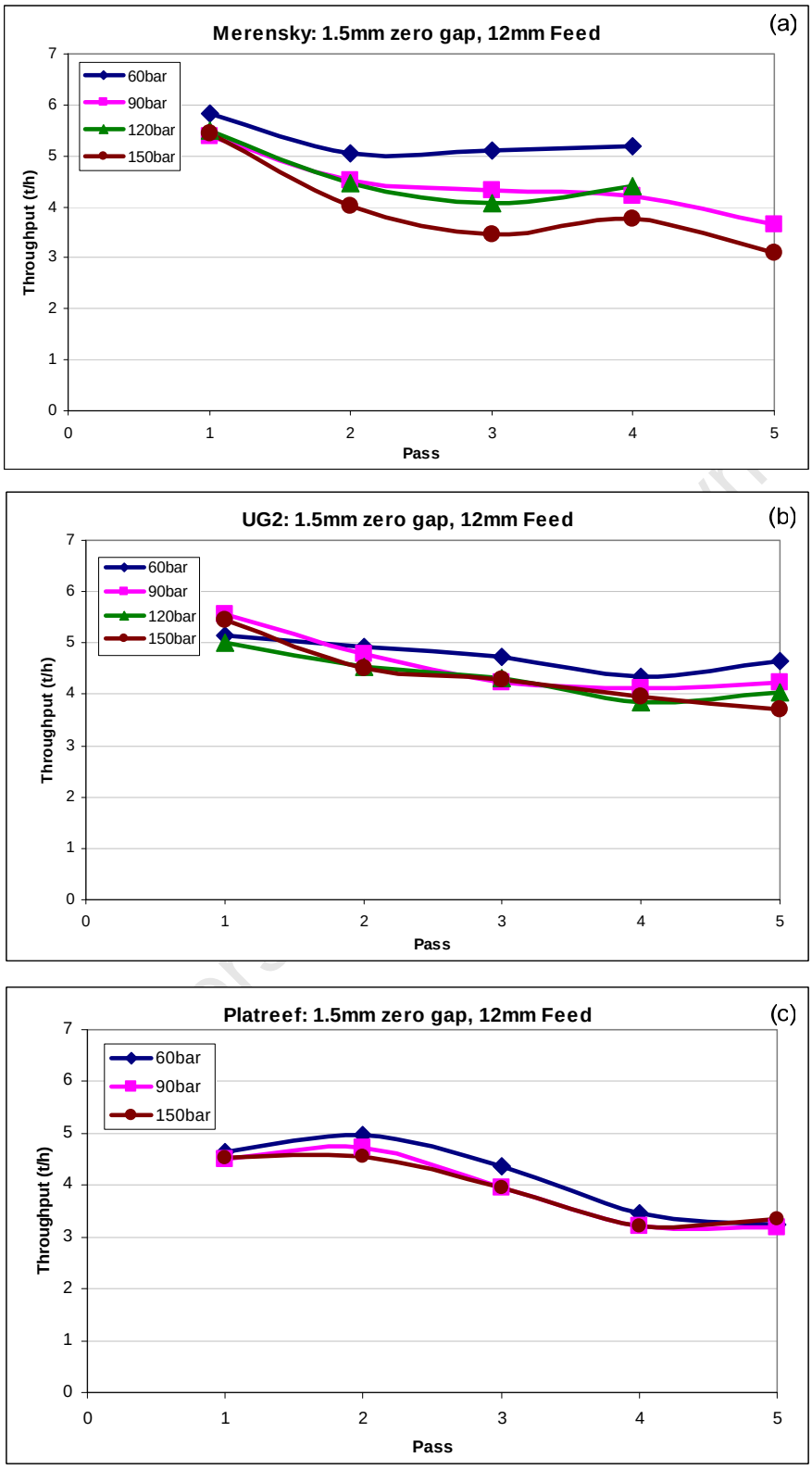

Figure 4-1: Effect of pressure and number of passes on throughput for Merensky (a), UG2 (b) and Platreef (c)

Zero gap effects

Figure 4-2 shows the effect of the number of passes and zero gap on throughput for Merensky (a), UG2 (b) and Platreef (c). A decrease in throughput was observed from the first to third passes for the 1.5mm and 3mm zero gaps after which there was an increase at the fourth passes. However, the 1.5mm zero gap shows a decrease in throughput at the fifth pass. No significant differences in throughput were observed at the first two passes between the two zero gaps. The 3mm zero gap showed higher throughputs compared to the 1.5mm zero gap after the second pass.

For UG2 (Figure 4-2(b)), the 3mm zero gap has slightly higher throughput compared to the 1.5mm zero gap except at the third pass. However, for the 4.5mm zero gap, the throughput remained constant at approximately 4.8t/h for the first three passes before increasing sharply to 5.7t/h at the fourth pass.

Platreef ore (Figure 4-2(c)) showed no significant difference in throughput between the 1.5mm and 3mm zero gaps for the first three passes. The 3mm zero showed a higher throughput at the fourth pass compared to the 1.5mm zero gap. The 4.5mm zero gap showed higher throughputs at the 2^{nd} and 3^{rd} passes compared to the 1.5mm and 3mm zero gaps.

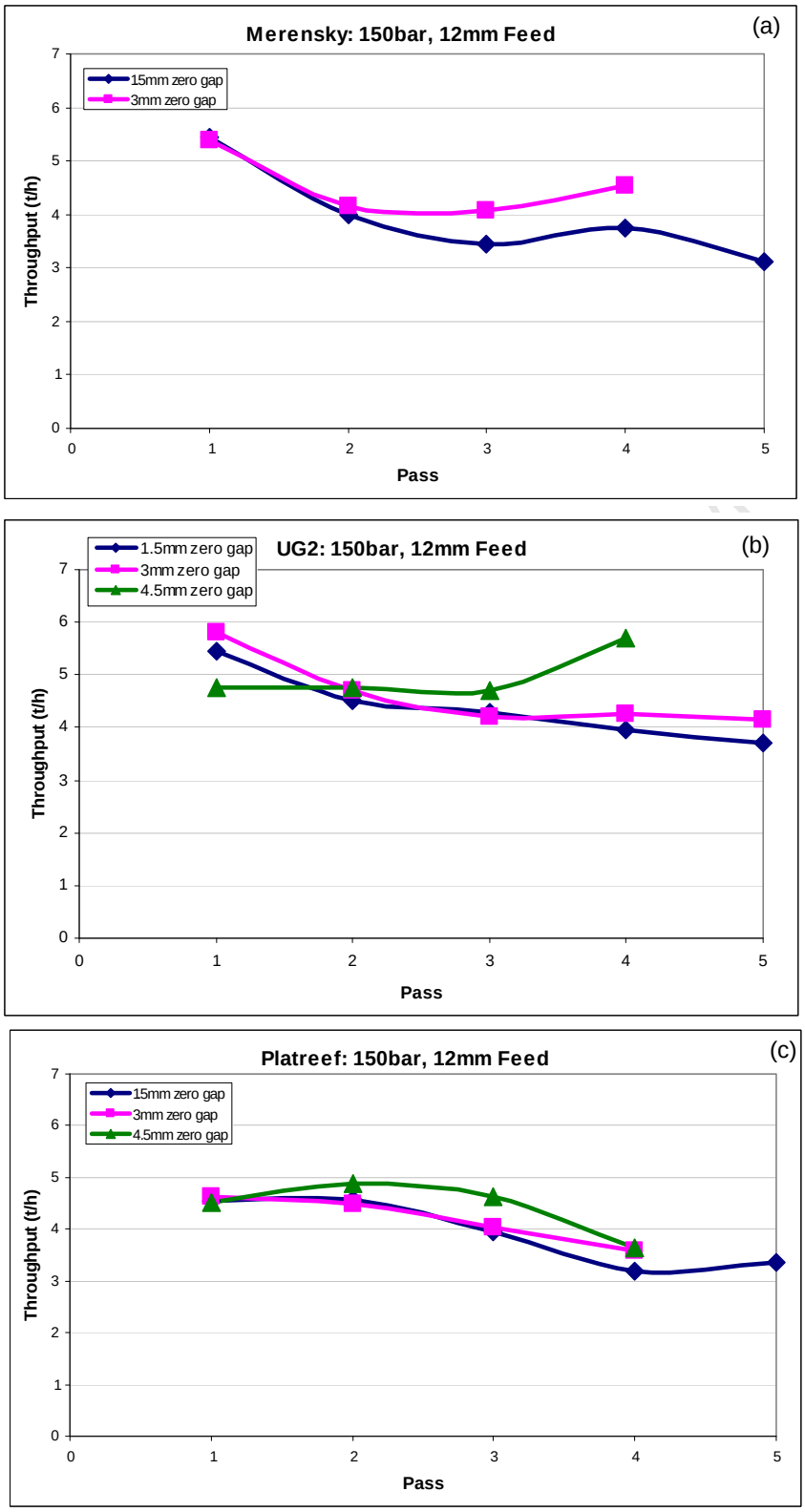

Figure 4-2: Effect of zero gap and number of passes on throughput for Merensky (a), UG2 (b) and Platreef (c)

4.1.3 Working gap

The working gap determines the largest particle that can pass through the rolls of the HPGR without being broken. This could have an effect on the product size distribution obtained. It is also an important variable that determines the throughput of the HPGR. Therefore in this work, the working gap has been presented to confirm the throughput results shown in the previous section.

Pressure effects

Figure 4-3 shows the effect of pressure and number of passes on the working gap for Merensky (a), UG2 (b) and Platreef (c) generated at a zero gap of 1.5mm and a feed topsize of 12mm. For Merensky ore, the general trend shows that as the number of passes increased, the working gap increased. At the first pass, there was no change in throughput observed with increasing pressure. However in subsequent passes the pressure showed general decreases in working gap as the pressure increased. This is consistent with the trends observed on the effects of the number of passes on throughput.

UG2 ore (Figure 4-3(b)) also showed general decreases in working gap with increasing number of passes. At 60bar and 90bar, no significant differences in working gap were observed for all passes. Slightly larger working gaps were observed at 150bar after the second pass compared to pressures at 60bar and 90bar. At 120bar, for the first pass the working gap was lower compared to the other pressures.

Platreef ore (Figure 4-3(c)) also showed decreases in working gap as the number of passes increased. A decrease in working gap was observed with increasing pressure for the first three passes. After the third pass, the 150bar pressure showed larger working gap compared to pressures at 60bar and 90bar.

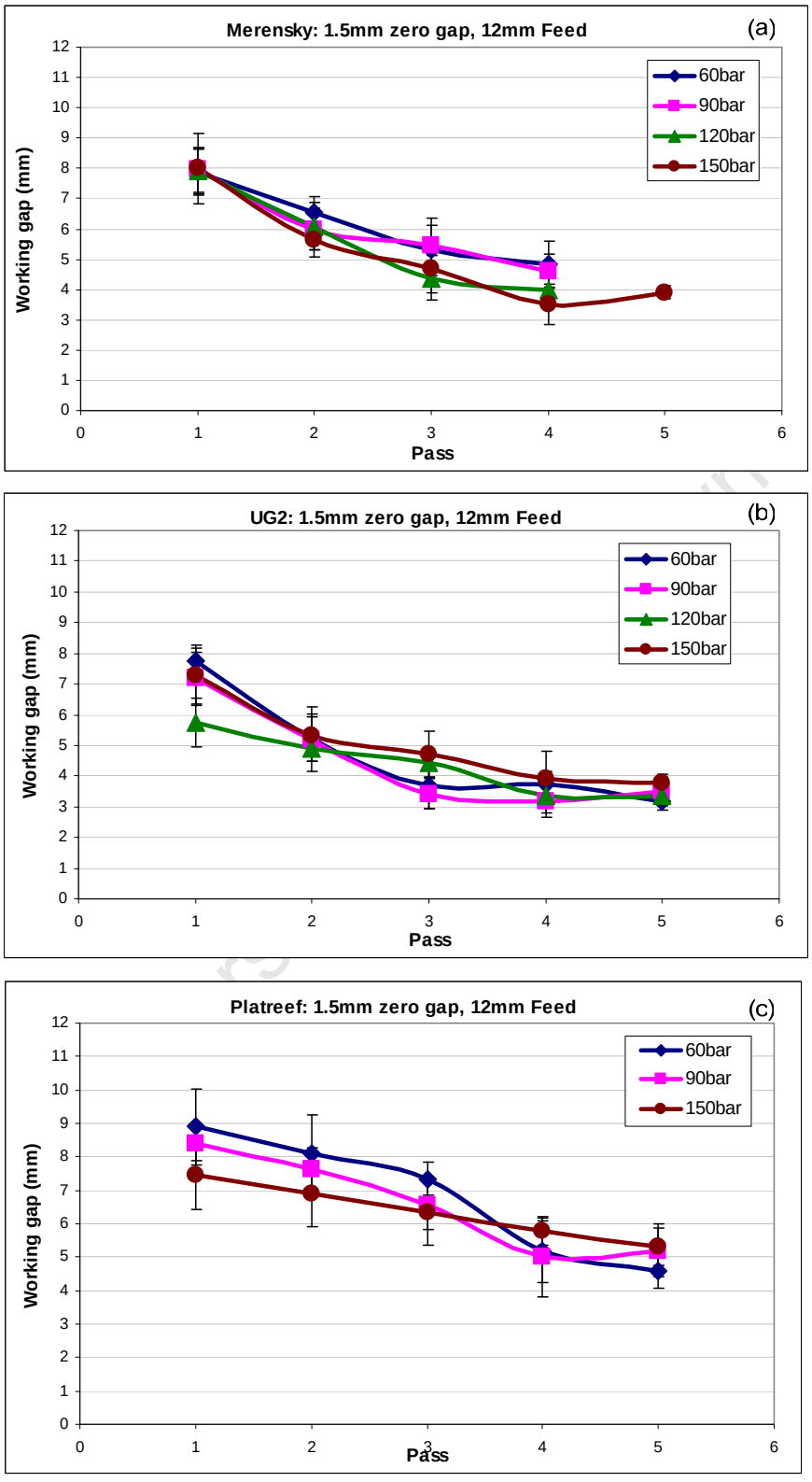

Figure 4-3: Effect of pressure and number of passes on the working gap of Merensky (a), UG2 (b) and Platreef (c)

Zero gap effects

Zero gap effects on working gap are shown in Figure 4-4 for Merensky (a), UG2 (b) and Platreef (c) at a pressure of 150bar and feed topsize of 12mm. Merensky ore showed larger working gaps for the 3mm zero gap after the first pass compared to the 1.5mm zero gap. This is consistent with the effect of zero gap on throughput for Merensky ore.

For UG2 ore (Figure 4-4(b)) shows larger working gaps at the 4.5mm zero gap compared to the 1.5mm and 3mm zero gaps. No flakes were formed at the fourth pass for the 4.5mm zero gap. Slightly larger working gaps were obtained at the 1.5mm zero gap compared to the 3mm zero gap.

Platreef ore showed no significant differences in working gap between the 1.5mm and 3mm zero gap for the first two passes. After the second pass, slightly larger zero gaps were obtained for the 1.5mm zero gap. At the 4.5mm zero gap, the number of passes did no change the working gap significantly.

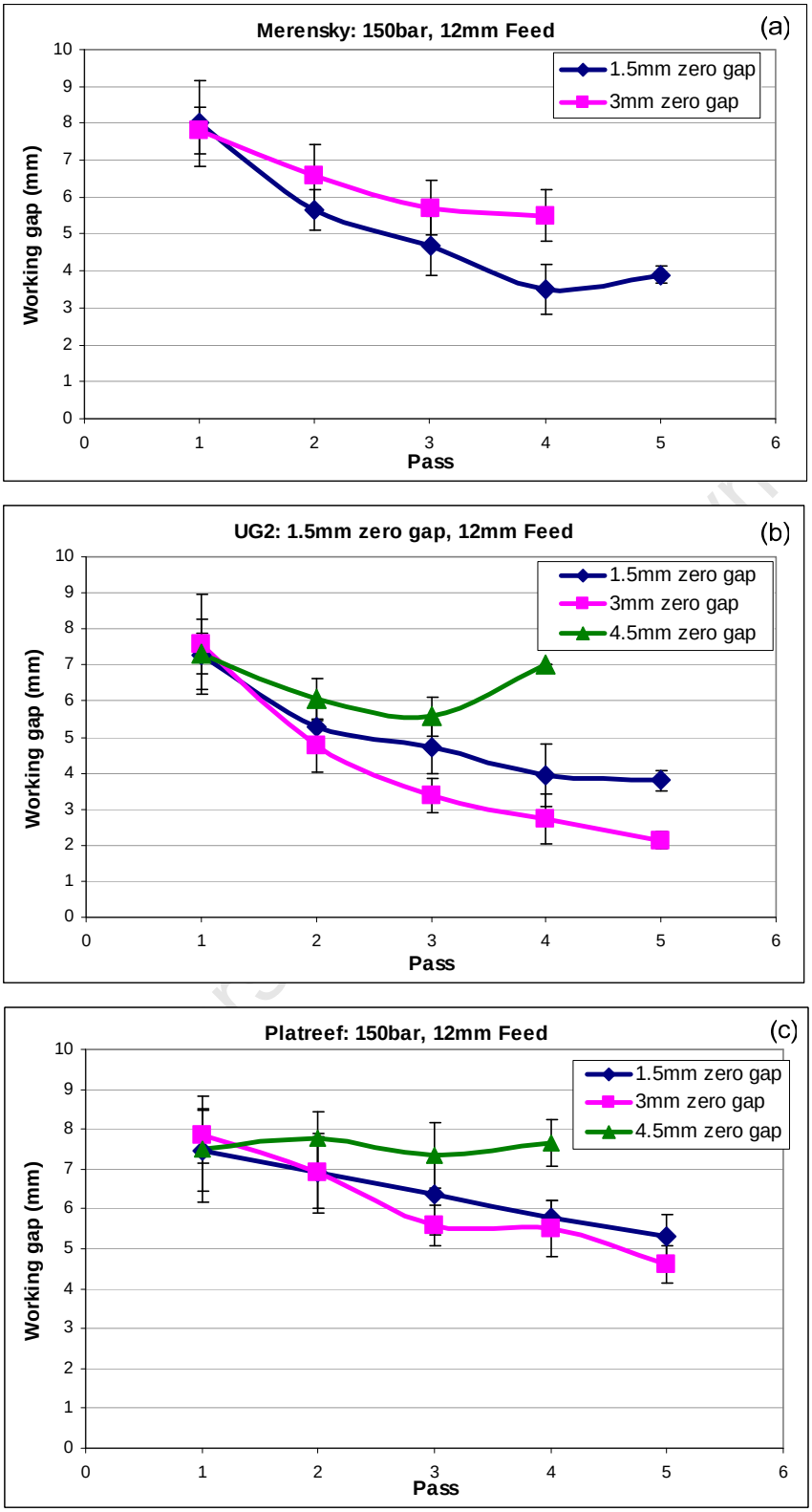

Figure 4-4: Effect of zero gap and number of passes on the working gap of Merensky (a), UG2 (b) and Platreef (c)

4.1.4 Effects on size distributions

The effects of the HPGR pressure and zero gap have been analysed to determine their effects on size distributions and the fineness of grind that can be achieved on the platinum bearing ores under consideration. The feed top size and the number of passes are also among the variables that have also been considered. In order to evaluate the effects of these variable individually, separate sections have been allocated to each for clarity. The following section looks at the effect of the number of passes.

Number of passes

Figure 4-5 shows the size distributions obtained at multiple passes for Merensky (a), UG2 (b) and Platreef (b) at a pressure of 150bar, a zero gap of 1.5mm and feed top size of 12mm. For Merensky ore, parallel size distributions were obtained as the material became progressively finer with each subsequent pass. However, the size reduction obtained appears to decrease with each pass until a point where the size distributions appear to be similar was reached. As discussed in section 2.2.4, this point is known as the saturation point. Merensky appears to have reached the saturation point after 4 passes as can be seen by the identical size distributions obtained at passes four and five.

Similarly for UG2 (Figure 4-5(b)) the material became finer with increasing number of passes. UG2 seams to also have reached saturation after the 4^{th} pass. The UG2 size distributions are bimodal, which is a common feature with this ore type.

For Platreef ore (Figure 4-5(c), it appears that the saturation point had not been reached even after five passes. Similar trends have been observed at different pressures, zero gaps and feed top sizes which are not shown here. The following section presents the effects of pressure and zero gap on the fineness of grind obtained (% passing 75μm) at different pressures and zero gap. This grind was used as a reference because it was on this basis that the samples for the flotation tests were selected.

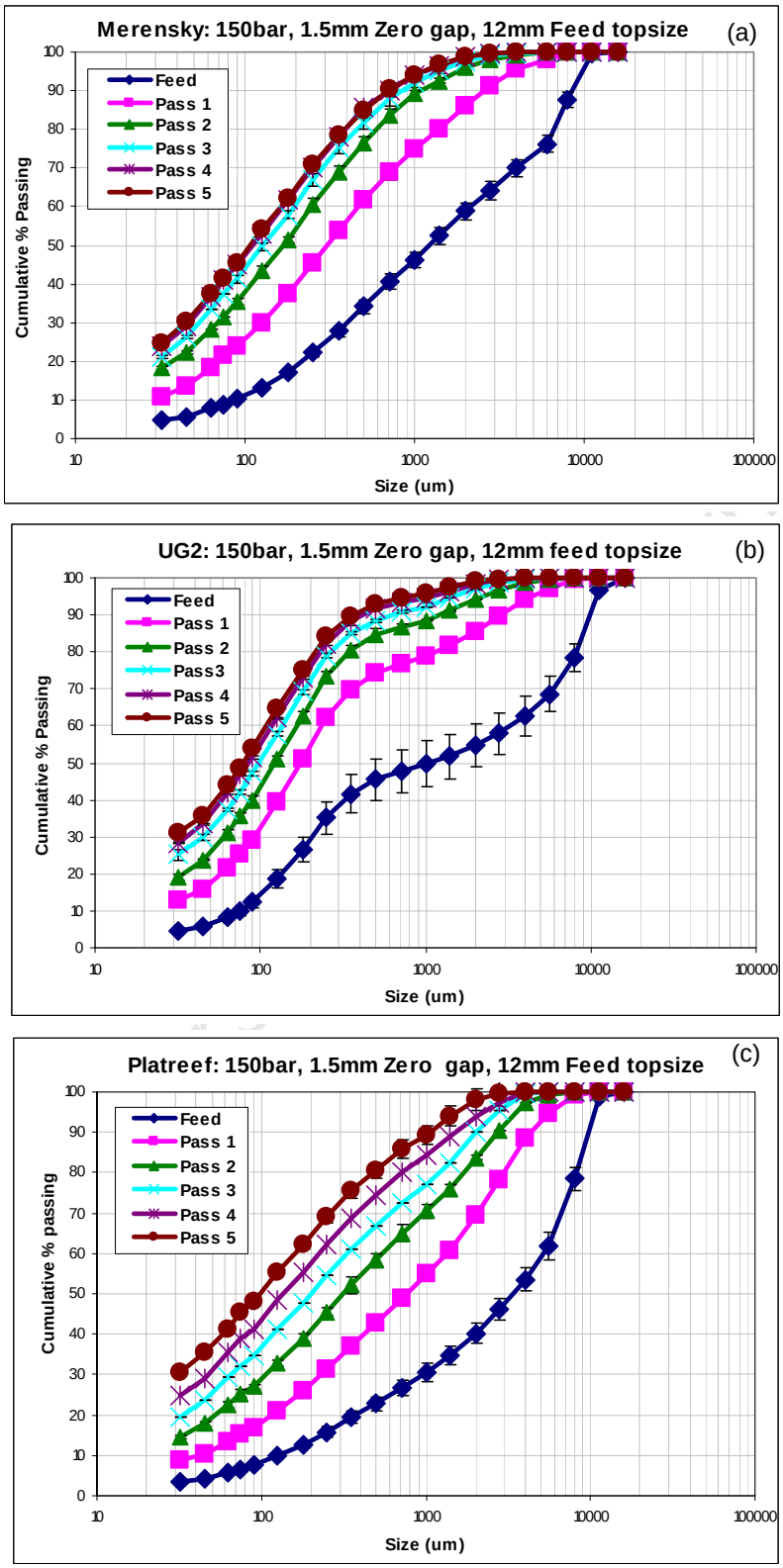

Figure 4-5: Effect of number of passes on the size distributions of Merensky (a), UG2 (b) and Platreef (c)

Effect of pressure on % passing 75µm

Figure 4-6 shows the effect of pressure and the number of passes on the % passing 75µm for Merensky (a), UG2 (b) and Platreef (c) at a zero gap of 1.5mm zero gap and 12mm feed top size. Merensky shows that the product became finer with increasing number of passes. This is consistent with the size distributions shown in Figure 4-5. Similar grinds were obtained at 90bar and 120bar however the general trend shows that increasing the pressure resulted in an increase in the fineness of grind. The difference in the fineness of the product between the tests performed at 60bar and 150bar appears to be significantly larger at the fourth passes compared to that at the first passes. Saturation points were reached after 4 passes for pressures 90bar and 150bar.

UG2 also shows increasing fineness of grind with increasing number of passes as shown in Figure 4-6(b). No differences in fineness of grind were observed for the first two passes at pressures 90bar, 120bar and 150bar. After the second pass, the grind became finer with increasing pressure. Coarser grinds were obtained at 60bar from the second to the fifth pass. Platreef ore shows increasing fineness of grind with increasing pressure for all the five passes shown in Figure 4-6(c).

Effect of zero gap on % passing 75µm

Figure 4-7 shows the effect of zero gap and the number of passes on the % passing 75µm for the three ore types at a pressure of 150bar and a feed top size of 12mm. For Merensky ore in Figure 4-7(a) there is no significant difference in the grind for the first and second pass. After the second pass, the grind becomes finer at the 1.5mm zero gap compared to the 3mm zero gap.

For UG2, there was no significant difference in the grind obtained at the 1.5mm and 3mm zero gaps in Figure 4-7(b). However, coarser material was generated at the 4.5mm zero gap where the saturation point was reached after the third pass. Platreef ore also showed no significant differences in grind at the 1.5mm and 3mm zero gaps for the first three passes. After the third pass, the 3mm zero gap had slight coarser grinds. At the 4.5mm zero gap, the grind was coarser than that at the 1.5mm and 3mm zero gaps.

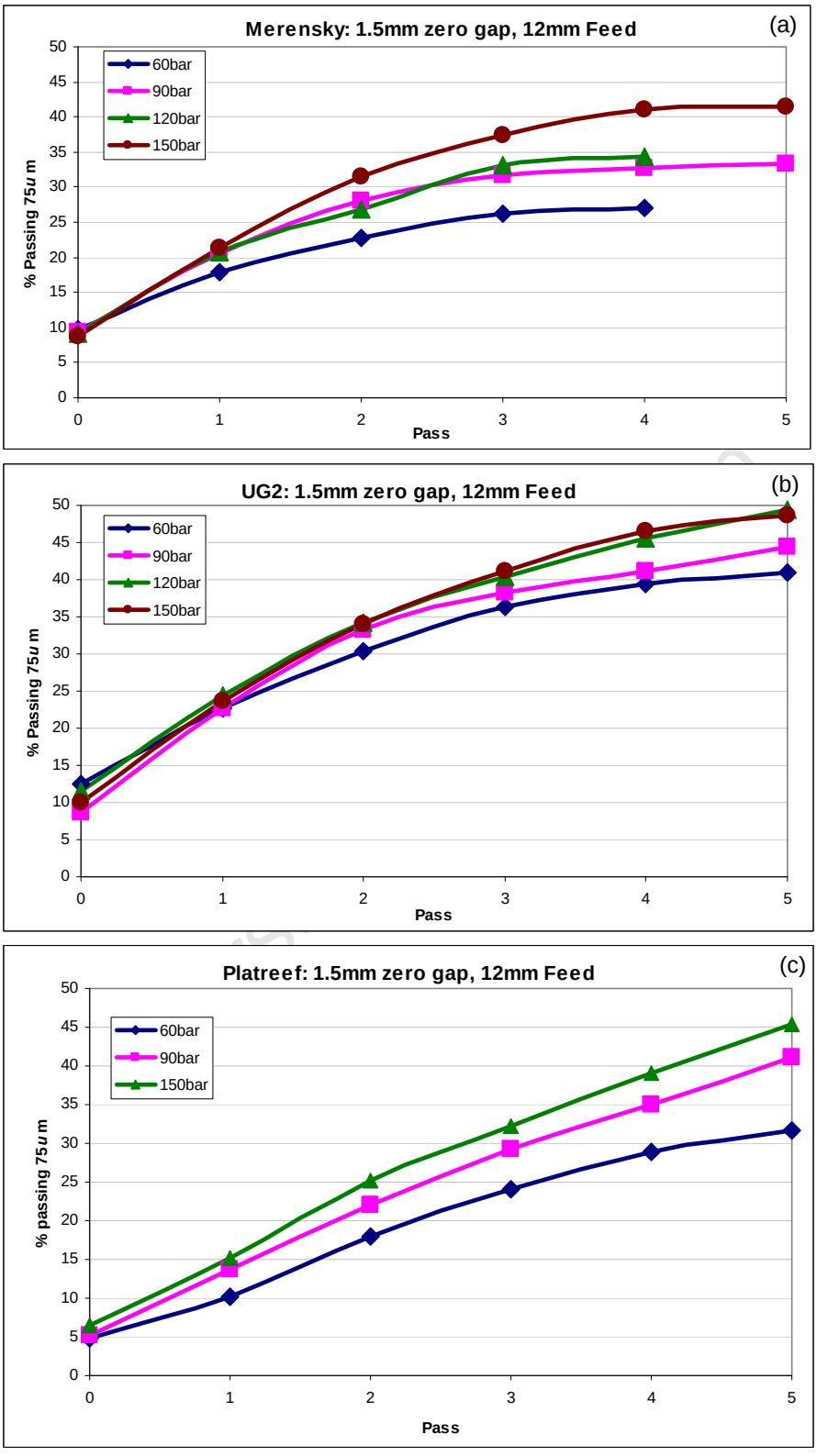

Figure 4-6: Effect of pressure and number of passes on % passing 75µm for Merensky (a), UG2 (b) and Platreef (c)

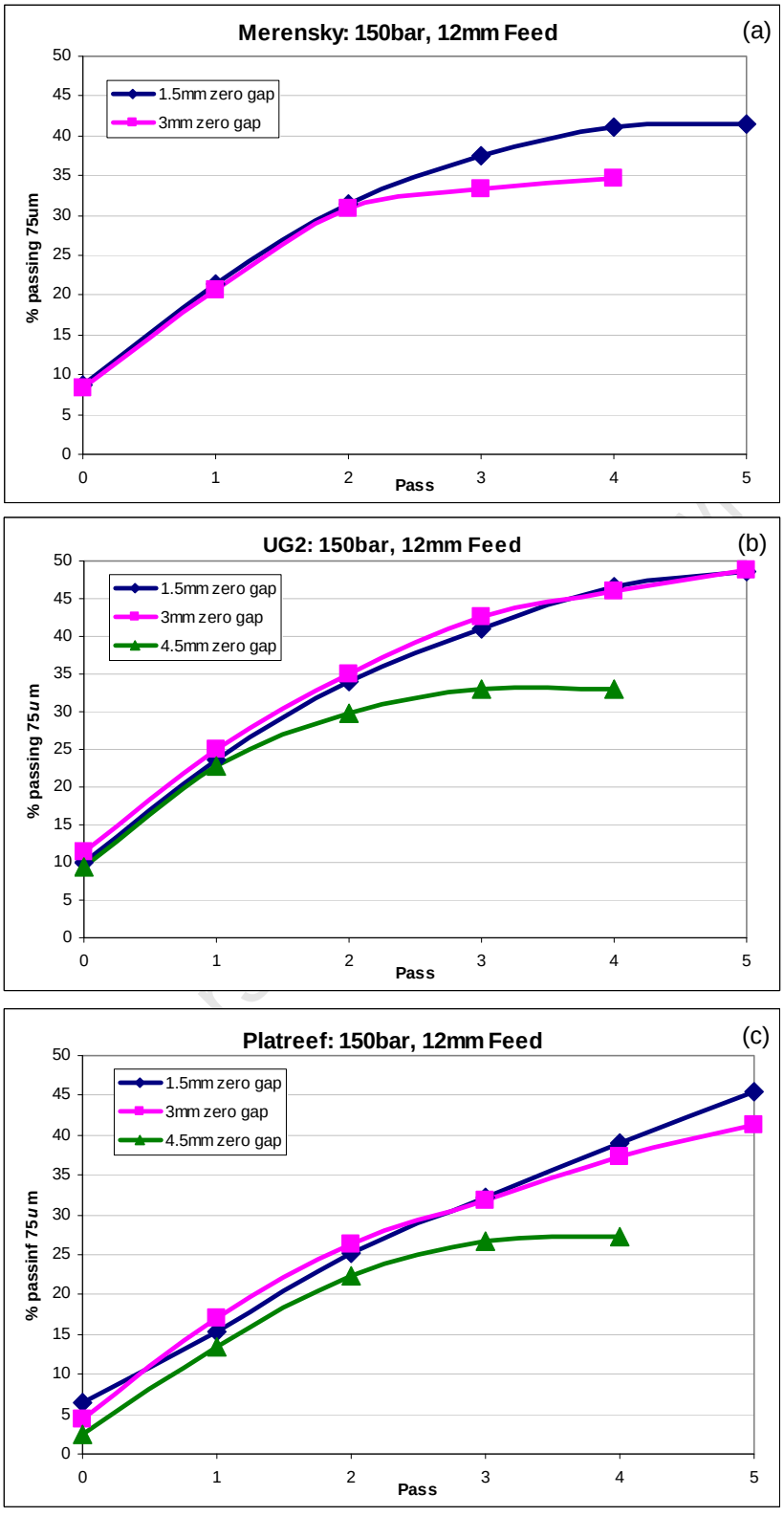

Figure 4-7: Effect of zero gap and number of passes on % passing 75µm for Merensky (a), UG2 (b) and Platreef (c)

4.1.5 Effects on cumulative specific energy

A comparison of the specific energies consumed by the three ore types was made to show the effect of ore type. The specific energy relationships shown in this section do not include the HPGR no-load power. Figure 4-8 shows the relationship between the pressure and the total specific energy consumed after four passes at a zero gap of 1.5mm and a feed top size of 12mm for Merensky, UG2 and Platreef. For each ore type, increasing the pressure resulted in an increase in the specific energy consumed. The error bars shown were obtained from repeat tests that were performed on selected tests to access repeatability. The error bars shown are within a 95% confidence interval. Platreef exhibits higher cumulative specific energy consumption compared to UG2 which in turn consumed more specific energy than Merensky. The following sub sections show the effects of pressure, zero gap and number of passes on specific energy consumed. Energy efficient application of the HPGR has been determined for each of the ores investigated with the use of reduction ratios (F_{50}/P_{50}).

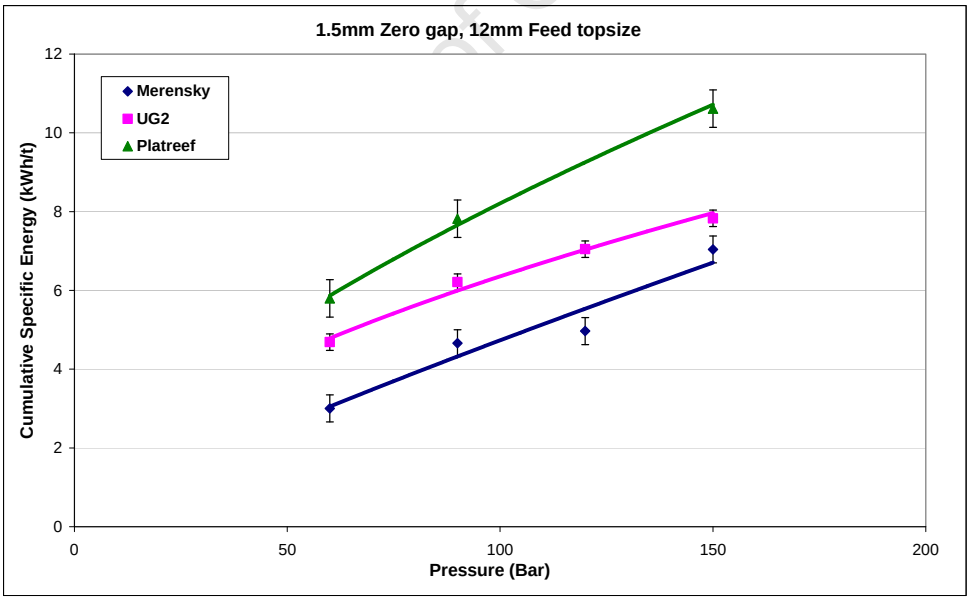

Figure 4-8: Effect of pressure on the total specific grinding energy consumed by the three platinum bearing ores

Pressure effects

Figure 4-9 shows the effect of the number of passes and pressure on the cumulative specific energy consumed for Merensky (a), UG2 (b) and Platreef (c) at a zero gap of 1.5mm and a feed topsize of 12mm. The cumulative specific energies were used to determine the effect of pressure on the total specific energy expenditure after each pass. Merensky ore shows decreasing gradients of the curves with each subsequent pass, indicating a decrease in specific energy consumption from one pass to the next. For example, at 90bar it can be seen that there was no significant difference in specific energy between passes 4 and 5, indicating that no specific energy was consumed between these passes. Increasing the pressure shows an increase in specific energy consumed. This is more evident after the first pass. Comparison of the trends observed are consistent with the results obtained with the fineness of grind analysis in Figure 4-6(a).

UG2 (Figure 4-9(b)) and Platreef (Figure 4-9(c)) also showed increasing cumulative specific energy consumption with increasing pressure. No saturation points were reached for both ore types for the HPGR variables shown.

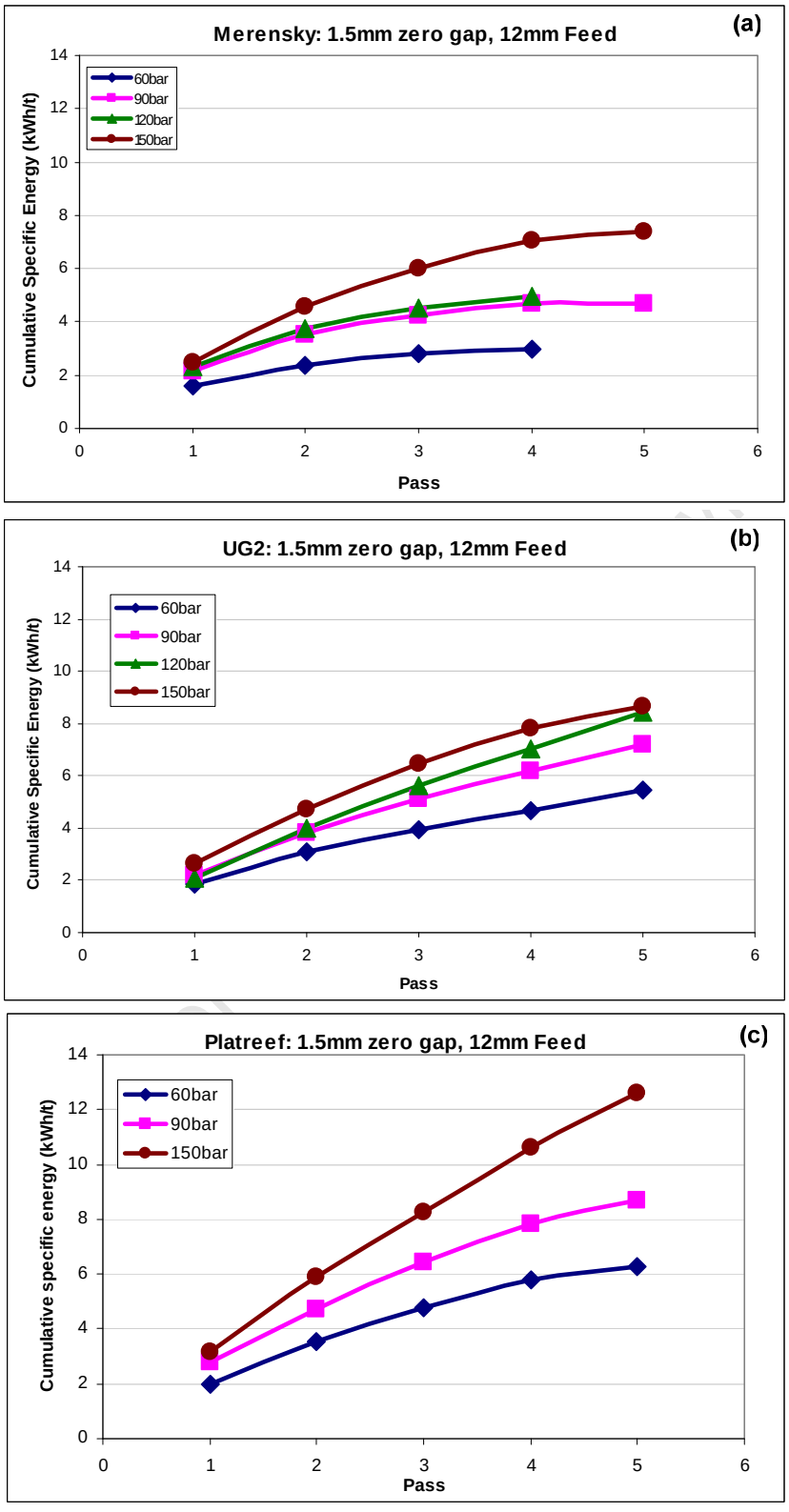

Figure 4-9: Effect of pressure on cumulative specific energy consumed for Merensky (a), UG2 (b) and Platreef (c)

Zero gap effects

Figure 4-10 shows the relationship between the cumulative specific energy and the number of passes at different zero gaps at a pressure of 150bar and a feed top size of 12mm for Merensky (a), UG2 (b) and Platreef (c). For Merensky ore, it can be seen that for the first two pass, similar cumulative specific energies were consumed at zero gaps 1.5mm and 3mm. After the second pass the 1.5mm zero gap begins to exhibit higher cumulative specific energies. At the 3mm zero gap, there was no significant difference in specific energy between passes 3 and 4, suggesting that saturation was reached. This is consistent with the % passing 75µm data (Figure 4-2(a)) which showed no significant change in the grind between pass 3 and 4.

For UG2, slightly higher cumulative specific energy was consumed at the 1.5mm zero gap compared to the 3mm zero gap. Much lower specific energies were consumed at the 4.5mm zero gap particularly at the higher passes where that material was finer. However, no significant difference in cumulative specific energy was observed between pass 3 and 4 at the 4.5mm zero gap.

Platreef ore showed similar specific energies at the first three passes after which the 3mm zero gap showed lower specific energies. At the 4.5mm zero gap, lower cumulative specific energies were consumed compared to the 1.5mm and 3mm zero gaps.

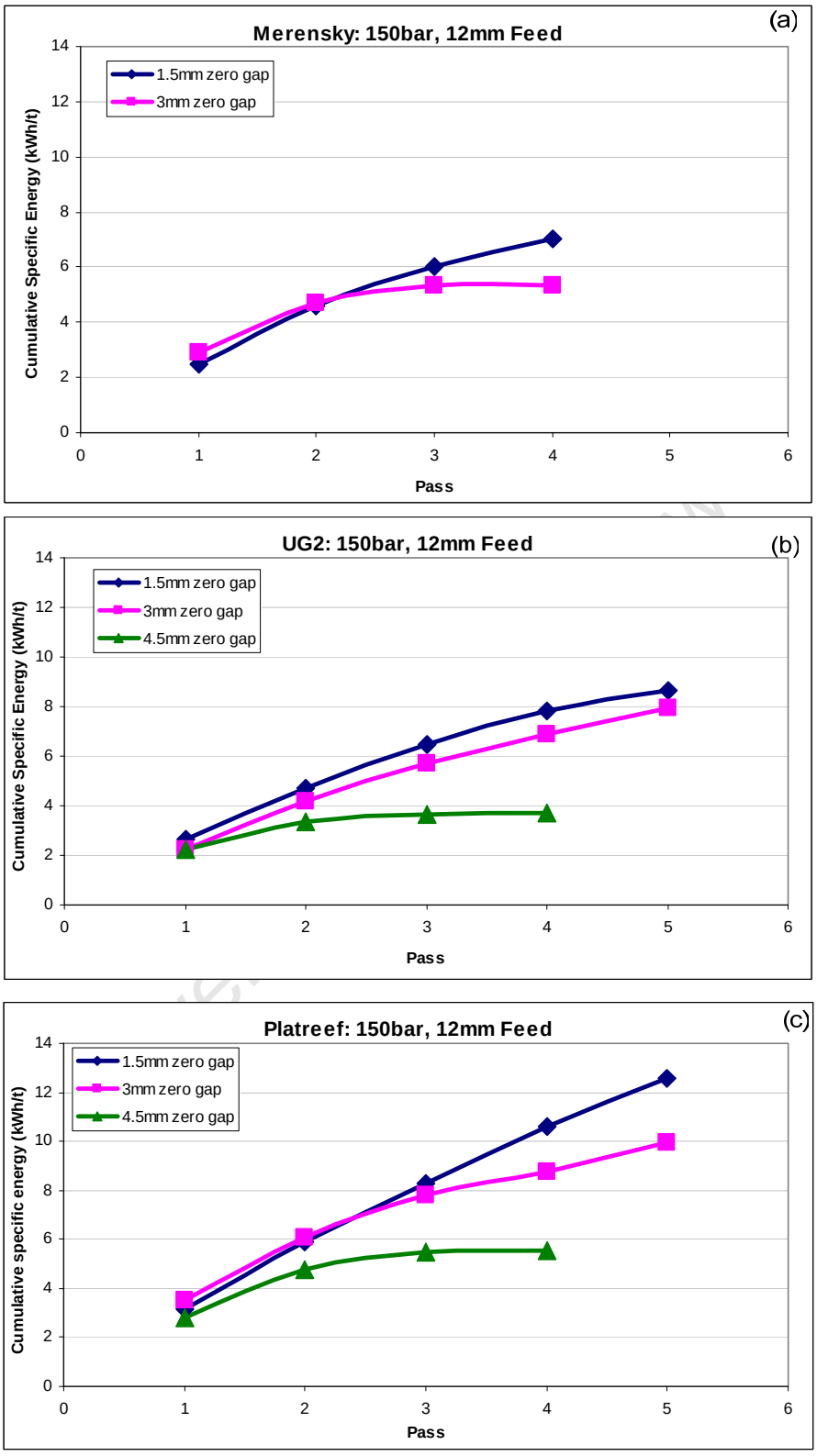

Figure 4-10: Effect of zero gap on cumulative specific energy consumed for Merensky (a), UG2 (b) and Platreef (c)

Similar specific grinding energies consumed

It was found that at different HPGR variables, some tests showed similarities in specific energy consumption. Comparisons have been made in terms for the grind obtained at these tests. Table 4-2 shows the percent passing 75µm of Merensky, UG2 and Platreef for tests where a similar amount of cumulative specific energy was obtained. The data presented is for a feed top size of 12mm. For Merensky ore, it has been observed that for tests performed at 60bar for a zero gap of 3mm after four passes, a specific energy of 3.36kWh/t was consumed while at 90bar after two passes, 3.40kWh/t was consumed. The percent passing 75µm under these conditions was 30.6% and 22%, respectively.

Table 4-2: Comparison of the grind (% passing 75µm) obtained at different HPGR settings exhibiting similar specific energies for a 12mm feed

Ore type	HPGR settings	Pass number	Total Specific energy (kWh/t)	% passing 75µm
Merensky	60bar, 3mm gap	4	3.36	30.6
	150bar, 3mm gap	2	3.40	22.0
UG2	60bar, 1.5mm gap	4	4.69	39.5
	150bar, 1.5mm gap	2	4.74	34.0
Platreef	60bar, 1.5mm gap	4	5.80	28.8
	150bar, 1.5mm gap	2	5.93	25.2

For UG2 ore, it was found that a 60bar at a zero gap of 1.5mm after four passes, a total specific energy of 4.69kWh/t was consumed and at 150bar for the same zero gap after two passes, 4.74kWh/t was consumed. However, the percent passing 75µm under these conditions was 39.5% and 34.0%, respectively. This suggests that to achieve a higher fineness of grind at lower specific energies, several passes are required at lower pressures. Similar results were obtained for Platreef ore where it was found that at for a zero gap of 1.5mm at 60bar after four passes the total specific energy consumed was 5.80kWh/t and that at 150bar for the same zero gap after two passes 5.93kWh/t. A finer grind of 28.8% passing 75µm was obtained at the lower pressure compared to the higher pressure where the grind was 25.2% passing 75µm.

Maximum grinds of up to 41.5%, 47.6% and 36.9% passing 75µm were obtained after five passes for Merensky, UG2 and Platreef, respectively. Depending on the grind required, the HPGR parameters can be adjusted to ensure that more energy efficient conditions are applied. The energy efficiency of the HPGR can be determined through the relationship between the reduction ratio (F_{50}/P_{50}) and the specific energy. The following section presents the data showing the effects of the HPGR variables on reduction ratio.

4.1.6 Effects on reduction ratios (F_{50}/P_{50})

The reduction ratio (F_{50}/P_{50}) is the relationship between the feed median size (F_{50}) and the product median size (P_{50}). This section shows effects of the pressure and zero gap settings on reduction ratios.

Pressure effects

Figure 4-11 shows the effects of pressure and number of passes on reduction ratios (F_{50}/P_{50}) for Merensky (a), UG2 (b) and Platreef (c) ores at a zero gap of 1.5mm and a feed top size of 12mm. Pass zero is the feed at which point the reduction ratio (F_{50}/F_{50}) is equal to one. For Merensky (Figure 4-11(a)), it can be seen that the reduction ratio at the first pass is much higher than those at subsequent passes. A sharp decrease in reduction ratio was observed between the first and second passes. At the first pass, as the pressure increased, the reduction ratios also increased. In subsequent passes, differences in reduction ratios with changing pressure are not significant. A similar outcome was observed for UG2 (Figure 4-11(b)) and Platreef (Figure 4-11(c)). However, for Platreef ore there is a more gradual decrease in reduction ratio as the number of passes increased. While Merensky and UG2 show a reduction ratio approaching 1 after the first pass, Platreef reached this point after four passes.

Zero gap effects

Figure 4-12 shows the effect of zero gap on reduction ratio for Merensky (a), UG2 (b) and Platreef (c) ores at a pressure of 150bar and a feed topsize of 12mm. For Merensky ore, the 1.5mm and 3mm zero gap show no effect on the reduction ratio achieved for all passes. For UG2 ore (Figure 4-12(b)), increasing the zero gap resulted in an increase in the reduction ratio at the first pass. However after the first pass, no significant differences in reduction ratios were observed for all pressures tested.

For Platreef ore (Figure 4-12(c)), the reduction ratios are significantly lower at the 4.5mm zero gap compared to the 1.5mm and the 3mm zero gap for the first pass. No significant differences in reduction ratios were observed from pass 2 to pass 5. At the 1.5mm, 3mm and 4.5mm zero gaps, there are no differences in reduction ratios from the second to the fifth pass. At the fourth and fifth passes, the reduction ratios are higher for the 3mm zero gap than at the 1.5mm zero gap.

The following section presents the relationship between the cumulative specific energy consumed and the reduction ratios. Using this relationship, energy efficient application of the HPGR for each ore type could be determined.

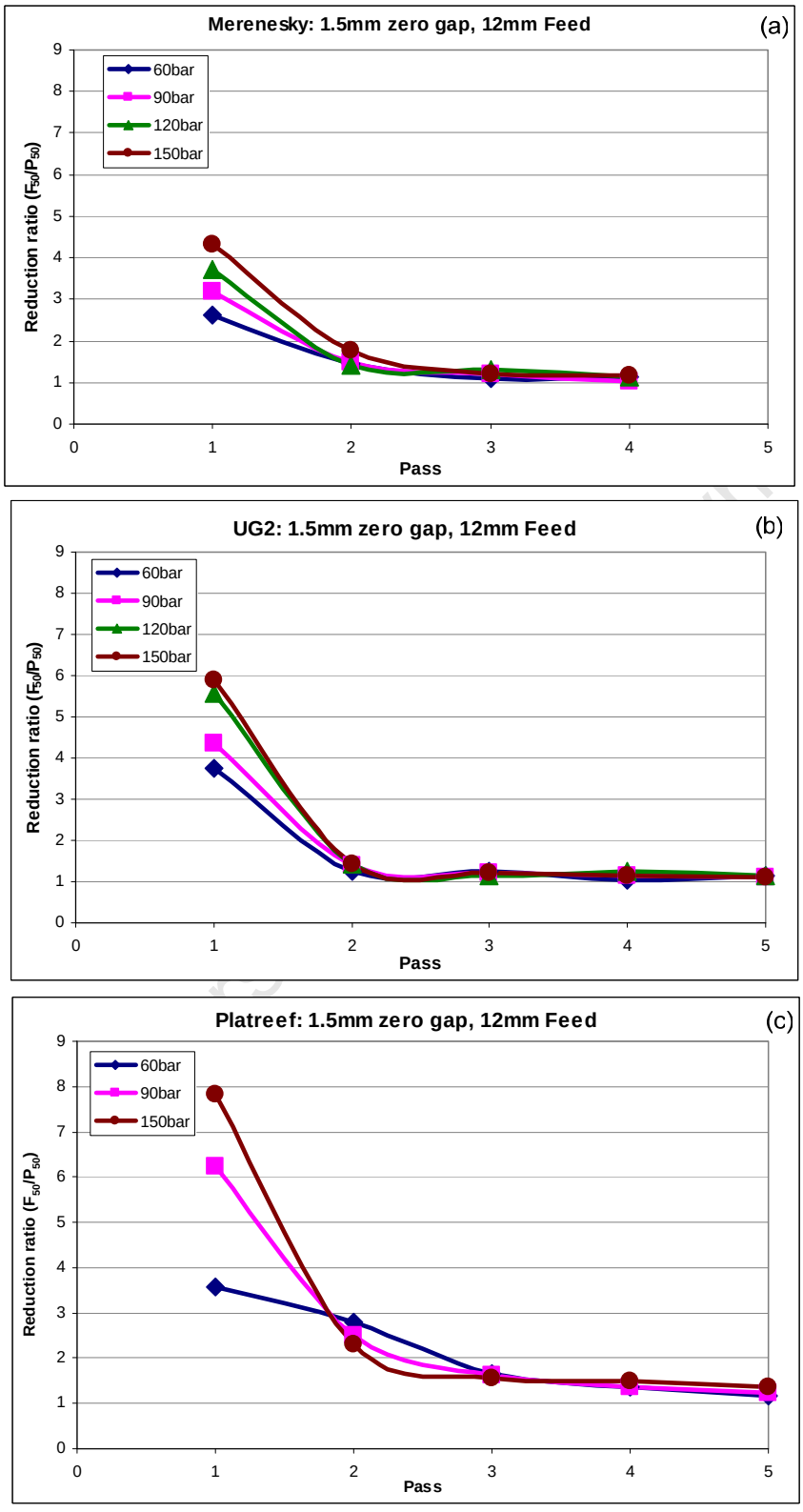

Figure 4-11: Effect of pressure and number of passes on reduction ratio (F_{50}/P_{50}) for Merensky (a), UG2(b) and Platreef ore (c) top size

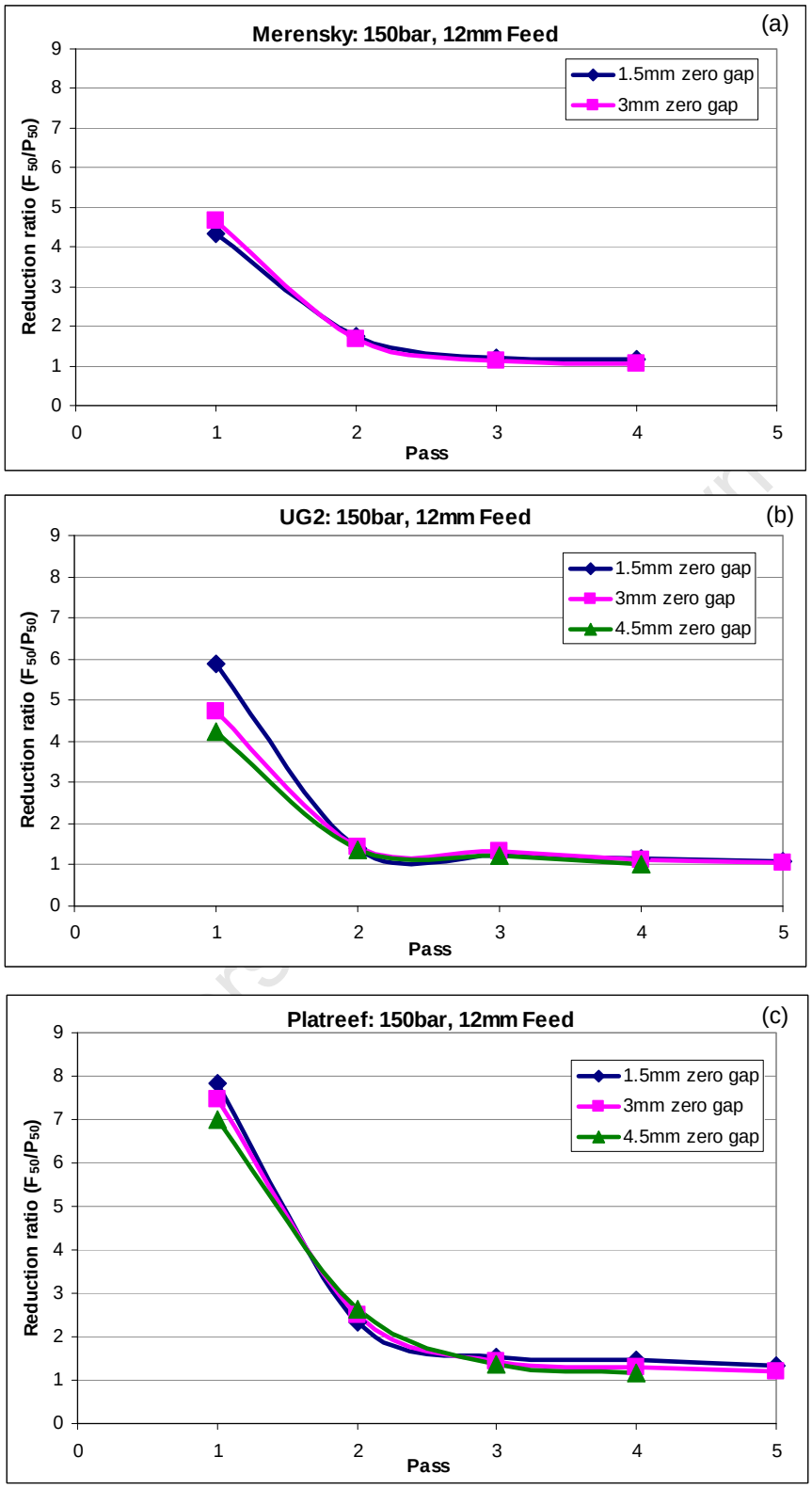

Figure 4-12: Effect of zero gap on reduction ratio for Merensky (a), UG2 (b) and Platreef (c) ores at 150bar pressure and 12mm feed top size

4.1.7 Effects on specific energy- reduction ratio relationship

This section presents the results showing the effect of pressure, zero gap and ore type on the specific energy – reduction ratio relationship. The specific energies and the reduction ratios quoted in this section are cumulative. Equation 11 developed by Norgate and Weller (1994) was fitted to the data generated in this study. As discussed in section 2.2.4, this relationship has previously been used to determine suitable operating conditions where it was more energy efficient to apply the HPGR for different ore types. Similarly, this equation has been applied to the data generated in this work to access the efficiency of the HPGR at different operating conditions for Merensky, UG2 and Platreef.

$$\frac{F_{50}}{P_{50}} = kE^{b} + 1 \qquad (11)$$

Where F_{50} is the feed median size

P_{50} is the product median size

k and b are constants that are ore dependent

E is the specific energy consumed in kWh/t

Plots of the reduction ratio (F_{50}/P_{50}) versus the cumulative specific energy after each subsequent pass were generated for each of the tests performed (Figure 4-13 and Figure 4-14). The values of k and b were generated for each ore type and have been presented for a feed top size of 12mm at different pressures and zero gaps shown in Table 4-3 and Table 4-4, respectively. The corresponding R^2 values which are an indication of how well the data fits the equation are also given. The R^2 values obtained were above 0.95 and close to unity indicating that the data generated in this work agrees with the relationship developed by Norgate and Weller (1994) for HPGR applications.

The k and b values appear to vary with pressure and zero gap for the three ore types. While no trend can be determine to show pressure and zero gap effects, the data suggests that the k and b values are dependent on ore type and HPGR operating conditions.

Table 4-3: k, b and R^2 values at different HPGR pressures

Ore type	HPGR settings	k	b	R^2
Merensky	60bar	0.912	1.24	0.952
	90bar	0.976	1.07	0.978
	120bar	0.417	1.41	0.997
	150bar	1.40	0.998	0.992
UG2	60 bar	1.69	0.756	0.977
	90bar	1.38	0.814	0.999
	120bar	1.57	0.774	0.990
	150bar	1.90	0.848	0.997
Platreef	60bar	0.829	1.86	0.999
	90bar	0.879	1.79	0.999
	150bar	0.966	1.59	0.997

Table 4-4: k, b and R^2 values at different HPGR zero gaps

Ore type	HPGR settings	k	b	R^2
Merensky	1.5mm	1.40	0.998	0.992
	3mm	1.34	1.13	0.998
UG2	1.5mm	1.90	0.848	0.997
	3mm	1.69	0.736	0.988
	4.5mm	1.95	0.864	0.990
Platreef	1.5mm	0.968	1.59	0.997
	3mm	1.02	1.60	0.980
	4.5mm	0.027	3.17	0.962

The following sub sections discuss the curves generated from the reduction ratio – specific energy data fitted using equation 11 and the pressure and zero gap effects.

Pressure effects

Figure 4-13 shows the influence of pressure on the cumulative specific energy-reduction ratio relationship for Merensky (a), UG2 (b) and Platreef (c) a zero gap of 1.5mm and a feed top size of 12mm. Although equation 11 fits well for all three ore types at the various HPGR settings, the shapes of the curves vary depending on the ore type. Merensky ore exhibits approximately linear relationships between the cumulative reduction ratio and the cumulative specific energy while both UG2 and Platreef ore exhibit non-linear relationships. Significantly larger reduction ratios were obtained for Platreef ore compared to Merensky and UG2 ore as shown in Figure 4-13. The different trends observed for the three ores emphasize the significance of ore type on the performance of the HPGR.

Table 4-5 shows some data extracted from Figure 4-13 showing the effects of pressure on reduction ratio and specific energy. The number of passes at these points has been included to assist in the discussion. For Merensky (Figure 4-13(a)), at 60bar after four passes a reduction ratio of 4.7 was achieved compared to 11 obtained at 150bar for the same number of passes. The specific energy consumed under these conditions was 3kWh/t and 7kWh/t, respectively. To achieve a reduction ratio of 4.7 at the 150 bar pressure, the ore would go through approximately one pass with a specific energy consumption of 2.6kWh/t. Therefore, approximately a 13% decrease in specific energy can be consumed if the HPGR were operated at 150bar for approximately one pass than at 60bar for four passes.

For UG2 ore (Figure 4-13(b)) at 60bar, after 4 passes a reduction ratio of 6.2 is obtained at a cumulative specific energy of 4.7kWh/t. For the same cumulative specific energy, a reduction ratio of 8 was obtained after only two passes at 150bar. It would therefore be more energy efficient to operate the HPGR at 150bar for the 1.5mm zero gap and 12mm feed top size for UG2 ore.

Table 4-5: Data extracted from Figure 4-13 showing effects of number of passes on reduction ratio (F_{50}/P_{50}) and specific energy (E_{sp})

Ore type	Pressure (bar)	Pass	F_{50}/P_{50}	E_{sp} (kWh/t)
Merensky	60	4	4.7	3.0
	150	4	11	7.0
	150	1	4.7	2.6
UG2	60	4	2.9	4.7
	150	2	8.0	4.7
Platreef	60	5	26	6.3
	90	3	26	6.5
	150	3	26	8.0

For Platreef ore (Figure 4-13(c)), to achieve a reduction ratio of 26, a cumulative specific energy of approximately 6.3kWh/t and 6.5kWh/t would be consumed at 60bar and 90bar, respectively. However, at 150bar, a cumulative specific energy of 8.0kWh/t would be consumed to achieve a similar reduction ratio. This suggests that about 20% savings in energy could be achieved if the HPGR was operated at 60bar or 90bar rather than at 150bar to achieve a reduction ratio of 26. However, it should be noted that at 60bar a reduction ratio of 26 is achieved after five passes, after three passes at 90bar and after three passes at 150bar as shown in Table 4-5. Therefore, for Platreef ore, under the conditions shown, it would be more energy efficient to operate the HPGR at lower pressures for multiple pass operations to achieve a certain reduction ratio.

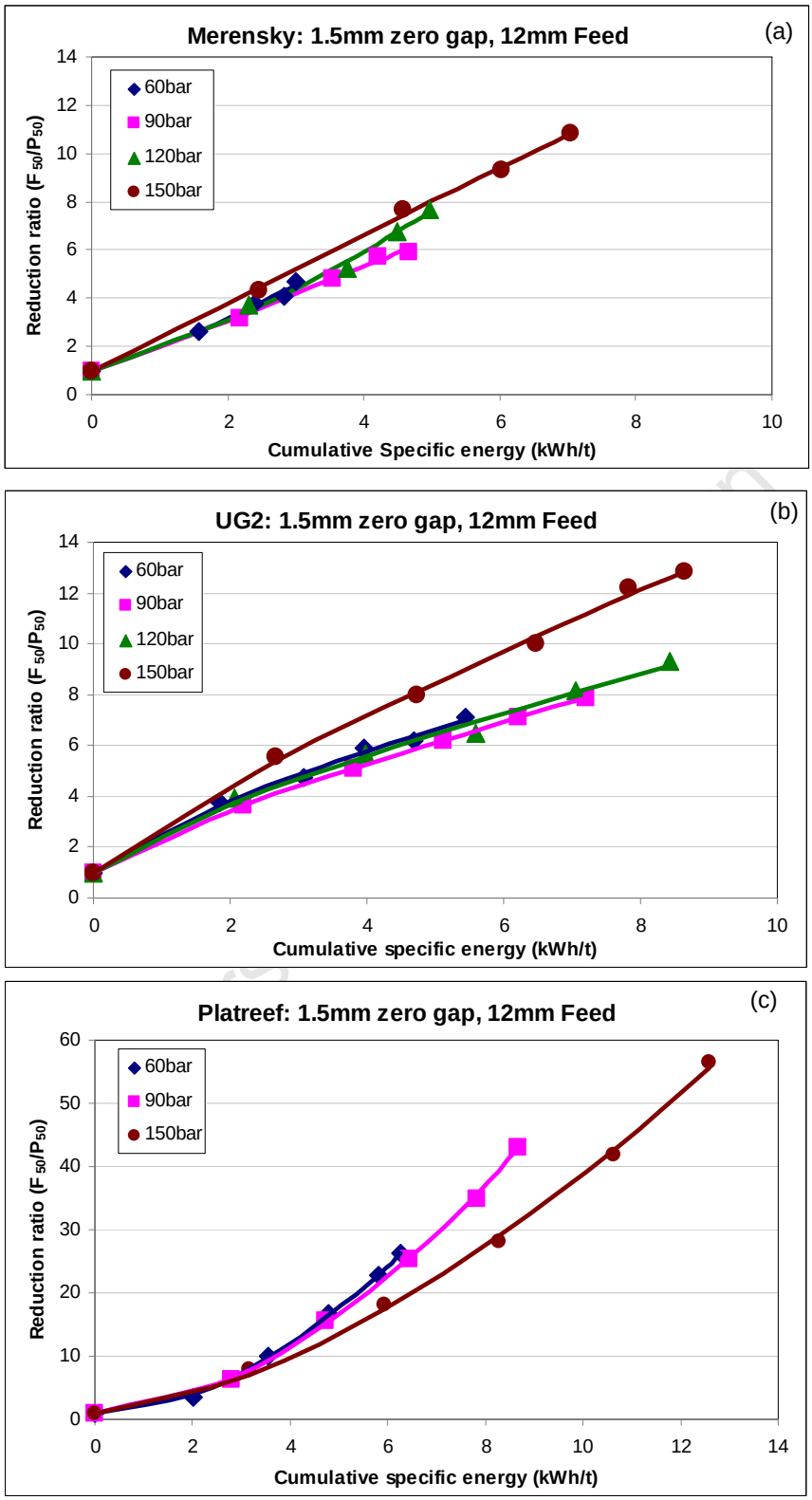

Figure 4-13: Effect of pressure on the specific energy-reduction ratio relationship for Merensky (a), UG2 (b) and Platreef (c) ores

Zero gap effects

Figure 4-14 shows the effect of zero gap on the specific energy-reduction ratio relationship for Merensky (a), UG2 (b) and Platreef (c). For Merensky ore (Figure 4-14 (a)), it can be seen that at the first pass, there is no difference in reduction ratio and specific energy between the 1.5mm and 3mm zero gap. However, the reduction ratio at the 3mm zero gap appeared to be larger than that of the 1.5mm zero gap at higher specific energies. Table 4-6 shows data that has been extracted from Figure 4-14 showing the corresponding number of passes.

For UG2 ore, the influence of 1.5mm, 3mm and 4.5mm zero gap effects have been presented in Figure 4-14 (b). At the 1.5mm zero gap it can be seen that larger reduction ratios are obtained at significantly reduced cumulative energy consumption compared to the 3mm and 4.5mm zero gaps. Table 4-6 shows that after four passes, a reduction ratio of 4.8 is obtained for a cumulative specific energy of 3.7kWh/t at the 4.5mm zero gap. However, for the same number of passes at the 1.5mm and 3mm zero gaps reduction ratios of 12.2 and 7.9 for cumulative specific energy consumptions of 7.8kWh/t and 6.9kWh/t, respectively were obtained.

For Platreef (Figure 4-14 (c)) on the other hand that it would be more energy efficient to apply the HPGR at the 1.5mm and 3mm zero gaps compared to the 4.5mm zero gap. After four passes, reduction ratios of 41.8 and 35.0 were obtained at the 1.5mm and 3mm zero gap at cumulative specific energy consumption of 10.6kWh/t and 8.73kWh/t respectively. At the 4.5mm zero gap, a relatively lower reduction ratio of 7.5 was obtained for a cumulative specific energy consumption of 5.5kWh/t for the same number of passes.

Table 4-6: Data extracted from Figure 4-14 showing effects of number of passes on reduction ratio (F_{50}/P_{50}) and specific energy (E_{sp})

Ore type	Zero gap	Pass	F_{50}/P_{50}	E_{sp} (kWh/t)
Merensky	1.5mm	2	7.7	4.6
	3mm	2	7.8	4.3
UG2	1.5mm	4	12.2	7.8
	3mm	4	7.9	6.9
	4.5mm	4	4.8	3.7
Platreef	1.5mm	4	42	11
	3mm	4	35	8.7
	4.5mm	4	7.5	5.5

This section has highlighted the effects of HPGR variables such as the pressure and the zero gap on outputs such as the specific energy consumed, throughput, size distributions and reduction ratios. The results reported show that the ore type has an effect on the energy efficiency of the HPGR as seen by the different trends generated for the different ore types. The increasing curves obtained for Platreef suggest that although more energy is consumed by Platreef compared to Merensky and UG2, it is more energy efficient to apply the HPGR on ore types such as Platreef ore.

In order to determine the benefits of using the HPGR, comparative tests must be made to comminution devices that are already being used in industry for the ore types being tested. Conventional ball mills are used in primary grinding sections of most industrial platinum processing comminution circuits. It is therefore reasonable to use the ball mill as a benchmark for the performance of the HPGR for comparative studies. The following section presents the data generated from the ball mill tests for comparative tests.

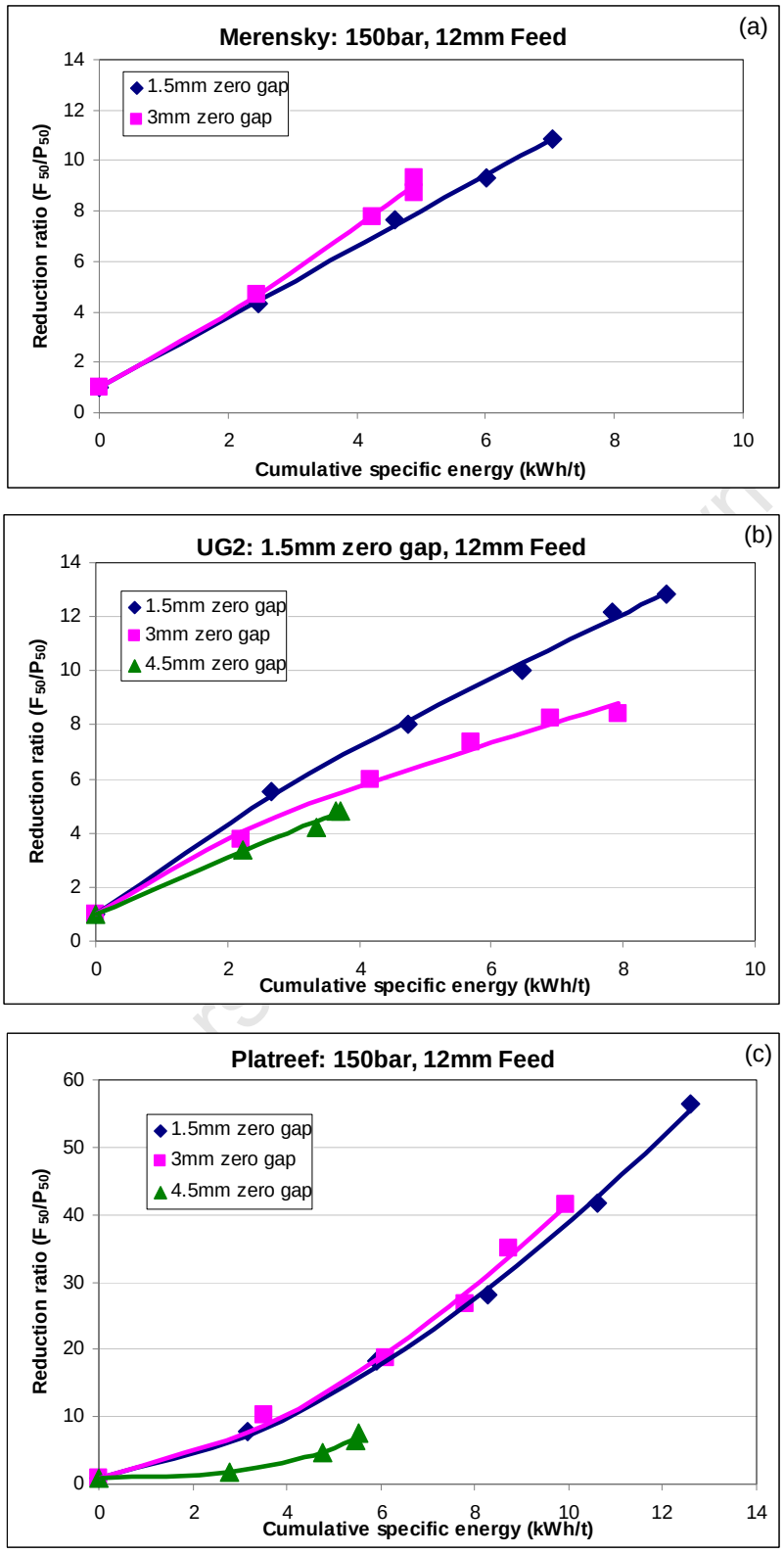

Figure 4-14: Effect of zero gap on specific energy – reduction ratio relationship for the Merensky (a), UG2 (b) and Platreef (c)ores

4.2 Comparison of HPGR data to Ball Mill data

Two types of ball mill tests were performed on the three ore types Merensky, UG2 and Platreef. The first tests performed were on a 6mm top size feed at a throughput of approximately 700kg/h of the ball mill. The second set of tests was performed on HPGR product at increasing ball mill throughput ranging between 700kg/h and 900kg/h for the three ore types under consideration. The results from these tests are discussed in this section and the comparison was performed on the basis of:

- specific energy consumed from the two types of ball mill tests.
- specific energy consumed by the HPGR and the ball mill at a similar grinds.
- size distributions obtained at the different ball mill tests performed.

4.2.1 Product size distributions

Figure 4-15 shows the size distributions obtained from the ball mill tests for Merensky (a), UG2 (b) and Platreef (c). For Merensky ore, steeper size distributions were obtained with the ball mill compared to that of the HPGR product. This suggests that more breakage of the coarser particles occurred with the application of the ball mill. Slightly finer grind was obtained with the HPGR-ball mill test performed at 743kg/h compared to that of the ball mill tests performed at a throughput of 720kg/h. Although the throughput of the HPGR-ball mill tests was increased to 936kg/h, there did not appear to be a significant change in grind compared to the test performed at 743kg/h.

For UG2 ore (Figure 4-15(b)), increasing the throughput of the HPGR-ball mill feed from 712kg/h to 932kg/h showed a decrease in the grind of the product. The grind obtained at a throughput 932kg/h was similar to that obtained with the ball mill tests grinding un-crushed ore performed at 709kg/h.

Platreef ore (Figure 4-15(c)) showed a coarser product of the ball mill product performed on 6mm feed at a throughput of 695kg/h compared to the HPGR-ball mill tests. A slight decrease in grind when the HPGR-ball mill throughput was increased from 710kg/h to 943kg/h was observed.

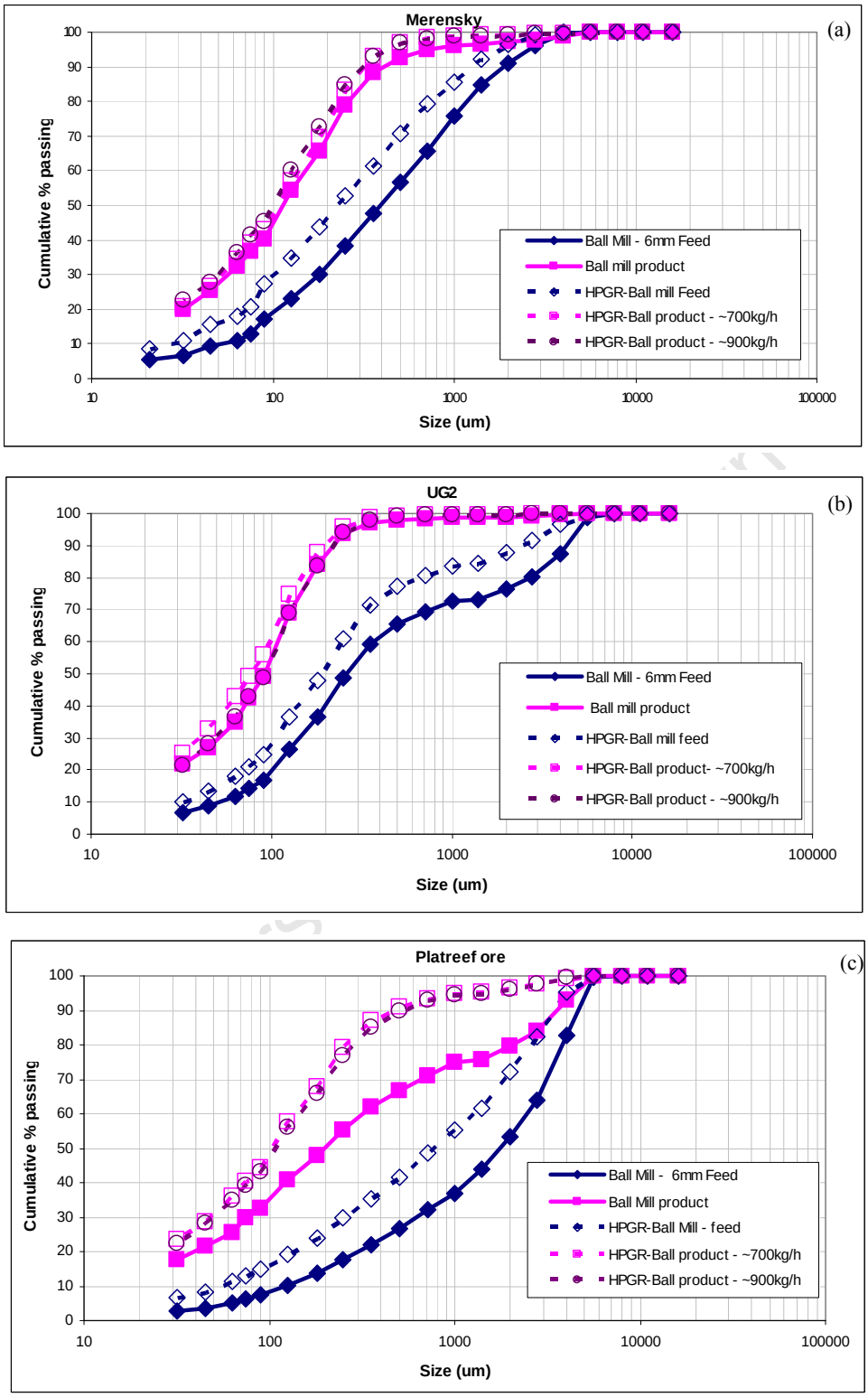

Figure 4-15: Size distributions obtained from the ball mill tests for Merensky (a), UG2 (b) and Platreef (c)

4.2.2 Specific energy consumption

Table 4-7 shows the data that was collected during the ball mill tests. The HPGR-Ball system represents the data obtained from the second set of ball mill tests where the material was comminuted using the HPGR and then the ball mill. For each ore type, low (~700kg/h) and high (900kg/h) throughput tests were performed. The voltage (V) and the current (I) were read off a digital meter and were used for the calculation of the power draw (kW) with the application of equation 12 (Daniel, 2007). A power factor (P_{factor}) of 0.75 was applied in all power draw calculations. However, this equation encompasses the total energy consumed including the no-load power. Therefore, for the purposes of comparisons of specific energy consumption between the HPGR and the ball mill, the specific energy consumed by the HPGR included the no-load power in this section.

$$Powerdraw(kW) = \frac{\sqrt{3} * I * V * P_{factor}}{1000} \quad (12)$$

Table 4-7: Ball mill tests data used to calculate the specific energy (E_{sp}) consumed for Merensky (MRY), UG2 and Platreef (PPL)

System	Ore type	Throughput (kg/h)	Voltage (V)	Current (A)	Power draw (kW)	E_{sp} (kWh/t)
Ball mill	MRY	720	424	11.2	6.58	9.1
	UG2	709	429	11.7	6.95	9.8
	PPL	695	429	11.9	7.07	10.2
HPGR-Ball Mill	MRY – high	936	424	11.2	6.58	8.2
	MRY – low	743	424	11.2	6.58	9.9
	UG2 – high	932	428	11.9	7.06	8.7
	UG2 – low	712	428	11.9	7.06	10.8
	PPL – high	943	429	11.7	6.95	8.8
	PPL – low	710	429	11.7	6.95	11.1

For Merensky, a specific energy of 9.1kWh/t was obtained for the ball mill test performed at a throughput of 720kg/h with a 6mm feed. For the material pre-crushed with the HPGR, a specific energy of 9.9kWh/t was consumed at a throughput of 743kg/h. An increase in throughput of the pre-crushed material to 936kg/h showed a decrease in specific energy consumed to 8.2kWh/t. This decrease in specific energy was obtained a significant change in grind as shown in Figure 4-15(a). A similar outcome was observed with UG2 and Platreef ore but with slight decreases in grind when the throughput was increased in the HPGR-ball mill tests.

4.2.3 Comparative tests

Figure 4-16 shows a comparison of the cumulative specific energy from selected HPGR and ball mill tests for Merensky, UG2 and Platreef. The no-load power from the HPGR tests had been included in the specific energies quoted in this section for comparison to the ball mill. For Merensky, the HPGR tests performed at a zero gap of 3mm and feed top size of 12mm exhibited lower specific energies and a coarser grind compared to the tests performed at a zero gap of 1.5mm and feed top sizes of 12 and 6mm. Comparisons of the specific energy from the ball mill tests performed at 700kg/h and 6mm feed top size appeared to be similar to those from the HPGR test performed at a zero gap of 1.5mm and feed top sizes of 12 and 6mm. The HPGR-ball mill test at ~700kg/h had a specific energy of 10.8kWh/t. An increase in throughput of the HPGR-ball mill test to ~900kg/h resulted in a decrease in specific energy from 10.8 to 8.6kWh/t. This was similar to the specific energy for the ball mill test operated at 700kg/h treated ore.

Similarly for UG2, a specific energy of 10.8kWh/t was obtained for the material ground using the HPGR-ball mill combination at 712kg/h. A decrease in specific energy from 10.8kWh/t to 8.65kWh/t was obtained when the throughput was increased to 932kg/h with a similar grind being obtained.

For Platreef ore, a specific energy of 11.1kWh/t was obtained for the material ground using the HPGR-ball mill combination at 710kg/h. A decrease in specific energy from

11.1kWh/t to 8.83kWh/t was obtained when the throughput was increased to 943kg/h. However, the grind measured using the percent passing 75μm at the higher throughput was higher than that for material ground with the ball mill alone at ~700kg/h. This suggests that for the HPGR-ball mill combination can be used to increase circuit capacity at a relatively good grind.

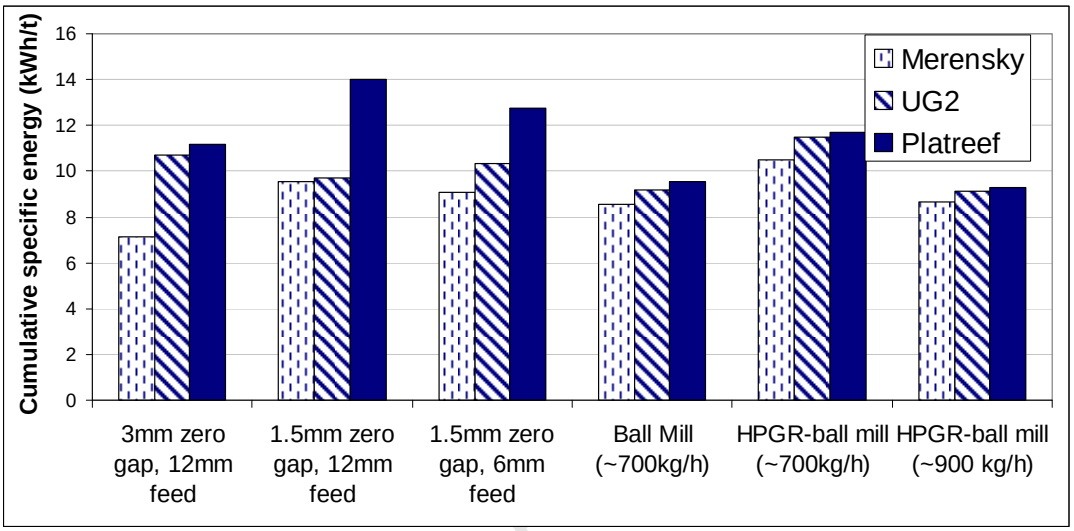

Figure 4-16: Specific energies from selected HPGR and ball mill tests

4.4 Summary of HPGR and ball milling results

This chapter highlighted the effects of the application of the different HPGR variables on throughput, energy efficiency and the product grind. Each of the aspects analysed in this study need to be considered in the optimisation of the HPGR variables to ensure desirable outcomes are obtained. Comparisons of the throughput and specific energy consumed were performed to determine the effect of the application of the HPGR as a pre-grinding stage to the ball mill. The results presented are discussed further in chapter 6 for each ore type. The following chapter presents the results from the flotation and mineralogical analyses.

Chapter 5

5 Effect of HPGR and Ball mill on flotation and mineral liberation

Overview: The results from the flotation along with the QEMSCAN and MLA analyses performed on selected samples from the HPGR and ball mill comminution tests are presented in this chapter. The effects of the HPGR on the PGM flotation response in terms of recovery-grade relationship and on mineral liberation are discussed in this chapter.

5.1 Flotation recovery

5.1.1 Repeatability analysis

Flotation tests were performed under the conditions discussed in section 3.6. The HPGR samples that were used for flotation analysis were obtained at a pressure of 150bar after four passes as discussed in section 3.6 (page 75). Table 5-1 shows an example of the masses of the concentrates and the corresponding PGE recoveries from duplicate flotation tests performed on Merensky, UG2 and Platreef ores. The data shown in this example is for the HPGR samples collected at 1.5mm zero gap and 12mm feed top size. The PGE recoveries shown were obtained from a mixture of concentrates C1+C2 and C3+C4 as described in Chapter 3. It can be seen that there are no significant differences between the primary and duplicate samples in terms of masses recovered and the PGE recoveries for each of the three ore types.

Table 5-1: A comparison of concentrate mass and PGE recovery between the primary and the duplicate sample for Merensky, UG2 and Platreef

MERENSKY				
Concentrate	**Primary**		**Duplicate**	
	Mass (g)	**PGE recovery**	**Mass (g)**	**PGE recovery**
C1	15.2	64.2	12.6	69.9
C2	15.8		13.3	
C3	17.1	74.1	14.5	76.1
C4	26.4		22.1	

UG2				
Concentrate	**Primary**		**Duplicate**	
	Mass (g)	**PGE recovery**	**Mass (g)**	**PGE recovery**
C1	35.7	54.5	39.5	57.5
C2	31.7		31.5	
C3	21.0	60.3	20.7	63.2
C4	20.3		20.8	

PLATREEF				
Concentrate	**Primary**		**Duplicate**	
	Mass (g)	**PGE recovery**	**Mass (g)**	**PGE recovery**
C1	32.9	63.9	32.8	66.1
C2	29.2		31.0	
C3	24.0	67.5	22.3	70.7
C4	22.8		24.3	

5.1.2 Mass-Water Recoveries

Figure 5-1 shows the mass-water recoveries for the flotation tests performed on the HPGR and ball mill product for Merensky (a), UG2 (b) and Platreef (c). The mass-water recovery graphs were generated to give an indication of the expected grade and recoveries of the concentrates relative to the other samples. Samples showing a higher mass pull could result in higher recoveries but lower grade concentrates. Samples that show similar mass pull but different water recoveries could indicate a more stable froth which could be as a result of one sample having more fines in the flotation feed (Palm *et al*, 2009). The relationship between mass and water recovery gives a good indication of the amount of floating ore obtained irrespective of the total water recovered (Wiese *et al*, 2006).

For Merensky ore (Figure 5-1 (a)) the lowest mass and water recoveries were obtained with the HPGR for the samples generated at a zero gap of 3mm and a feed topsize of 12mm. Similar mass and water recoveries were obtained with the HPGR tests performed at a zero gap of 1.5mm and feed top sizes 12mm and 6mm. these were also similar to those obtained with the ball mill.

For UG2 (Figure 5-1 (b)) the highest mass and water recoveries were obtained for the HPGR sample generated at a zero gap of 3mm and a feed topsize of 12mm. The HPGR samples generated at a zero gap of 1.5mm and feed topsizes of 12mm and 6mm showed similarities in mass and water recoveries. Although the ball mill showed similarities in water recovery to those obtained with the HPGR at a zero gap of 1.5mm and feed topsizes of 12mm and 6mm, differences in mass pull were observed.

For Platreef ore (Figure 5-1(c)) showed that the lowest mass and water recoveries were obtained with the ball mill compares to the HPGR tests. The differences in mass and water recoveries could be explained by the flotation feed size distributions obtained for these tests. These have been shown and discussed in Chapter 6 for the three ore types.

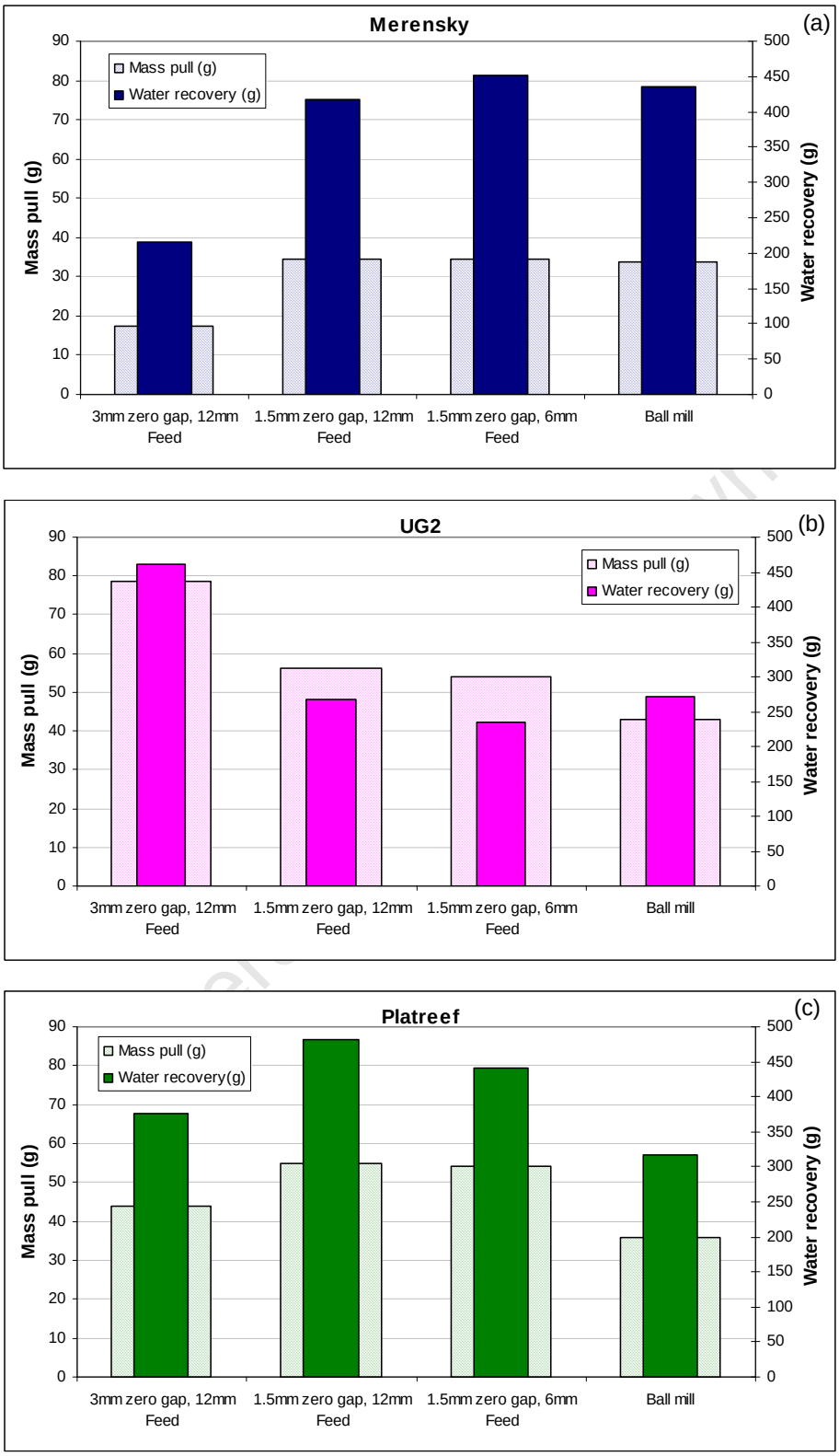

Figure 5-1: Mass-water recoveries for Merensky (a), UG2 (b) and Platreef ore (c)

5.1.3 Overall PGE recovery

Figure 5-2 shows the PGE recoveries for Merensky, UG2 and Platreef ore obtained from the selected HPGR and ball mill tests. For Merensky ore, the PGE recoveries lie in the range 71 – 83% with the ball mill test exhibiting the highest recoveries (83%). The three HPGR samples tested for PGE recovery show variations in recovery. Comparisons in grinds obtained from these tests could explain the differences observed.

For UG2 ore, the PGE recoveries obtained were in the range 55 – 67% as shown in Figure 5-2. The lowest PGE recovery (55%) was obtained from the test performed at a zero gap of 1.5mm and a feed top size of 6mm. Similar recoveries were obtained from the ball mill (67%) and the HPGR material generated at a zero gap of 3mm and a feed top size of 12mm (68%).

For Platreef ore, no significant differences in PGE recovery were observed among the HPGR tests (67 – 68%). Slightly lower recoveries were obtained for the ball mill compared to the HPGR generated samples.

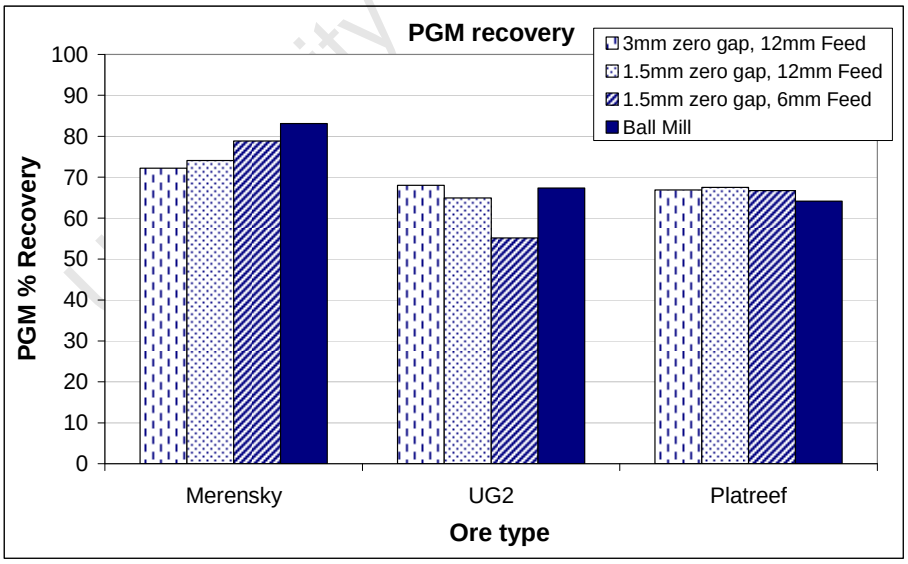

Figure 5-2: Overall recovery of PGM in Merensky, UG2 and Platreef ore from the ball mill tests and at different HPGR parameters

Confirmation of weather the differences in PGE recoveries could be considered significantly different or not was performed with the application of the analysis of variance (ANOVA) (Napier – Munn, 2005). This is a statistical analysis that was performed on the data to ensure that a reasonable interpretation of the results was achieved. Table 5-2 shows the results obtained for the ANOVA analyses for Merensky, UG2 and Platreef. A confidence interval of >95% means that there is a significant difference between the PGE recoveries of the samples analysed.

The ANOVA analysis confirms the observation previously discussed. For Merensky ore, the 99.5% confidence interval highlighted in red shows that the PGE recoveries between the HPGR samples generated at 3mm zero gap,12mm feed and 1.5mm zero gap, 6mm feed are significantly different. Significant differences were observed when comparing the three HPGR tests (97.5% confidence interval). UG2 shows significant differences in PGE recoveries with a few exceptions as shown in Table 5-2 by the confidence intervals that are not highlighted. For Platreef ore, none of the comparisons performed show significant differences in overall PGE recovery.

Table 5-2: ANOVA analysis used to determine any differences in PGE recovery among the different samples tested for Merensky, UG2 and Platreef

Comparison between samples	*Confidence level (%)*		
	Merensky	**UG2**	**Platreef**
3mm zero gap, 12mm feed 1.5mm zero gap, 12mm feed	88.6	93.1	68.9
3mm zero gap, 12mm feed 1.5mm zero gap, 6mm feed	**99.5**	**98.9**	69.1
3mm zero gap, 12mm feed Ball mill	62.5	70.6	35.4
1.5mm zero gap, 12mm feed 1.5mm zero gap, 6mm feed	82.4	**97.4**	77.7
1.5mm zero gap, 12mm feed Ball mill	28.5	93.4	12.2
1.5mm zero gap, 6mm feed Ball mill	0.12	**99.8**	27.0
3mm zero gap, 12mm feed 1.5mm zero gap, 12mm feed 1.5mm zero gap, 6mm feed	**97.5**	**99.4**	76.4
3mm zero gap, 12mm feed 1.5mm zero gap, 12mm feed Ball mill	51.3	**95.2**	17.7
3mm zero gap, 12mm feed 1.5mm zero gap, 6mm feed Ball mill	62.3	**99.8**	28.6
1.5mm zero gap, 12mm feed 1.5mm zero gap, 6mm feed Ball mill	18.7	**99.7**	26.4
3mm zero gap, 12mm feed 1.5mm zero gap, 12mm feed 1.5mm zero gap, 6mm feed Ball mill	57.5	**99.8**	21.4

5.1.4 PGE grade-recovery curves

Figure 5-3 shows the PGM grade-recoveries for Merensky (a), UG2 (b) and Platreef (c). It should be noted that the results presented here are normalized and do not reflect the absolute values obtained in the actual operation due to the differences in scale and flotation conditions applied. The shapes of the grade-recovery curves for all three ore types are typical of those obtained for the platinum ores. For Merensky ore, better grades were obtained from the HPGR sample generated at a zero gap of 3mm and feed top size of 12mm. The material generated from this HPGR condition was coarser than the other Merensky samples on which flotation tests were performed. Better PGE grades and recoveries were obtained from the ball mill compared to the material generated at a zero gap of 1.5mm and feed top sizes 12mm and 6mm.

For UG2, the flotation response for the material ground under different HPGR conditions is similar and appears to be inferior when compared to the material ground with the ball mill. The UG2 results indicate that a lot of gangue material would report to the concentrate if the HPGR is used to grind the ore. Using the HPGR at different design and operating variables did not appear to show any significant improvements in response.

It can be seen from Figure 5-3 (c) that Platreef ore ground at different HPGR conditions exhibited a similar flotation response. An average recovery of 67% was obtained in all cases with fairly similar grades of 31g/t. The flotation response for the material ground with the ball mill was significantly superior compared to that ground with the HPGR. It is not clear at this stage why the material ground with the ball mill would respond better to flotation compared to those ground with the HPGR.

The mineralogical analysis presented in section 5.2 was performed on the flotation feed to assess the degree of liberation and the PGM associations that could assist in explaining the flotation results observed.

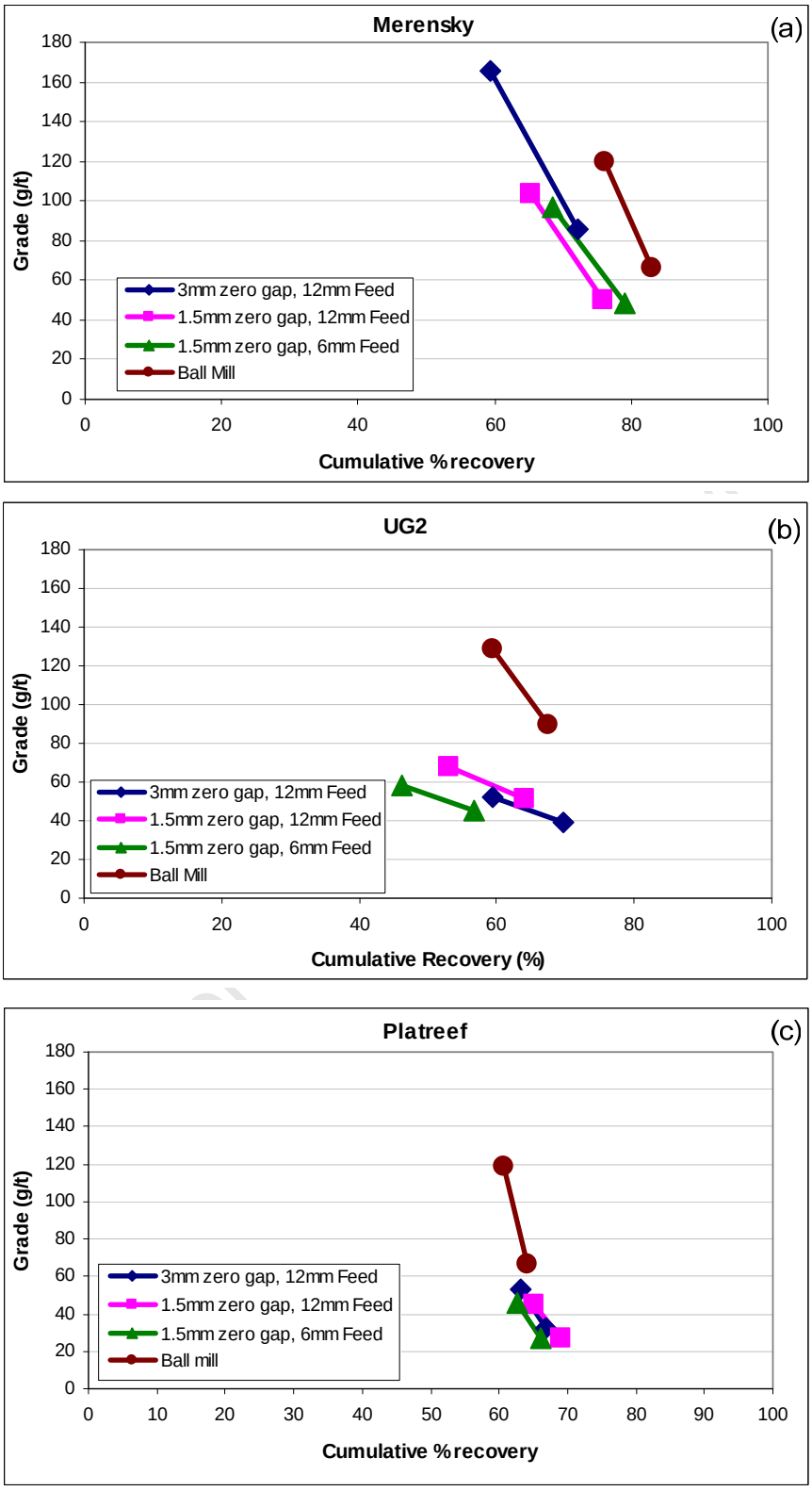

Figure 5-3: PGE Grade-recovery curves for Merensky (a), UG2 (b) and Platreef (c)

5.2 Mineralogical Characterisation

5.2.1 Bulk mineralogical analysis

The bulk mineralogical analysis was performed to obtain a quantitative description of the minerals present in the three ore types under consideration. The major minerals in the three ore types have been identified and quantified with the use of QEMSCAN. The discussion of the minerals present has been split in to two sections, the major gangue minerals present and the base metal sulphides present. According to literature reviewed in chapter 2, the PGM are typically associated with the base metal sulphides.

Gangue minerals

Table 5-3 shows the quantitative abundance of the minerals present in the platinum bearing ores Merensky, UG2 and Platreef obtained from the QEMSCAN analysis performed for this work. Distinct differences in mineral abundance of the main minerals are observed in the different ore types. The main minerals present in the three ores are chromite, pyroxene and plagioclase. UG2 ore has significantly higher chromite content of 62.1 wt% compared to Merensky (5.0 wt%) and Platreef ore (4.8 wt%). The bulk of Merensky and Platreef ores consist mainly of pyroxene which is a combination of orthopyroxene and clinopyroxene. Merensky ore contained 45.9 wt% orthopyroxene and 8.0 wt% clinopyroxene while Platreef had 21.8 wt% and 24.8 wt%, respectively. UG2 ores consists of only 12.8 wt% orthopyroxene and 0.91 wt% clinopyroxene. A significant portion of Merensky ore is made up of plagioclase (33.3 wt%) while UG2 and Platreef ore contain 14.5 wt% and 15.6 wt% of the same mineral. The naturally floatable gangue mineral talc content was 0.1 wt%, 0.3 wt% and 0.4 wt% in Merensky, UG2 and Platreef, respectively. Although the three ore types contain similar types of minerals, the differences in proportions may have significant effects on the metallurgical requirements.

Table 5-3: Mineral abundance in weight % within each of the three platinum bearing ores measured with QEMSCAN

Mineral	Merensky (wt%)	UG2 (wt%)	Platreef (wt%)
Pentlandite	0.63	0.06	0.23
Pyrrhotite	0.47	0.01	0.11
Pyrite	0.20	0.04	0.16
Chalcopyrite	0.33	0.02	0.13
Other sulphide	0.00	0.00	0.04
Orthopyroxene	45.9	12.8	21.8
Clinopyroxene	7.95	0.91	24.8
Olivine	0.64	0.15	0.72
Talc	0.10	0.28	0.36
Serpentine	1.22	1.61	8.56
Amphibole	0.72	0.24	4.17
Chlorite	1.50	2.76	7.87
Plagioclase	33.4	14.5	15.6
Mica	0.71	0.74	0.40
Chromite	5.03	62.13	4.79
Quartz	0.50	0.28	4.99
Oxides	0.58	1.10	0.67
Calcite	0.16	0.18	1.27
Other	0.61	2.30	4.18
Total sulphides	1.63	0.14	0.67

Base metal sulphides

Figure 5-4 shows the relative abundances of the sulphides present in the three ore types. It can be seen that Merensky ore has a higher sulphide content (1.6 wt%) compared to UG2 (0.1 wt%) and Platreef ore (0.7 wt%). These values are consistent with those obtained in the literature review in chapter 2. The main sulphides present in these ore types are chalcopyrite, pentlandite, pyrrhotite and pyrite and are present in varying abundances in the three ore types. It can be seen that the sulphide content in UG2 is very low compared to Merensky and Platreef ore. Pentlandite ($(Fe,Ni)_9S_8$) is the most common sulphide in the three ores with abundances of 0.6 wt% in Merensky, 0.1 wt% in UG2 and 0.2 wt% in Platreef ore. While traces of pyrrhotite ($Fe_{1-x}S$) were found in UG2

ore (0.01 wt%), larger proportions were found in Merensky (0.5 wt%) and Platreef ore (0.1 wt%). Chalcopyrite ($CuFeS_2$) abundances of 0.3 wt% in Merensky, 0.02 wt% in UG2 and 0.1 wt% in Platreef ore were obtained and pyrite abundances of 0.2 wt%, 0.04 wt% and 0.2 wt% respectively.

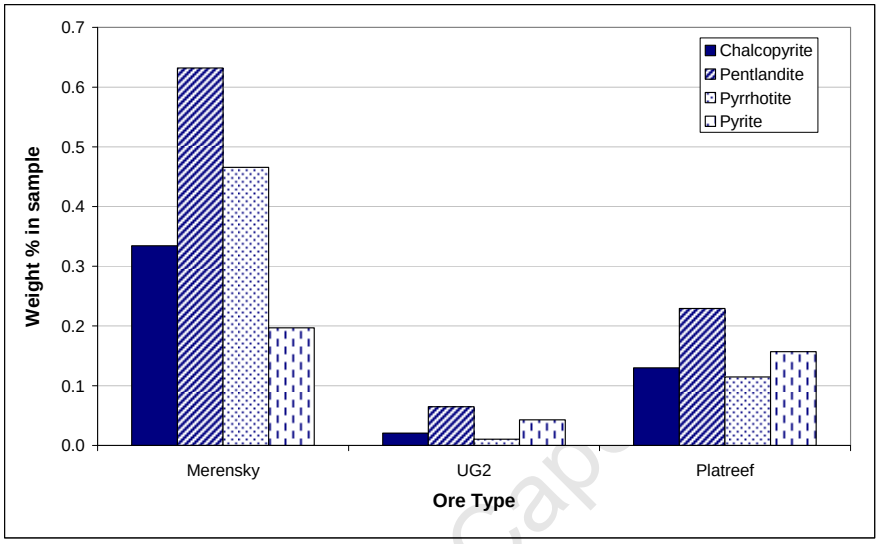

Figure 5-4: Sulphide modal mineralogy in the three ore types

The significance of performing a modal analysis of the major minerals present in each ore type is to be able to sufficiently characterize the minerals of interest by analysing the associations of these minerals with other gangue minerals in the sample. In this thesis, the minerals of interest are the PGMs and their associations with other minerals in each ore type. Any differences in association of these minerals between the three ore types could assist in finding reasons for the different metallurgical requirements. It is the associations of the valuable minerals that will give an indication of whether adequate liberation has been achieved. Therefore, the next section describes the PGM mineralogy in terms of particle size, abundance and association with the other minerals present. The effect of the various operational parameters of the HPGR and comminution device on mineral liberation has been discussed.

5.2.2 PGM mineralogical analysis

Mineralogical analysis was performed on the Merensky, UG2 and Platreef ore samples that were comminuted with the use of the HPGR and ball mill and were selected for flotation analysis. Comparisons of the two comminution devices have been made. The main points of discussion in the mineralogical analysis of the PGM in the three ore types are:

- Size
- Liberation
- Association
- Theoretical grade and recovery

Determination of these characteristics for minerals of interest is essential in the development of a suitable metallurgical processing route for any ore type.

PGM Associations

The absolute grade of the PGM was not available in this study therefore, the PGM have been ranked based on the associations with other minerals in each ore type. The PGM mineralogical analysis obtained from the MLA tests show that there are four main PGM associations in the three ore types. These are:

- Liberated
- PGM locked in floatable base metal sulphide (BMS)
- PGM occluded in locked BMS
- PGM locked in gangue mineral

These associations vary in occurrence depending on the ore type and the comminution device applied. Figure 5-5 shows selected images of the various PGM associations obtained from Merensky, UG2 and Platreef ore. The different BSE grey levels represent the different minerals present in a particle. The labeled bright white particles represent the PGM particles. The minerals that are associated with the PGM have also been labeled.

Figure 5-5 (a) and (b) show liberated PGM from Merensky and UG2 ore, respectively. Figure 5-5(c) and (d) show the PGM locked in liberated, floatable sulphides such as pentlandite and pyrite. Figure 5-5 (e) and (f) show the PGM associated with base metal sulphides that are locked in gangue minerals. Figure 5-5 (g) and (h) show the PGM locked in gangue minerals. In these associations, it would be more difficult to recover the PGM by flotation in the primary flotation stage due to insufficient liberation. Further grinding of these minerals to less than 10μm would be required to liberate the locked PGM.

The locked PGM are typically located at grain boundaries, (e) and (f) or in particles that are fragile looking due to the many cracks on the sulphide surfaces shown in (c) and (d). The images shown in (c) and (d) were obtained from the HPGR, showing evidence of micro-cracks being formed. However, the location of the PGM at grain boundaries and at points of weakness could mean easier access for leaching solutions. The following sections give more quantitative analyses of the mineralogical analysis of the PGM in the three ore types.

Better chances of PGM recovery are expected if the PGM are associated with liberated base metal sulphides. For Merensky and Platreef ore, approximately 65% of the PGM that are associated with liberated floatable base metal sulphides are locked in pentlandite. The rest are locked in pyrrhotite (25%), pyrite and chalcopyrite (10%) for Merensky, and in chalcopyrite (21%) and pyrrhotite (10%) for Platreef ore. For UG2 ore, 73% of the PGM associated with liberated floatable base metal sulphides are associated with pentlandite, with 18% associated with chalcopyrite and 6% with pyrite.

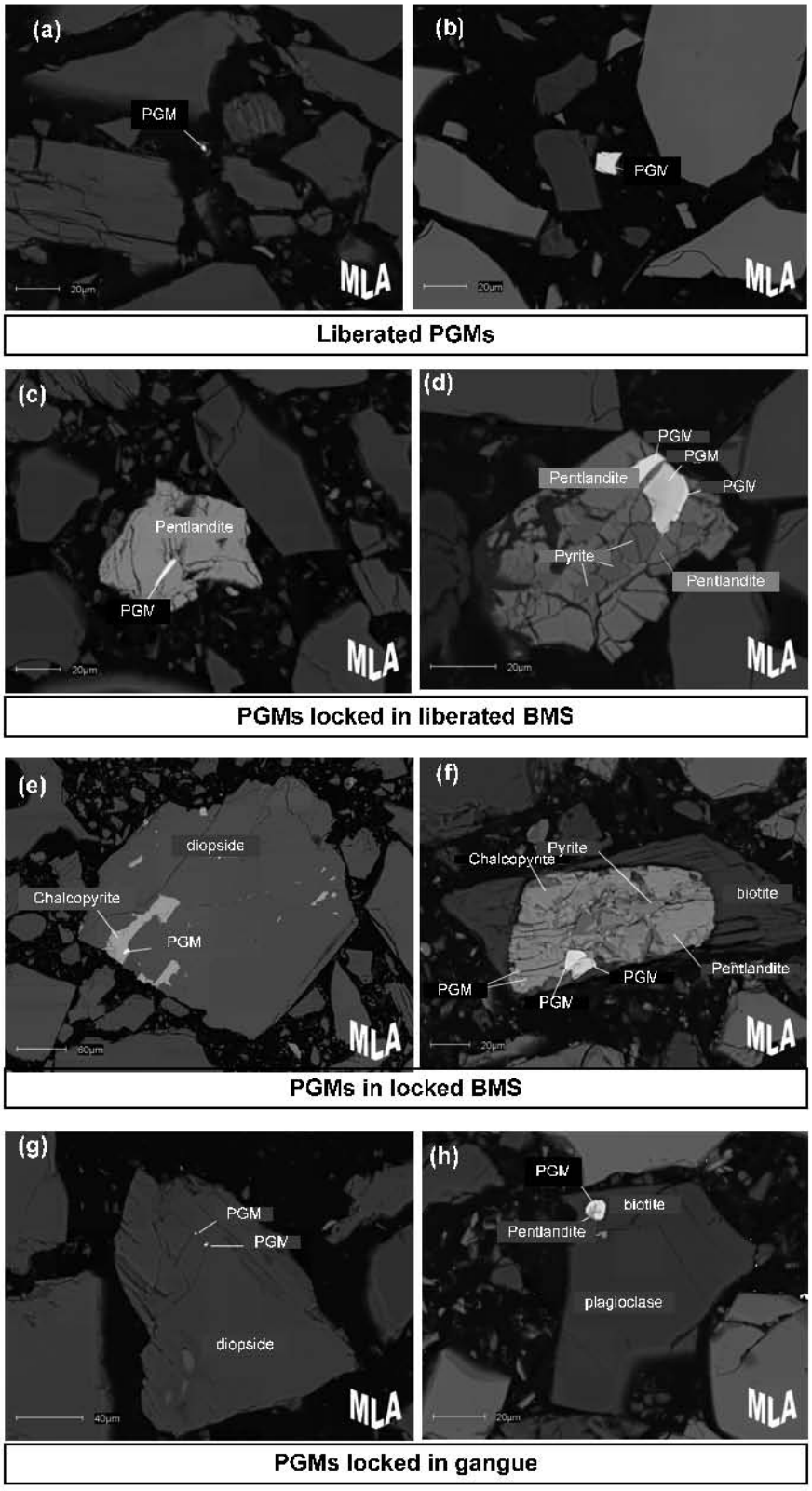

Figure 5-5: MLA back scattered electron images showing the various PGM associations in the three ore types Merensky and UG2 ore

PGM grain sizes

A comparison of the size of the PGMs has been performed for the three ore types for the various samples tested. The size of the PGMs is a significant parameter in the determination of the suitable grind required for effective liberation of the PGMs. The mean sizes in each PGMs grade have been used.

Table 5-4 shows the mean grain sizes for the PGMs in each association group for the HPGR and ball mill samples for Merensky (a), UG2 (b) and Platreef ore (c). It can be seen that all the PGM are less than 10µm with Merensky ore generally exhibiting slightly larger PGM compared to UG2. For Merensky ore, it can also be seen that the liberated PGM in all four samples analysed are generally larger (>4µm) than those from the other association groups (<4µm). This suggests that the larger PGMs have successfully been liberated while further size reduction would be required to liberate the smaller PGMs. The largest liberated PGMs were from the ball mill sample with a mean size of 6.2µm.

For UG2 ore, the PGMs are generally less than 4µm in size for all samples with the exception of the 5µm mean size PGM found in the 3mm zero gap, 12mm feed top size HPGR sample. The liberated PGMs in the ball mill sample have the largest mean size (4µm) compared to the liberated PGMs in the HPGR samples.

The PGMs in Platreef ore seem to be larger than those in UG2 ore. The liberated PGMs are generally larger than those in the different groups shown. For the HPGR samples obtained at 3mm zero gap and 12mm feed top size, the PGM are generally less than 2µm for the PGM that are associated with other minerals.

Table 5-4: PGM mean grain sizes (microns) for different associations for Merensky, UG2 and Platreef for the HPGR and ball mill samples

MERENSKY				
Association	**3mm zero gap, 12mm Feed**	**1.5mm zero gap, 12mm Feed**	**1.5mm zero gap, 6mm Feed**	**Ball Mill**
Liberated PGM	4.2	5.0	4.3	6.2
PGM in floatable BMS	3.8	2.7	2.5	3.1
PGM in locked BMS	3.8	3.7	2.2	1.5
PGM locked in gangue	3.1	3.0	3.1	2.4

UG2				
Association	**3mm zero gap, 12mm Feed**	**1.5mm zero gap, 12mm Feed**	**1.5mm zero gap, 6mm Feed**	**Ball Mill**
Liberated PGM	3.3	3.5	3.3	4.0
PGM in floatable BMS	5.0	2.6	3.9	2.5
PGM in locked BMS	2.9	2.1	2.1	2.4
PGM locked in gangue	3.7	2.6	3.6	3.0

PLATREEF				
Association	**3mm zero gap, 12mm Feed**	**1.5mm zero gap, 12mm Feed**	**1.5mm zero gap, 6mm Feed**	**Ball Mill**
Liberated PGM	4.7	5.1	3.0	3.6
PGM in floatable BMS	1.5	3.9	2.3	1.6
PGM in locked BMS	1.7	3.3	2.6	3.0
PGM locked in gangue	2.1	3.2	3.6	2.3

PGM Liberation

Figure 5-6 shows the PGM liberation profiles of the selected HPGR and ball mill samples for Merensky (a), UG2 (b) and Platreef (c). For Merensky ore it can be seen that different liberation profiles were obtained for different HPGR operational variables. The sample from the HPGR operated at a zero gap of 3mm and a feed top size of 12mm had the lowest amount of liberated PGMs (43%) while the product obtained at a zero gap of 1.5mm and a feed top size of 6mm had up to 70% liberated PGMs. Better liberation profiles were obtained with the ball mill in which 74% of the PGMs were liberated and the proportion of PGMs occluded in locked BMS and locked in gangue minerals was the least (6.5%).

For UG2 ore (Figure 5-6(b)), the HPGR sample obtained at a zero gap of 3mm and feed top size 12mm had the lowest amount of liberated PGM (27%). The liberation profile of the sample generated at a 1.5mm zero gap and 6mm feed top size compared well with the ball mill product with both showing approximately 45% liberated PGM. The highest amount of liberated PGM (53%) was from the HPGR sample generated at 1.5mm zero gap and 12mm feed.

For Platreef ore (Figure 5-6(c)), the HPGR samples generated showed comparable liberation profiles with the liberated PGMs in the range 45 – 55%. The ball mill had the least amount of liberated PGMs (11%) with a significant amount (80%) locked in gangue minerals.

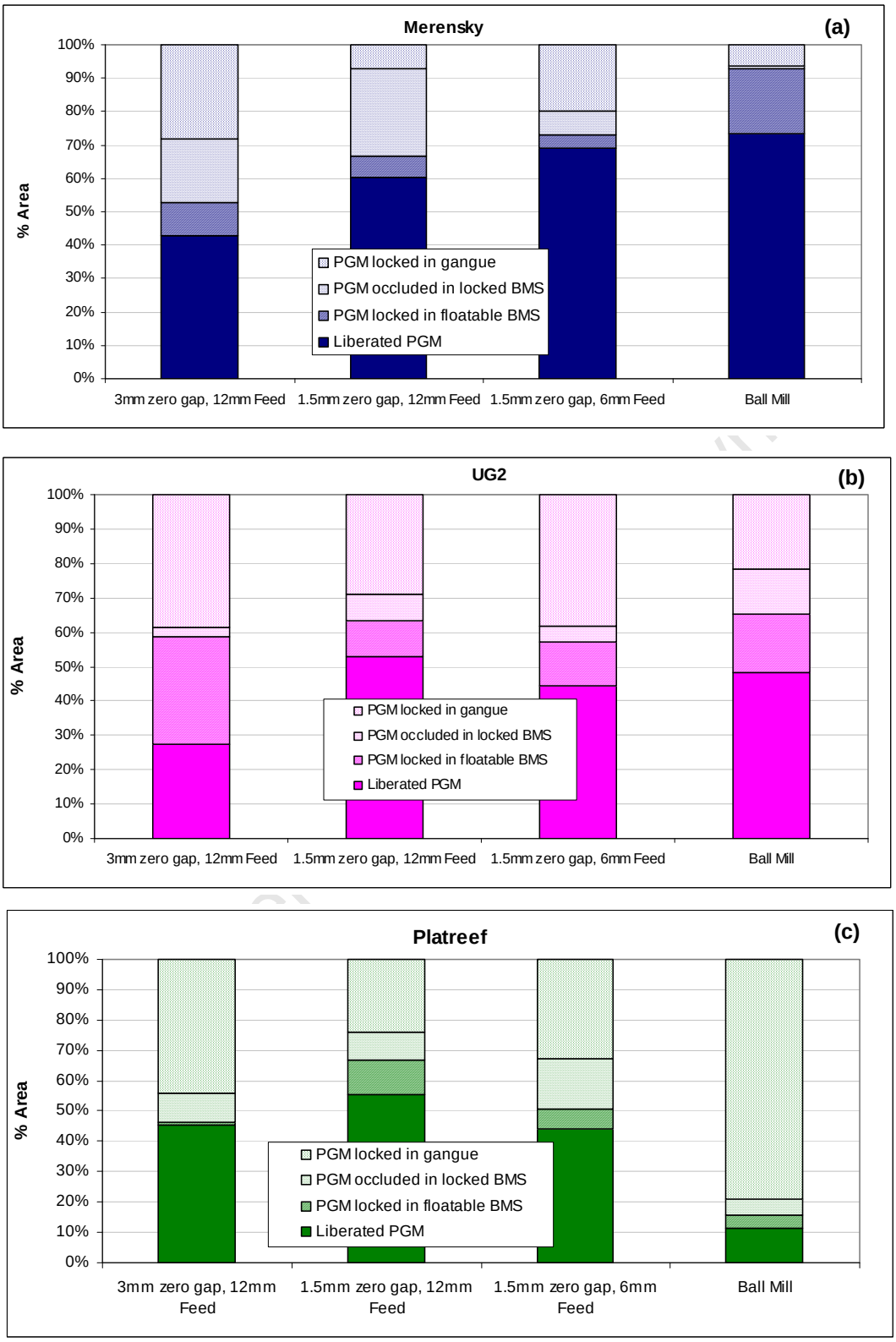

Figure 5-6: PGM Liberation profiles in Merensky (a), UG2 (b) and Platreef (c) ore using the area

Theoretical grade-recovery

Theoretical or potential grade-recoveries were generated to determine the potential of the recovery process. Two methods of analysis were applied in the analysis of the theoretical grade-recoveries: the PGM area and the number of PGMs in each association. Since no differences were noted between the two methods of analyses, only area information was used here.

Figure 5-7 is a comparison of the theoretical PGM grade-recovery of the samples obtained from the HPGR and ball mill tests for Merensky (a), UG2 (b) and Platreef (c) ore with the use of the exposed areas analysis. The grades shown here are not absolute values and are ranked based on the association of PGM particles with other minerals. For Merensky ore, better potential grade-recovery profiles occur with the ball mill compared to the three HPGR samples. For all mineral associations indicated, the ball mill exhibits better theoretical recoveries. It can also be seen that the HPGR variables, zero gap and feed top size have an influence on the theoretical grade-recovery. The least desirable theoretical grade-recovery was observed for the HPGR sample obtained at the 3mm zero gap and 12mm feed top size.

For UG2 ore, although the area of liberated PGM for the ball mill tests is slightly lower compared to the HPGR product obtained at 1.5mm zero gap and 12mm feed top size, better theoretical grade-recovery is obtained from the ore ground using the ball mill. It can also be seen that at different variables of the HPGR there are differences in the theoretical grade-recoveries obtained. For the HPGR sample obtained at the 1.5mm zero gap and 12mm feed top size better theoretical grade-recoveries are obtained compared to the other two HPGR samples.

For Platreef ore, at the HPGR settings of 1.5mm zero gap and 12mm feed top size, the highest theoretical grade and recoveries are obtained. Lower PGM potential grade recoveries were observed for the ball mill.

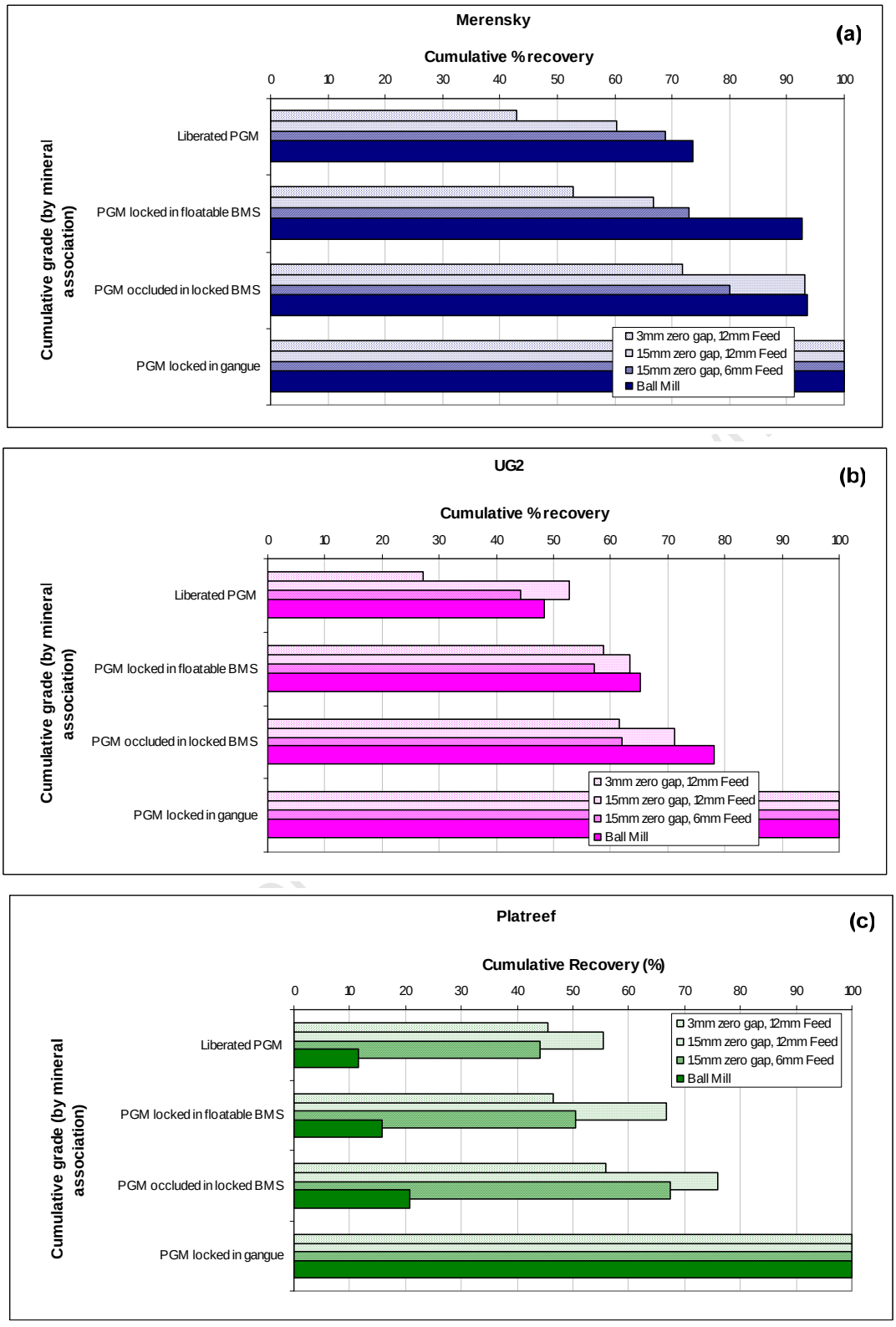

Figure 5-7: PGM Theoretical grade-recovery in Merensky (a), UG2 (b) and Platreef ore (c) for samples obtained from the HPGR and ball mill tests

5.3 Summary

This chapter presented the results obtained from the flotation and mineralogical analysis tests. The flotation results showed that the mass-water recoveries gave an indication of the PGE grade and recoveries expected. The ball mill generally showed better grades and recoveries compared to the HPGR. The grind of the flotation feed was required to explain the trends observed. These have been shown and discussed in the following chapter.

A bulk mineralogical analysis of the three ore types showed that while similar minerals are present in the three ore types, differences in abundance could result in dissimilarities in metallurgical behaviour. The MLA analyses showed that size of PGMs in the three ore types was less than 10µm. The liberation profiles showed that more liberated PGMs were obtained with Merensky compared to UG2 and Platreef. Variations in liberation profiles could be explained with the use of the size distribution of the samples analysed.

Chapter 6

6 Discussion

Overview: The effect of using HPGR to comminute Merensky, UG2 and Platreef ore on throughput, energy consumption, size reduction, flotation performance and liberation have been discussed in this chapter. The influence of using the HPGR on the performance indicators mentioned above have been discussed for each ore separately because the results indicated that different ore types behave differently.

6.1 Merensky

6.1.1 Throughput

In this thesis the main focus was determining how the pressure, zero gap, number of passes and feed characteristics such as feed top size and ore type affected the throughput. The effects of pressure and the number of passes for Merensky are shown in Figure 4-1 (a). An increase in pressure resulted in a decrease in the throughput. This is in line with what has been found in literature (Klymowsky *et al*, 2002; Lubjuhn and Schonert, 1993; Austen *et al*, 1993). This is due to the decreased working gap as a result of increased pressure (Austen *et al*, 1993). The increased pressure results in the increase in the bulk density of the particle bed between the rolls. As such, less separation of the rolls is achieved at the critical angle of nip (α_c) shown in Figure 2-4. Therefore, the material is pulled into the gap at a slower rate.

As the number of passes increased, the throughput decreased as seen in Figure 4-1 (a). The same phenomenon as that used to explain the effect of pressure can be applied to explain the effect of the number of passes on throughput. The only variable that changed as the number of passes increased during the testwork was the fineness of the feed. The first pass consisted of a higher coarse content which forced the rolls apart, resulting in the collapse of the particle bed, causing the material to fall between the rolls without being nipped. This effect as explained by Klymowsky *et al* (2002) is referred to as internal by-

pass, where the material falls through the gap and is accelerated by the rolls. As the fineness of the feed increases, the separation of the rolls is decreased, resulting in the material being pulled into the gap at a slower rate.

The working gap determines the amount of material that can pass between the rolls during operation and hence the throughput. Figure 4-3(a) showing the effect of pressure and number of passes on the working gap confirms the throughput trends observed. As the number of passes increased, the working gap decreased which in turn resulted in a decrease in throughput. Lim *et al* (1997) showed a similar trend to that obtained in this study. The effect of the zero gap on the working gap in Figure 4-4(a) show that the 3mm zero gap resulted in wider working gaps compared to that at 1.5mm particularly after the first pass. This is consistent with the throughput trends observed in Figure 4-2(a) at different zero gaps. Greater compaction of the particle bed is experienced at the narrower zero gap (1.5mm) resulting in lower working gaps.

An increase in fines content of the feed to the HPGR means that the particle bed was less porous. The material stream becomes narrower as it moves towards the gap between the rolls. Therefore the particles have to move relative to each other (Austin *et al*, 1993). At higher coarse content, the friction between the particles and between the particles and the rolls surface is higher. The combination of the frictional forces and the movable rolls results in higher throughput. For finer material the opposite effect occurs, less slip between the rolls and the particles, and between particles results in reduced throughput.

The effect of the zero gap on throughput shown in Figure 4-2(a) show no significant effect on the throughput for the first two passes. This is postulated to be due to the higher coarse content outweighing the effect of zero gap at the first two passes. From the third pass onwards, the material is finer and the zero gap effects outweigh the material effects. This is postulated to be due to lower compaction forces experienced after the second pass at the 3mm zero gap compared to the 1.5mm zero gap. Therefore the bulk density of the material is lower at the 3mm zero gap, making it easier for the material to be pulled down wards into the gap between the rolls.

6.1.2 Size distributions

The size distribution for increasing number of passes shown in Figure 4-5 (a) for Merensky ore indicate that the product becomes progressively finer with increasing number of passes. Hosten and Cimilli (2009), Schönert (1988) and Lim *et al* (1996) obtained similar results when they performed experiments at varying grinding pressures. The size distributions appear to be reaching a point where no changes in size distributions can be seen. Figure 4-6 (a) showing the effect of pressure on the fineness of grind (% passing 75µm) confirms that there is a point reached where the product fineness does not change. This point is referred to as the saturation point. When the saturation point is reached the bed porosity is at a maximum such that when a compaction force is applied on the bed, there is no displacement of the device applying the force.

The fineness of grind obtained at the saturation point is dependent on the pressure applied (Figure 4-6 (a)). The saturation points appear to have been reached after four passes for all the pressures for the experiments performed at a 1.5mm zero gap and 12mm feed top size. Table 6-1 shows the % passing 75µm obtained after reaching the saturation points for the full range of pressures tested on Merensky ore. At 150bar, product with more fines content is generated within the first pass compared to that at 60bar. Therefore, the presence of more fines assists in further generation of more fines. As a result, after four passes, more fines were generated at the higher pressure.

Table 6-1: % passing 75µm at saturation points reached at a zero gap of 1.5mm after four passes

Pressure (bar)	% passing 75µm
60	27
90	33
120	34
150	41

Figure 4-7 (a) suggests that the zero gap does not have an effect on the product fineness for the first three passes. Lower compaction forces were experienced by the particle bed

after the third pass for the 3mm zero gap compared to the 1.5mm zero gap. As a result, the fineness of grind is lower for the 3mm zero gap compared to the 1.5mm zero after the third pass. Therefore, the zero gap has an effect on the product fineness achieved at the saturation point. At the 1.5mm zero gap, a grind of 41% passing 75µm was obtained while that at the 3mm zero gap was 35% passing 75µm. This is consistent with the trends observed on the effect of zero gap on the working gap (Figure 4-4(a)). At the saturation point, the 3mm zero gap had a higher working gap compared to the 1.5mm zero gap.

6.1.3 Specific energy consumption and energy efficiency

Figure 4-9 (a) shows the effect of pressure and the number of passes on the cumulative specific energy consumed. An increase in pressure resulted in an increase in the cumulative specific energy consumed. The data generated in this work is presented differently compared to that in literature due to the addition of a third variable (the number of passes). The general trends which show an increase in pressure resulting in an increase in specific energy consumed were also observed by Klymowsky *et al* (2002), Schönert (1988) and Lim *et al* (1997) for ore types such as gold, zinc, iron, kimberlite and quartz. However differences in terms of whether the relationship was linear or non-linear appeared to be dependent on the ore type and the range of pressures tested. The increasing specific energy as a result of the increasing pressure is due to the rising forces required to push the rolls apart as the pressure increases.

The specific energy consumed decreased after each subsequent passes with the sharpest decrease being between the first and second passes. This could be due to the higher coarse content at the first pass which caused more forcing apart of the rolls. Norgate and Weller (1994) also found that for a multi-stage operation of the HPGR on a gold ore, the specific energy consumed after each subsequent pass decreased sharply between the first and second passes. Norgate and Weller (1994) suggest that the trends observed are as a result of the decreasing fineness of the grind as the number of passes increases.

Comparisons between Figure 4-9(a) and Figure 4-6(a) show that the saturation point is reached at the fourth pass at pressures 150bar and 90bar. At this point no increase in the cumulative specific energy was observed, only the no-load power was being drawn. This could be the reason that led Klymowsky *et al* (2002) to suggest that it is more energy efficient to operate the HPGR up to the saturation point where maximum size reduction of the material is obtained without wasting energy.

The effect of pressure, zero gap and number of passes on reduction ratios for Merensky ore are shown in Figure 4-11(a) and Figure 4-12(a), respectively. As the number of passes increased the reduction ratio after each subsequent pass decreased. The greatest decrease in reduction ratio is from the first to the second pass after which, the third and fourth passes show slight decreases. Viljoen *et al* (2001) showed that the bed porosity had a significant effect on the size reduction obtained on a nickel sulphide ore. The results generated from their work showed that increasing the porosity of the bed reduced the extent of secondary breakage. Therefore a similar explanation can be applied to the results obtained in this work. Higher compaction forces were experienced at the first pass compared to subsequent passes due to a more porous particle bed as a result of the high coarse content.

An increase in pressure resulted in larger reduction ratios due to the increasing compaction forces. The gap between the rolls is narrower at higher pressures, making it more difficult for the ore to force the rolls apart. This is confirmed in Figure 4-3(a) which shows a decrease in working gap as the pressure increased. Although differences in working gap were observed at varying zero gaps, no significant distinctions in reduction ratios were observed at the 1.5mm and 3mm zero gaps. The specific energies consumed at these zero gaps did not differ significantly particularly for the first three passes (Figure 4-10(a)). This suggests that the HPGR zero gap does not significantly affect the outcome of the results obtained for Merensky ore.

Figure 4-13(a) and Figure 4-14(a) show the effect of pressure and zero gap on the reduction ratio-specific energy relationship for Merensky. The energy efficiency of the

HPGR is determined by analysing the relationship between the reduction ratio and the specific energy consumed (Norgate and Weller, 1994; Fuerstenau and Kapur, 1995; Lim *et al*, 1997). Linear relationships between the reduction ratios (F_{50}/P_{50}) and the cumulative specific energies were obtained showing that increasing the specific energy results in increasing reduction ratios for the specific energies tested in this work. This is consistent with what Fuerstenau and Kapur (1995) obtained for limestone and quartz. Lim *et al* (1997) also obtained linear relationships for two gold ores but the bauxite and diamond ores did not exhibit linear trends. These findings appear to suggest that the reduction ratio-specific energy relationship is ore dependent.

Table 4-5 shows that for Merensky, to achieve a reduction ratio of 4.7, 13% less energy is used if the HPGR is operated at a pressure of 150bar for a single pass compared to a multi-stage operation at a lower pressure. Therefore, it is more energy efficient to apply the HPGR at higher pressures as a single pass application. This is contradictory to the results that were obtained by Norgate and Weller (1994) on a gold ore. These authors found that a 50% reduction in specific energy was obtained when the HPGR was applied as a multi-stage operation at a lower specific force compared to a single stage application to achieve a reduction ratio of 6 (Table 6-2). The range of specific forces (3 – 7.5N/mm^2) and specific energies (1.5 – 7kWh/t) applied on Merensky ore in this study were also used by Norgate and Weller (1994). Since the operating conditions and design variables were similar, the dissimilarities in the results obtained could only be due to the differences in the ore characteristics. The specific forces used by Norgate and Weller (1994), i.e. 3N/mm^2 and 12N/mm^2 correspond to pressures 60bar and 240bar on the HPGR used in this work.

Table 6-2: Results obtained by Norgate and Weller (1994) showing specific energies for a single and multi-stage HPGR application

Specific force (N/mm^2)	F_{50}/P_{50}	Pass	E_{sp} (kWh/t)
3	6	2	4
12	6	1	8

The specific energy-reduction ratio relationship can be used to determine the most energy efficient application of the HPGR for a particular ore. However, the evaluation of suitable applications of the HPGR should also consider factors such as the fineness of grind achieved. Consideration of the fineness of grind achieved would enable one to determine if it is feasible to obtain a favourable reduction ratio. If it is assumed that the saturation points have been reached after four passes, the highest pressure of 150bar appears to produce a much finer grind of 41.0% passing 75µm compared to the lower pressures (Table 6-3). An increase in the fineness of grind with pressure is evident in Table 6-4 where the lowest pressure used in the experimental work produced a grind of 27% passing 75µm. Therefore to achieve a certain reduction ratio is required for any particular ore type, the saturation points should be considered in determining the suitable operational variables for the application of the HPGR.

Table 6-3: % passing 75µm and reduction ratios obtained at the saturation points at varying pressures for Merensky

Pressure (bar)	Cumulative E_{sp} (kWh/t)	F_{50}/P_{50}	% passing 75µm
60	3.00	4.7	27.1
90	4.66	5.9	32.6
120	4.97	7.7	34.4
150	7.04	10.8	41.0

Tavares (2005) established that an optimum level that can be applied with the HPGR must not only consider the size distribution of the product but also its amenability to subsequent grinding stages. The following section discusses the effects on throughput and specific energy when the HPGR is applied as a pre-grinding stage to the ball mill. As discussed in section 3.3.2 a single pass through the HPGR product generated at a pressure of 60bar and a zero gap of 3mm was ground with the ball mill. The results obtained are shown in section 4.2 and are discussed in the following section.

6.1.4 Comparison to ball mill

Table 4-7 shows the data from the ball mill tests that was used to calculate the specific energies consumed. Equation 12 was applied to determine the specific energy consumed for each ball mill test performed. Differences in specific energy between ore pre-crushed with the HPGR and uncrushed ore could not be determined with the application of the above equation. Therefore, the Bond equation which includes the Bond Work Index that accounts for the hardness of the ore was applied. However, it was found that the Bond Work Indices of the HPGR product used as a feed to the ball mill did not change significantly compared to that of the feed to the HPGR for the three ore types tested in this study. Tavares (2005) found that compression breakage with the application of the HPGR resulted in the weakening of the ore structure. Therefore, the Bond Work Index of HPGR treated ores become lower and this was not the case for the ores in this study. Norgate and Weller (1994) on the other hand, found that Bond work indices for zinc and gold ores that were ground with the HPGR were lower than those of untreated ore. Therefore, the dissimilarities in results generated in this study and those obtained by Norgate and Weller (1994) could be due to differences in ore type.

The size distributions generated from the ball mill tests for Merensky ore (Figure 4-6(a)) shows that the ball mill produced steeper size distributions compared to the HPGR. Similar results were obtained by Palm *et al* (2009) where the size distributions generated by the HPGR were broader than those generated by the cone crusher which is known to produce particle size distributions that are broader that those of the ball mill. This is due to the differences in breakage mechanism applied by the two comminution devices. The HPGR applies interparticle breakage while the ball mill has a combination of impact and abrasion breakage as the ore moves in the tumbling motion. Similar trends were observed for UG2 and Platreef ores.

In this study it has been shown that for Merensky ore an increase in throughput of more than 30% could be obtained when the HPGR was applied as a prelude to ball mill grinding without changing the fineness of grind (Figure 4-15(a)). Aydoğan *et al* (2006) also showed that the application of the HPGR in open circuit or as a hybrid (HPGR-Ball

mill) can increase the capacity of existing comminution circuits. Tavares (2005) suggest that this is due to the weakening of the particles produced from the HPGR which make breakage in downstream grinding easier. A grind of 36.4% passing 75µm was obtained for a 6mm feed to the ball mill at a throughput of 720kg/h. For the feed that was pre-ground with the HPGR, a throughput of 936kg/h a grind of 39.1% passing 75µm was achieved. This shows that the throughput can be increased further to match the grind produced by ball mill alone treating 720kg/h of feed with a 6mm feed topsize.

Table 6-4 shows the fineness of grind (% passing 75µm) and the specific energies consumed during the ball mill tests for Merensky ore. Slightly lower specific energy (3.2%) was consumed in the HPGR-Ball mill test with a throughput of 936kg/h compared to the ball mill test performed on untreated ore at a throughput of 720kg/h. This suggests that it is more energy efficient to treat HPGR ground ore with the ball mill due to benefits such as improved throughput and reduced energy consumption. Therefore the addition of the HPGR to existing comminution circuits has the potential to reduce energy consumption at increased throughput. Similar outcomes were obtained by Rule *et al* (2008) on a UG2 ore at Northam Platinum. In their work, further tests were performed to determine the effects of HPGR on PGM flotation recovery. A similar step was taken in this study and the flotation results obtained from the HPGR and ball mill tests are discussed in the following section.

Table 6-4: % passing 75µm and the specific energies (E_{sp}) consumed by Merensky ore during the ball mill tests

Ore type	Ball Mill (720kg/h)	HPGR-Ball (743kg/h)	HPGR-Ball (936kg/h)
% passing 75µm	36.4	41.0	39.1
E_{sp} (kWh/t)	8.57	9.95	8.24

6.1.5 Flotation

The relationship between the mass and water recoveries shown in Figure 5-1 have been used in this work to give an indication of the PGE grade and recoveries that could be obtained (Wiese *et al*, 2006). For Merensky ore (Figure 5-1(a)) the lowest mass recoveries were obtained for the HPGR test performed at a zero gap of 3mm and a feed top size of 12mm. This is consistent with the higher PGE grades that were obtained under these conditions as shown in Figure 5-3(a). This could be due to the coarser grind of the flotation feed as shown in Figure 6-1. The lower fines content and water recovery of the above mentioned test compared to the other flotation tests suggest that there was less recovery by entrainment. This is in agreement with Shi *et al* (2006) who found that coarser feeds achieved better grades but lower recoveries.

Similarities in the mass pull were obtained for the ball mill and HPGR tested performed at a zero gap of 1.5mm and feed top sizes 12mm and 6mm. This correlated with the similarities in grades obtained for these tests. However, although similarities in mass pull were observed for the above mentioned tests; there were some differences in the water recoveries. A higher water recovery indicates a more stable froth and is mainly due to higher fines content (Feng and Aldrich, 1999; Palm *et al*, 2009). The ball mill sample shows slightly lower water recoveries compared to the two HPGR samples (1.5mm and feed top sizes 12mm and 6mm). Although the % passing 75µm of the ball mill feed (36.4%) is less than that of the HPGR flotation feeds generated at 1.5mm and feed top sizes 12mm and 6mm (41.0% and 41.5%), a lower coarse content was obtained for the ball mill product (Figure 6-1). The slightly higher water and PGE recoveries obtained from the ball mill flotation results could be due to the lower coarse content in the 125µm - 1000µm size fraction.

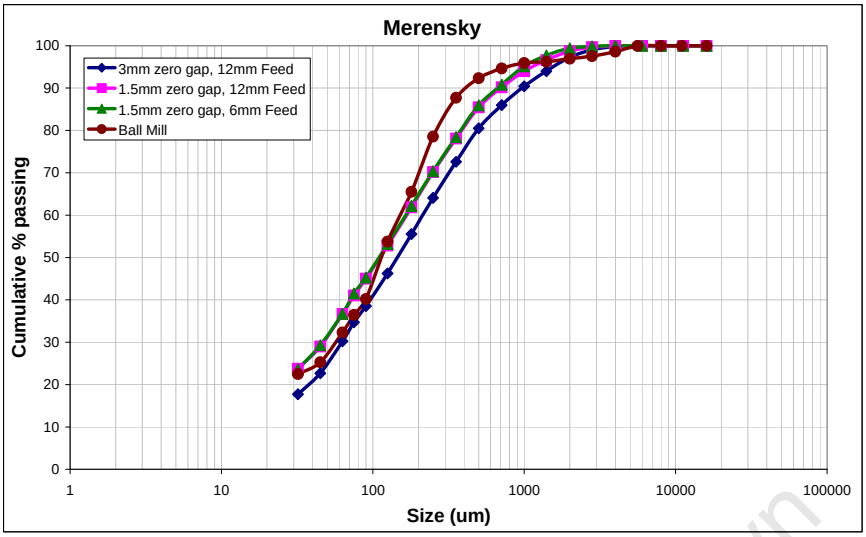

Figure 6-1: Flotation feed size distributions from the HPGR and the ball mill for Merensky

6.1.6 PGM mineralogy

The Merensky liberation profiles in Figure 5-6(a) show that better liberation was obtained with the ball mill compared to the HPGR. The majority of the PGMs were either liberated (73.6%) or associated with base metal sulphides (19.1%). This is consistent with lower coarse content obtained with the ball mill compared to the HPGR (Figure 6-1). Penberthy *et al* (2000) indicated that some mineralogical factors that may affect the recovery of PGEs include the degree of liberation and the association with minerals in the ore body. PGMs that are associated with liberated base metal sulphides are more likely to be recovered compared to those that are locked in gangue or associated with locked base metal sulphides. The average grain sizes of the PGMs in Merensky obtained in this work are less than 10µm as shown in Table 5-4. Liberated PGMs generally report to concentrates but at a slower rate due to the small grain sizes (Penberthy *et al*, 2000; Johnson, 2005).

Figure 5-6(a) also shows that the coarser feed obtained with the HPGR at a zero gap of 3mm and feed top size of 12mm had 43% of the PGMs liberated and 10% associated with liberated base metal sulphides. The remaining PGMs were locked in gangue (28.2%) or

associated with base metal sulphides that were locked in gangue minerals (19.1%). Therefore, further grinding would be required to further liberate the locked PGMs.

The results obtained in this study suggest that the application of the ball mill on Merensky resulted in the generation of product with a lower coarse content and hence better liberation. As a result, better PGE recoveries were obtained with the ball mill compared to the HPGR. However, slightly lower grades were obtained with the ball mill. These results are consistent with what has been obtained by Palm *et al* (2009) and Shi *et al* (2006) for finer size fractions.

6.2 UG2

6.2.1 Throughput

UG2 showed no significant differences in throughput as the pressure increased (Figure 4-1(b)). This is similar to the results obtained by Lim et al (1997) on a gold and diamond ore. However, for other ore types such as iron and bauxite, Lim *et al* (1997) found that there were slight decreases in throughput with increasing pressure. Similarly, Merensky ore showed a decrease in throughput with an increase in pressure. This suggests that the effect of pressure is dependent on the ore type. The fineness of the ore also has an effect on throughput obtained. Lim *et al* (1997) found that a finer feed could either result in a higher or lower throughput depending on the ore type. For UG2 ore, it was found that increasing the number of passes decreased the throughput. This is due to the reduced separation of the rolls as the feed became finer after each subsequent pass resulting in the material being pulled into the gap between the rolls at a slower rate.

Figure 4-2(b) shows that the zero gap also has an effect on the throughput. Slightly higher throughputs were obtained at the 3mm zero gap compared to that at 1.5mm. However, for the 4.5mm zero gap a constant throughput (4.7t/h) was observed for the first three passes and then a sharp increase at the fourth pass to 5.7t/h. Lunjuhn and Schönert (1993) also found that the throughput remained constant for limestone and quartz as the specific force

increased for the same feed topsize. While Lunjuhn and Schönert (1993) do not site reasons for this behaviour, this author believes that the operational variables and the feed top sizes applied in their work may have resulted in this effect. Similarly, in the work performed in this thesis, the 4.5mm zero gap had no significant effect on the throughput of UG2 ore until the material became too fine. This suggests that the ore passed through without being nipped resulting in the sharp increase in throughput at the fourth pass. This was confirmed by analysing the sizing data.

6.2.2 Size distributions

The size distributions obtained for UG2 ore are bimodal as shown in Figure 4-5(b). Daniel (2007) obtained similar size distributions for a Lonmin platinum/chrome ore. The mineralogical analysis performed by Daniel (2007) on this ore showed that un-liberated chromite particles were obtained for the -850 + 600µm size fraction while the -425 + 300µm size fraction showed fully liberated chromite particles. Daniel (2007) postulated that this bimodal effect on the liberation of the chromite particle is the cause of the kink observed in the size distributions at the 425µm size. Similarly, in this thesis, a kink in the size distribution was observed at 500µm as shown in Figure 6-2 which could be due to the reasons described by Daniel (2007). It is for this reason that Daniel (2007) suggests that the P_{80} and Bond test methodology should not be used on this ore type.

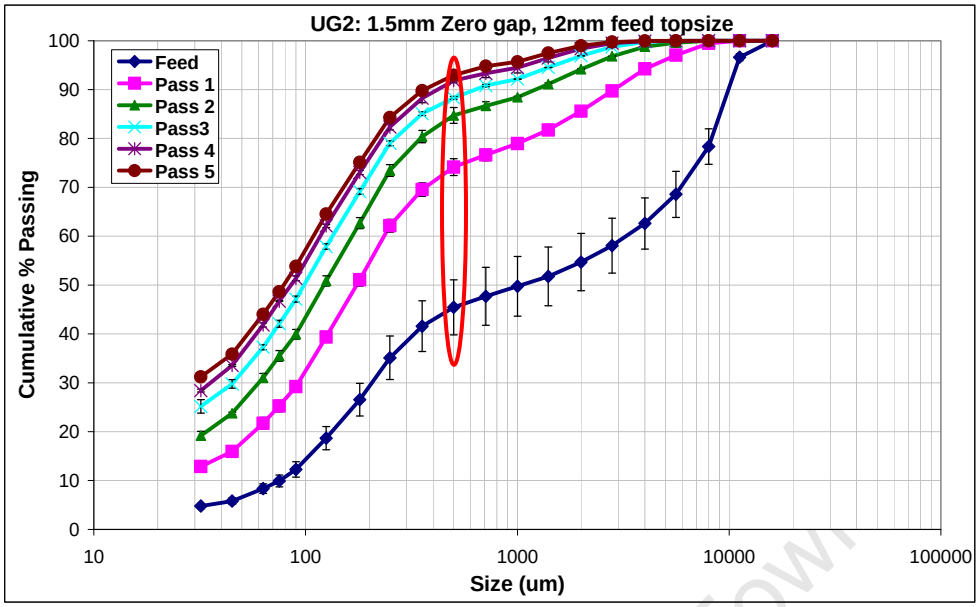

Figure 6-2: UG2 size distributions showing the kink obtained at the 500µm size

UG2 showed no significant differences in fineness of grind for the first two passes at pressures 90, 120 and 150bar (Figure 4-6(b)). From the third pass onwards, distinctions in pressure effect could be seen. Increasing the pressure resulted in an increase in the percent passing 75µm. No significant differences in the percent passing 75µm were observed at zero gaps 1.5mm and 3mm. The 4.5mm zero gap showed that a saturation point had been reached after three passes. This is consistent with the throughput observations at the same zero gap. At the fourth pass, there was a sharp increase in throughput because the ore was too fine for the 4.5mm zero gap resulting in the ore passing through the rolls without being nipped.

In the Los Bronces project performed on different quartz ores discussed in section 2.2.2 (page 30), similar size distributions were obtained in the pressure range of 60 – 90bar (Van Drunick and Smit, 2006).This was postulated to be due to the properties of the ore and the feed size distribution. Therefore, Van Drunick and Smit (2006) suggest that attention must be paid to the optimisation of the HPGR grinding pressures with respect to feed properties. The specific energy consumed at different HPGR operational variables where similar grinds are generated must also be considered during optimisation.

6.2.3 Specific energy consumption and energy efficiency

Although the pressures 90, 120 and 150bar generated a similar grind for the first two passes for UG2 ore, Figure 4-9(b) shows that increasing the pressure resulted in an increase in the cumulative specific energy consumed. A 25% increase in specific energy was obtained when changing the pressure from 90bar to 150bar while generating a similar grind of 33.5% passing 75µm. Therefore when optimizing the processes, it is essential to consider the grinds achieved and the specific energies consumed for each ore type.

In Figure 4-10(b) at a zero gap of 4.5mm the saturation point was reached which is consistent with the throughput and fineness of grind data discussed in previous sections. It was also found that at pass four there was no flake formation, little compaction was experienced by the material and hence an insignificant amount of specific energy was consumed. Similar grinds were obtained after five passes at the 1.5mm and 3mm zero gap but at the 3mm zero gap, 8% less specific energies was consumed. However, depending on the stability of a plant, this may not be considered to be a significant difference in specific energy consumed.

In section 4.1.3 it was shown that similar specific energies were consumed at 150bar after two passes (4.74kWh/t) and at 60bar after four passes (4.69kWh/t). Finer product was obtained at 60bar (39.5% passing 75µm) compared to that at 150bar (34.0% passing 75µm). However, the reduction ratio-specific energy relationships generated for UG2 (Figure 4-13(b)) show that at 150bar after two passes a reduction ratio (F_{50}/P_{50}) of 8 was obtained while at 60bar after four passes a reduction ratio of 6.2 was obtained. This suggests that in terms of reduction ratios it was more energy efficient to apply the HPGR at the higher pressures for fewer passes (Table 6-5). The differences in outcome observed when analysing the data based on the grind obtained compared to reduction ratio suggest that it is better to analyse the data in terms of the reduction ratios. This is because the reduction ratio takes into account the feed size distribution when determining the most energy efficient HPGR applications for any ore type. Therefore, based on the reduction ratios, it was more energy efficient to apply the HPGR at the higher pressure of 150bar

for two passes due to the larger reduction ratio obtained compared to that at 60bar for four passes.

Table 6-5: Effect of pressure and number of passes on specific energy (E_{sp}), fineness of grind and reduction ratio for UG2

Pressure (bar)	E_{sp} (kWh/t)	Pass	% passing 75µm	F_{50}/P_{50}
60	4.69	4	39.5	6.2
150	4.74	2	34.0	8.0

6.2.4 Comparison to ball mill

In section 4.2.2 it was shown that for UG2 ore a 31% increase in throughput was obtained when the feed to the ball mill was pre-ground with the HPGR with a 6% decrease in specific energy consumed for the same grind produced (Table 6-6). This confirms what has been obtained in literature where it was found that the HPGR has the potential to increase the capacity in the circuit containing the conventional ball mill (Aydoğan *et al*, 2006; Rule *et al,* 2009; Patzelt *et al,* 2001). Therefore, the HPGR can be used as a pre-grinding stage to increase ball mill capacity with no significant changes in the specific energy consumed and the grind generated.

Table 6-6: % passing 75µm and the specific energies (E_{sp}) consumed by UG2 ore during the ball mill tests

Ore type	Ball Mill (709kg/h)	HPGR-Ball (712kg/h)	HPGR-Ball (932kg/h)
% passing 75µm	42.3	49.1	42.0
E_{sp} (kWh/t)	9.20	10.8	8.65

6.2.5 Flotation

The mass-water recoveries for UG2 in Figure 5-1(b) show that the lowest mass pull was obtained from the ball mill tests. The feed size distributions used in the flotation tests given in Figure 6-3 show that while the ball mill product had a lower coarse content, it also showed lower fines content compared to the three HPGR products shown. Slightly more mass pull was obtained with the ball mill compared to the HPGR tests performed at a zero gap of 1.5mm and feed topsizes 6mm and 12mm. This corresponds to the slightly higher PGE recoveries obtained for the ball mill. The water recovery obtained with the ball mill tests was slightly lower than that obtained with the two HPGR tests previously mentioned. This is consistent with the lower fines fraction and the better grades obtained with the ball mill (Palm *et al*, 2009).

It was found that the higher PGE recoveries and lower grade for the HPGR product generated at a zero gap of 3mm and a feed topsize of 12mm are due to a higher frother dosage that was used.

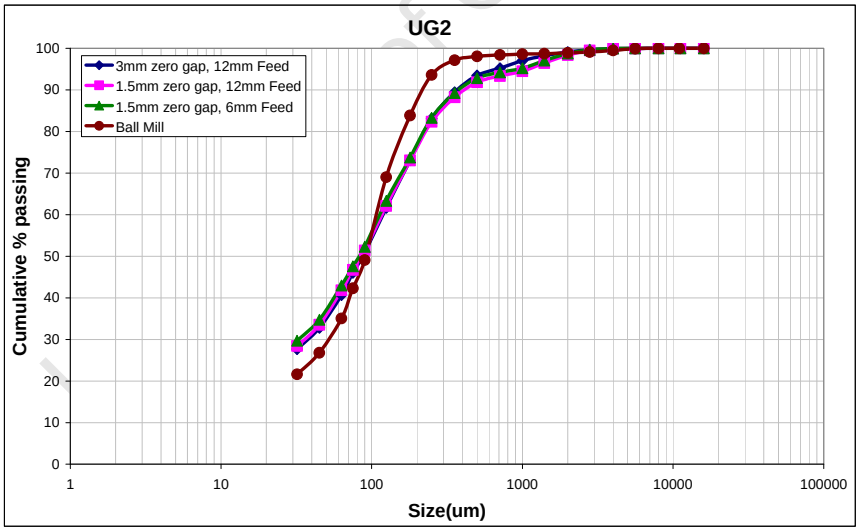

Figure 6-3: Flotation feed size distributions from the HPGR and ball mill for UG2

6.2.6 PGM liberation

Although similar size distributions were obtained for the three HPGR products shown in Figure 6-3, differences in liberation profiles were observed. The UG2 liberation profiles

shown in Figure 5-6(b) show that the HPGR product generated at a zero gap of 3mm and a feed topsize of 12mm had the least amount of liberated PGMs (27.3%). The HPGR product generated at a zero gap of 1.5mm and feed top sizes 12mm and 6mm had 52.8% and 44.0% liberated PGMs, respectively.

The ball mill liberation profile showed that 48.3% of the PGMs present were liberated which is comparable to the liberation profiles obtained from the HPGR products generated at a zero gap of 1.5mm and feed topsizes 12mm and 6mm. Therefore the better PGM grade and recoveries obtained with the ball mill compared to the HPGR could be due to the differences in grind as observed Figure 6-3. A lower coarse content was observed for the ball mill between size fractions 125µm - 1000µm. Therefore the application of the ball mill resulted in the reduction of the coarser particles which could mean better liberation in this size fraction.

6.3 Platreef

6.3.1 Throughput

The Platreef throughput decreased with increasing number of passes (Figure 4-1(c) and Figure 4-2(c)). However, there was no significant difference in throughput between the first and second passes for pressures in the range 60 – 150bar (Figure 4-1(c)). This could to be due to the hardness of Platreef ore and the high coarse content. The slip between the rolls and the particles may have been similar at passes 1 and 2, which resulted in similar throughputs being obtained at these passes. The reduction in throughput after the second pass is due to the increasing fineness of the HPGR feed as the number of passes increased. The higher fines content in subsequent passes resulted in reduced slip between the particles and the rolls, and between particles which contributed to the lower throughput observed at higher passes (Austen *et al*, 1993). In addition, there was less separation of the rolls as the feed became finer which resulted in the material being pulled into the gap between the rolls at a slower rate.

The zero gap effects in Figure 4-2(c) show that no significant differences in throughput were observed at the 1.5mm and 3mm zero gaps for the first three passes. After the third pass when the material was finer, the 3mm zero gap showed a slightly higher throughput than that at 1.5mm. The 4.5mm zero gap showed higher throughputs than the 1.5mm and 3mm zero gaps at the second and third passes. The working gap results (Figure 4-4(c)) shown are consistent with the results showing effect of zero gap on throughput (Figure 4-2(c)).

The working gap was obtained by measuring the thickness of several flakes formed during the tests and averaging the values obtained. However, this is not an accurate measurement of the working gap because the flakes tend to expand after passing through the compression zone (Lim and Weller, 1998). The results in Figure 4-4 (c) show that no significant differences in working gap were observed over fives passes for the 1.5mm and 3mm zero gaps. This is consistent with the throughput trends observed at the above mentioned zero gaps, particularly at the first three passes. The working gap at the 4.5mm zero gap was higher than that at the 1.5mm and 3mm zero gaps. No significant differences in working gap were observed at the 4.5mm zero gap as the number of passes increased. This could be because the 4.5mm zero gap was too wide such that it did not have an effect on the working gap.

During operation, it was observed that for Platreef ore, instead of being pulled between the rolls, some of the ore accumulated on the outside of the rolls particularly at the first pass. This effect was described as external by-pass of the material by Klymowsky *et al* (2002) who attributed this behaviour to be due hardness of the ore. This effect was not observed with the Merensky and UG2 ore.

6.3.2 Size distributions

For Platreef ore, as the number of passes increased, the material became progressive finer as shown in Figure 4-5(c). The material did not appear to have reached saturation points for pressures in the range 60 – 150bar at the 1.5mm zero gap. This is confirmed in Figure

4-6(c) which shows that the percent passing 75µm increased with increasing pressure and number of passes with no indication of the saturation point being reached. The zero gap effects (Figure 4-7(c)) show that for the 1.5mm and 3mm zero gaps, the fineness of grind was similar up to the third pass after which the 3mm zero gap showed slightly coarser grinds at the fourth and fifth passes. At the 4.5mm zero gap, a saturation point was reached after the third pass and this could be because the gap between the rolls was too wide to have any impact on size reduction.

6.3.3 Specific energy consumption

The cumulative specific energy trends observed for Platreef ore are consistent with what was observed with the fineness of grind in Figure 4-6(c). There was an increase in specific energy consumed with increasing pressure but with no saturation point being reached. The zero gap effects showed that there were no differences in cumulative specific energy at the 1.5mm and 3mm zero gaps for the first three passes after which the 1.5mm zero gap exhibited higher cumulative specific energies. This is also in conformity with the fineness of grind behaviour shown in Figure 4-7(c). At the 4.5mm zero gap, a saturation point was reached after the third pass which is also consistent with the fineness of grind trends observed for UG2 (Figure 4-7(c)) at the same zero gap.

Platreef ore consumed more specific energy compared to Merensky and UG2. This is because Platreef is more competent compared to the other two as shown by the characterisation indices presented by Mainza and Powell (2006). A maximum cumulative specific energy of 12.6kWh/t was consumed by Platreef after four passes at a pressure of 150bar and a zero gap of 12mm. Under the same HPGR conditions, lower cumulative specific energies of 7.0kWh/t and 8.4kWh/t were consumed by Merensky and UG2, respectively.

The reduction ratio-specific energy relationships for Platreef ore (Figure 4-13(c)) are non-linear with increasing slopes. This relationship suggests that the application of the HPGR on Platreef ore is more energy efficient compared to Merensky and UG2. A

similar relationship was obtained by Norgate and Weller (1994) for a multi-pass operation of the HPGR on a gold ore (Figure 2-14). However, they used a linear model which did not fit the data well. Application of the power-law (equation 5) could fit the data better and will result in a relationship similar to that obtained in this work for Platreef ore.

It was found that at 60bar after four passes, a similar amount of energy (5.8kWh/t) was consumed as at 150bar (5.9kWh/t) after two passes. The cumulative reduction ratios obtained at these conditions were 22.7 and 18.2 respectively. This suggests that for Platreef ore, it was more energy efficient to operate the HPGR at the lower pressure (60bar) for multiple passes if a certain reduction ratio is required. In practical applications this suggests that several HPGRs operating at low pressures operating in series would be required to generate finer product with no significant change in specific energy consumed. While there are some benefits with this set up in terms of specific energy, it would be undesirable for other aspects such as throughput, capital costs and maintenance costs.

6.3.4 Comparison to ball mill

For Platreef ore it was found that although a 33% increase in the throughput of the material in the HPGR-ball mill tests from 710kg/h to 943kg/h did not alter the fineness of grind to a large extent (Figure 4-6(c)), there was a decrease of 20.5% in specific energy consumed (Table 6-7). Comparison of the ball mill test performed with the 6mm feed showed a coarser product compared to that obtained with the HPGR-ball mill tests (Figure 4-15(c)). This suggests that further increases in ball mill throughput of the pre-ground ore could eventually generated a grind similar to that obtained with the un-ground ore. However, further tests are required to determine if this outcome can be achieved.

Table 6-7: % passing 75µm and the specific energies (E_{sp}) consumed by Platreef ore during the ball mill tests

Ore type	Ball Mill (695kg/h)	HPGR-Ball (710kg/h)	HPGR-Ball (943kg/h)
% passing 75µm	29.7	40.2	39.3
E_{sp} (kWh/t)	9.54	11.1	8.83

Comparisons of the percent passing 75µm generated for Merensky (36.4%), UG2 (42.3%) and Platreef (29.7%) further emphasizes the hardness of Platreef. However, the application of the HPGR at a ball mill throughput of approximately 900kg/h resulted in similar percent passing 75µm for Merensky (39.1%), UG2 (42.0%) and Platreef (39.3%). The total specific energies consumed under these conditions using a combination of the HPGR and ball mill were 8.24kWh/t, 8.65kWh/t and 8.83kWh/t, respectively. This suggests that the application of the HPGR on hard ore types such as Platreef ore has the potential to soften the ore and generate grinds similar to those obtained with Merensky and UG2 under similar ball mill conditions.

6.3.5 Flotation

The ball mill product, which had a coarser size distribution compared to the HPGR products as shown in Figure 6-4 had the lowest mass pull. This is consistent with the grades observed in Figure 5-3(c) which show that better grades were obtained with the ball mill compared to the HPGR. Higher PGE grades (66.8g/t) and lower recoveries (64.1%) were obtained with the ball mill. The HPGR PGE grades and recoveries were in the range 20 – 60g/t and 64% - 70%, respectively. The two HPGR tests performed at a zero gap of 1.5mm and feed top sizes 12mm and 6mm had similar grinds (39% passing 75µm) and hence showed similarities in the mass pull. However, the HPGR test performed at a zero gap of 1.5mm and feed top sizes 12mm had a slightly higher water recovery. This is consistent with the slightly higher PGE recovery at lower grade obtained (Figure 5-3(c)). The results obtained here can be used to draw a conclusion to

determine whether the flotation response is better for the ore comminuted with the ball mill or the HPGR. This is due to the differences in the grind which could have contributed to the differences noted in the behaviour.

The Platreef ball mill size distribution has a shape that is typically observed in industry. The ball mill appears to struggle to grind Platreef particularly in the coarse size fraction (1mm – 5mm). This trend is typically observed in industrial grinding of Platreef ore. In some instances, the presence of scats in the grinding media could be the cause of the insufficient grinding of the Platreef ore. Scats are balls that have worn out and become smaller due to the grinding action in the mill. In this work, there was no presence of scats in the mill however difficulties were still experienced in grinding the coarser size fraction. The HPGR-ball size distributions show that the application of the HPGR as a pre-grinding stage for Platreef ore could assist in the breakage of the harder, coarser particles.

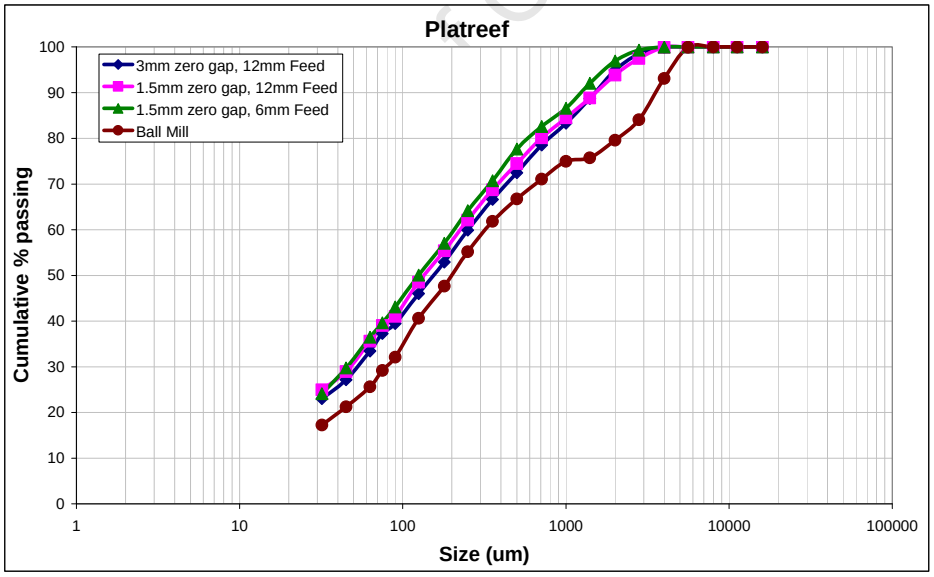

Figure 6-4: Flotation feed size distributions from the HPGR and ball mill for Platreef

6.3.6 PGM liberation

The liberation profiles shown in Figure 5-6(c) show that better liberation was obtained with the HPGR tests performed at a zero gap of 1.5mm and a feed top size of 12mm with 55.5% of the PGMs being liberated. Due to the similarities in grind between the HPGR samples generated at a zero gap of 1.5mm and feed top sizes 12mm and 6mm, similarities in liberation profiles were expected. The ball mill product showed the least amount of liberated PGMs (11%). This could be due to the coarser grind obtained with the ball mill particularly at the coarser end of the size distribution (Figure 6-4).

6.4 Summary

This chapter discussed the effects of the HPGR on throughput, specific energy consumption and size reduction on Merensky, UG2 and Platreef ores. The effects on PGE flotation recovery and mineral liberation of the HPGR in comparison to the ball mill were also discussed. Consistency with regards to trends observed in throughput, specific energy and fineness of grind were observed for all three ore types. It was found that the pressure, zero gap and ore characteristics play a significant roll in the grind of the product obtained from the HPGR. Platreef showed higher specific energies compared to Merensky and UG2 postulated to be due to the differences in hardness of the ores. Generally, the trends observed with respect to the application of the HPGR showed conformity to those obtained in literature on different ore types.

Differences in the specific energy-reduction ratio relationships for the three ores further emphasized the importance of ore type. For ore types such as Platreef, it was more energy efficient to operate the HPGR at lower pressures for multiple pass operations to achieve a certain reduction ratio. However, it is more desirable to achieve the reduction ratio in as fewer passes as possible. Therefore, from the perspective of a design plant, fewer process stages may be required to minimize capital cost which would result in the higher pressure scenario being preferable.

Chapter 7

7 Conclusions and Recommendations

Overview: This chapter gives conclusions and recommendations based on the findings and the objectives set out for this study.

7.1 Conclusions

This section gives conclusions in the form of answers to the key questions and the outcomes obtained in testing the hypotheses.

7.1.1 Key questions

1. Is it possible to apply the HPGR as an alternative to the highly energy inefficient ball mill in a grinding circuit processing platinum bearing ores?

Based on the sizing analyses, it was found that a circuit with a series of HPGRs could be applied as an alternative to the ball mills particularly in the primary comminution stage. Grinds of up to 41.5%, 47.6% and 36.9% passing 75μm were obtained after five passes for Merensky, UG2 and Platreef, respectively. This is within the range of grinds applied in the primary comminution circuits in platinum processing plants. Depending on the grind required, the HPGR parameters can be adjusted to ensure that more energy efficient conditions are applied. Indicators are that if operated in closed circuit with efficient screens or other forms of classifiers, HPGRs can be used to produce fine product that is comparable to primary ball mills in a single stage and at a reasonable tonnage.

2. How does the application of the HPGR affect downstream PGE recovery?

Although the material comminuted with the HPGR was able to float, the PGE grade and recoveries were consistently inferior to that of the ball mill. Therefore no benefits in PGE recovery were observed with the application of the HPGR.

3. How does the HPGR affect energy efficiency and size reduction of each ore type?

Generally, it was found that increasing the energy input resulted in the generation of more fines due to higher breakage rates. However, the extent of size reduction and energy consumption is ore dependent. While Merensky and UG2 showed better energy efficiencies at higher pressures for fewer pass, Platreef produced better results at lower pressures with a higher number of passes.

7.1.2 Hypotheses

1. **The operational variables where the HPGR can comminute the ore with minimal energy requirements vary for different ore types because material with dissimilar mineralogical compositions will respond differently to the applied force.**

The results obtained in this work showed that effects of the HPGR variables on specific energy consumption and the extent of size reduction is dependent on the ore type. Merensky ore showed that saturation points were reached after four passes for the different pressures tested at a zero gap of 1.5mm and a feed top size of 12mm. At the different saturation points reached for varying pressures, differences in the grind obtained were observed. For UG2ore, while no significant differences were observed in the grind obtained for the first three passes between pressures and 90bar and 150bar, variations in the specific energy consumption were observed. For Platreef ore, the general trends showed that increasing the pressure resulted in an increase in specific energy consumed and the fineness of grind obtained. Therefore, in the determination of the optimum operational variables of the HPGR, for different ore types, factors such as the saturation points and the specific energy consumed for similar grinds produced must be considered.

The energy efficient application of the HPGR also varied for the different ore types and this was observed with the differences in the trends observed in the specific energy-reduction ratio relationships. Linear relationships were obtained for Merensky at varying pressures while UG2 and Platreef exhibited non-linear relationships. While the reduction ratio-specific energy relationship is essential for determining the most energy efficient

operational conditions of the HPGR for each ore type, it does not take into account the saturation points. Therefore reference to the grinds and specific energy relationships is required to determine possible HPGR operational variables for each ore type.

2. **The HPGR can be used to prepare the ore for flotation without any subsequent grinding at reduced specific energy. This is due to the different breakage mechanism applied by the HPGR which can potentially liberate valuable minerals at a coarser grind.**

Grinds that are comparable to those obtained in platinum processing circuits were obtained. However, in this work, this was achieved through multiple passes of the ore through the HPGR. In practice, this would require several HPGRs in series to achieve similar results which would result in high capital and maintenance costs. In terms of the energy consumed, it was found that the HPGR generally consumed higher specific energies compared to the ball mill to produce similar grinds. The differences were most significant with Platreef ore compared to Merensky and UG2.

Generally, better PGE recoveries were obtained with the ball mill compared to the HPGR. Steeper size distributions were obtained with the ball mill suggesting that the lower coarse and fines content contributed to the better grades and recoveries obtained with the ball mill. The liberation profiles for Merensky ore showed more liberated PGMs obtained with the ball mill compared to the HPGR. UG2 showed no significant difference in liberation profiles between the HPGR and the ball mill while Platreef showed better liberation profiles with the HPGR.

7.2 Recommendations

Based on the investigations performed in this work, the following recommendations for further work have been made.

- Further tests could be performed on the platinum ore to determine more energy efficient methods of generating a grind that can be applied in the primary comminution stage at reduced energy consumption. This could be through the application of the HPGR in closed circuit with screens or classifiers. The following scenario would be preferred:
    - Recycling a portion of the HPGR product before screening out the coarse material to introduce more fines into the feed to promote the generation of more fines in the product.
    - The addition of a screen with 1mm apertures to screen the HPGR product and recycling the screen oversize. This will ensure that only sub 1mm product sizes report to the downstream process
    - To install air classifiers to classify the HPGR product and recycle the oversize while sending the fines to downstream processes.

- An investigation of the size by size mineralogical analysis of the HPGR and ball mill product and flotation concentrate is required to fully understand the implications of generating particles with different comminution devices on downstream processes. Daniel (2007) found that the differences in breakage modes of the HPGR and the ball mill did not affect the liberation characteristics of the valuable mineral in bauxite and lead/zinc ore for a size fraction of -53 + 38μm. Differences in liberation characteristics were observed with respect to chromite in the Lonmin platinum ore. However the liberation characteristics of the PGMs were not investigated and therefore inconclusive with regards to PGM liberation characteristics (Daniel, 2007). Therefore a similar analysis in terms of a size by size analysis of PGM liberation would assist in the determination of the effect of HPGR on downstream processes.

- A size by size mineralogical analysis of the concentrate and tails along with other flotation chemistry measurements could further assist in explaining some of the PGE grade and recoveries obtained.

References

Apling, A., Bwalya., M., 1997, Evaluating high pressure milling for liberation enhancement and energy saving, Minerals Engineering, Vol. 10, Issue 9, 1013-1022.

Austin, L. G., Weller, K. R., Lim, I. R., 1993, Phenomenological Modelling of the High Pressure Grinding Rolls, XVIII International Mineral Processing Congress, pp87 – 95

Aydogan, N.A., Ergun, L., Benzer, H., 2005, High pressure grinding rolls (HPGR) applications in the cement industry, Minerals Engineering, Vol. 19, 130-139.

Brachthauser, M., Kellerwessel, H., 1988, High Pressure Comminution with Roller Press in mineral processing, XVI International Mineral Processing Congress, Vol. 10A, pp209 – 219

Cabri, L. J., 2004 New Developments in Process Mineralogy of Platinum-Bearing Ores, Proceedings of Canadian Mineral Processors, 189-198.

Cabri, L.J., Beattie, M., Rudashevsky, V.N., 2005, Process Mineralogy of Au, Pd, Pt ores from the Skaergaard intrusion, Greenland, using new technology, Minerals Engineering, Vol. 18, 887-897.

Celik, I.B., Oner, M., 2006, The influence of grinding mechanisms on the liberation characteristics of clinker minerals, Cement and concrete research, Vol. 36, 422-427

Clarke, A. J., Will, B. A., 1989, Enhancement of cassiterite liberation by High Pressure Roller comminution, Minerals Engineering, Vol. 2, Issue 2, pp 259 – 262

Clarke, B., Uken, R., Reinhardt, J., 2008, Structural and compositional constraints on the emplacement of the Bushveld Complex, South Africa, Lithos-01857

Cole, S., Ferron, C. J., A review of the beneficiation and extractive metallurgy of the platinum-group elements, highlighting recent process innovations, Canadian Institute of Metallurgy, Special volume 54, pp811 – 840

Cramer, L. A., 2001, The extractive metallurgy of South Africa's Platinum ores, Journal of Metals, pp14 – 18

Daniel, M., 2007, Energy efficient mineral liberation using HPGR technology, PhD Thesis, Julius Kruttschnitt Research Center, University of Queensland

Daniel, M.J., Morrell, S., 2004, HPGR model verification and scale-up, Minerals Engineering, Vol. 17, 1149–1161

Djordjevic, N., Morrison, R., 2006, Exploratory modeling of grinding pressure within a compressed particle bed, Minerals Engineering, Vol. 19, pp995 – 1004

Dunne, R., Goulsbra, A., Dunlop, I., 1996, High Pressure Grinding Rolls and the effect on Liberation: Comparative Test Results, Randol Gold Forum, pp 49 – 54

Esna-Ashari, M., Kellerwessel, H., 1988, Interparticle crushing of gold ore improves leaching, Randol Gold Forum, pp141 – 146

Feng, D., Aldrich, C., 1999, Effect of particle size on flotation performance of complex sulphide ores, Minerals Engineering, Vol. 12, Issue 7, 721 – 731

Fonseca, E., Sá, L. R. B. M., 2005, Methodological evaluation of a liberation study in sulfide copper ore, Centenary of Flotation Symposium, Brisbane, Queensland, pp953 - 958

Fuerstenau, D. W., Lutch, J. J., De, A., 1991, The effect of ball size on the energy efficiency of hybrid high pressure roll mill/ball mill grinding, Powder Technology, 105, pp199–204

Fuerstenau, D. W., Kapur, P. C., 1995, Newer energy efficient approach to particle production by comminution, Powder Technology, 82, pp 51 – 57

Fuerstenau, D.W., Lutch, J.J., De, A., 1999, The effect of ball size on the energy efficiency of hybrid high-pressure roll mill ball mill grinding, Powder Technology , Issue 105, pp199–204

Fuerstenau, D.W., Abouzeid, A.Z.M., 2002, The energy efficiency of ball milling in comminution, International Journal of Mineral Processing, Issue 67, pp 161 – 185

Gay, S.L., Morrison, R., 2005, Using two dimensional information to interpret three dimensional information – validation using tomography, 4th World Congress on Industrial Process Tomography, Aziu, Japan.

Goodall, W.R., Scales, P.J.,Butcher, A.R., 2005, The use of QEMSCAN and diagnostic leaching in the characterisation of visible gold in complex ores, Minerals Engineering, Vol. 18, 877-886.

Grano, S., 2009, The critical importance of the grinding environment on fine particle recovery in flotation, Minerals Engineering, Vol. 22, 386 - 394

Henley, K.J., 1983, Ore-dressing mineralogy – A review of techniques, applications and recent developments, Spec. Publ. geol. Soc. S. Afr., Vol. 7, 175-200

Holwell, D. A., McDonald, I., 2006, Platinum-group mineral assemblages in the Platreef at the Sandsloot Mine, northern Bushveld Complex, South Africa, Mineralogical Magazine, Vol. 70(1), pp83 – 101

Hosten, C., Cimilli, H., 2009, The effects of feed size distribution on confined-bed comminution of quartz and calcite in piston-die press, International Journal of Mineral Processing, Article in press

Hosten, C., Ozbay, C., Technical note: A comparison of particle bed breakage and rod mill grinding with regard to mineral liberation and particle shape effects, Minerals Engineering, Vol. 11, No. 9, pp871 – 874

Humphries, G., Rule C., Wolmarans, E., 2006, The development of a process flowsheet for the new Anglo Platinum PPRust north concentrator; incorporating HPGR technology, International platinum conference 'Platinum Surges Ahead', The Southern African Institute of Mining Metallurgy

Johnson, N. W., 2005, Liberated 0-10 μm particles from sulphide ores, their production and separation – Recent developments and future need, Minerals engineering, Vol. 19, 666-674.

Klimpel, 1984, Froth flotation: The kinetic approach International Journal of Mineral Processing, Vol. 12, Issue 4, pp323 – 324

Klymowsky, R., Patzelt, N., Knecht, J., Burchardt, E., 2002, Selection and sizing of High Pressure Grinding Rolls, Mineral Processing Plant Design, Practice and Control, Proceedings, Vol. 1, pp 636 – 668

Lastra, R., 2002, Comparison of liberation determinations by particle area percentage and exposed particle perimeter percentage in a flotation concentrator, Minerals and Metallurgical Processing, Vol.19, No. 4

Lastra, R., 2007, Seven practical application cases of liberation analysis, International Journal of Mineral Processing, 84, pp337 – 347

Lee, C. A., 1996, A review of Mineralization in the Bushveld Complex and some other Layered Intrusions, Elseveir Science, 103-145.

Lee, C. A., 2000, A short geological review of the Bushveld Complex, Platinum Metals Review, Vol. 44(1), pp33 – 39

Liddell, K.S., McRae, L. B., Dunne, R. C., 1986, Process routes for the beneficiation of Noble metals from Merensky and UG2 ores, Mintek Review, No. 4, pp33 – 44

Lim, W.I.L., Campbell, J.J., Tondo, L.A., 1997, The effect of rolls speed and rolls surface on high pressure grinding rolls performance, Minerals Engineering, Vol. 10, Issue 3, 401-419.

Lim, I.L.,Voight, W., Weller, K.R., 1996, Product size distribution and energy expenditure in grinding minerals and ores in high pressure rolls, International Journal of Mineral Processing, 44-45, pg 539-559.

Lim, W.I.L. , Weller, K.R., 1998, Some benefits of using studded surfaces in high pressure grinding rolls, International Journal of Minerals Engineering, Vol. 12, Issue 2, pp. 187-203.

Lubjuhn, U., Schonert, K., 1993, Material flow in the acceleration zone and throughput of high pressure roller mills, XVIII International Mineral Processing Congress, pp161 – 168

Mainza, A. N., Powell, M. S., 2006, RoM Ball Mills - A comparison with AG/SAG Milling, Proceedings of International Autogenous and Semi-Autogenous Grinding Technology, vol. 2, pp. 314–325

Morley, C., 2006, Flowsheets for HPGR, Proceedings of International Autogenous and Semi-Autogenous Grinding Technology, Vol. 4., pp. 172 – 189

Merkle, R.K.W., McKenzie, A.D., 2002, The mining and beneficiation of South African PGE ores—an overview. The Geology, Geochemistry, Mineralogy and Mineral Beneficiation of the Platinum-Group Elements, L.J. Cabri, (ed.). Canadian Institute of Mining, Metallurgy and Petroleum, vol. 54, pp. 793–809.

Napier – Munn, T. J., 2005, An introduction to comparative statistics and experimental design for mineral engineers, JKMRC, University of Queensland, Course notes, second edition, version 5.2

Napier-Munn, T. J., Morrel, S., Morrison, R. D., Kojovic, T., 1996, Mineral Comminution Circuits – Their Operation and Optimisation, JKMRC Monograph series in Mining and Mineral processing 2

Norgate, T. E., Weller, K. R., 1994, Selection and operation of High Pressure Grinding Rolls Circuits for Minimum Energy Consumption, Minerals Engineering, Vol. 7, Issue 10, pp 1253 – 1287

Ntsele, C., Sauermann, G., 2007, HPGR technology – the heart and future of the diamond liberation processing, The South African Institute of Mining and Technology,

Oestreicher., C., Spollen, C. F., 2006, HPGR versus SAG mill selection for the Los Bronces grinding circuit expansion, Proceedings of International Autogenous and Semi-Autogenous Grinding Technology, Vol. 4, pp110 – 123

Palm, N., Shackleton, V., Malysiak, V., O'Connor, C. T., 2009, The effect of using different comminution procedures on the flotation of sphalerite, Unpublished

Parker, B., Rowe, P., Lane, G., Morrell,S., 2001, The decision to opt for high pressure grinding rolls for the Boddington expansion, Mining and Mineral Process Engineering, University of British Columbia, pp 93 – 106

Patzelt, N., Knecht, H., Baum, W., 1995, Case made for high-pressure roll-grinding in gold plants, Mining Engineering, pp 524 – 529

Patzelt, N., Knetch, J., Baum, W., 1997, The metallurgical potential of high-pressure roll grinding, XX IMPC, pp155 – 164

Patzelt, N., Klymowsky, R., Burchardt, E., Knecht, J., 2001, High Pressure Grinding Rolls in AG/SAG Mill Circuits – The next step in the evolution of grinding plants for the new millennium, SAG 2001

Pease, J. D., Curry, D. C., Young, M. F., 2006, Designing flotation circuits for high fines recovery, Minerals Engineering, Vol. 19, pp 831-840

Penburthy, C. J., Oosthuyzen, J., Merkle, K. W., 2000, The recovery of platinum-group elements from the UG-2 chromitite, Bushveld Complex – a mineralogical perspective, Mineralogy and Petrology, 68: 213 – 222

Petruk, W., 2000, Applied Mineralogy in the Mining Industry, Elsevier Science, Oxford, ISBN: 0 444 500774

Rule, C.M., Minnaar, D.M., Sauermann, G.M., 2008, HPGR – revolution in Platinum?, The Southern African Institute of Mining and Metallurgy, Vol. 109, Issue 1, pp23 – 30

Schönert., K., 1988, A first survey of grinding with high-compression roller mills, International Journal of Mineral Processing, 22, pp401 – 412

Shi, F., Lambert, S., and Daniel, M., 2006, A study of HPGR treating platinum ores, Proceedings of International Autogenous and Semi-Autogenous Grinding Technology, Vol. 4, pp 154 – 171

Siedel, J., Logan, T. C., LeVier, K. M., Veillette, G., 2006, Case study – Investigating for HPGR suitability for two gold/copper prospects, Proceedings of International Autogenous and Semi-Autogenous Grinding Technology, Vol. 4, pp 140 – 153

Sutherland, D., 2007, Estimation of mineral grain size using automated mineralogy, Minerals Engineering, Vol. 20, Issue 5, pp452 - 460

Tavares, L.M., 2005, Particle weakening in high-pressure roll grinding, Minerals Engineering, Vol. 18, 651-657

Tromans, D., 2008, Mineral comminution: Energy efficiency considerations, Minerals Engineering, Vol. 21, pp613 – 620

Van Alphen, C., 2007, Automated mineralogical analysis of coal and ash products – Challenges and requirements, Minerals Engineering, Article in press

Van der Meer, F. P., Gruendken, A., 2009, Flowsheet considerations for optimal use of high pressure grinding rolls, Minerals Engineering, Article in press

Van Drunick, W., Smit, I., 2006, Energy efficient comminution – HPGR experience at Anglo Research, Proceedings of International Autogenous and Semi-Autogenous Grinding Technology, Vol. 4, pp124 – 139

Viljoen, R. M., Smit, J. T., Du Plessis, I., Ser, V., 2001, The development and application of in-bed compression breakage principles, Mineral Engineering, Vol. 14, No. 5, pp465 – 471

Wen, S. B., Yang., C. S., Hsih, C.S., 1998, The abnormal size distribution of comminuted heterogeneous ores due to detachment of grain boundaries fracturing, International Journal of Mineral Processing, Issue 53, pp183 – 200

Wiese, J., Harris, P., Bradshaw, D., 2006, The role of the reagent suite in optimizing pentlandite recoveries from the Merensky reef, Minerals Engineering, Vol. 19, pp1290 – 1300

Wills, B. A., 1988, Enhancement of Mineral Liberation, XVI International Mineral Processing Congress, Vol. 10A, pp293 – 297

Wills, B.A., Napier – Munn, T. J., 2005, Mineral processing technology: an introduction to the practical aspects of ore treatment and mineral recovery, 7th ed., Butterworth-Heinemann, ISBN: 0750644508

Wightman, E., Evans, C. L., Vizcarra, T., Sandoval, G., 2008 Process Mineralogy as a tool in modelling mineral processing operations, Ninth International Congress for Applied Mineralogy, pp 475 – 481.

Xiao, Z., Laplante, A.R., 2004, Characterizing and recovering the platinum group minerals – a review, Minerals Engineering, Vol. 17, 961-969

Appendix A – HPGR raw data

Equations applied

$$P = \frac{E * 3600}{t}$$

$$m = \frac{M * 3.6}{t}$$

$$E_{sp} = \frac{P - P_{no-load}}{m}$$

Where E_{sp} is specific energy (kWh/t)

E is the energy consumed (kWh)

P is power draw (kW)

$P_{no\text{-}load}$ is no load power (kW)

m is throughput (t/h)

M is the mass of sample (kg)

t is time taken to grind sample (s)

12mm feed, 1.5mm zero gap

Ore type	*Pressure (bar)*	*t (s)*	*Pass*	*M (kg)*	*m (t/h)*	*Energy (roll 1, kWh)*	*Energy (roll 2, kWh)*	*Total energy (kWh)*	$P_{no\text{-}load}$ *(kW)*	*P (kW)*	E_{sp} *(kWh/t)*	x_g *(mm)*
Merensky	150	320	1	484.3	5.45	0.75	0.67	1.42	2.52	13.45	2.47	8.0
	150	360	2	400.5	4.01	0.56	0.54	1.10	2.52	8.46	2.11	5.6
	150	331	3	317.2	3.45	0.35	0.34	0.69	2.52	4.95	1.44	4.7
	150	233	4	243.3	3.76	0.20	0.21	0.41	2.52	3.85	1.02	3.5
	150	195	5	168.3	3.11	0.09	0.1	0.19	2.52	1.08	0.35	3.9
Merensky	120	334	1	509.9	5.50	0.68	0.73	1.41	2.52	12.70	2.31	7.9
	120	350	2	434.3	4.47	0.44	0.43	0.87	2.52	6.42	1.44	6.1
	120	311	3	352.7	4.08	0.24	0.24	0.48	2.52	3.08	0.76	4.4
	120	216	4	264.6	4.41	0.12	0.15	0.27	2.52	2.05	0.46	4.0
Merensky	90	335	1	501.9	5.39	0.65	0.68	1.33	2.52	11.73	2.17	8.0
	90	335	2	420.2	4.52	0.40	0.41	0.81	2.52	6.20	1.37	6.0
	90	294	3	353.9	4.33	0.21	0.23	0.44	2.52	2.90	0.67	5.5
	90	237	4	276.4	4.20	0.10	0.19	0.29	2.52	1.85	0.44	4.6
	90	195	5	198.2	3.66	0.06	0.05	0.11	2.52	-0.54	-0.15	no flakes
Merensky	60	304	1	492.2	5.83	0.48	0.51	0.99	2.52	9.22	1.58	7.9
	60	292	2	409.2	5.04	0.27	0.27	0.54	2.52	4.11	0.82	6.5
	60	231	3	327.4	5.10	0.15	0.15	0.30	2.52	2.16	0.42	5.3
	60	177	4	254.8	5.18	0.08	0.09	0.17	2.52	0.96	0.18	4.8

6mm feed, 1.5mm zero gap

Ore type	*Pressure (bar)*	*t (s)*	*Pass*	*M (kg)*	*m (t/h)*	*Energy (roll 1, kWh)*	*Energy (roll 2, kWh)*	*Total energy (kWh)*	$P_{no\text{-}load}$ *(kW)*	*P (kW)*	E_{sp} *(kWh/t)*	x_g (mm)
Merensky	150	380	1	506.2	4.80	0.77	0.79	1.56	2.52	12.27	2.56	6.7
	150	389	2	427.6	3.96	0.59	0.58	1.17	2.52	8.31	2.10	6.1
	150	345	3	350.1	3.65	0.35	0.34	0.69	2.52	4.72	1.29	4.3
	150	243	4	276	4.09	0.18	0.18	0.36	2.52	2.75	0.67	3.8
	150	156	5	189.8	4.38	0.06	0.06	0.12	2.52	0.20	0.05	3.3
Merensky	90	369	1	503.5	4.91	0.55	0.57	1.12	2.52	8.39	1.71	7.6
	90	395	2	435.4	3.97	0.43	0.42	0.85	2.52	5.24	1.32	6.0
	90	327	3	354	3.90	0.30	0.31	0.61	2.52	4.24	1.09	4.9
	90	244	4	274.1	4.04	0.19	0.19	0.38	2.52	3.01	0.74	4.9
Merensky	60	349	1	503.5	5.19	0.42	0.45	0.87	2.52	6.50	1.25	7.2
	60	349	2	419.2	4.32	0.34	0.36	0.70	2.52	4.67	1.08	6.7
	60	285	3	340	4.29	0.25	0.25	0.50	2.52	3.75	0.87	5.2
	60	223	4	261	4.21	0.16	0.15	0.31	2.52	2.45	0.58	4.9

12mm feed, 3mm zero gap

Ore type	*Pressure (bar)*	*t (s)*	*Pass*	*M (kg)*	*m (t/h)*	*Energy (roll 1, kWh)*	*Energy (roll 2, kWh)*	*Total energy (kWh)*	$P_{no\text{-}load}$ *(kW)*	*P (kW)*	E_{sp} *(kWh/t)*	x_g (mm)
Merensky	150	340	1	508.3	5.38	0.76	0.72	1.48	2.52	13.12	2.44	7.8
	150	337	2	389.1	4.16	0.43	0.51	0.94	2.52	7.50	1.80	6.6
	150	269	3	304.1	4.07	0.19	0.19	0.38	2.52	2.62	0.64	5.7
	150	173	4	218.2	4.54	0.06	0.06	0.12	2.52	-0.06	-0.01	5.5
Merensky	90	326	1	518.1	5.72	0.57	0.74	1.31	2.52	11.90	2.08	8.2
	90	336	2	435.3	4.66	0.41	0.40	0.81	2.52	6.15	1.32	6.3
	90	292	3	359.5	4.43	0.16	0.18	0.34	2.52	1.73	0.39	6.4
Merensky	60	301	1	503.9	6.03	0.44	0.50	0.94	2.52	8.77	1.46	8.0
	60	298	2	423.4	5.11	0.30	0.29	0.59	2.52	4.55	0.89	6.7
	60	268	3	346.4	4.65	0.21	0.20	0.41	2.52	2.96	0.64	6.1
	60	198	4	270.6	4.92	0.12	0.12	0.24	2.52	1.88	0.38	5.6

6mm feed, 3mm zero gap

Ore type	*Pressure (bar)*	*t (s)*	*Pass*	*M (kg)*	*m (t/h)*	*Energy (roll 1, kWh)*	*Energy (roll 2, kWh)*	*Total energy (kWh)*	$P_{no\text{-}load}$ *(kW)*	*P (kW)*	E_{sp} *(kWh/t)*	x_g (mm)
Merensky	150	369	1	499.4	4.87	0.71	0.76	1.47	2.52	11.81	2.42	6.9
	150	353	2	416.1	4.24	0.44	0.44	0.88	2.52	6.43	1.52	5.7
	150	269	3	335.9	4.50	0.14	0.14	0.28	2.52	1.29	0.29	5.1
	150	177	4	258.6	5.26	0.06	0.06	0.12	2.52	-0.02	0.00	no flakes
Merensky	90	345	1	490.9	5.12	0.49	0.53	1.02	2.52	8.07	1.58	7.4
	90	321	2	404.5	4.54	0.37	0.37	0.74	2.52	5.72	1.26	6.0
	90	255	3	325.2	4.59	0.17	0.19	0.36	2.52	2.63	0.57	5.4
	90	173	4	250.9	5.22	0.08	0.07	0.15	2.52	0.54	0.10	5.0
Merensky	60	338	1	497.4	5.30	0.38	0.44	0.82	2.52	6.20	1.17	7.5
	60	322	2	416.1	4.65	0.30	0.32	0.62	2.52	4.40	0.95	6.1
	60	268	3	346.4	4.65	0.21	0.21	0.42	2.52	3.18	0.68	5.2
	60	198	4	270.6	4.92	0.12	0.11	0.23	2.52	1.59	0.32	5.1

12mm feed topsize, 1.5mm zero gap

Ore type	*Pressure (bar)*	*t (s)*	*Pass*	*M (kg)*	*m (t/h)*	*Energy (roll 1, kWh)*	*Energy (roll 2, kWh)*	*Total energy (kWh)*	*no load power(kW)*	*power-draw (kW)*	E_{sp} *(kWh/t)*	x_g (mm)
UG2	150	318	1	501.5	5.68	0.67	0.60	1.27	2.52	11.83	2.08	7.4
	150	318	2	411.2	4.66	0.54	0.53	1.07	2.52	9.55	2.05	5.2
	150	270	3	320.9	4.28	0.38	0.37	0.75	2.52	7.44	1.74	3.8
	150	198	4	237.3	4.31	0.26	0.26	0.52	2.52	6.92	1.60	3.9
UG2 (repeat)	150	328	1	497.2	5.46	0.72	0.69	1.41	2.52	12.96	2.37	7.3
	150	328	2	409.7	4.50	0.55	0.53	1.08	2.52	9.29	2.07	5.3
	150	269	3	320.5	4.29	0.37	0.38	0.75	2.52	7.46	1.74	4.7
	150	220	4	242.2	3.96	0.24	0.24	0.48	2.52	5.37	1.35	3.9
	150	155	5	159.4	3.70	0.12	0.12	0.24	2.52	3.05	0.82	3.8
UG2	120	360	1	500.8	5.01	0.67	0.62	1.29	2.52	10.37	2.07	5.8
	120	317	2	400.2	4.54	0.50	0.49	0.99	2.52	8.67	1.91	4.9
	120	261	3	312.7	4.31	0.35	0.34	0.69	2.52	7.00	1.62	4.4
	120	211	4	225.6	3.85	0.23	0.24	0.47	2.52	5.57	1.45	3.4
	120	131	5	147.2	4.05	0.15	0.15	0.30	2.52	5.59	1.38	3.4
UG2	90	329	1	508.6	5.57	0.69	0.66	1.35	2.52	12.23	2.20	7.2
	90	308	2	410.6	4.80	0.44	0.43	0.87	2.52	7.68	1.60	5.2
	90	275	3	323.5	4.23	0.31	0.31	0.62	2.52	5.54	1.31	3.4
	90	208	4	238	4.12	0.20	0.21	0.41	2.52	4.54	1.10	3.2
	90	124	5	146.1	4.24	0.11	0.12	0.23	2.52	4.19	0.99	3.5
UG2	60	353	1	504	5.14	0.58	0.60	1.18	2.52	9.54	1.86	7.8
	60	301	2	411.8	4.93	0.36	0.35	0.71	2.52	5.95	1.21	5.3
	60	236	3	309.9	4.73	0.20	0.24	0.44	2.52	4.19	0.89	3.7
	60	178	4	215.3	4.35	0.14	0.14	0.28	2.52	3.20	0.74	3.8
	60	107	5	138.2	4.65	0.09	0.09	0.18	2.52	3.54	0.76	3.2

6mm feed topsize, 1.5mm zero gap

Ore type	*Pressure (bar)*	*t (s)*	*Pass*	*M (kg)*	*m (t/h)*	*Energy (roll 1, kWh)*	*Energy (roll 2, kWh)*	*Total energy (kWh)*	*no load power(kW)*	*power-draw (kW)*	E_{sp} *(kWh/t)*	x_g (mm)
UG2	150	345	1	498	5.20	0.79	0.74	1.53	2.52	13.39	2.58	6.6
	150	334	2	402	4.33	0.57	0.56	1.13	2.52	9.69	2.24	5.4
	150	288	3	313.1	3.91	0.40	0.42	0.82	2.52	7.77	1.98	3.9
	150	204	4	228.2	4.03	0.25	0.25	0.50	2.52	6.32	1.57	3.2
UG2 (repeat)	150	347	1	511.6	5.31	0.79	0.72	1.51	2.52	13.17	2.48	5.9
	150	344	2	420	4.40	0.57	0.57	1.14	2.52	9.41	2.14	5.3
	150	280	3	330.1	4.24	0.38	0.38	0.76	2.52	7.29	1.72	4.4
	150	197	4	243.3	4.45	0.24	0.24	0.48	2.52	6.31	1.42	3.8
UG2	90	309	1	505	5.88	0.55	0.52	1.07	2.52	9.95	1.69	6.9
	90	313	2	412.2	4.74	0.40	0.40	0.80	2.52	6.66	1.40	5.1
	90	270	3	323.1	4.31	0.28	0.27	0.55	2.52	4.79	1.11	4.6
	90	195	4	236.5	4.37	0.18	0.18	0.36	2.52	4.09	0.94	4.0
UG2	60	285	1	500.5	6.32	0.38	0.45	0.83	2.52	7.93	1.25	7.8
	60	288	2	412.2	5.15	0.29	0.30	0.59	2.52	4.90	0.95	6.5
	60	247	3	321.1	4.68	0.21	0.21	0.42	2.52	3.66	0.78	4.6
	60	196	4	234	4.30	0.14	0.13	0.27	2.52	2.37	0.55	4.0

12mm feed topsize, 3mm zero gap

Ore type	*Pressure (bar)*	*t (s)*	*Pass*	*M (kg)*	*m (t/h)*	*Energy (roll 1, kWh)*	*Energy (roll 2, kWh)*	*Total energy (kWh)*	*no load power(kW)*	*power-draw (kW)*	E_{sp} *(kWh/t)*	x_g (mm)
UG2	150	308	1	496.60	5.80	0.69	0.62	1.31	2.52	12.83	2.21	7.6
	150	304	2	396.90	4.70	0.50	0.49	0.99	2.52	9.24	1.97	4.8
	150	263	3	307.30	4.21	0.32	0.33	0.65	2.52	6.42	1.53	3.4
	150	183	4	217.20	4.27	0.20	0.19	0.39	2.52	5.15	1.21	2.7
	150	111	5	127.70	4.14	0.11	0.10	0.21	2.52	4.23	1.02	2.1
UG2	90	343	1	497.40	5.22	0.67	0.63	1.30	2.52	11.16	2.14	7.7
	90	304	2	409.60	4.85	0.39	0.39	0.78	2.52	6.75	1.39	4.8
	90	269	3	326.10	4.36	0.26	0.27	0.53	2.52	4.60	1.05	3.2
	90	266	4	253.70	3.43	0.16	0.18	0.34	2.52	2.14	0.62	2.9
	90	145	5	178.60	4.43	0.10	0.12	0.22	2.52	2.87	0.65	2.8
	90	127	6	113.60	3.22	0.04	0.06	0.10	2.52	0.34	0.11	no flakes
UG2	60	280	1	490.80	6.31	0.54	0.49	1.03	2.52	10.68	1.69	
	60	257	2	341.20	4.78	0.28	0.27	0.55	2.52	5.24	1.10	5.3
	60	178	3	265.60	5.37	0.16	0.15	0.31	2.52	3.81	0.71	3.5
	60	129	4	154.20	4.30	0.09	0.09	0.18	2.52	2.56	0.59	
UG2 (repeat)	60	281	1	501.20	6.42	0.57	0.53	1.10	2.52	11.60	1.81	6.9
	60	351	2	413.70	4.24	0.29	0.27	0.56	2.52	3.23	0.76	5.9
	60	227	3	323.90	5.14	0.20	0.21	0.41	2.52	3.97	0.77	4.4
	60	183	4	234.70	4.62	0.11	0.12	0.23	2.52	2.02	0.44	3.6
	60	136	5	149.10	3.95	0.05	0.06	0.11	2.52	0.44	0.11	3.6

6mm feed topsize, 3mm zero gap

Ore type	*Pressure (bar)*	*t (s)*	*Pass*	*M (kg)*	*m (t/h)*	*Energy (roll 1, kWh)*	*Energy (roll 2, kWh)*	*Total energy (kWh)*	$P_{no\text{-}load}$ *(kW)*	*P (kW)*	E_{sp} *(kWh/t)*	x_g (mm)
UG2	150	354	1	489.30	4.98	0.70	0.65	1.35	2.52	11.2	2.25	6.8
	150	299	2	401.50	4.83	0.44	0.41	0.85	2.52	7.70	1.59	6.1
	150		3	324.40	#DIV/0!	0.20	0.19	0.39	2.52	#DIV/0!	#DIV/0!	5.7
	150	176	4	253.90	5.19	0.08	0.09	0.17	2.52	0.92	0.18	
UG2	90	332	1	489.80	5.31	0.50	0.45	0.95	2.52	7.80	1.47	7.0
	90	308	2	407.70	4.77	0.35	0.32	0.67	2.52	5.30	1.11	5.8
	90	241	3	390.60	5.83	0.18	0.16	0.34	2.52	2.48	0.43	5.0
	90	176	4	259.20	5.30	0.08	0.09	0.17	2.52	0.88	0.17	5.0
UG2	60	311	1	491.00	5.68	0.41	0.36	0.77	2.52	6.34	1.11	7.6
	60	293	2	405.20	4.98	0.28	0.27	0.55	2.52	4.20	0.84	6.3
	60	236	3	328.60	5.01	0.18	0.18	0.36	2.52	2.90	0.58	5.0
	60	181	4	256.10	5.09	0.10	0.12	0.22	2.52	1.80	0.35	no flakes

12mm feed topsize, 4.5mm zero gap

Ore type	*Pressure (bar)*	*t (s)*	*Pass*	*M (kg)*	*m (t/h)*	*Energy (roll 1, kWh)*	*Energy (roll 2, kWh)*	*Total energy (kWh)*	$P_{no\text{-}load}$ *(kW)*	*P (kW)*	E_{sp} *(kWh/t)*	x_g (mm)
UG2	150	377	1	499.6	4.77	0.72	0.66	1.38	2.52	10.7	2.24	7.3
	150	304	2	401.2	4.75	0.33	0.33	0.66	2.52	5.27	1.11	6.1
	150	238	3	310.9	4.70	0.13	0.13	0.26	2.52	1.38	0.29	5.6
	150	139	4	220	5.70	0.05	0.06	0.11	2.52	0.43	0.08	no flakes
UG2	120	380	1	497.5	4.71	0.60	0.56	1.16	2.52	8.47	1.80	6.1
	120	280	2	404	5.19	0.28	0.26	0.54	2.52	4.44	0.85	6.0
	120	229	3	304.5	4.79	0.10	0.09	0.19	2.52	0.48	0.10	5.4
	120	190	4	211.3	4.00	0.07	0.09	0.16	2.52	0.51	0.13	no flakes
UG2	90	317	1	493.3	5.60	0.49	0.49	0.98	2.52	8.56	1.53	7.9
	90	263	2	392.3	5.37	0.31	0.28	0.59	2.52	5.56	1.03	6.2
	90	199	3	302.9	5.48	0.12	0.12	0.24	2.52	1.88	0.34	5.7
	90	225	4	211.4	3.38	0.08	0.07	0.15	2.52	-0.14	-0.04	no flakes
UG2	60	274	1	494.1	6.49	0.37	0.34	0.71	2.52	6.78	1.04	6.8
	60	261	2	403.3	5.56	0.25	0.22	0.47	2.52	3.96	0.71	6.8
	60	238	3	311.2	4.71	0.11	0.12	0.23	2.52	1.02	0.22	4.8
	60	207	4	230.5	4.01	0.07	0.06	0.13	2.52	-0.24	-0.06	no flakes

12mm feed topsize, 1.5mm zero gap

Ore type	*Pressure (bar)*	*t (s)*	*Pass*	*M (kg)*	*m (t/h)*	*Energy (roll 1, kWh)*	*Energy (roll 2, kWh)*	*Total energy (kWh)*	$P_{no\text{-}load}$ *(kW)*	*P (kW)*	E_{sp} *(kWh/t)*	x_g (mm)
Platreef	150	545	1	501.7	3.31	0.92	1.06	1.98	2.52	10.5	3.18	7.4
	150	346	2	383.3	3.99	0.78	0.72	1.50	2.52	13.0	3.27	6.9
	150	280	3	349.7	4.50	0.49	0.50	0.99	2.52	10.2	2.26	6.4
	150	262	4	240.6	3.31	0.41	0.39	0.80	2.52	8.51	2.58	5.8
	150	170	5	204.2	4.32	0.24	0.22	0.46	2.52	7.18	1.66	5.3
	150	191	6	135.0	0.66	0.30	0.27	0.57	2.52	8.20	12.44	5.3
Platreef	150	397	1	500	4.53	0.92	0.94	1.86	2.52	14.3	3.16	7.3
(repeat)	150	331	2	419.3	4.56	0.69	0.70	1.39	2.52	12.6	2.76	7.0
	150	305	3	335.6	3.96	0.51	0.49	1.01	2.52	9.34	2.36	6.2
	150	270	4	240.2	3.20	0.38	0.37	0.75	2.52	7.47	2.33	5.6
	150	195	5	181.2	3.35	0.25	0.24	0.49	2.52	6.62	1.98	5.1
Platreef	90	403	1	503.2	4.50	0.77	0.92	1.69	2.52	12.6	2.80	8.4
	90	324	2	426.0	4.73	0.51	0.53	1.04	2.52	9.1	1.92	7.6
	90	319	3	349.5	3.94	0.41	0.42	0.83	2.52	6.9	1.74	6.6
	90	312	4	279.2	3.22	0.31	0.31	0.62	2.52	4.67	1.45	5.0
	90	231	5	204.9	3.19	0.22	0.22	0.44	2.52	4.35	1.36	5.2
	90	218	6	119.8	1.98	0.13	0.13	0.26	2.52	1.71	0.86	3.7
Platreef	60	392	1	505.0	4.64	0.57	0.72	1.29	2.52	9.3	2.01	8.9
	60	312	2	431.1	4.97	0.39	0.50	0.89	2.52	7.7	1.56	8.1
	60	292	3	353.2	4.35	0.30	0.34	0.64	2.52	5.4	1.24	7.3
	60	292	4	281.0	3.46	0.25	0.24	0.48	2.52	3.46	1.00	5.2
	60	232	5	209.6	3.25	0.18	0.08	0.26	2.52	1.53	0.47	4.6
	60	157	6	138.3	3.17	0.11	0.12	0.23	2.52	2.82	0.89	4.7

6mm feed topsize, 1.5mm zero gap

Ore type	*Pressure (bar)*	*t (s)*	*Pass*	*M (kg)*	*m (t/h)*	*Energy (roll 1, kWh)*	*Energy (roll 2, kWh)*	*Total energy (kWh)*	$P_{no\text{-}load}$ *(kW)*	*P (kW)*	E_{sp} *(kWh/t)*	x_g (mm)
Platreef	150	402	1	473.5	4.24	0.76	0.91	1.67	2.52	12.48	2.94	6.6
	150	344	2	383.9	4.02	0.62	0.61	1.23	2.52	10.30	2.56	6.6
	150	293	3	312.2	3.84	0.51	0.49	1.00	2.52	9.73	2.54	6.5
	150	257	4	241.4	3.38	0.35	0.33	0.68	2.52	6.96	2.06	6.0
Platreef	90	395	1	495.8	4.52	0.75	0.87	1.62	2.52	12.24	2.71	7.3
	90	336	2	410	4.39	0.51	0.53	1.04	2.52	8.60	1.96	6.5
	90	321	3	326.4	3.66	0.35	0.34	0.69	2.52	5.23	1.43	6.1
	90	288	4	254.5	3.18	0.26	0.26	0.52	2.52	3.98	1.25	5.2
	90	210	5	187.4	3.21	0.18	0.18	0.36	2.52	3.65	1.14	4.7
Platreef	60	429	1	488.2	4.10	0.59	0.78	1.37	2.52	8.98	2.19	7.3
	60	332	2	405.8	4.40	0.42	0.50	0.92	2.52	7.48	1.70	7.1
	60	311	3	343.4	3.98	0.32	0.34	0.66	2.52	5.17	1.30	6.6
	60	301	4	276.6	3.31	0.23	0.24	0.47	2.52	3.10	0.94	5.6
	60	228	5	201.8	3.19	0.16	0.17	0.33	2.52	2.72	0.85	

12mm feed topsize, 3mm zero gap

Ore type	*Pressure (bar)*	*t (s)*	*Pass*	*M (kg)*	*m (t/h)*	*Energy (roll 1, kWh)*	*Energy (roll 2, kWh)*	*Total energy (kWh)*	$P_{no\text{-}load}$ *(kW)*	*P (kW)*	E_{sp} *(kWh/t)*	x_g (mm)
Platreef	150	397	1	509.7	4.62	1.166	0.9	2.066	2.52	16.21	3.51	7.8
	150	345	2	429	4.48	0.706	0.65	1.356	2.52	11.63	2.60	6.9
	150	315	3	352.2	4.03	0.419	0.4	0.819	2.52	6.84	1.70	5.6
	150	275	4	274.1	3.59	0.226	0.22	0.446	2.52	3.32	0.92	5.5
	150	200	5	203.3	3.66	0.114	0.13	0.244	2.52	1.87	0.51	4.6
Platreef	90	394	1	505.9	4.62	0.73	0.79	1.52	2.52	11.37	2.46	7.6
	90	332	2	435.2	4.72	0.448	0.46	0.908	2.52	7.33	1.55	6.9
	90	315	3	365.9	4.18	0.333	0.34	0.673	2.52	5.17	1.24	6.1
	90	297	4	294.4	3.57	0.194	0.21	0.404	2.52	2.38	0.67	5.1
	90	202	5	224.3	4.00	0.104	0.09	0.194	2.52	0.94	0.23	4.8
Platreef	60	376	1	507.4	4.86	0.508	0.63	1.138	2.52	8.38	1.72	8.4
	60	313	2	437	5.03	0.327	0.44	0.767	2.52	6.30	1.25	7.5
	60	294	3	365.8	4.48	0.258	0.31	0.568	2.52	4.44	0.99	5.6
	60	262	4	294.1	4.04	0.182	0.19	0.372	2.52	2.59	0.64	5.8
	60	233	5	233.3	3.60	0.12	0.12	0.24	2.52	1.19	0.33	5.2

6mm feed topsize, 3mm zero gap

Ore type	*Pressure (bar)*	*t (s)*	*Pass*	*M (kg)*	*m (t/h)*	*Energy (roll 1, kWh)*	*Energy (roll 2, kWh)*	*Total energy (kWh)*	$P_{no\text{-}load}$ *(kW)*	*P (kW)*	E_{sp} *(kWh/t)*	x_g (mm)
Platreef	150	399	1	497.5	4.49	0.861	1.02	1.881	2.52	14.45	3.22	7.1
	150	350	2	422.5	4.35	0.65	0.67	1.32	2.52	11.06	2.54	6.5
	150	327	3	355.9	3.92	0.434	0.41	0.844	2.52	6.77	1.73	5.7
	150	284	4	279.7	3.55	0.221	0.22	0.441	2.52	3.07	0.87	5.5
	150	209	5	124.3	2.14	0.106	0.11	0.216	2.52	1.20	0.56	5.2
Platreef	90	396	1	529.4	4.81	0.578	1.12	1.698	2.52	12.92	2.68	6.9
	90	357	2	444	4.48	0.429	0.48	0.909	2.52	6.65	1.48	6.3
	90	354	3	374.8	3.81	0.3	0.31	0.61	2.52	3.68	0.97	5.5
	90	302	4	305.4	3.64	0.174	0.17	0.344	2.52	1.58	0.43	5.4
	90	224	5	235.3	3.78	0.1	0.12	0.22	2.52	1.02	0.27	4.9
Platreef	60	370	1	497	4.84	0.391	0.56	0.951	2.52	6.73	1.39	6.8
	60	313	2	409.3	4.71	0.293	0.4	0.693	2.52	5.45	1.16	6.9
	60	292	3	342.2	4.22	0.244	0.27	0.514	2.52	3.82	0.90	6.2
	60	271	4	280.5	3.73	0.168	0.17	0.338	2.52	1.97	0.53	4.9
	60	210	5	219.6	3.76	0.11	0.1	0.21	2.52	1.08	0.29	5.0

12mm feed topsize, 4.5mm zero gap

Ore type	*Pressure (bar)*	*t (s)*	*Pass*	*M (kg)*	*m (t/h)*	*Energy (roll 1, kWh)*	*Energy (roll 2, kWh)*	*Total energy (kWh)*	$P_{no\text{-}load}$ *(kW)*	*P (kW)*	E_{sp} *(kWh/t)*	x_g (mm)
Platreef	150	404	1	505.9	4.51	0.75	0.94	1.69	2.52	12.5	2.78	7.5
	150	315	2	426.9	4.88	0.51	0.56	1.07	2.52	9.66	1.98	7.8
	150	266	3	342.8	4.64	0.20	0.22	0.42	2.52	3.23	0.70	7.3
	150	268	4	271.2	3.64	0.10	0.11	0.21	2.52	0.30	0.08	7.7

Appendix C – Sizing analysis data

Merensky

150bar, 1.5mm zero gap, 12mm Feed						
Size (µm)	**Feed**	**Pass 1**	**Pass 2**	**Pass 3**	**Pass 4**	**Pass 5**
16000	100.0	100.0	100.0	100.0	100.0	100.0
11200	99.5	100.0	100.0	100.0	100.0	100.0
8000	87.7	99.8	100.0	100.0	100.0	100.0
6000	76.3	98.0	99.9	100.0	100.0	100.0
4000	70.0	95.5	99.3	99.8	99.9	100.0
2800	64.3	91.1	97.9	99.2	99.6	99.7
2000	58.8	86.2	95.9	97.8	98.7	98.9
1400	52.5	80.2	92.6	95.2	96.6	96.9
1000	46.2	75.1	89.1	92.0	94.0	93.9
710	40.6	69.0	83.5	88.0	90.2	90.3
500	34.3	61.8	76.3	81.8	85.5	84.7
355	27.9	53.8	69.0	75.3	78.1	78.5
250	22.1	45.3	60.6	67.0	70.2	71.1
180	17.3	37.6	51.5	58.0	61.9	62.3
125	13.2	30.0	43.4	49.7	52.8	54.2
90	10.2	24.0	35.4	41.3	45.0	45.6
75	8.80	21.4	31.5	37.4	41.0	41.6
63	7.82	18.3	28.3	33.5	36.7	37.5
45	5.59	13.5	22.2	26.1	29.0	30.4
32	4.86	10.7	18.2	21.0	23.7	24.6

120 bar, 1.5mm zero gap, 12mm Feed					
Size (µm)	**Feed**	**Pass 1**	**Pass 2**	**Pass 3**	**Pass 4**
16000	100.0	100.0	100.0	100.0	100.0
11200	99.9	100.0	100.0	100.0	100.0
8000	90.0	99.9	100.0	100.0	100.0
6000	78.2	98.0	99.8	100.0	100.0
4000	72.0	95.5	99.1	99.8	99.9
2800	66.2	90.5	97.2	98.6	99.3
2000	60.8	86.0	94.3	96.3	98.0
1400	54.6	79.9	89.6	92.4	95.3
1000	48.1	74.8	85.0	88.1	92.0
710	42.3	68.8	77.2	82.4	86.4
500	35.7	61.8	70.7	75.9	79.6
355	29.1	53.3	62.2	68.5	72.5
250	23.0	44.6	54.2	60.8	64.3
180	18.0	37.1	45.7	52.3	54.9
125	13.8	29.5	37.8	44.0	46.8
90	10.6	23.5	30.2	36.6	38.1
75	9.11	20.8	26.9	33.2	34.4
63	8.20	17.7	24.1	29.3	30.0
45	5.98	13.2	18.2	22.6	23.4
32	5.04	10.6	14.1	18.5	18.2

90bar, 1.5mm zero gap, 12mm Feed						
Size (µm)	**Feed**	**Pass 1**	**Pass 2**	**Pass 3**	**Pass 4**	**Pass 5**
16000	100.0	100.0	100.0	100.0	100.0	100.0
11200	99.6	100.0	100.0	100.0	100.0	100.0
8000	90.2	99.8	100.0	100.0	100.0	100.0
6000	78.5	98.0	99.6	99.9	100.0	100.0
4000	72.5	95.3	98.8	99.6	99.8	99.9
2800	67.6	90.4	96.5	98.5	99.0	99.2
2000	62.6	85.6	93.0	96.6	97.1	97.5
1400	56.2	79.4	88.1	93.3	93.9	94.4
1000	49.5	74.4	83.5	89.6	90.3	91.0
710	43.7	68.5	78.3	83.8	84.6	85.4
500	36.4	61.5	71.0	76.5	77.6	79.4
355	30.0	53.1	63.6	69.1	70.4	71.2
250	24.0	44.7	55.4	60.9	62.2	62.5
180	18.6	37.0	46.4	51.6	53.0	53.8
125	14.2	29.4	38.6	43.5	44.7	44.9
90	10.8	23.5	30.8	35.3	36.2	37.1
75	9.39	20.6	28.1	31.7	32.6	33.4
63	8.09	17.8	24.5	28.3	28.8	29.3
45	5.78	13.3	18.6	21.4	22.5	22.3
32	4.93	10.8	14.8	17.4	18.1	18.0

60bar, 1.5mm zero gap, 12mm Feed					
Size (µm)	**Feed**	**Pass 1**	**Pass 2**	**Pass 3**	**Pass 4**
16000	100.0	100.0	100.0	100.0	100.0
11200	99.8	100.0	100.0	100.0	100.0
8000	90.5	99.8	99.9	100.0	100.0
6000	80.4	97.6	99.5	99.9	99.9
4000	74.7	94.2	98.5	99.1	99.5
2800	69.5	88.5	95.2	96.7	97.5
2000	64.1	83.4	91.1	93.5	94.4
1400	57.7	76.6	85.6	88.7	89.8
1000	51.0	71.2	80.4	83.6	85.2
710	45.0	64.9	74.4	75.9	79.7
500	38.3	56.8	66.5	68.9	72.2
355	31.3	49.3	58.6	60.6	64.6
250	24.8	41.1	50.1	52.3	56.2
180	19.3	33.0	40.9	43.6	46.9
125	14.7	26.4	33.1	35.5	38.6
90	11.1	20.3	25.8	28.3	30.7
75	9.85	17.8	22.7	26.2	27.1
63	8.64	15.5	20.0	22.1	23.5
45	6.29	11.4	14.5	16.0	17.2
32	5.33	8.85	11.4	12.6	13.7

150bar, 3mm zero gap, 12mm Feed					
Size (µm)	**Feed**	**Pass 1**	**Pass 2**	**Pass 3**	**Pass 4**
16000	100.0	100.0	100.0	100.0	100.0
11200	99.7	100.0	100.0	100.0	100.0
8000	86.4	99.7	100.0	100.0	100.0
6000	74.2	98.1	99.7	100.0	100.0
4000	68.0	95.1	98.9	99.8	99.8
2800	62.6	90.3	97.5	99.0	99.0
2000	57.9	85.4	95.5	97.3	97.3
1400	51.9	79.4	92.3	94.2	94.0
1000	45.6	74.4	89.0	90.8	90.4
710	39.5	68.5	82.9	85.4	86.0
500	32.9	62.0	75.7	78.4	80.5
355	27.1	53.5	67.7	71.3	72.6
250	21.6	45.1	59.0	63.1	64.1
180	16.7	37.2	50.5	53.9	55.5
125	12.8	29.6	41.6	45.7	46.3
90	9.81	23.5	34.4	37.4	38.5
75	8.39	20.6	30.9	33.4	34.7
63	7.19	17.4	26.9	30.2	30.2
45	5.26	12.5	20.2	22.9	22.7
32	4.39	9.8	15.9	17.6	17.7

90bar, 3mm zero gap, 12mm Feed				
Size (µm)	**Feed**	**Pass 1**	**Pass 2**	**Pass 3**
16000	100.0	100.0	100.0	100.0
11200	99.7	100.0	100.0	100.0
8000	86.0	99.8	100.0	100.0
6000	74.6	97.6	99.7	100.0
4000	68.6	94.8	99.0	99.8
2800	63.2	90.3	97.0	98.6
2000	58.5	86.1	94.1	96.2
1400	52.3	80.6	90.1	92.5
1000	46.1	76.1	85.9	88.5
710	40.4	68.7	79.0	82.2
500	33.6	61.6	71.0	75.5
355	27.7	52.8	62.2	66.9
250	22.2	44.0	52.8	58.0
180	16.7	36.1	43.8	49.5
125	13.2	28.5	34.4	40.6
90	10.2	22.4	25.1	33.4
75	8.71	19.6	22.0	29.7
63	7.53	16.6	17.8	25.9
45	5.53	12.1	11.8	19.4
32	4.64	9.80	7.01	14.7

60bar, 3mm zero gap, 12mm Feed					
Size (µm)	**Feed**	**Pass 1**	**Pass 2**	**Pass 3**	**Pass 4**
16000	100.0	100.0	100.0	100.0	100.0
11200	99.6	100.0	100.0	100.0	100.0
8000	85.7	99.7	100.0	100.0	100.0
6000	75.0	97.3	99.6	99.9	100.0
4000	69.2	94.0	98.6	99.5	99.9
2800	63.8	89.1	95.5	98.0	99.2
2000	59.1	84.8	91.7	95.5	97.9
1400	52.7	79.4	86.5	91.5	95.6
1000	46.6	74.9	81.9	87.7	93.1
710	41.3	67.3	76.1	81.0	86.6
500	34.3	59.3	68.1	73.1	79.5
355	28.3	51.9	60.2	65.3	70.8
250	22.7	44.4	51.7	56.5	61.3
180	16.7	36.8	42.4	46.7	52.2
125	13.6	30.7	34.5	38.2	42.4
90	10.6	25.2	26.7	30.0	34.1
75	9.03	22.8	23.5	26.8	30.6
63	7.86	20.6	20.5	23.4	26.6
45	5.80	16.9	14.7	17.0	19.8
32	4.89	14.7	11.6	12.9	14.8

150bar, 1.5mm zero gap, 12mm Feed						
Size (µm)	**Feed**	**Pass 1**	**Pass 2**	**Pass 3**	**Pass 4**	**Pass 5**
16000	100.0	100.0	100.0	100.0	100.0	100
11200	100.0	100.0	100.0	100.0	100.0	100
8000	100.0	100.0	100.0	100.0	100.0	100
6000	99.4	100.0	100.0	100.0	100.0	100
4000	94.1	99.4	99.9	100.0	100.0	100
2800	87.8	97.6	99.1	99.8	99.8	100
2000	80.8	94.5	97.5	98.8	99.4	99
1400	70.5	88.8	93.7	96.4	97.7	97
1000	59.8	82.4	89.2	93.1	95.1	94
710	52.9	74.4	84.1	88.8	90.8	90
500	44.2	66.3	77.0	83.3	85.9	85
355	35.5	57.4	69.6	75.8	78.4	78
250	27.7	48.7	61.3	67.5	70.4	70
180	21.2	40.0	52.0	59.0	62.2	61
125	15.7	32.3	43.7	49.9	53.2	52
90	11.4	25.6	35.7	41.5	45.3	44
75	9.88	23.1	32.3	38.3	41.5	41
63	8.27	19.7	28.6	33.6	36.7	36
45	5.77	13.7	21.8	26.9	29.3	29
32	4.52	10.6	17.7	21.2	23.6	23

90bar, 1.5mm zero gap, 6mm Feed					
Size (µm)	**Feed**	**Pass 1**	**Pass 2**	**Pass 3**	**Pass 4**
16000	100.0	100.0	100.0	100.0	100.0
11200	100.0	100.0	100.0	100.0	100.0
8000	100.0	100.0	100.0	100.0	100.0
6000	99.6	100.0	100.0	100.0	100.0
4000	95.3	99.2	99.8	99.9	100.0
2800	89.0	97.0	99.1	99.5	99.8
2000	81.0	93.6	97.3	98.6	99.2
1400	71.5	87.8	93.5	96.0	97.1
1000	60.9	81.9	89.3	92.5	94.0
710	53.1	73.6	82.7	86.7	89.0
500	43.2	64.4	75.1	79.6	83.0
355	35.1	55.7	66.4	72.2	75.2
250	27.4	46.7	57.2	63.9	66.7
180	19.8	37.5	48.4	54.4	58.1
125	15.6	30.0	39.1	45.9	48.9
90	11.6	23.1	31.6	37.6	40.6
75	10.12	20.2	28.2	33.8	37.1
63	8.68	17.5	24.4	30.2	32.6
45	6.21	12.5	17.9	23.4	25.5
32	5.13	9.5	14.0	18.3	20.4

60bar, 1.5mm zero gap, 6mm Feed					
Size (µm)	**Feed**	**Pass 1**	**Pass 2**	**Pass 3**	**Pass 4**
16000	100.0	100.0	100.0	100.0	100.0
11200	100.0	100.0	100.0	100.0	100.0
8000	100.0	100.0	100.0	100.0	100.0
6000	99.5	100.0	100.0	100.0	100.0
4000	93.7	99.2	99.8	100.0	100.0
2800	88.5	96.6	98.6	99.2	99.8
2000	81.5	92.7	96.4	97.5	98.8
1400	70.2	86.2	92.1	93.5	96.0
1000	60.5	80.1	87.8	88.8	92.2
710	52.3	71.2	80.9	83.1	86.2
500	42.8	62.4	73.1	75.8	78.8
355	34.8	52.9	64.5	67.7	71.2
250	27.4	43.6	55.6	58.8	62.7
180	20.7	35.2	47.2	50.2	53.0
125	15.4	27.2	38.7	41.2	44.6
90	11.4	20.9	31.8	33.7	35.9
75	9.57	18.1	28.9	29.8	32.4
63	8.15	15.2	25.4	26.1	28.5
45	5.64	10.7	19.8	19.5	21.4
32	4.38	8.2	15.9	14.7	16.7

150bar, 3mm zero gap, 6mm Feed					
Size (µm)	**Feed**	**Pass 1**	**Pass 2**	**Pass 3**	**Pass 4**
16000	100.0	100.0	100.0	100.0	100.0
11200	100.0	100.0	100.0	100.0	100.0
8000	100.0	100.0	100.0	100.0	100.0
6000	99.3	100.0	100.0	100.0	100.0
4000	95.0	99.3	99.8	99.9	100.0
2800	88.9	97.4	99.3	99.7	99.6
2000	81.7	94.3	97.9	98.7	98.7
1400	70.9	88.8	94.8	96.1	96.0
1000	61.5	83.3	91.2	92.7	92.6
710	53.4	74.2	85.0	86.7	86.8
500	43.6	64.1	78.4	79.5	80.6
355	35.4	55.0	69.6	72.1	72.5
250	27.9	45.1	60.6	63.7	63.8
180	21.3	34.6	51.7	54.1	55.2
125	16.0	30.7	42.5	45.9	46.0
90	11.9	27.0	34.8	37.7	38.1
75	10.19	23.8	31.5	33.9	34.3
63	8.55	20.6	27.4	30.3	30.2
45	6.04	14.8	20.4	23.0	22.9
32	4.84	11.4	16.2	18.4	17.8

90bar, 3mm zero gap, 6mm Feed					
Size (µm)	**Feed**	**Pass 1**	**Pass 2**	**Pass 3**	**Pass 4**
16000	100.0	100.0	100.0	100.0	100.0
11200	100.0	100.0	100.0	100.0	100.0
8000	100.0	100.0	100.0	100.0	100.0
6000	99.6	100.0	100.0	100.0	100.0
4000	94.8	99.2	99.7	99.8	100.0
2800	89.1	97.0	98.6	98.7	99.7
2000	82.3	93.6	96.3	96.8	98.6
1400	71.5	87.4	91.5	93.0	95.7
1000	61.6	81.7	85.8	88.0	91.9
710	52.5	73.4	80.3	81.1	85.8
500	43.7	64.1	72.6	73.8	78.4
355	35.1	55.5	64.9	66.4	70.7
250	27.5	46.5	55.7	57.9	62.2
180	21.2	37.3	46.8	49.4	52.7
125	16.1	30.0	38.2	40.8	44.1
90	11.8	23.1	30.2	32.8	35.5
75	10.39	19.9	27.7	30.4	31.1
63	8.99	17.1	24.1	26.6	27.6
45	6.41	12.3	17.6	20.3	20.7
32	5.19	9.6	13.4	15.7	16.1

60bar, 3mm zero gap, 6mm Feed					
Size (µm)	**Feed**	**Pass 1**	**Pass 2**	**Pass 3**	**Pass 4**
16000	100.0	100.0	100.0	100.0	100.0
11200	100.0	100.0	100.0	100.0	100.0
8000	100.0	100.0	100.0	100.0	100.0
6000	99.6	100.0	100.0	99.9	100.0
4000	95.9	99.1	99.7	99.6	99.9
2800	91.1	96.4	98.4	98.4	99.3
2000	84.7	92.3	95.4	96.3	97.7
1400	75.7	85.4	89.6	92.4	94.3
1000	65.7	79.2	84.0	88.1	90.6
710	56.7	70.8	77.6	81.4	84.0
500	47.5	61.4	69.7	73.6	77.1
355	38.2	52.6	60.9	65.7	68.5
250	29.9	43.8	51.5	56.9	59.3
180	23.0	34.8	43.0	47.3	50.6
125	17.2	27.5	34.0	39.0	41.4
90	12.7	20.9	26.7	30.8	33.6
75	10.95	18.0	23.8	27.3	29.8
63	9.29	15.6	20.5	23.4	25.9
45	6.67	11.0	14.4	17.4	19.1
32	5.48	8.8	11.4	13.0	14.6

UG2

150bar, 1.5mm zero gap, 12mm Feed						
Size (µm)	**Feed**	**Pass 1**	**Pass 2**	**Pass 3**	**Pass 4**	**Pass 5**
16000	100.0	100.0	100.0	100.0	100.0	100.0
11200	96.6	100.0	100.0	100.0	100.0	100.0
8000	78.3	99.5	100.0	100.0	100.0	100.0
5600	68.6	97.0	99.6	100.0	100.0	100.0
4000	62.6	94.2	98.8	99.8	99.9	100.0
2800	58.1	89.7	96.8	98.7	99.5	99.7
2000	54.7	85.6	94.2	96.9	98.4	99.0
1400	51.8	81.7	91.1	94.5	96.5	97.5
1000	49.8	79.0	88.4	92.2	94.5	95.7
710	47.7	76.6	86.7	90.8	93.3	94.8
500	45.4	74.2	84.7	88.3	91.8	93.0
355	41.6	69.5	80.4	85.1	88.2	89.8
250	35.1	62.1	73.5	79.0	82.3	84.3
180	26.5	51.1	62.7	69.1	73.0	75.1
125	18.7	39.4	50.8	57.9	62.1	64.5
90	12.3	29.2	39.9	47.1	51.4	53.8
75	9.92	25.2	35.5	42.1	46.7	48.6
63	8.35	21.7	31.0	37.3	41.8	44.0
45	5.79	15.9	23.8	29.8	33.5	35.9
32	4.76	12.9	19.2	25.2	28.4	31.2

120 bar, 1.5mm zero gap, 12mm Feed						
Size (µm)	**Feed**	**Pass 1**	**Pass 2**	**Pass 3**	**Pass 4**	**Pass 5**
16000	100.0	100.0	100.0	100.0	100.0	100.0
11200	97.4	100.0	100.0	100.0	100.0	100.0
8000	82.9	100.0	100.0	100.0	100.0	100.0
5600	74.8	97.9	99.6	100.0	100.0	100.0
4000	69.0	94.8	98.7	99.7	99.9	100.0
2800	64.4	90.7	97.1	99.0	99.5	99.8
2000	60.8	87.0	94.9	97.9	98.7	99.3
1400	57.7	83.5	92.5	96.3	97.2	98.2
1000	55.6	80.4	89.5	93.6	95.3	96.9
710	53.6	77.7	87.7	91.8	93.8	95.8
500	50.8	75.1	85.6	89.8	91.4	94.4
355	46.8	70.0	80.9	85.4	88.2	90.8
250	39.9	61.9	73.4	78.7	82.1	85.1
180	30.2	50.3	62.1	68.1	72.5	75.8
125	21.2	38.4	50.4	56.3	61.5	65.4
90	14.2	28.3	38.7	45.1	50.7	54.4
75	11.45	24.4	34.2	40.3	45.7	49.5
63	9.36	20.7	29.8	35.4	41.0	44.6
45	6.44	15.0	22.6	28.6	33.1	36.4
32	5.40	12.1	18.6	24.1	27.9	30.3

90bar, 1.5mm zero gap, 12mm Feed						
Size (µm)	**Feed**	**Pass 1**	**Pass 2**	**Pass 3**	**Pass 4**	**Pass 5**
16000	100.0	100.0	100.0	100.0	100.0	100.0
11200	95.5	100.0	100.0	100.0	100.0	100.0
8000	73.0	99.3	100.0	100.0	100.0	100.0
5600	62.3	96.2	99.5	99.9	100.0	100.0
4000	55.7	92.6	98.3	99.5	99.8	99.9
2800	50.4	87.0	95.7	98.4	99.0	99.8
2000	46.8	82.0	92.6	96.4	97.5	99.2
1400	44.0	77.7	89.1	93.4	95.0	98.0
1000	41.9	74.7	86.4	90.8	92.6	96.7
710	40.1	72.3	84.3	89.1	91.1	94.7
500	38.0	69.9	82.1	86.4	89.4	92.8
355	34.8	65.4	77.8	83.1	85.3	88.8
250	29.4	58.1	70.8	76.4	79.1	82.4
180	22.3	47.3	60.2	66.0	68.9	72.5
125	15.7	36.1	48.3	54.5	57.5	60.8
90	10.5	26.3	37.7	43.8	46.0	49.5
75	8.74	22.7	33.4	38.3	41.2	44.5
63	7.18	19.1	28.8	33.4	36.2	39.5
45	5.04	14.1	20.6	25.5	28.7	31.5
32	4.15	11.3	16.7	20.9	23.7	26.6

60bar, 1.5mm zero gap, 12mm Feed						
Size (µm)	**Feed**	**Pass 1**	**Pass 2**	**Pass 3**	**Pass 4**	**Pass 5**
16000	100.0	100.0	100.0	100.0	100.0	100.0
11200	96.9	100.0	100.0	100.0	100.0	100.0
8000	83.3	99.8	99.9	100.0	100.0	100.0
5600	75.5	97.3	99.5	99.9	100.0	100.0
4000	71.6	92.9	98.2	99.4	99.8	99.9
2800	68.0	87.7	95.6	98.1	99.1	99.5
2000	65.6	83.4	92.1	96.1	97.5	98.0
1400	63.4	79.8	88.4	93.6	94.9	95.7
1000	61.8	76.7	85.5	90.8	92.5	93.3
710	59.5	74.2	83.1	88.7	90.7	91.9
500	56.6	71.5	79.9	85.8	88.1	89.0
355	51.6	66.9	76.0	82.2	84.6	85.5
250	43.5	59.2	68.8	75.2	77.8	79.2
180	32.9	48.0	57.7	64.4	67.4	69.0
125	23.0	36.3	45.8	52.7	55.8	57.5
90	15.2	26.7	35.2	41.7	45.1	46.4
75	12.48	22.7	30.4	36.4	39.5	41.0
63	10.22	19.5	26.3	31.8	34.6	36.3
45	7.15	14.2	19.8	24.3	27.4	28.8
32	5.83	11.4	16.0	19.5	21.7	23.8

150bar, 3mm zero gap, 12mm Feed						
Size (µm)	**Feed**	**Pass 1**	**Pass 3**	**Pass 4**	**Pass 5**	
16000	100.0	100.0	100.0	100.0	100.0	
11200	96.5	100.0	100.0	100.0	100.0	
8000	79.0	99.5	99.9	100.0	100.0	
5600	70.0	97.1	99.9	100.0	100.0	
4000	64.6	94.3	99.7	99.9	100.0	
2800	60.2	90.0	99.1	99.6	99.7	
2000	57.0	86.0	98.1	99.1	99.0	
1400	54.3	82.2	96.7	98.2	97.6	
1000	52.3	79.5	95.2	97.0	95.9	
710	50.2	77.1	93.3	95.2	94.7	
500	47.8	74.7	90.7	93.5	92.6	
355	43.9	69.8	87.3	89.4	89.8	
250	37.2	62.3	80.6	83.1	84.2	
180	28.2	50.9	70.3	73.1	75.0	
125	19.8	39.0	58.8	61.6	64.4	
90	13.2	28.9	48.0	50.9	53.7	
75	10.67	25.1	42.6	46.0	48.8	
63	8.69	21.3	36.7	40.7	44.1	
45	6.05	15.5	29.6	32.8	36.2	
32	5.05	12.6	25.0	27.7	29.5	

90bar, 3mm zero gap, 12mm Feed							
Size (µm)	**Feed**	**Pass 1**	**Pass 2**	**Pass 3**	**Pass 4**	**Pass 5**	**Pass 6**
16000	100.0	100.0	100.0	100.0	100.0	100.0	100.0
11200	96.0	100.0	100.0	100.0	100.0	100.0	100.0
8000	77.9	99.2	100.0	100.0	100.0	100.0	100.0
5600	68.5	96.1	99.6	99.9	100.0	100.0	100.0
4000	63.1	92.8	98.6	99.4	99.9	99.9	100.0
2800	58.7	88.1	96.8	98.5	99.4	99.5	99.7
2000	55.5	83.9	94.7	96.7	98.5	98.4	98.6
1400	52.7	80.1	92.3	94.1	97.1	96.3	96.6
1000	50.9	77.5	90.3	92.0	95.6	94.0	94.5
710	48.9	76.1	87.1	90.6	93.3	92.6	92.7
500	46.3	73.8	83.6	88.3	90.1	90.8	90.8
355	42.7	68.6	79.6	83.5	86.3	86.9	86.8
250	36.4	61.1	72.2	76.5	79.9	80.6	80.5
180	27.7	49.8	60.7	65.4	69.1	70.4	70.6
125	19.6	38.3	48.3	52.8	57.2	59.1	59.2
90	13.2	27.8	37.2	41.6	45.3	47.4	47.2
75	10.63	23.3	32.2	37.2	40.3	42.5	42.4
63	8.58	19.8	27.3	32.4	35.3	37.3	37.5
45	5.87	14.6	20.9	24.9	27.2	30.1	29.5
32	4.88	12.1	17.1	21.3	23.3	23.5	24.9

60bar, 3mm zero gap, 12mm Feed						
Size (µm)	**Feed**	**Pass 1**	**Pass 2**	**Pass 3**	**Pass 4**	**Pass 5**
16000	100.0	100.0	100.0	100.0	100.0	100.0
11200	97.0	100.0	100.0	100.0	100.0	100.0
8000	80.2	99.3	100.0	100.0	100.0	100.0
5600	71.6	95.9	99.7	99.9	100.0	100.0
4000	66.1	93.0	98.9	99.3	99.8	99.8
2800	61.7	88.5	97.1	97.5	99.0	99.0
2000	58.6	85.0	94.4	94.7	96.9	97.1
1400	55.8	81.8	91.3	91.3	94.0	94.1
1000	53.8	79.4	88.5	88.4	91.7	91.4
710	51.6	76.0	86.6	86.2	89.7	89.0
500	49.2	72.2	83.6	82.9	87.4	86.0
355	45.1	67.7	79.9	78.9	82.6	82.1
250	38.0	60.4	72.9	71.8	75.3	75.5
180	28.8	49.1	62.1	60.7	63.9	64.6
125	20.0	37.4	50.2	48.3	51.7	52.6
90	13.2	27.4	39.1	37.0	39.8	41.1
75	10.72	22.9	34.4	32.1	34.9	36.0
63	8.80	19.4	29.8	27.5	30.0	31.2
45	6.24	14.1	23.2	20.9	22.8	23.6
32	5.23	11.7	18.8	17.0	19.0	18.8

150bar, 4.5mm zero gap, 12mm Feed					
Size (µm)	**Feed**	**Pass 1**	**Pass 2**	**Pass 3**	**Pass 4**
16000	100.0	100.0	100.0	100.0	100.0
11200	95.1	100.0	100.0	100.0	100.0
8000	74.5	99.3	100.0	100.0	100.0
5600	64.5	96.0	99.1	99.7	100.0
4000	58.9	91.8	97.8	99.3	99.5
2800	54.3	86.4	94.7	97.4	97.6
2000	51.0	81.8	91.2	94.4	94.6
1400	48.2	77.7	87.5	91.0	91.2
1000	46.1	74.8	84.7	88.1	88.4
710	44.2	72.4	82.4	85.9	86.0
500	42.0	70.1	80.1	83.5	82.9
355	38.5	65.4	75.4	79.1	79.1
250	32.5	58.3	68.1	72.0	72.3
180	24.6	47.4	57.0	61.0	61.4
125	17.1	36.1	44.9	48.7	49.2
90	11.6	26.4	34.2	37.2	37.8
75	9.54	22.7	29.8	33.0	33.1
63	7.91	19.3	25.5	28.5	28.7
45	5.56	14.1	19.0	21.7	21.2
32	4.65	11.3	15.4	17.0	17.4

90bar, 4.5mm zero gap, 12mm Feed					
Size (µm)	**Feed**	**Pass 1**	**Pass 2**	**Pass 3**	**Pass 4**
16000	100.0	100.0	100.0	100.0	100.0
11200	96.4	100.0	100.0	100.0	100.0
8000	75.3	99.3	99.9	100.0	100.0
5600	65.5	96.2	98.9	99.9	99.6
4000	59.7	91.5	97.3	99.3	98.7
2800	55.2	85.9	93.6	97.0	96.1
2000	52.1	81.3	89.4	94.1	92.9
1400	49.4	77.4	85.2	90.9	89.2
1000	47.7	74.1	82.0	87.4	86.3
710	45.8	71.4	79.5	84.9	84.1
500	43.5	67.9	76.1	82.5	80.8
355	39.9	63.6	72.1	77.6	76.7
250	33.7	56.3	65.0	70.0	69.5
180	25.6	45.3	53.8	58.3	58.1
125	17.8	34.0	41.8	45.8	45.7
90	12.0	24.2	31.1	33.9	34.4
75	9.75	20.2	26.8	29.1	29.5
63	7.98	17.1	22.6	24.7	24.7
45	5.61	12.3	16.8	18.1	18.5
32	4.68	9.8	12.7	14.7	15.2

60bar, 4.5mm zero gap, 12mm Feed					
Size (µm)	**Feed**	**Pass 1**	**Pass 2**	**Pass 3**	**Pass 4**
16000	100.0	100.0	100.0	100.0	100.0
11200	97.6	100.0	100.0	100.0	100.0
8000	81.4	98.8	100.0	100.0	100.0
5600	73.5	95.5	99.0	99.6	99.8
4000	68.4	91.4	97.3	98.5	98.8
2800	64.0	86.0	93.3	95.0	95.8
2000	60.6	81.7	89.0	90.9	91.9
1400	57.7	77.8	84.6	86.6	87.7
1000	55.2	75.1	81.4	83.5	84.6
710	53.1	71.7	78.7	80.9	81.7
500	50.7	68.7	76.0	78.1	78.7
355	46.5	63.6	71.0	73.4	73.8
250	39.2	55.3	63.1	65.5	65.8
180	29.6	43.7	51.3	53.7	54.0
125	20.5	32.0	38.7	40.7	41.3
90	13.5	22.3	27.9	29.9	29.9
75	11.04	18.7	23.9	25.8	25.4
63	9.04	15.5	19.9	21.4	21.5
45	6.29	10.8	14.0	15.2	14.9
32	5.19	8.8	11.5	12.3	11.4

150bar, 1.5mm zero gap, 6mm Feed					
Size (µm)	**Feed**	**Pass 1**	**Pass 2**	**Pass 3**	**Pass 4**
16000	100.0	100.0	100.0	100.0	100.0
11200	100.0	100.0	100.0	100.0	100.0
8000	100.0	100.0	100.0	100.0	100.0
5600	99.7	100.0	100.0	100.0	100.0
4000	93.2	98.8	99.7	99.9	100.0
2800	83.7	94.1	98.0	99.3	99.8
2000	78.0	89.3	95.3	97.8	99.2
1400	74.0	84.5	91.9	95.5	98.1
1000	71.3	81.2	89.0	93.2	96.7
710	67.6	78.7	87.4	91.9	95.0
500	63.8	75.5	85.5	89.7	93.3
355	58.1	71.4	80.9	86.7	90.0
250	48.5	63.8	74.1	80.6	83.4
180	35.9	52.5	63.1	70.8	73.4
125	24.2	40.8	51.8	59.7	62.2
90	15.8	30.8	40.6	49.0	51.3
75	12.84	26.0	36.1	44.1	46.6
63	9.92	22.1	31.7	38.9	40.9
45	6.62	16.2	24.4	30.9	33.0
32	5.44	13.0	20.6	25.4	28.3

90bar, 1.5mm zero gap, 6mm Feed					
Size (µm)	**Feed**	**Pass 1**	**Pass 3**		**Pass 4**
16000	100.0	100.0	100.0		
11200	100.0	100.0	100.0		
8000	100.0	100.0	100.0		
5600	100.0	100.0	100.0		
4000	98.0	99.5	100.0		
2800	92.2	97.2	99.6		
2000	86.4	93.9	98.6		
1400	81.2	89.9	96.8		
1000	77.9	86.8	94.8		
710	75.2	84.9	93.4		
500	72.6	82.9	90.9		
355	67.7	78.4	87.6		
250	59.9	70.9	81.7		
180	48.5	59.4	71.9		
125	36.5	47.5	60.7		
90	26.1	35.9	50.2		
75	22.40	31.5	44.9		
63	18.83	27.1	39.4		
45	13.23	20.3	32.0		
32	10.84	16.1	27.0		

60bar, 1.5mm zero gap, 6mm Feed					
Size (µm)	**Feed**	**Pass 1**	**Pass 2**	**Pass 3**	**Pass 4**
16000	100.0	100.0	100.0	100.0	100.0
11200	100.0	100.0	100.0	100.0	100.0
8000	100.0	100.0	100.0	100.0	100.0
5600	98.7	99.9	100.0	100.0	100.0
4000	80.8	96.8	99.1	99.7	99.9
2800	65.7	88.3	95.0	97.8	99.0
2000	59.2	81.2	89.9	94.5	96.6
1400	55.2	75.3	85.3	90.3	92.9
1000	52.9	71.6	81.2	87.0	89.6
710	50.1	68.5	76.3	84.3	87.1
500	47.2	65.0	73.1	81.0	84.5
355	43.0	60.8	67.9	77.2	80.0
250	36.1	53.9	60.5	70.3	73.1
180	26.9	43.4	49.1	59.5	62.4
125	18.5	32.6	36.8	47.7	50.3
90	12.2	23.2	25.9	36.9	39.0
75	9.96	19.3	20.8	31.7	34.5
63	7.87	16.0	16.9	27.0	29.6
45	5.58	11.0	10.6	20.2	22.3
32	4.57	8.9	6.4	15.8	18.5

150bar, 3mm zero gap, 6mm Feed					
Size (µm)	**Feed**	**Pass 1**	**Pass 2**	**Pass 3**	**Pass 4**
16000	100.0	100.0	100.0	100.0	100.0
11200	100.0	100.0	100.0	100.0	100.0
8000	100.0	100.0	100.0	100.0	100.0
5600	99.7	100.0	100.0	100.0	100.0
4000	90.8	98.2	99.6	99.9	99.9
2800	79.8	94.0	97.7	98.9	99.2
2000	73.8	89.8	94.5	96.9	97.6
1400	70.1	86.0	90.7	94.2	95.2
1000	67.6	83.5	87.9	91.8	92.4
710	64.8	79.5	85.5	89.7	90.4
500	61.2	75.3	82.8	87.6	87.5
355	56.3	70.6	78.0	83.0	83.9
250	47.9	62.8	70.0	76.2	77.2
180	35.9	50.9	58.7	65.2	66.9
125	24.3	38.7	46.6	53.6	55.3
90	15.5	28.1	36.0	42.1	44.4
75	12.32	23.4	31.3	36.8	38.7
63	9.56	19.6	28.7	32.3	33.9
45	6.44	13.6	21.3	25.2	26.2
32	5.16	11.3	17.3	19.7	21.6

90bar, 3mm zero gap, 6mm Feed					
Size (µm)	**Feed**	**Pass 2**	**Pass 3**	**Pass 4**	
16000	100.0	100.0	100.0	100.0	
11200	100.0	100.0	100.0	100.0	
8000	100.0	100.0	100.0	100.0	
5600	99.8	100.0	100.0	100.0	
4000	93.6	99.5	99.8	99.9	
2800	83.1	97.3	98.7	99.2	
2000	76.2	94.3	96.6	97.4	
1400	70.8	91.0	93.9	94.5	
1000	67.7	87.6	91.0	91.9	
710	64.6	85.0	88.6	89.7	
500	60.8	82.3	85.3	86.7	
355	55.6	77.3	81.3	82.8	
250	47.0	69.2	74.0	75.7	
180	34.9	57.4	62.6	64.4	
125	23.5	44.9	50.1	51.5	
90	14.7	33.6	38.4	39.3	
75	11.4	29.0	33.4	34.2	
63	8.84	24.9	28.5	29.5	
45	5.83	18.3	21.5	21.8	
32	4.84	14.3	16.2	17.8	

60bar, 3mm zero gap, 6mm Feed					
Size (µm)	**Feed**	**Pass 1**	**Pass 2**	**Pass 3**	**Pass 4**
16000	100.0	100.0	100.0	100.0	100.0
11200	100.0	100.0	100.0	100.0	100.0
8000	100.0	100.0	100.0	100.0	100.0
5600	99.7	100.0	100.0	100.0	100.0
4000	94.3	98.2	99.5	99.8	99.9
2800	86.4	92.9	97.2	98.6	99.0
2000	81.5	87.4	93.3	95.9	96.8
1400	78.0	82.4	89.1	92.5	93.7
1000	75.2	79.1	86.2	89.6	90.9
710	72.1	76.2	83.6	86.9	88.5
500	68.5	72.4	80.3	83.6	85.3
355	62.3	67.7	75.9	79.4	81.1
250	51.9	59.5	67.9	71.7	73.8
180	38.4	47.4	56.0	60.0	62.2
125	26.1	35.2	43.3	47.4	49.3
90	16.4	24.7	32.2	36.4	37.3
75	13.03	20.4	27.0	30.8	32.1
63	10.50	16.8	22.1	25.6	27.6
45	6.82	11.6	15.9	18.7	20.3
32	5.47	9.4	12.9	15.0	15.8

Platreef

150bar, 1.5mm zero gap, 12mm Feed						
Size (µm)	**Feed**	**Pass 1**	**Pass 2**	**Pass 3**	**Pass 4**	**Pass 5**
16000	100.0	100.0	100.0	100.0	100.0	100.0
11200	98.9	100.0	100.0	100.0	100.0	100.0
8000	78.4	99.1	100.0	100.0	100.0	100.0
5600	62.0	94.8	99.3	99.9	100.0	100.0
4000	53.6	88.7	97.1	99.6	99.9	100.0
2800	46.3	78.4	90.4	95.6	97.5	99.6
2000	40.2	69.5	83.8	90.0	93.9	98.0
1400	34.7	60.8	76.0	82.6	88.8	93.9
1000	30.4	54.8	70.4	77.1	84.5	89.2
710	26.7	49.0	64.9	72.6	80.1	85.7
500	22.9	42.6	58.2	66.6	74.5	80.5
355	19.3	37.1	52.1	61.1	68.7	75.4
250	15.8	31.4	45.5	54.5	62.1	69.2
180	12.6	26.0	39.0	47.7	55.4	62.2
125	9.9	21.2	33.0	41.4	48.5	55.4
90	7.5	16.7	27.0	34.6	41.0	48.0
75	6.39	15.2	25.2	32.2	39.0	45.4
63	5.63	13.3	22.6	29.3	35.6	41.4
45	4.05	10.2	17.8	23.8	28.9	35.6
32	3.37	8.6	14.5	19.6	25.0	30.7

90bar, 1.5mm zero gap, 12mm Feed						
Size (µm)	**Feed**	**Pass 1**	**Pass 2**	**Pass 3**	**Pass 4**	**Pass 5**
16000	100.0	100.0	100.0	100.0	100.0	100.0
11200	98.8	100.0	100.0	100.0	100.0	100.0
8000	69.5	98.9	100.0	100.0	100.0	100.0
5600	50.1	93.3	99.4	100.0	100.0	100.0
4000	43.6	86.4	97.0	99.4	99.9	100.0
2800	36.9	75.3	89.8	95.9	98.4	99.2
2000	31.8	66.4	82.4	90.6	94.9	97.0
1400	27.3	57.5	74.0	83.7	89.1	92.5
1000	24.0	51.7	68.1	78.2	83.8	88.0
710	20.5	45.9	62.3	72.7	78.7	82.6
500	17.4	40.1	55.2	66.3	73.1	76.2
355	14.8	34.3	49.1	59.1	65.8	70.1
250	12.3	29.1	42.3	52.3	59.0	63.2
180	9.8	23.9	35.6	45.2	51.8	56.2
125	7.8	19.5	29.5	38.6	44.9	49.3
90	6.0	15.6	23.5	32.6	38.2	42.5
75	5.27	13.7	22.0	29.3	34.9	41.1
63	4.62	12.3	19.5	26.4	32.1	36.4
45	3.33	9.1	15.2	20.8	26.0	30.2
32	2.75	7.3	12.2	17.8	21.5	25.9

60bar, 1.5mm zero gap, 12mm Feed							
Size (µm)	**Feed**	**Pass 1**	**Pass 2**	**Pass 3**	**Pass 4**	**Pass 5**	**Pass 6**
16000	100.0	100.0	100.0	100.0	100.0	100.0	100.0
11200	98.5	100.0	100.0	100.0	100.0	100.0	100.0
8000	72.7	98.6	99.9	100.0	100.0	100.0	100.0
5600	53.3	90.9	99.0	99.8	100.0	100.0	100.0
4000	44.8	81.5	95.7	98.9	99.7	99.9	99.9
2800	37.4	68.8	87.3	94.0	97.1	98.8	98.9
2000	31.8	59.4	79.1	87.6	92.4	95.1	95.2
1400	27.2	50.3	69.7	79.4	85.2	88.8	88.1
1000	23.6	44.6	63.3	73.5	79.5	83.0	82.3
710	20.4	39.0	56.9	67.4	73.2	77.0	76.7
500	17.2	33.1	49.9	60.7	66.4	70.2	70.6
355	14.5	28.1	43.2	53.3	58.9	63.1	63.3
250	11.9	23.2	36.9	46.5	51.9	56.1	57.1
180	9.4	18.8	30.8	39.4	44.6	48.7	50.3
125	7.2	15.0	25.3	32.9	37.9	41.7	44.0
90	5.5	11.5	20.2	27.0	31.7	35.0	37.8
75	4.74	10.2	18.0	24.2	28.8	31.7	34.2
63	4.06	9.1	16.5	22.0	25.8	29.0	32.1
45	2.97	6.8	12.3	17.0	20.6	23.3	26.1
32	2.50	5.4	10.3	13.9	17.1	19.6	21.8

150bar, 3mm zero gap, 12mm Feed						
Size (µm)	**Feed**	**Pass 1**	**Pass 2**	**Pass 3**	**Pass 4**	**Pass 5**
16000	100.0	100.0	100.0	100.0	100.0	100.0
11200	98.1	100.0	100.0	100.0	100.0	100.0
8000	69.9	100.0	99.9	100.0	100.0	100.0
5600	50.4	100.0	99.4	99.9	100.0	100.0
4000	41.2	97.2	97.8	99.5	99.9	100.0
2800	33.3	87.0	91.8	96.2	98.5	99.2
2000	27.8	77.1	85.1	90.9	94.9	96.7
1400	23.1	67.2	77.2	83.6	88.7	91.8
1000	19.7	61.0	71.7	77.6	83.3	86.8
710	17.0	55.2	66.2	72.7	78.5	81.9
500	14.5	48.6	59.5	66.4	72.5	75.7
355	12.2	41.8	53.6	60.6	66.6	69.8
250	10.1	35.7	46.9	53.8	59.9	62.8
180	8.2	29.6	40.4	47.0	52.9	55.7
125	6.6	24.0	34.4	40.5	46.0	48.7
90	5.1	19.3	28.4	33.8	39.5	42.0
75	4.39	17.1	26.3	31.8	37.3	41.2
63	3.93	15.3	23.7	28.6	33.5	35.8
45	2.90	11.6	19.2	23.3	27.1	29.0
32	2.42	9.3	16.2	19.6	23.0	23.9

90bar, 3mm zero gap, 12mm Feed						
Size (µm)	**Feed**	**Pass 1**	**Pass 2**	**Pass 3**	**Pass 4**	**Pass 5**
16000	100.0	100.0	100.0	100.0	100.0	100.0
11200	98.7	100.0	100.0	100.0	100.0	100.0
8000	61.6	98.9	100.0	100.0	100.0	100.0
5600	39.8	93.3	99.4	99.9	100.0	100.0
4000	30.4	85.2	97.0	99.2	99.8	99.9
2800	23.7	73.9	90.4	95.2	97.5	98.6
2000	19.1	64.7	83.0	89.4	93.5	95.3
1400	15.7	55.4	74.1	81.8	86.8	89.5
1000	13.1	49.0	68.2	75.7	81.2	84.0
710	11.2	43.4	61.7	69.7	75.2	77.7
500	9.4	37.7	55.3	63.0	68.1	70.5
355	7.9	32.0	48.0	55.7	61.5	63.7
250	6.6	27.1	41.5	48.8	54.3	56.4
180	5.3	22.2	35.0	41.8	47.1	49.1
125	4.2	18.0	29.2	35.4	40.4	42.1
90	3.2	14.3	23.9	29.5	33.7	35.6
75	2.80	12.7	21.2	25.7	31.5	34.5
63	2.46	11.1	19.1	23.7	28.4	29.9
45	1.75	8.4	14.8	19.0	22.7	23.5
32	1.47	6.8	12.1	15.6	19.0	19.8

60bar, 3mm zero gap, 12mm Feed						
Size (µm)	**Feed**	**Pass 1**	**Pass 2**	**Pass 3**	**Pass 4**	**Pass 5**
16000	100.0	100.0	100.0	100.0	100.0	100.0
11200	99.0	100.0	100.0	100.0	100.0	100.0
8000	69.8	98.1	99.8	100.0	100.0	100.0
5600	51.1	90.3	98.4	99.8	100.0	100.0
4000	43.0	81.5	94.3	98.7	99.5	99.9
2800	35.9	68.8	85.9	93.8	96.7	97.7
2000	30.6	60.0	77.6	87.3	91.5	93.2
1400	26.0	51.3	68.5	79.0	84.4	86.3
1000	22.3	46.0	62.4	73.0	78.5	80.3
710	19.6	40.5	56.0	66.4	71.1	74.1
500	16.5	34.6	49.4	59.2	64.0	67.2
355	14.1	29.7	42.6	51.9	56.6	59.6
250	11.7	24.7	36.4	45.0	49.6	52.4
180	9.5	20.3	30.3	38.1	42.4	44.9
125	7.6	16.4	24.9	31.7	35.8	38.1
90	5.9	12.7	20.2	25.7	29.5	31.9
75	5.22	11.7	17.6	22.8	26.7	28.4
63	4.54	10.2	15.9	21.1	24.7	26.0
45	3.33	7.6	12.2	16.2	19.3	20.3
32	2.77	6.2	9.9	13.4	15.6	16.8

150bar, 1.5mm zero gap, 6mm Feed					
Size (µm)	**Feed**	**Pass 1**	**Pass 2**	**Pass 3**	**Pass 4**
16000	100.0	100.0	100.0	100.0	100.0
11200	100.0	100.0	100.0	100.0	100.0
8000	100.0	100.0	100.0	100.0	100.0
5600	98.5	100.0	100.0	100.0	100.0
4000	77.2	96.9	99.4	99.8	100.0
2800	55.1	86.7	93.8	97.0	99.3
2000	42.7	77.2	86.0	92.1	96.9
1400	33.5	67.6	76.8	85.2	92.0
1000	27.7	61.1	70.6	79.9	86.6
710	22.9	54.2	65.1	75.2	82.6
500	18.7	47.7	58.3	69.7	77.6
355	15.3	40.8	52.4	62.8	70.7
250	12.3	34.7	45.6	56.3	64.2
180	9.4	28.8	39.0	49.4	57.0
125	7.0	23.5	32.8	42.7	50.0
90	5.1	18.8	27.2	36.2	43.1
75	4.35	16.6	25.9	33.0	39.6
63	3.67	14.9	22.0	30.4	36.5
45	2.52	11.4	17.2	24.3	29.7
32	2.04	9.4	14.2	20.2	24.1

90bar, 1.5mm zero gap, 6mm Feed						
Size (µm)	**Feed**	**Pass 1**	**Pass 2**	**Pass 3**	**Pass 4**	**Pass 5**
16000	100.0	100.0	100.0	100.0	100.0	100.0
11200	100.0	100.0	100.0	100.0	100.0	100.0
8000	100.0	100.0	100.0	100.0	100.0	100.0
5600	98.8	100.0	100.0	100.0	100.0	100.0
4000	72.9	97.3	99.4	99.9	99.9	100.0
2800	48.0	87.5	96.0	98.5	99.1	99.5
2000	35.3	78.4	90.5	95.8	96.1	97.8
1400	26.4	68.5	83.0	91.4	90.9	93.5
1000	21.3	62.1	77.2	86.9	85.9	88.8
710	17.1	55.2	71.1	80.2	79.8	84.1
500	13.7	47.7	64.4	73.6	72.6	77.9
355	11.2	41.4	56.9	65.9	65.9	72.1
250	9.0	34.6	49.9	58.8	58.5	65.2
180	6.9	28.4	42.5	51.1	51.2	57.9
125	5.3	22.9	35.7	43.9	44.3	50.9
90	3.9	17.8	29.4	36.8	37.6	43.2
75	3.30	16.0	26.7	33.7	35.3	40.9
63	2.79	14.4	23.8	30.6	32.2	37.2
45	1.90	10.8	18.9	24.8	26.1	30.8
32	1.55	8.6	15.7	20.4	21.5	26.2

60bar, 1.5mm zero gap, 6mm Feed						
Size (µm)	**Feed**	**Pass 1**	**Pass 2**	**Pass 3**	**Pass 4**	**Pass 5**
16000	100.0	100.0	100.0	100.0	100.0	100.0
11200	100.0	100.0	100.0	100.0	100.0	100.0
8000	100.0	100.0	100.0	100.0	100.0	100.0
5600	99.1	99.9	100.0	100.0	100.0	100.0
4000	68.7	95.7	98.9	99.7	100.0	100.0
2800	41.0	81.4	92.8	96.3	98.7	99.2
2000	27.9	69.9	85.1	90.6	95.2	96.6
1400	19.3	58.6	76.0	82.9	88.9	91.7
1000	14.8	51.8	69.1	75.5	83.2	87.3
710	11.3	44.8	62.1	68.6	76.5	81.2
500	8.8	38.1	54.3	61.5	68.9	74.6
355	7.1	32.0	47.5	55.0	62.0	67.1
250	5.7	26.7	40.3	48.0	54.6	60.1
180	4.5	21.5	33.6	41.4	47.4	52.7
125	3.5	17.2	27.5	35.0	40.5	45.7
90	2.6	13.5	21.6	28.9	34.1	39.1
75	2.25	11.8	20.0	26.9	33.5	35.3
63	1.92	10.3	17.5	24.1	28.6	32.6
45	1.29	7.4	13.2	19.3	22.6	26.4
32	1.07	6.2	10.4	15.7	19.1	22.1

150bar, 3mm zero gap, 6mm Feed						
Size (µm)	**Feed**	**Pass 2**	**Pass 3**	**Pass 4**	**Pass 5**	
16000	100.0	100.0	100.0	100.0	100.0	
11200	100.0	100.0	100.0	100.0	100.0	
8000	100.0	100.0	100.0	100.0	100.0	
5600	98.8	100.0	100.0	100.0	100.0	
4000	81.9	99.4	99.7	99.9	100.0	
2800	63.3	93.5	96.8	98.5	99.4	
2000	51.9	85.3	92.0	93.9	97.1	
1400	42.7	75.4	85.1	86.6	92.5	
1000	35.9	68.6	79.7	79.0	88.2	
710	31.3	63.4	74.8	74.2	83.3	
500	25.8	57.3	68.9	71.1	77.3	
355	21.2	50.7	62.1	66.0	71.2	
250	16.8	44.6	55.5	58.9	64.4	
180	12.9	38.1	48.2	47.7	57.5	
125	9.7	32.2	41.5	35.8	50.4	
90	7.0	26.8	34.9	25.2	43.5	
75	5.83	23.8	31.7	20.2	40.7	
63	4.95	21.9	29.1	16.5	37.1	
45	3.42	17.1	23.1	10.3	30.1	
32	2.81	14.4	19.3	6.2	25.2	

90bar, 3mm zero gap, 6mm Feed						
Size (µm)	**Feed**	**Pass 1**	**Pass 2**	**Pass 3**	**Pass 4**	**Pass 5**
16000	100.0	100.0	100.0	100.0	100.0	100.0
11200	100.0	100.0	100.0	100.0	100.0	100.0
8000	100.0	100.0	100.0	100.0	100.0	100.0
5600	99.5	99.9	100.0	100.0	100.0	100.0
4000	80.5	97.0	99.2	99.8	99.9	100.0
2800	59.8	88.9	94.2	97.1	98.3	98.9
2000	47.7	82.1	87.5	92.2	94.6	95.7
1400	38.1	74.8	79.1	85.1	88.3	89.8
1000	31.6	69.4	72.7	79.2	82.8	84.2
710	26.1	59.6	66.4	73.1	76.7	78.5
500	21.4	51.5	58.8	66.1	69.4	72.0
355	17.5	44.6	52.1	58.9	62.8	64.8
250	13.8	37.4	44.8	52.0	55.3	57.8
180	10.7	30.8	37.7	44.6	47.8	50.2
125	8.0	24.7	31.2	37.6	40.7	43.0
90	5.8	19.0	24.9	31.1	33.7	36.3
75	5.00	17.4	22.4	27.6	32.6	32.9
63	4.25	15.5	20.3	25.7	28.4	30.0
45	2.81	11.4	15.6	19.9	22.7	24.2
32	2.30	9.1	12.9	16.7	18.5	20.1

60bar, 3mm zero gap, 6mm Feed						
Size (µm)	**Feed**	**Pass 1**	**Pass 2**	**Pass 3**	**Pass 4**	**Pass 5**
16000	100.0	100.0	100.0	100.0	100.0	100.0
11200	100.0	100.0	100.0	100.0	100.0	100.0
8000	100.0	100.0	100.0	100.0	99.7	100.0
5600	99.5	99.9	100.0	100.0	98.1	100.0
4000	82.9	95.2	98.8	99.6	95.6	99.9
2800	63.9	82.4	92.7	95.8	89.5	98.7
2000	53.4	72.0	85.0	89.8	80.7	95.1
1400	43.8	61.7	75.6	81.6	68.8	88.9
1000	37.1	55.2	68.8	75.1	59.9	82.7
710	32.2	48.5	61.9	68.5	54.0	76.7
500	26.6	41.8	54.6	60.7	48.4	69.1
355	22.0	35.4	46.9	53.7	42.5	62.1
250	17.7	29.6	39.9	46.2	37.1	54.4
180	13.6	24.0	33.1	38.9	31.6	46.8
125	10.2	19.0	26.9	32.2	26.6	39.4
90	7.5	14.8	21.6	26.1	22.1	32.1
75	6.25	12.8	18.8	23.9	20.1	29.8
63	5.11	11.4	16.7	21.1	17.6	26.5
45	3.51	8.4	12.4	16.3	13.8	20.8
32	2.91	6.7	10.1	13.4	11.1	17.3

150bar, 4.5mm zero gap, 12mm Feed					
Size (µm)	**Feed**	**Pass 1**	**Pass 2**	**Pass 3**	**Pass 4**
16000	100.0	100.0	100.0	100.0	100.0
11200	97.8	100.0	100.0	100.0	100.0
8000	58.8	99.2	100.0	100.0	100.0
5600	37.6	92.9	99.1	99.8	99.9
4000	28.6	85.4	96.8	98.8	99.3
2800	22.0	74.4	90.0	94.5	95.9
2000	17.9	65.3	82.9	88.8	90.8
1400	14.5	56.5	74.6	81.4	83.7
1000	12.2	50.5	68.9	75.6	77.8
710	10.3	44.4	62.5	69.5	71.8
500	8.68	38.3	55.8	62.3	65.1
355	7.28	33.1	48.9	55.8	57.9
250	5.93	27.6	42.6	48.6	50.9
180	4.73	22.9	36.0	41.7	43.7
125	3.69	18.6	30.1	35.2	36.9
90	2.81	14.6	24.8	28.9	30.6
75	2.41	13.4	22.3	26.6	27.2
63	2.17	11.9	20.0	23.9	24.8
45	1.55	8.92	15.7	19.0	19.7
32	1.30	7.58	13.1	15.9	16.5

Appendix D – Flotation data

Merensky

150bar, 3mm zero gap, 12mm Feed - 4th pass

Concentrate	Float 1		Float 2		Float 3		Float 4	
	Cumulative Mass pull (g)	Cum. Water recovery (g)	Cumulative Mass pull (g)	Cum. Water recovery (g)	Cumulative Mass pull (g)	Cum. Water recovery (g)	Cumulative Mass pull (g)	Cum. Water recovery (g)
C1	3.37	38.8	2.38	20.5	1.78	13.5	5.12	39.3
C2	7.39	116.2	5.83	73.9	4.65	54.2	11.7	103.0
C3	9.77	165.7	9.02	128.2	8.06	118.4	17.5	149.0
C4	14.4	236.9	14.6	202.0	13.7	203.8	26.9	222.6
Total feed	1015		1039		1013		1038	

150bar, 1.5mm zero gap, 12mm Feed - 4th pass

Concentrate	Float 1		Float 2		Float 3		Float 4	
	Cumulative Mass pull (g)	Cum. Water recovery (g)	Cumulative Mass pull (g)	Cum. Water recovery (g)	Cumulative Mass pull (g)	Cum. Water recovery (g)	Cumulative Mass pull (g)	Cum. Water recovery (g)
C1	7.24	87.6	7.92	92.4	6.06	71.7	6.55	74.1
C2	15.5	217.0	15.5	197.5	12.4	169.8	13.6	182.1
C3	23.4	310.0	24.7	301.4	19.9	275.1	20.9	272.1
C4	36.7	447.0	37.8	432.2	30.0	387.4	32.8	400.2
Total feed	1030		1051		1051		1033	

150bar, 1.5mm zero gap, 6mm Feed - 4th pass

Concentrate	Float 1		Float 2		Float 3		Float 4	
	Cumulative Mass pull (g)	Cum. Water recovery (g)	Cumulative Mass pull (g)	Cum. Water recovery (g)	Cumulative Mass pull (g)	Cum. Water recovery (g)	Cumulative Mass pull (g)	Cum. Water recovery (g)
C1	5.66	81.5	5.38	47.5	6	52.2	5.81	55.6
C2	17.6	321.6	14.3	169.3	14.2	159.7	14.0	167.9
C3	27.0	520.9	21.9	250.3	21.8	244.6	22.0	258.9
C4	38.0	731.6	34.0	361.2	32.4	346.6	33.7	369.1
Total feed	1001		1005		1007		1009	

Ball Mill

Concentrate	Float 1		Float 2		Float 3		Float 4	
	Cumulative Mass pull (g)	Cum. Water recovery (g)	Cumulative Mass pull (g)	Cum. Water recovery (g)	Cumulative Mass pull (g)	Cum. Water recovery (g)	Cumulative Mass pull (g)	Cum. Water recovery (g)
C1	21.8	86.4	15	83.3	31.7	10.0	7.9	34.8
C2	39	184.1	26.8	183.5	135.4	23.8	17.5	99.1
C3	54.7	281.4	40	295.1	248.3	36.8	26.5	172.1
C4	73.6	414.8	56.4	435.2	402.2	53.6	40.2	299.5
Total feed	1015		1040		1013		1038	

UG2

150bar, 3mm zero gap, 12mm Feed - 4th pass

Concentrate	Float 1		Float 2		Float 3		Float 4	
	Cumulative Mass pull (g)	Cum. Water recovery (g)	Cumulative Mass pull (g)	Cum. Water recovery (g)	Cumulative Mass pull (g)	Cum. Water recovery (g)	Cumulative Mass pull (g)	Cum. Water recovery (g)
C1	30.64	171.63	28.04	159.23	27.7	159.06	29.07	151.07
C2	54.64	307.29	48.98	284.61	48.39	269.74	52.28	273.74
C3	70.49	405.63	63.9	383.01	63.01	360.94	67.92	364.49
C4	83.64	492.91	74.83	457.39	74.47	440.8	81.58	455.38
Total feed	1083.12		1346.71		1343.94		1353.07	

150bar, 1.5mm zero gap, 12mm Feed - 4th pass

Concentrate	Float 1		Float 2		Float 3		Float 4	
	Cumulative Mass pull (g)	Cum. Water recovery (g)	Cumulative Mass pull (g)	Cum. Water recovery (g)	Cumulative Mass pull (g)	Cum. Water recovery (g)	Cumulative Mass pull (g)	Cum. Water recovery (g)
C1	16.4	64.6	19.3	86.4	20.1	89.4	19.5	88.6
C2	32.6	135.3	34.8	157.9	35.5	157.9	35.5	157.9
C3	42.7	182.1	45.7	214.8	46.3	209.6	45.3	203.7
C4	52.5	233.3	56.1	275.2	56.8	265.8	55.7	258.2
Total feed	1325		1334		1325		1327	

150bar, 1.5mm zero gap, 6mm Feed - 4th pass

Concentrate	Float 1		Float 2		Float 3		Float 4	
	Cumulative Mass pull (g)	Cum. Water recovery (g)	Cumulative Mass pull (g)	Cum. Water recovery (g)	Cumulative Mass pull (g)	Cum. Water recovery (g)	Cumulative Mass pull (g)	Cum. Water recovery (g)
C1	29.9	156.5	17.6	68.3	15.6	55.7	19.3	81.3
C2	52.7	280.9	33.0	130.6	30.1	112.1	34.4	146.2
C3	68.4	380.1	44.0	182.0	40.7	159.2	44.0	190.1
C4	80.5	463.9	55.2	238.4	49.8	200.6	52.8	232.4
Total feed	1351		1343		1344		1356	

Ball Mill

Concentrate	Float 1		Float 2		Float 3		Float 4	
	Cumulative Mass pull (g)	Cum. Water recovery (g)	Cumulative Mass pull (g)	Cum. Water recovery (g)	Cumulative Mass pull (g)	Cum. Water recovery (g)	Cumulative Mass pull (g)	Cum. Water recovery (g)
C1	13.8	62	13.7	60.9	19.7	121.3	8.1	18.7
C2	26.4	129.1	25.6	125.8	32.1	174.2	19	36
C3	34.9	187.1	34.2	187	40.8	239	27.1	75.2
C4	43.9	273.6	42.1	270.6	48.7	319.3	34.2	138.3
Total feed	1360.2		1302.4		1398.2		1461.7	

Platreef

150bar, 3mm zero gap, 12mm Feed - 4th pass

Concentrate	Float 1		Float 2		Float 3		Float 4	
	Cumulative Mass pull (g)	Cum. Water recovery (g)	Cumulative Mass pull (g)	Cum. Water recovery (g)	Cumulative Mass pull (g)	Cum. Water recovery (g)	Cumulative Mass pull (g)	Cum. Water recovery (g)
C1	13.2	127.7	14.3	142.1	13.0	132.3	12.9	129.1
C2	25.1	236.2	26.0	247.0	25.2	250.6	23.9	225.2
C3	34.6	306.9	35.6	318.5	35.1	338.3	32.9	297.1
C4	44.4	375.0	45.5	388.1	43.5	379.1	42.1	359.8
Total feed	1003		1007		1005		1005	

150bar, 1.5mm zero gap, 12mm Feed - 4th pass

Concentrate	Float 1		Float 2		Float 3		Float 4	
	Cumulative Mass pull (g)	Cum. Water recovery (g)	Cumulative Mass pull (g)	Cum. Water recovery (g)	Cumulative Mass pull (g)	Cum. Water recovery (g)	Cumulative Mass pull (g)	Cum. Water recovery (g)
C1	19.0	167.1	13.9	128.8	17.6	158.0	15.3	123.5
C2	33.9	305.7	28.1	272.5	32.4	281.3	31.5	262.1
C3	46.7	431.1	39.4	389.4	43.4	362.1	42.8	343.1
C4	59.3	549.6	49.7	487.1	55.3	455.6	55.1	435.2
Total feed	1008		960		1002		1004	

150bar, 1.5mm zero gap, 6mm Feed - 4th pass

Concentrate	Float 1		Float 2		Float 3		Float 4	
	Cumulative Mass pull (g)	Cum. Water recovery (g)	Cumulative Mass pull (g)	Cum. Water recovery (g)	Cumulative Mass pull (g)	Cum. Water recovery (g)	Cumulative Mass pull (g)	Cum. Water recovery (g)
C1	15.9	133.9	17.0	152.0	17.4	154.7	14.7	120.6
C2	30.4	256.6	32.0	283.9	32.4	286.2	29.1	232.4
C3	42.7	366.0	43.1	378.0	43.6	355.3	41.4	327.1
C4	53.6	442.5	54.4	464.6	54.8	433.6	53.8	427.2
Total feed	1013		1015		1016		1013	

Ball mill

Concentrate	Float 1		Float 2		Float 3		Float 4	
	Cumulative Mass pull (g)	Cum. Water recovery (g)	Cumulative Mass pull (g)	Cum. Water recovery (g)	Cumulative Mass pull (g)	Cum. Water recovery (g)	Cumulative Mass pull (g)	Cum. Water recovery (g)
C1	8.1	90.0	11.0	110.6	12.3	136.5	100.1	9.8
C2	16.6	148.7	19.7	207.9	21.3	230.4	197.0	18.4
C3	23.7	182.4	26.4	230.3	28.8	264.7	226.1	25.4
C4	32.0	245.1	34.0	300.2	37.9	338.5	296.5	34.0
Total feed	1120.6		1146.2		1189.9		110.5	

Grade and Recovery data

Equations used

The data obtained from the PGE assays was presented in terms of grade (ppm) for each sample as shown in the following tables for each ore type. Therefore the following equation was used for the calculation of the PGE recovery into the concentrate.

$$\%R = \frac{C_T * m_c}{C_T * m_c + T_T * m_T} * 100$$

Where R is the recovery of PGE into concentrated

C_T is the total amount of PGE in the concentrate

m_c is the mass of concentrate

T_T is the total amount of PGE in the tailings

Merensky

150bar, 3mm zero gap, 12mm Feed - 4th pass

Sample	sample mass (g)	Au (ppm)	Pd (ppm)	Pt (ppm)	Rh (ppm)	Ru (ppm)	Ir (ppm)
Conc 1	29.59	14.4	45.9	120	5.41	11.4	2.33
Conc 2	39.97	1.15	14.1	12.7	2.09	4.06	0.6
Feed	61.03	0.1	0.67	1.24	<0.1	0.13	<0.1
Tail 1	68.83	<0.1	0.22	0.37	<0.1	<0.1	<0.1
Tail 2	64.73	<0.1	0.2	0.38	<0.1	<0.1	<0.1
T2 (repeat)		<0.1	0.16	0.35	<0.1	<0.1	0.6

150bar, 1.5mm zero gap, 12mm Feed - 4th pass

Sample	sample mass (g)	Au (ppm)	Pd (ppm)	Pt (ppm)	Rh (ppm)	Ru (ppm)	Ir (ppm)
Conc 1a	31.0	7.06	26.7	71.4	3.29	7.19	1.2
Conc 2a	43.5	0.46	5.2	5.56	0.82	1.74	0.29
Feed a	24.8	0.12	0.89	1.55	0.12	0.15	0.15
Tail 1a	57.5	<0.1	0.22	0.4	<0.1	<0.1	<0.1
Conc 1b	25.9	8.25	28.8	79.9	3.65	7.74	1.2
Conc 2b	36.9	0.55	6.36	6.69	0.97	2.04	0.29
Feed b	30.7	0.1	0.72	1.47	0.23	0.18	0.1
Tail 1b	56.7	<0.1	0.18	0.3	<0.1	<0.1	0.14
Tail 1b(repeat)		<0.1	0.18	0.3	<0.1	<0.1	0.18

150bar, 1.5mm zero gap, 6mm Feed - 4th pass

Sample	sample mass (g)	Au (ppm)	Pd (ppm)	Pt (ppm)	Rh (ppm)	Ru (ppm)	Ir (ppm)
Conc 1a	31.9	6.1	25.6	63.6	3.09	6.63	3.67
Conc 2a	40.1	0.47	5.09	6.2	0.78	1.58	0.56
Feed a	18.8	<0.1	0.78	1.52	0.11	0.2	0.27
Tail 1a	35.5	<0.1	0.16	0.34	<0.1	<0.1	0.15
Conc 1b	28.2	8.11	30	74.5	3.71	7.8	4.22
Conc 2b	37.9	0.48	5.22	6.18	0.83	1.71	0.58
Feed b	27.6	0.2	1.1	2.58	0.15	0.32	0.36
Tail 1b	47.0	<0.1	0.17	0.29	<0.1	<0.1	0.32

Ball Mill

Sample	sample mass (g)	Au (ppm)	Pd (ppm)	Pt (ppm)	Rh (ppm)	Ru (ppm)	Ir (ppm)
Conc 1a	65.8	5.23	38.3	81	5.33	11.1	1.96
Conc 2a	64.2	0.45	4.79	6.4	0.86	2	0.54
Feed a	153.9	0.22	1.02	1.84	0.17	0.35	0.1
Tail 1a	154.4	<0.1	0.3	0.58	<0.1	<0.1	0.1
Tail 1a(repeat)		0.14	0.22	0.41	<0.1	<0.1	<0.1
Tail 2a	133.6	0.86	0.24	0.48	<0.1	<0.1	0.34
Conc 1b	41.3	4.63	29.4	64.6	4.09	8.54	2.75
Conc 2b	52.5	0.58	5.71	8.86	1.02	2.51	0.56
Feed b	110.7	0.15	1.08	2	0.18	0.35	0.18
Tail 1b	133.6	<0.1	0.2	0.36	<0.1	<0.1	0.16
Tail 2b	97.6	<0.1	0.26	0.5	<0.1	<0.1	0.15

UG2

150bar, 3mm zero gap, 12mm Feed - 4th pass

Sample	sample mass (g)	Au (ppm)	Pd (ppm)	Pt (ppm)	Rh (ppm)	Ru (ppm)	Ir (ppm)
Conc 1a	69.6	0.27	16.2	33.8	6.68	12.1	2.13
Conc 2a	42.9	<0.1	4.81	10.7	2.44	4.17	0.96
Feed a	44.0	<0.1	1.16	2.32	0.5	0.87	0.19
Tail 1a	89.5	<0.1	0.25	0.53	0.14	0.25	<0.1
Conc 1b	100.7	0.26	16.9	35.8	6.94	12.5	2.24
Conc 1b(repeat)		0.3	17.6	37.2	7.06	13	2.39
Conc 2b	55.4	<0.1	4.76	11.1	2.41	4.15	0.94
Feed b	44.7	<0.1	1.21	2.45	0.53	0.94	0.2
Tail 1b	85.1	<0.1	0.34	0.69	0.19	0.34	<0.1

150bar, 1.5mm zero gap, 12mm Feed - 4th pass

Sample	sample mass (g)	Au (ppm)	Pd (ppm)	Pt (ppm)	Rh (ppm)	Ru (ppm)	Ir (ppm)
Conc 1a	71.0	0.37	22	47.6	8.1	15.6	2.98
Conc 2a	41.5	0.14	8.65	16.1	4.14	6.64	1.47
Feed a	38.7	<0.1	1.21	2.7	0.58	1.02	0.21
Tail 1a	88.1	<0.1	0.49	0.9	0.27	0.45	0.12
Tail 1a(repeat)		<0.1	0.37	0.67	0.2	0.32	0.15
Conc 1b	71.0	0.33	19.9	45.3	7.69	14.4	2.8
Conc 2b	41.5	0.13	8.06	15.4	3.74	5	1.35
Feed b	39.1	<0.1	1.33	2.76	0.58	1.02	0.28
Tail 1b	78.1	<0.1	0.43	0.78	0.22	0.37	0.11

150bar, 1.5mm zero gap, 6mm Feed - 4th pass

Sample	sample mass (g)	Au (ppm)	Pd (ppm)	Pt (ppm)	Rh (ppm)	Ru (ppm)	Ir (ppm)
Conc 1a	85.7	0.27	16.3	33.4	6.08	11.3	2.2
Conc 2a	50.1	<0.1	6.22	12.4	2.83	4.49	0.48
Feed a	37.7	<0.1	1.39	2.86	0.57	1	<0.1
Tail 1a	69.4	<0.1	0.46	1.01	0.21	0.36	<0.1
Conc 1b	64.5	0.39	22.2	44.5	7.52	14.5	1.86
Conc 1b(repeat)		0.35	21.7	45.6	7.93	15.5	1.79
Conc 2b	38.1	0.12	8.92	18.5	4	6.25	0.84
Feed b	36.0	<0.1	1.31	3.23	0.54	0.95	0.35
Tail 1b	76.1	<0.1	0.45	1.26	0.23	0.35	0.18

Ball Mill

Sample	sample mass (g)	Au (ppm)	Pd (ppm)	Pt (ppm)	Rh (ppm)	Ru (ppm)	Ir (ppm)
Conc 1a	52.0	1.05	41.4	97.9	19.1	34.1	5.96
Conc 2a	34.0	0.2	9.69	20.4	4.65	8.87	1.4
Feed 1a	91.5	<0.1	1.3	2.8	0.54	1.02	0.16
Feed 2a	89.0	<0.1	1.42	3.13	0.65	1.17	0.16
Tail 1a	124.8	<0.1	0.3	0.65	0.15	0.29	<0.1
Tail 2a	92.3	<0.1	0.34	0.78	0.18	0.33	<0.1
Conc 1b	51.1	0.8	33.5	84.8	16.4	28.5	5.88
Conc 2b	31.8	0.17	8.04	17.2	3.64	6.97	1.37
Feed 1b	103.8	<0.1	1.21	2.62	0.52	0.98	0.13
Feed 2b	185.3	<0.1	1.31	2.82	0.59	1.06	0.16
Feed 2b(repeat)		<0.1	1.24	2.66	0.57	1.04	0.1
Tail 1b	89.3	<0.1	0.3	0.65	0.15	0.29	<0.1
Tail 2b	94.7	<0.1	0.34	0.76	0.17	0.34	<0.1

Platreef

150bar, 3mm zero gap, 12mm Feed - 4th pass

Sample	sample mass (g)	Au (ppm)	Pd (ppm)	Pt (ppm)	Rh (ppm)	Ru (ppm)	Ir (ppm)
Conc 1a	51.1	2.44	24.8	26.7	2.82	3.18	1.09
Conc 2a	38.9	0.16	3.82	3.5	0.44	0.65	0.45
Feed a	26.8	<0.1	1.19	1.17	0.11	0.1	4.62
Tail 1a	59.6	<0.1	0.4	0.34	<0.1	<0.1	0.25
Tail 1a(repeat)		<0.1	0.4	0.34	<0.1	<0.1	<0.1
Conc 1b	49.1	2.08	25.7	29.1	2.5	2.98	1.03
Conc 2b	36.4	0.18	4.22	3.5	0.48	0.66	0.41
Feed b	26.5	<0.1	1.13	1.08	0.12	0.14	0.33
Tail 1b	51.1	<0.1	0.44	0.33	<0.1	<0.1	0.31

150bar, 1.5mm zero gap, 12mm Feed - 4th pass

Sample	sample mass (g)	Au (ppm)	Pd (ppm)	Pt (ppm)	Rh (ppm)	Ru (ppm)	Ir (ppm)
Conc 1a	62.0	1.69	21.2	23.7	1.94	2.13	0.43
Conc 2a	46.9	0.14	3.11	3.01	0.33	0.47	0.12
Feed a	25.0	<0.1	1.14	1.18	0.11	<0.1	0.14
Tail 1a	23.4	<0.1	0.38	0.41	<0.1	<0.1	<0.1
Tail 1a(repeat)		<0.1	0.43	0.43	<0.1	<0.1	<0.1
Conc 1b	63.8	1.64	20	24.8	1.73	2	0.43
Conc 2b	46.7	0.16	3.99	3.42	0.39	0.54	0.15
Feed b	31.5	<0.1	1.15	1.37	0.11	0.11	0.1
Tail 1b	56.8	<0.1	0.36	0.33	<0.1	<0.1	<0.1

150bar, 1.5mm zero gap, 6mm Feed - 4th pass

Sample	sample mass (g)	Au (ppm)	Pd (ppm)	Pt (ppm)	Rh (ppm)	Ru (ppm)	Ir (ppm)
Conc 1a	62.4	1.61	21.1	25.2	1.98	2.28	0.44
Conc 2a	45.7	0.15	3.38	3.13	0.36	0.5	0.14
Feed a	32.0	<0.1	0.95	1.15	<0.1	<0.1	0.18
Tail 1a	67.0	<0.1	0.4	0.44	<0.1	<0.1	0.14
Conc 1b	61.4	1.61	20.7	23.9	1.83	2.29	0.53
Conc 2b	47.1	0.15	2.96	3.06	0.33	0.46	0.16
Feed b	28.6	<0.1	1.13	1.27	0.12	<0.1	0.19
Tail 1b	65.9	<0.1	0.38	0.44	<0.1	<0.1	<0.1
Tail 1b(repeat)		<0.1	0.34	0.43	<0.1	<0.1	<0.1

Ball Mill

Sample	sample mass (g)	Au (ppm)	Pd (ppm)	Pt (ppm)	Rh (ppm)	Ru (ppm)	Ir (ppm)
Conc 1a	33.6	4.23	57.7	61.4	5.38	6.99	1.51
Conc 2a	29.7	0.81	6.3	6.38	0.73	1.4	0.25
Feed 1a	121.9	<0.1	1.26	1.4	0.2	0.28	<0.1
Feed 2a	117.8	<0.1	1.23	1.18	0.12	0.17	<0.1
Tail 1a	122.1	<0.1	0.51	0.67	0.1	0.14	<0.1
Tail 2a		<0.1	0.39	0.59	<0.1	0.12	<0.1
Conc 1b	39.7	3.98	56.8	55.3	4.84	6.18	1.11
Conc 2b	32.2	0.36	6.68	5.99	0.79	1.43	0.26
Feed 1b	112.0	<0.1	1.42	1.81	0.21	0.33	0.1
Feed 2b	124.3	0.11	1.94	3.54	0.42	0.72	0.16
Tail 1b	133.8	<0.1	0.35	0.38	<0.1	<0.1	<0.1
Tail 2b	133.3	<0.1	0.31	0.36	<0.1	<0.1	<0.1

Appendix E – MLA data

A summary of the MLA data obtained is given in this section, showing the total PGM area in each liberation class for the three ore types.

Merensky

Liberation class	3mm zero gap, 12mm Feed	1.5mm zero gap, 12mm Feed	1.5mm zero gap, 6mm Feed	Ball Mill
Liberated PGM	667.06	1495.92	1108.07	2807.64
PGM locked in gangue	439.15	157.85	63.94	729.77
PGM locked in floatable BMS	155.97	654.12	116.89	33.28
PGM occluded in locked BMS	297.13	172.73	319.73	243.93
Total area (μm^2)	**1559.30**	**2480.63**	**1608.63**	**3814.63**

UG2

Liberation class	3mm zero gap, 12mm Feed	1.5mm zero gap, 12mm Feed	1.5mm zero gap, 6mm Feed	Ball Mill
Liberated PGM	569.78	594.80	701.15	742.53
PGM locked in floatable BMS	656.66	118.37	203.99	261.84
PGM occluded in locked BMS	60.44	87.94	75.34	197.88
PGM locked in gangue	803.61	324.37	601.91	335.34
Total area(μm^2)	**2090.49**	**1125.48**	**1582.39**	**1537.59**

Platreef

Liberation class	3mm zero gap, 12mm Feed	1.5mm zero gap, 12mm Feed	1.5mm zero gap, 6mm Feed	Ball Mill
Liberated PGM	488.07	1253.09	166.28	471.76
PGM locked in floatable BMS	9.36	251.64	64.43	67.12
PGM occluded in locked BMS	99.59	212.12	70.58	180.90
PGM locked in gangue	473.05	541.37	1150.63	347.72
Total area(μm^2)	**1070.07**	**2258.22**	**1451.92**	**1067.50**